The Relationship between Rock Mass Conditions and Alteration and Weathering in the Lower Hamersley Group Iron Formations, Western Australia

---

A thesis submitted in partial fulfilment of the requirements for the Degree of

Master of Science in Engineering Geology

at the

University of Canterbury

By

Hanna Donders

September 2009

FRONTISPIECE

WEST ANGELAS IRON ORE MINE, WESTERN AUSTRALIA

ABSTRACT

The Pilbara region of Western Australia hosts the Hamersley Province, an area of abundant iron ore resources located in the lower Hamersley Groups, Brockman and Marra Mamba Iron Formations. This study consists of a geotechnical and a geochemical and mineralogical investigation into the Banded Iron Formation (BIF) and shale deposits of the lower Hamersley Group that reside in the pit walls of RTIO mines in Western Australia. Areas throughout Tom Price, Paraburdoo, Marandoo and West Angelas iron ore mines are geotechnically investigated for rock mass conditions through the use of the Slope Mass Rating (SMR) classification system and through point load and slake durability testing. Selected samples from these areas were then geochemically and mineralogically tested by X-ray Fluorescence (XRF), X-ray Diffraction (XRD) and microscopic analysis, to determine the geochemical and mineralogical changes of BIF and shale as they alter and weather through hypogene and supergene alteration and Recent weathering. It was found that the most efficient method for determining the alteration and/or weathering of lower Hamersley Group BIF and shale deposits was by the use of a chemical alteration index, calculated from enriched and depleted major elements in the BIF and shale as they alter and weather. It has been suggested here that this *Pilbara Iron* alteration index can be calculated efficiently and effectively from geochemical testing in intervals down boreholes throughout future or developing open pit mines to assist in estimating slope stability conditions. It is also suggested that many boreholes should be analysed in section or in 3D space to create cross sections or block models showing the varying extent of alteration and weathering throughout the area being studied. From the geotechnical investigation, it was found that the weakest region, in terms of pit slope stability, were the highly and extremely altered and/or weathered regions with *Pilbara Iron* alteration indices of between 61 and 80, and 81 and 100, respectively. If these zones are identified, slope stability analysis can be focused on these geotechnically vulnerable areas. Slope stability analysis should be completed by using a suitable technique, such as by the use of SMR, which, along with other risk identification measures, will identify potentially unstable areas and suggest the required course of action. Further hazard and risk analysis should be undertaken in potentially unstable areas and remedial measures undertaken as appropriate. Thereby, the *Pilbara Iron* alteration index can be used in the Hamersley Province as a predictive tool for pit slope stability.

ACKNOWLEDGEMENTS

Firstly, I would like to thank Rio Tinto Iron Ore for the opportunity to work with the geotechnical team in Tom Price, Paraburdoo, Marandoo and West Angelas mine sites and the Perth office, and also for their financial contribution that made this project possible. Thanks goes out especially to my supervisor at RTIO, Joe Seery, who was always on call when I needed him and was always happy to help. Thank you for your time and support, it was much appreciated. Thank you to all the rest of the RTIO crew that contributed. Especially, thank you to Richard Mould, Jon Lapwood, Sihaba Mbano, Leigh Nicholas, Leo Souza, Fred Sadiiki, Matt Zanin and Matt Fetcher. Also, thank you to Peter Croft and Mark Eggers for your helpful insights.

I would also like to thank the crew at the University of Canterbury. Thank you to my supervisor, David Bell, who organized my scholarship and provided many insights along the way. Thank you to the technical crew, Vannesa Tappenden, Cathy Higgins, Kerry Swanson and Rob Spiers, for helping me with the geotechnical, geochemical and mineralogical lab work and for taking care of me when I got my thumb squashed by the rock crusher. Thank you to Steven Brown who analysed all of my XRF and XRD samples and was always happy to answer my questions and help me out with my geochemical study. Thank you to Pat Roberts and Janet Warburton for your eternal support of students. Also, to John Southward, thank you with for continuously fixing my laptop, for without your expertise, I would possibly have gone mad.

Last, but not least, I would like to thank my family and friends. Thank you to Dannielle Belcher, my friend and fellow classmate, who listened and feigned listening to everything I had to say over the past six years. Your support will never be forgotten. Thank you also to Kelly Sparks and Liz Carnousus who stuck by Dannielle and I during undergrad, during rain and shine and everything in between. Thank you to my fellow officemate and friend, Angela Doherty, who gave me advice and friendship. I wish you the very best for your future. Thank you to my flat mates, Andrew Brown, Quentin Goodman, Dave McRobert, Johnny Winter, Paul Thornley and Toni McLean who have always put up with my student ways and who were always there to have a good time. Thank you to Morgan Lynn and Amanda England, your support and encouragement have always meant so much to me.

Thank you to my family. To Eran and Karel, thank you for your unconditional friendship. Thank you especially to my mother, Apakura. You were always a major influence in my life. Thank you for being so strong and unconditionally supportive. Your sacrifices did not go unnoticed.

Lastly, thank you to my partner, Scott Johnston. You have always been there for me, through thick and thin. Thank you for the many laughs we have shared. Your support through this thesis has been limitless.

TABLE OF CONTENTS

TABLE OF FIGURES

TABLE OF TABLES

1 INTRODUCTION

1.1 BACKGROUND

The Pilbara region lies in the north of Western Australia. It contains an area known as the Hamersley Basin where numerous iron ore mines reside due to its abundant mineralised Banded Iron Formation (BIF) deposits.

The Rio Tinto Iron Ore Company (RTIO) mines iron ore throughout the Pilbara. RTIO currently owns and operates eleven iron ore mines in the Pilbara region and their operations are expanding. Last year the Pilbara operations produced over 150 million tonnes of iron ore.

The RTIO mines are open cast mines mined using mainly drill and blast methods.

Geotechnical engineering at these mines allows the open pit mines to be mined safely and economically. Geotechnical studies of the mines ensures adequate stability of the pit slopes for the life of the mine and, therefore, ensures safety of personnel and machinery that operate in the vicinity of pit walls and ensures optimum design of the pits so that the mined iron ore to waste ratio is maximised.

This study focussed on deposits at Tom Price, Paraburdoo, Marandoo and West Angelas mine sites in the Hamersley Province of the Pilbara region, Western Australia (refer to Figure 1.1).

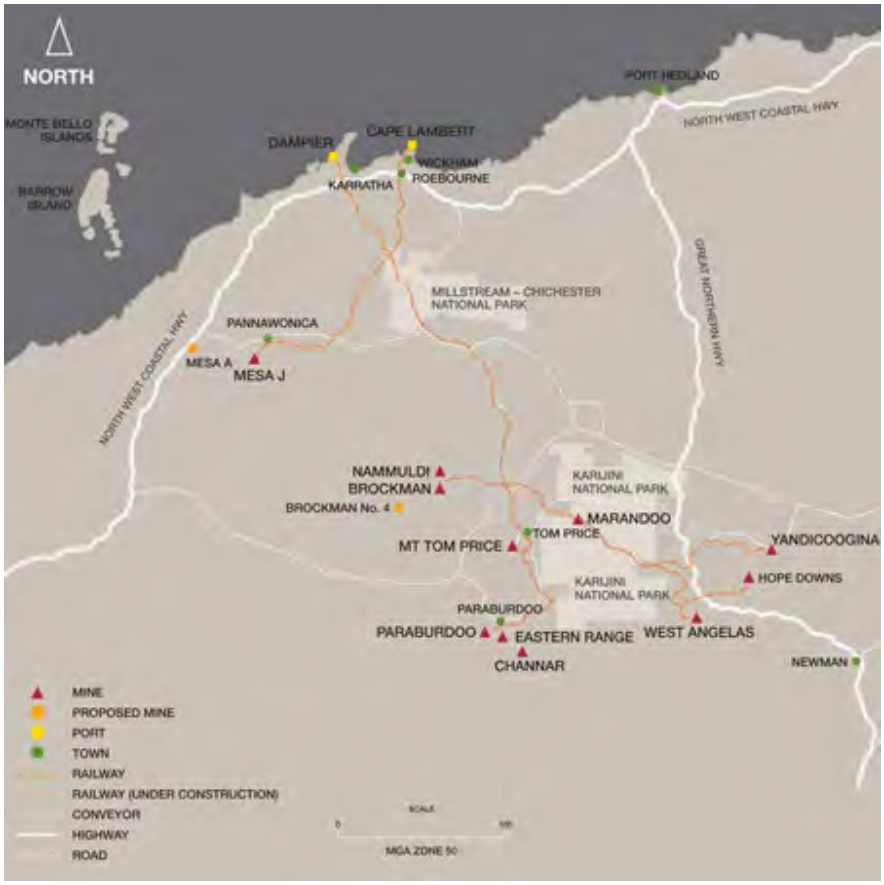

FIGURE 1.1 RTIO MINING OPERATIONS IN THE PILBARA, WESTERN AUSTRALIA (RIO TINTO IRON ORE, 2009)

1.2 AIMS AND OBJECTIVES

The aim of this research project is to develop a method of estimating aspects of the slope stability of open-cast pit slopes in iron ore mines in the Hamersley Province by analysing the geochemistry and mineralogy of the rock.

The rock mass classification system, used to classify the pit slope stability in this study, was Slope Mass Rating (SMR). SMR is a method modified by Romana (1985) from the Rock Mass Rating (RMR) method, which was developed by Bieniawski (1976 and 1989) and which is commonly used as a tool for estimating rock mass strength in civil and mining projects.

The geochemistry of the rocks was determined by X-Ray Florescence (XRF) major and minor element analysis. The mineralogy of the rocks was determined by X-Ray Diffraction (XRD) mineral analysis and transmitted and reflected microscopic analysis.

This research has three specific objectives which are as follows:

- To document, analyse and classify pit slope stability throughout RTIO mines;
- To document, analyse and classify the geochemical and mineralogical characteristics of altered and weathered BIF and shale that cause instability issues and
- To link the geochemical and mineralogical parameters, caused by alteration and weathering, to specific rock mass conditions and use this as a predictive tool for open pit slope stability in the Lower Hamersley Group deposits in the Pilbara, Western Australia.

1.3 INVESTIGATION METHODOLOGY

1.3.1 LITERATURE REVIEW

Firstly, a literature review was undertaken to evaluate the geology of the Hamersley Province. In particular, the mineralogical evolution of iron ore genesis from BIF to iron ore was studied, as well as the structural influences on ore genesis and the theories of iron ore genesis itself.

Secondly, rock mass classification techniques were studied. The geomechanics of slope stability with an emphasis on open pit slopes and the transfer of these ideas into rock mass classification systems were considered.

1.3.2 GEOTECHNICAL CLASSIFICATION AND LABORATORY TESTING

Field investigations were undertaken at Tom Price, Paraburdoo, Marandoo and West Angelas iron ore mines. Excavated slopes and diamond drill core were studied. SMR was performed on selected rock mass exposures and point load testing and slake durability testing was performed where possible. The rock masses studied were chosen from fresh through to extremely altered and extremely weathered BIF and shale from the lower Hamersley Group deposits including the Brockman Iron Formation and the Marra Mamba Iron Formation.

Ore Type:	Study Site:
Low P Brockman Iron Formation	Southern Ridge, North Deposit, 23 East
High P Brockman Iron Formation	Section Seven, 32 East
Marra Mamba Iron Formation	Marandoo, West Angelas

TABLE 1.1 ORE TYPES MINED AND THEIR CORRESPONDING STUDY SITES

1.3.3 GEOCHEMICAL AND MINERALOGICAL LABORATORY TESTING

Samples were taken from each study area to provide lab specimens for geochemical and mineralogical analysis. Rock samples were taken of fresh through to extremely altered and weathered BIF and shale over the three ore types studied. Using XRF and XRD analysis, the chemical components and mineral components of the rock specimens were identified. Polished thin section analysis was also used to determine the petrology of typical BIF and shale deposits in the region. Using these techniques, the typical alteration and weathering geochemical and mineralogical signatures in the lower Hamersley Group BIF and shale deposits were determined as they alter through hypogene and supergene alteration and Recent weathering.

	Testing Methods:
Geotechnical	SMR, Point load Testing, Slake Durability Testing
Geochemical	XRF
Mineralogical	XRD, Microscopic Analysis

TABLE 1.2 TESTING METHODS COMPLETED IN THIS STUDY

1.3.4 INTERPRETATION

Using the geotechnical, geochemical and mineralogical analyses, the effect of alteration and weathering on rock mass conditions throughout the Hamersley Province was analysed. This was then followed by a discussion on the possible techniques for using geochemical data in open pit mining, to determine the link to potential instability issues.

1.4 THESIS ORGANISATION

This thesis comprises of eight chapters and associated appendices. The first chapter outlines the background and setting of the project and introduces the methodology of the research.

Chapter two reviews the geology of the Hamersley Province, paying particular attention to the genesis of iron ore in the Hamersley Province and to the structure of the province and its role in ore genesis.

Chapter three investigates rock mechanics and rock mass classification techniques.

Chapter four discusses the results from rock mass classification, taken from in the field, completed throughout the four study areas; and from geomechanical laboratory testing of Hamersley Province BIF and shale.

Chapter five discusses the results of geochemical and mineralogical laboratory testing of selected BIF and shale samples from the Hamersley Province and their evolution with alteration and/or weathering.

Chapter six analyses the relationship between alteration and weathering of the BIF and shale deposits with rock mass conditions in the Hamersley Province.

Chapter seven discusses the application of geochemistry to characterise the stability of open pit slopes in RTIO mines.

And finally, chapter eight provides an overview of the research and several conclusions made by the author.

2 GEOLOGY OF THE HAMERSLEY PROVINCE

2.1 REGIONAL GEOLOGY

The Hamersley Province covers 80 000 km^2 of land in the Pilbara region in the north of Western Australia. It is host to many mines including over 20 iron ore mines, many of these are owned and operated by RTIO.

Iron ore in the Hamersley Province is mainly found in the Hamersley Group Iron Formations which, along with the Fortescue Group and the Turee Creek Group, make up the Mount Bruce Supergroup and is found throughout the Pilbara region alongside older Archaean granite and greenstone deposits and the younger sedimentary and volcanic Wyloo Group.

The largest iron ore deposits found in the region are the Mount Whaleback deposit in the south-east of the Pilbara and the Mount Tom Price deposit found in the west Pilbara.

The Hamersley Group was deposited on a continental shelf environment over 2,500 Ma ago. It has an overall stratigraphic thickness of 2,500 m and comprises mainly of BIF deposits interbedded with shale, dolomite and acid volcanics and are intruded by dolerite sills and dykes. The BIF is composed of thin chert layers alternating with layers of mainly iron minerals.

The north of the Hamersley province is characterised by gentle folding caused by mild deformation. The southern region is extensively folded with en echelon folding occurring in the southwest and tight east trending folding occurring in the southeast (Horwitz, 1987).

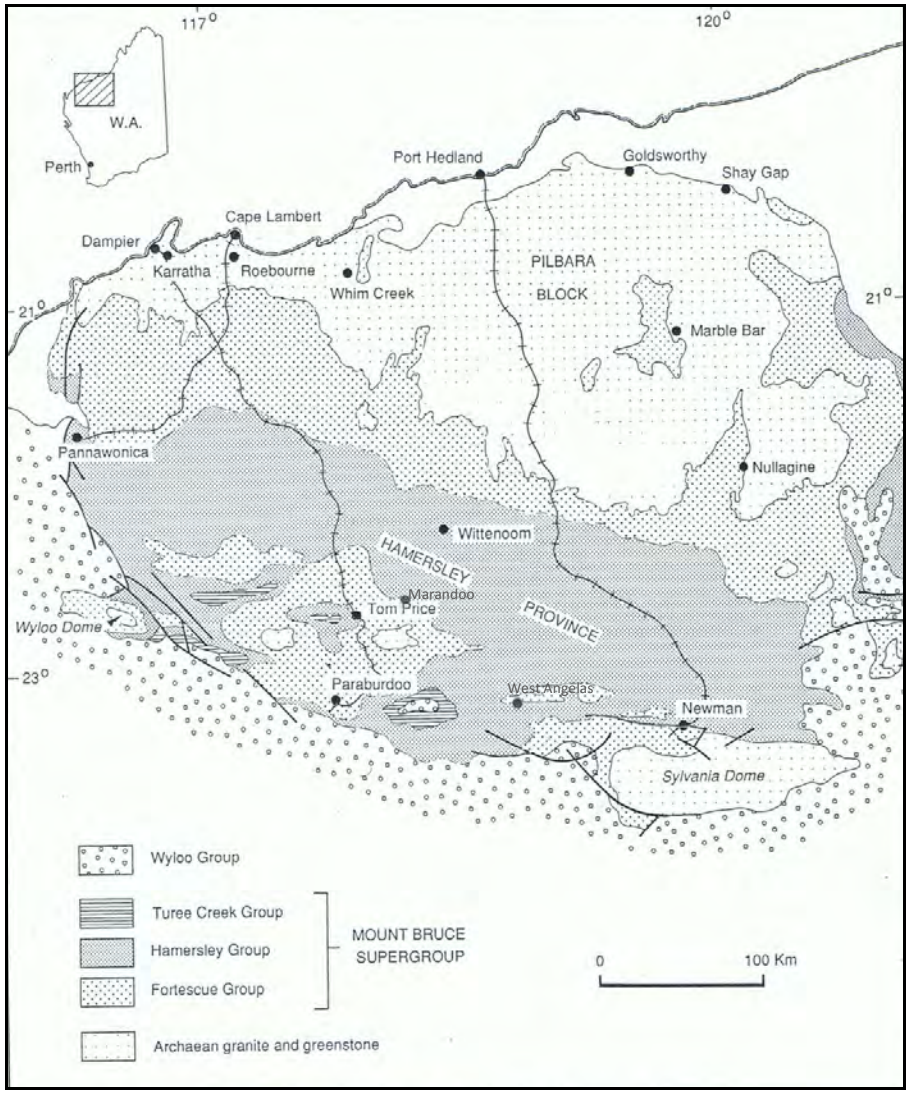

FIGURE 2.1 GEOLOGY OF THE HAMERSLEY PROVINCE (FROM HARMSWORTH ET AL., 1990)

2.2 STRATIGRAPHY

2.2.1 FORTESCUE GROUP

The Fortescue Group has a stratigraphic thickness of 4,500 m made up of the Bellary Formation, the Hardy Formation, the Tumbiana Formation and the Jeerinah Formation. The Bellary Formation consists of clastic sedimentary and mafic volcanic rocks. Unconformably overlying the Bellary Formation is the thick Hardy Formation consisting of mostly sandstones and a basal conglomerate. The Hardy Formation was deposited during the beginning of regional subsidence and is thickened in the south of the Hamersley Province with mafic intrusions. The conformably overlying Tumbiana Formation consists of interbedded volcanic and sedimentary rocks and has also been intruded towards the south. The Jeerinah Formation conformably overlies the Tumbiana Formation and consists entirely of fine clastic sedimentary rock with a high organic content in the north and over 50% interbedded mafic volcanic rock and intrusions in the central Hamersley Province.

2.2.2 HAMERSLEY GROUP

An overview of the Hamersley Group stratigraphy is shown in Figure 2.2. It is 2,500 m thick but can locally decrease in thickness by over 50% in areas of iron enrichment. The Hamersley Group consists of the Marra Mamba Iron Formation, the Wittenoom Formation, the Mount Sylvia Formation, the Mount McRae Formation, the Brockman Iron Formation, the Weeli Wolli Formation, the Woongarra Formation and the Boolgeeda Iron Formation.

The Marra Mamba Iron Formation conformably overlies the Jeerinah Formation and consists of the Nammuldi Member, the MacLeod Member and the Mount Newman Member. The Nammuldi Member consists of interbedded cherty BIF and thin shale bands. The MacLeod Member consists of interbedded chert, BIF, carbonates and shale. The Mount Newman Member consists of interbedded BIF, carbonates and shale. Iron enrichment forming iron ore from BIF is often found in this formation, especially in the Mount Newman Member, and is mined extensively in areas such as the Marandoo and West Angelas mine sites.

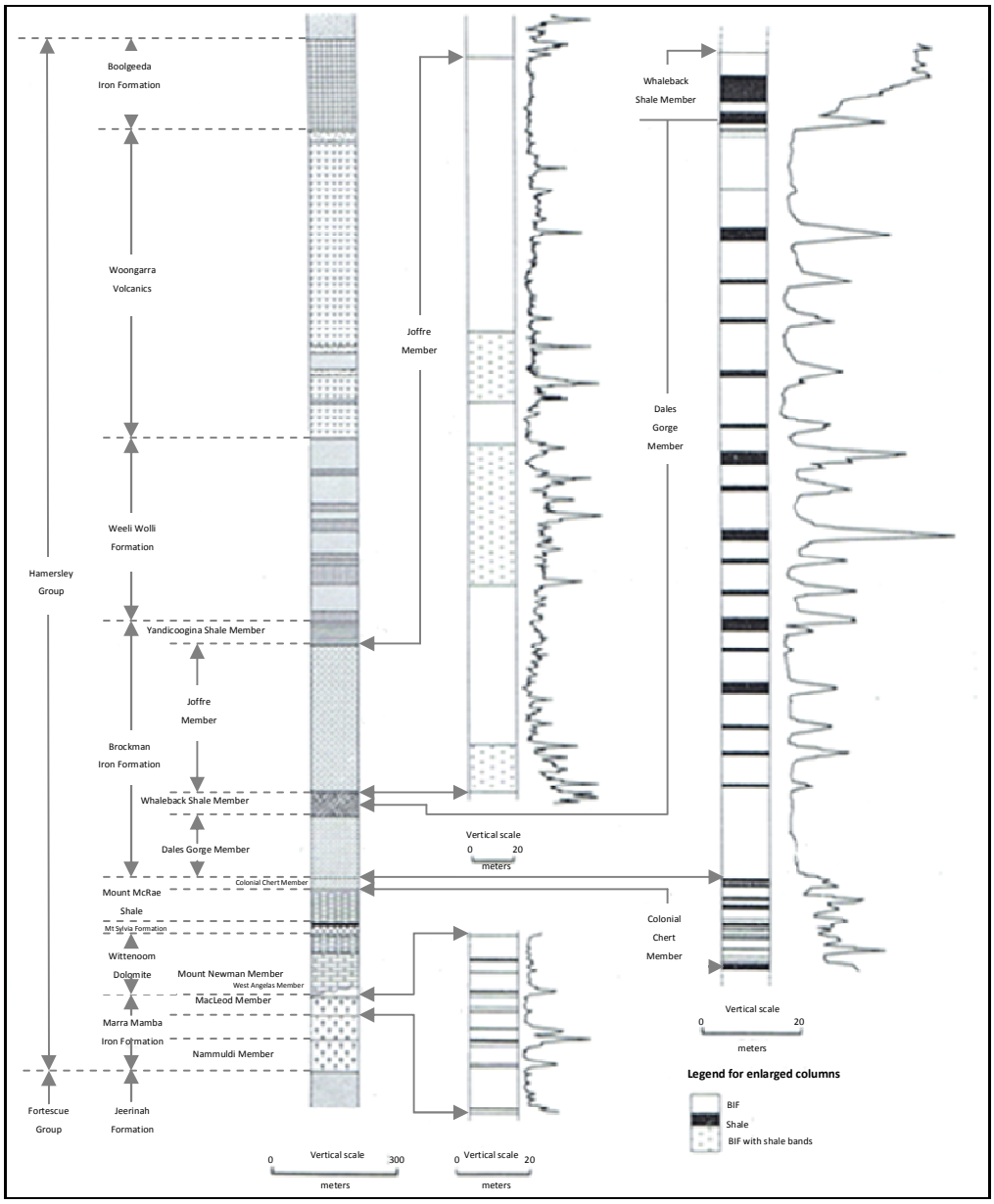

FIGURE 2.2 STRATIGRAPHIC COLUMNS OF THE HAMERSLEY GROUP AND ASSOCIATED GAMMA PROFILES OF THE MAJOR IRON DEPOSITS (FROM HARMSWORTH ET AL., 1990)

The Wittenoom Formation conformably overlies the Marra Mamba Iron Formation. It includes the West Angelas Shale Member at its base which consists of shale, chert and dolomite with some BIF. The middle unit comprises of interbedded dolomite and minor chert. The upper unit consists of interbedded shale, dolomite and minor chert and BIF.

The Mount Sylvia Formation conformably overlies the Wittenoom Formation and comprises of three prominent BIF and chert units separated by chert and shale beds.

The Mount McRae Formation conformably overlies the Mount Sylvia Formation. At its base is a unit of interbedded black carbonaceous shale and chert. The middle layer is a pyrite rich unit consisting of interbedded chert, black shale and minor dolomitic shale. The top unit is the Colonial Chert Member which consists of interbedded BIF and shale.

The Brockman Iron Formation conformably overlies the Mount McRae Formation and consists of the Dales Gorge Member, the Whaleback Shale Member, the Joffre Member and the Yandicoogina Member and is the most economically valuable formation in the Hamersley Province for producing iron ore. The Dales Gorge Member consists of interbedded BIF and shale. 16 shale and 17 BIF macrobands are recognised in the Dales Gorge Member throughout the province. The Whaleback Shale Member comprises of five units of four interbedded shale and BIF bands and an upper unit of interbedded chert and shale. The Joffre Member consists of mostly BIF with numerous thin shale bands that are not continuous throughout the Hamersley Province such as in the Dales Gorge Member. The Yandicoogina Member consists of interbedded shale and chert.

The Weeli Wolli Formation conformably overlies the Brockman Iron Formation and comprises of interbedded BIF, shale and intruded dolerite.

The Woongarra Formation is a volcanic formation and overlies the Weeli Wolli Formation. It consists of acid intrusives, mainly rhyolite; and tuff deposits. Some BIF can also be found in this formation.

The Boolgeeda Iron Formation overlies the Woongarra Formation and comprises of three units. The lower unit consists of interbedded shaly BIF, chert and shale while the middle unit consists of interbedded BIF and shale and the upper unit consists of a basal chert zone and interbedded BIF and shale.

2.2.3 TUREE GROUP

The Turee Group is the uppermost formation of the Mount Bruce Supergroup. It conformably overlies the Boolgeeda Formation and has a stratigraphic thickness of 5,000 m. The Turee Group is made up of the Kungarra Formation and an upper unit. The Kungarra Formation consists of siltstone, greywacke and sandstone. The upper unit consists of quartzite, carbonate and shale (Trendall, 1983).

2.2.4 WYLOO GROUP

The Wyloo Group unconformably overlies the Mount Bruce Supergroup and is broken up into the Lower Wyloo Group and the Upper Wyloo Group separated by an unconformity.

The Lower Wyloo Group is a thick sequence of up to 12,000 m and is made up of the basal Beasley River Formation and the upper Cheela Springs formation. The Beasley River Formation comprises of quartz sandstone with some channels of BIF conglomerate. The Cheela Springs Formation consists of basalts.

The Upper Wyloo Group has a stratigraphic thickness of up to 13,000 m and is made up of four formations including the basal Mount McGrath Formation, the Duck Creek Formation, the June Hill Formation and the uppermost Ashburton Formation. The Mount McGrath Formation consists of ferruginous mudstone and sandstone with some hematite conglomerates. The Duck Creek Formation consists of interbedded dolomite and chert. The June Hill Formation is a volcanic sequence. And, lastly, the Ashburton Formation consists of interbedded mudstone, conglomerate, sandstone and siltstone.

2.3 GENESIS OF HAMERSLEY GROUP IRON ORE

2.3.1 OVERVIEW

In the RTIO mines, iron enriched BIF, mainly from the Brockman Iron Formation and the Marra Mamba Iron Formation, are mined. The lithologies in and around these formations are important to the stability of the mines. These lithologies are geochemically and mineralogically altered with ore genesis and, therefore, affect the mechanical nature of these rocks. It is believed that iron enrichment was the product of hypogene and/or supergene alteration, enriching iron and removing gangue minerals.

Hypogene alteration is a relatively recent hypothesis for the formation of high grade hematite ore deposits in the Hamersley Province. Hypogene alteration involves the process of metasomatic alteration from fluids circulating through the earth's crust, preferentially flowing through weakened areas such as fault systems. An example of areas where this mineralisation type has occurred is Southern Ridge and North Deposit at Mount Tom Price and 23 East Deposit at Eastern Ranges in Paraburdoo. The second iron enrichment process is supergene alteration. Supergene alteration generally follows the landscape and creates extensive and flat lying deposits and is, therefore, believed to have been caused by alteration from circulating meteoric water from the surface creating martite-goethite ores in primary BIF and is also believed to be the final stage of the process in creating high grade hematite iron ore after hypogene alteration. Examples of this mineralisation occur at Section Seven deposit at Mount Tom Price, 32 East 6 Deposit at Eastern Ranges in Paraburdoo, Marandoo deposit and West Angelas Deposit A.

In this section the deposition of primary BIF is briefly discussed followed by an overview of current iron ore genesis theories with concentration on the hypogene model for high grade hematite iron ore and the supergene model for martite-goethite ore.

2.3.2 DEPOSITION OF BIF

BIF is a chemical sedimentary deposit of alternating bands of iron, chert and shale and contains approximately 25 to 45% (wt) Fe. BIF is generally believed to have been deposited in shallow ocean areas such as continental shelves, and are mainly Precambrian in age. It is believed that

blue green algae during this time created an oxidising environment in these areas for the then-abundant iron in the earth's oceans to precipitate. This caused the iron, along with anoxic mud, to form sedimentary bands of iron oxide, chert and shale on the ocean's floor (Morris, 1993). It is believed that seasonal cycles caused the characteristic banding. In addition, Barley et al. (1997) suggested that the Hamersley BIF deposits were deposited during a time of increased submarine magmatic and hydrothermal activity and was deposited as a result of iron and silica being subsequently deposited into the ocean, upwelling along the continental shelf where the BIF was forming.

2.3.3 GENESIS OF BIF-DERIVED IRON ORE

There are two types of BIF-hosted iron ore mined in the Hamersley Province. These are high grade hematite ore in which, it is believed, BIF has been enriched by hypogene or metamorphic processes and overprinted by supergene enrichment and contains approximately 60 to 68% (wt) Fe, and martite goethite ore in which BIF has been enriched in Fe by supergene processes and contains approximately 60 to 63% (wt) Fe.

Early iron ore genesis models for the Hamersley Province iron ore mines included Phanerozoic supergene leaching and replacement as the iron enrichment process for martite-goethite ore (Morris, 1980; and Morris, 1985) and later regional metamorphism of supergene altered ore to form high grade hematite deposits (Harmsworth et al., 1990; and Morris, 1985). The supergene metamorphic model involved an early stage of iron enrichment by supergene alteration by oxidising meteoric water during the Proterozoic, replacing silica with goethite and oxidising magnetite to hematite, and later burial and metamorphism during the Proterozoic resulting in dehydration of the goethite to microplaty hematite and finally removal of phosphorous by leaching. Several research papers have disputed this hypothesis more recently, however, and have instead suggested that high grade hematite ore deposits in the Hamersley Province have formed through high temperature alteration and low temperature oxidation before supergene alteration (Barley et al., 1999; Martin et al., 1998; Oliver & Dickens, 1999; Powell et al., 1999; Taylor et al., 2001; Thorne et al., 2004; Thorne et al., 2006; Webb et al., 2003; Webb et al., 2004; and Webb et al., 2006). Some of these papers have proposed that carbonate replacement

of silica in the BIF is a required first step to high grade hematite ore formation as evidenced by the absence of silica in carbonate rich rocks found below high grade hematite ore deposits in the Hamersley Province (Barley et al., 1999; Hagemann et al., 1999; Taylor et al., 2001; and Webb et al., 2006).

2.3.4 HYPOGENE MODEL

Hypogene alteration is currently believed to be the first stage of development for high grade hematite ore in the Hamersley Province. The high grade hematite ore deposits are believed to be a product of both deep basinal hypogene iron enrichment and shallow supergene enrichment and are found mainly within the Brockman Iron Formation at Mount Tom Price, Paraburdoo and Mount Whaleback in the Hamersley Province.

Hypogene mineralisation is believed to have taken place sometime between 2,209 and 1,843 Ma (Taylor et al., 2001) during the Paleoproterozoic. These ore bodies are found in the Hamersley Province to lie along medium scale faults of hundreds of meters offset and are found up to great depths along these faults. At Mount Tom Price, the high grade ore is found along the Southern Batter Fault. At Mount Whaleback, the ore is thought to be associated with the Central fault and the Eastern Footwall fault. This ore type is dominantly found in the Brockman Iron Formation.

There are four stages of alteration distinguished for the development of high grade hematite ore in the Hamersley Province (Taylor et al., 2001):

1) Hypogene Stage (refer to Figure 2.3). This primary alteration stage is believed to have resulted from low temperature, highly saline fluids that flowed up from underlying basin-wide aquifers and focussed flow around early faults during the Paleoproterozoic. This stage mainly involves the removal of silica from the primary BIF and the shale bands resulting in considerable thinning of the sedimentary succession. Carbonate is also slightly enriched in the BIF and shale during this stage from the basinal fluids passing up through the underlying stratigraphy. The characteristic mineral assemblage resulting is magnetite-siderite-stilpnomelane-pyrite-apatite.

2) Deep Meteoric Circulation Stage (refer to Figure 2.3). This secondary stage is believed to have resulted from oxidising, low saline, deeply circulating, heated meteoric fluids during the Proterozoic. This stage involves the oxidation of magnetite to martite and the development of microplaty hematite. No change in silica content or volume is associated with this stage. The characteristic mineral assemblage resulting from this stage is microplaty hematite-martite-apatite-ankerite.
3) Leaching Stage. This third stage involves the leaching of carbonate and remaining silica during the Proterozoic to form a characteristic mineral assemblage of microplaty hematite-martite-apatite.
4) Supergene stage. This final stage is believed to have resulted from shallow meteoric fluids during the Phanerozoic, possibly during the Cretaceous (Taylor et al., 2001). During this stage, shale bands lose magnesium and calcium and become enriched in aluminium and titanium. BIF loses calcium and phosphorous to form a remaining characteristic mineral assemblage of microplaty hematite-martite ore (refer to Figure 2.4).

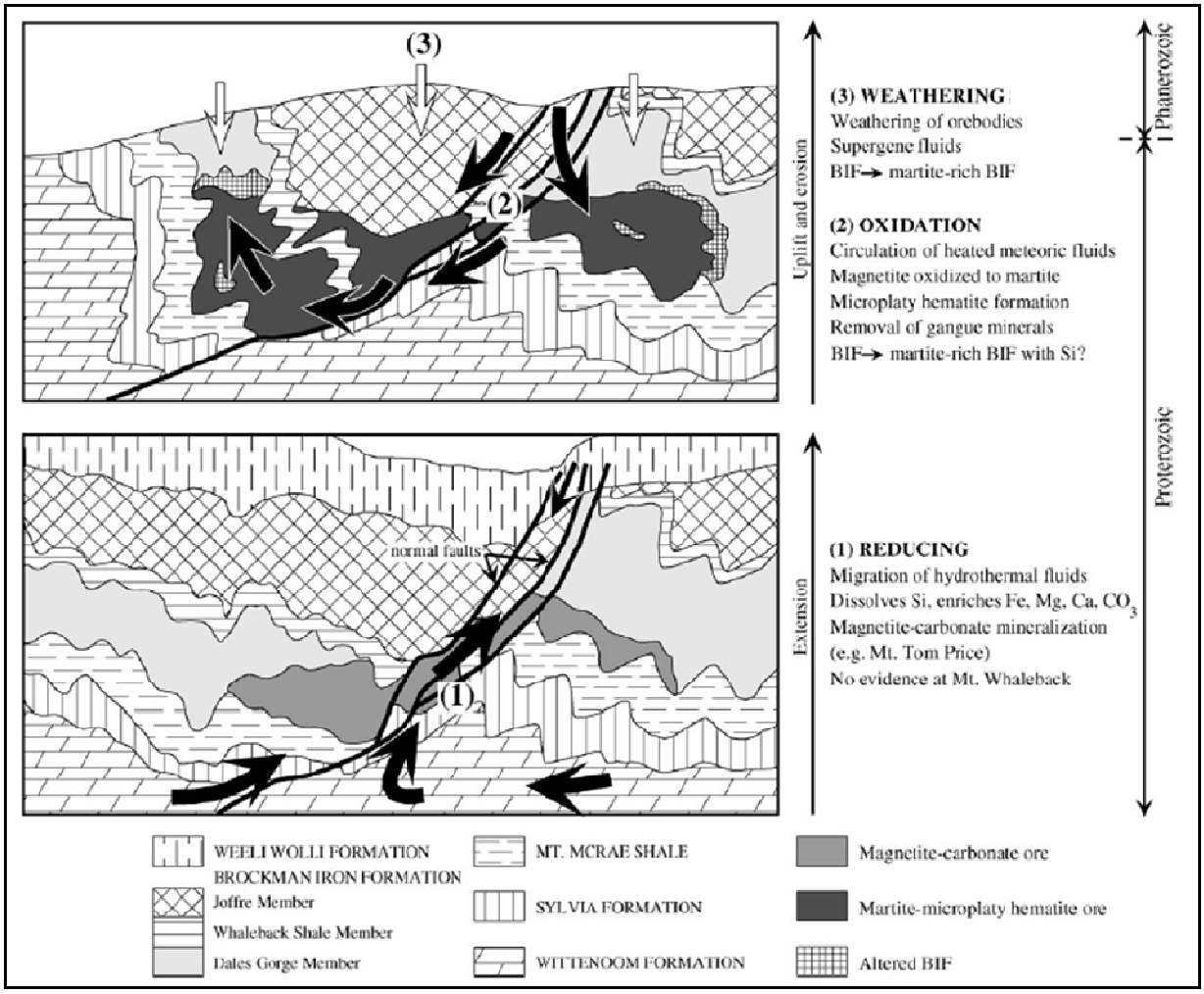

FIGURE 2.3 CROSS SECTIONAL DIAGRAMS OF THE EVOLUTION OF PRIMARY BIF TO HIGH GRADE HEMATITE ORE IN THE HAMERSLEY PROVINCE (MODIFIED FROM WEBB ET AL., 2003)

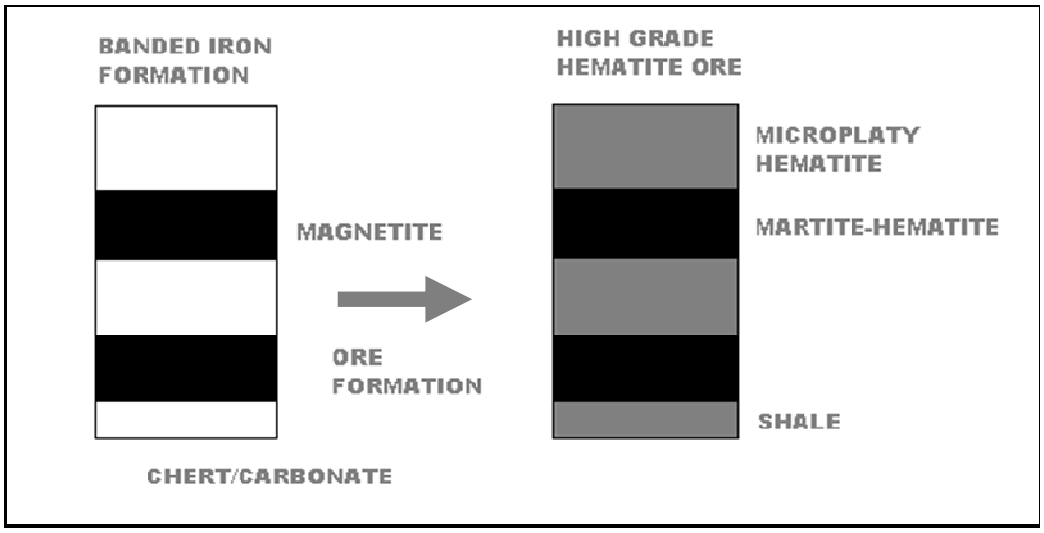

FIGURE 2.4 SIMPLIFIED SUMMARY OF PRIMARY BIF MINERAL ASSEMBLEGE AND THE RESULTING HIGH GRADE HEMATITE ORE MINERAL ASSEBLAGE AFTER HYPOGENE AND SUPERGENE ALTERATION (MODIFIED FROM CLOUT, 2003)

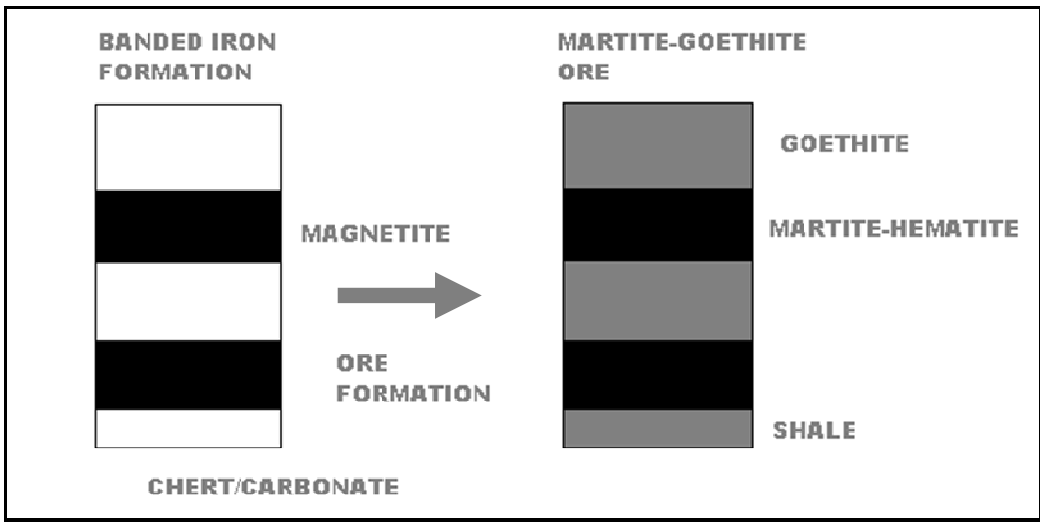

FIGURE 2.5 SIMPLIFIED SUMMARY OF PRIMARY BIF MINERAL ASSEMBLAGE AND THE RESULTING MARTITE-GEOTHITE ORE MINERAL ASSEMBLAGE AFTER SUPERGENE ORE FORMATION (MODIFIED FROM CLOUT, 2003)

2.3.5 SUPERGENE MODEL

Supergene alteration, without hypogene alteration, is the accepted theory for the development of martite-goethite ore in the Hamersley Province. Martite-goethite ores in the Hamersley Province are believed to have undergone only the final stage of ore enrichment that formed the high grade hematite ore deposits. This model involves supergene alteration and leaching of primary BIF from shallow, low temperature, meteoric waters.

It is believed that martite-goethite ores were developed during the Phanerozoic, possibly during the Cretaceous. They are extensive and flat-lying deposits that typically follow the present land surface. Though they do not form large ore deposits such as at Mount Tom Price and Mount Whaleback, they are much more numerous in the Hamersley Province and includes deposits such as Section 6 and Section 7 deposits at Tom Price mine, Brockman No 2 deposit, Nammuldi deposit, Eastern Ranges deposits at Paraburdoo, Marandoo deposit, and West Angelas Deposit A. Martite-goethite ores commonly occur in both the Brockman Iron Formation and the Marra Mamba Iron Formation.

In martite-goethite ores the original hematite in the Primary BIF typically remains unaffected while the magnetite has oxidised to mainly martite and some goethite (refer to figure 2.5). Iron silicates and carbonates have been oxidised and hydrated to goethite and other carbonates and silica is replaced by goethite or leached. This results in thinning of the BIF sequence and a high phosphorus content in the final ore product.

2.3.6 PHOSPHORUS IN IRON ORE

The phosphorus content in iron ore is important to the iron industry as a high phosphorus content in ore creates a more brittle and less desired final steel product, therefore, low phosphorus iron ore has a higher value than high phosphorus iron ore. Phosphorus is present in primary BIF almost entirely as apatite, however, during iron enrichment it is present in association with goethite and to a lesser extent, hematite (Harmsworth et al., 1990). Taylor et al. (2001) explains that as primary BIF is altered and enriched in iron, phosphorus increases. However, with further alteration to high grade hematite iron ore, there is a significant fall in phosphorus. This suggests that apatite has broken down in the high grade ore, possibly

transferring out of the system and into other areas such as the hydrated zones, leaving a more desirable low phosphorus iron ore.

2.3.7 VOLUME CHANGES

The difference in volume from primary BIF to iron ore is significant. This phenomenon was recorded at Mount Tom Price and Paraburdoo in the early 1970s. Harmsworth et al. (1990) recorded a 52% reduction in thickness between mineralised ore and primary BIF in the Dales Gorge Member at Mount Whaleback. Porosity also increases with ore genesis creating a highly permeable orebody, allowing a greater fluid flow in these areas.

2.3.8 RECENT WEATHERING

Recent weathering from climatic factors reaches depths of over 100 meters in the Hamersley Province and is characterised by vughs in both BIF and shale bands. Recent studies have shown that under the detrital top surface in the Hamersley Province, the vertical profile can be divided into five zones (Figure 2.6).

A hard crust-like layer that is common on the surface in the Hamersley Province is known as the 'hardcap' layer. The hardcap layer is an intense zone of weathering at the surface consisting of abundant pores, or 'vughs', and brown or virtuous goethite. This zone contains high levels of silica and aluminium (Clout, 2006). In this layer, hematite and goethite are dissolved by surface waters and re-precipitated further down the profile.

Under the hardcap layer is the hydrated zone. In this zone, hematite is hydrated to goethite. Secondary goethite also fills pores and cavities in this zone. The hydrated zone is less porous and contains more goethite then the ore zone.

Horizontal dehydrated zones can be found within the hydrated zones, often above impermeable structures such as shale bands and faults. These zones are characterised by goethite dehydrated to hematite but retaining the goethite structure. These zones can also have high manganese content.

ZONE	MICROPLATY HEMATITE	MARTITE-GOETHITE
Detrital		
Hardcap	Vitreous Goethite-Microplaty Hematite	Vitreous Goethite-Martite
	Goethite-Microplaty Hematite	Goethite-Martite
Dehydrated	Hematite-Goethite	Hematite-Goethite
Hydrated	Goethite-Microplaty Hematite	Goethite-Martite
Ore	Micorplaty Hematite	Martite-Goethite
Unmineralised	BIF	BIF

FIGURE 2.6 VERTICAL ZONATION PROFILE OF ORE MINERALS IN THE HAMERSLEY PROVINCE (MODIFIED FROM CLOUT, 2006)

2.4 STRUCTURAL GEOLOGY OF THE HAMERSLEY PROVINCE

2.4.1 OVERVIEW

The structural history of the Hamersley Province comprises four major compression events generating folding in the province, and three major extensional events and several minor extensional events in between the compressional episodes, causing normal faulting in the Province. A clear spatial relationship can be seen between the high grade mineralisation in the Hamersley Province and normal basement faults, especially those which link the Wittenoom Formation with the BIF formations, and is therefore important in understanding the genesis of such deposits and in the exploration of iron ore. The structural history of the Hamersley Province is discussed below and a tectonostratigraphic column (developed by Dalstra, 2006) is shown in Figure 2.7.

2.4.2 COMPRESSION EVENTS

Four compression events, creating characteristic fold structures, are recognised in the Hamersley Province (refer to Figure 2.7). The first compressional event (F1) occurred during the deposition of the Hamersley Group creating recumbent isoclinal folds and podding. It is interpreted as being caused by vertical loading and deformation of the sedimentary unconsolidated rocks (Dalstra, 2006). The Ophthalmia orogeny (F2) occurred after deposition of the Turee Creek Group but before deposition of the Wyloo Group (Tyler & Thorne, 1990).

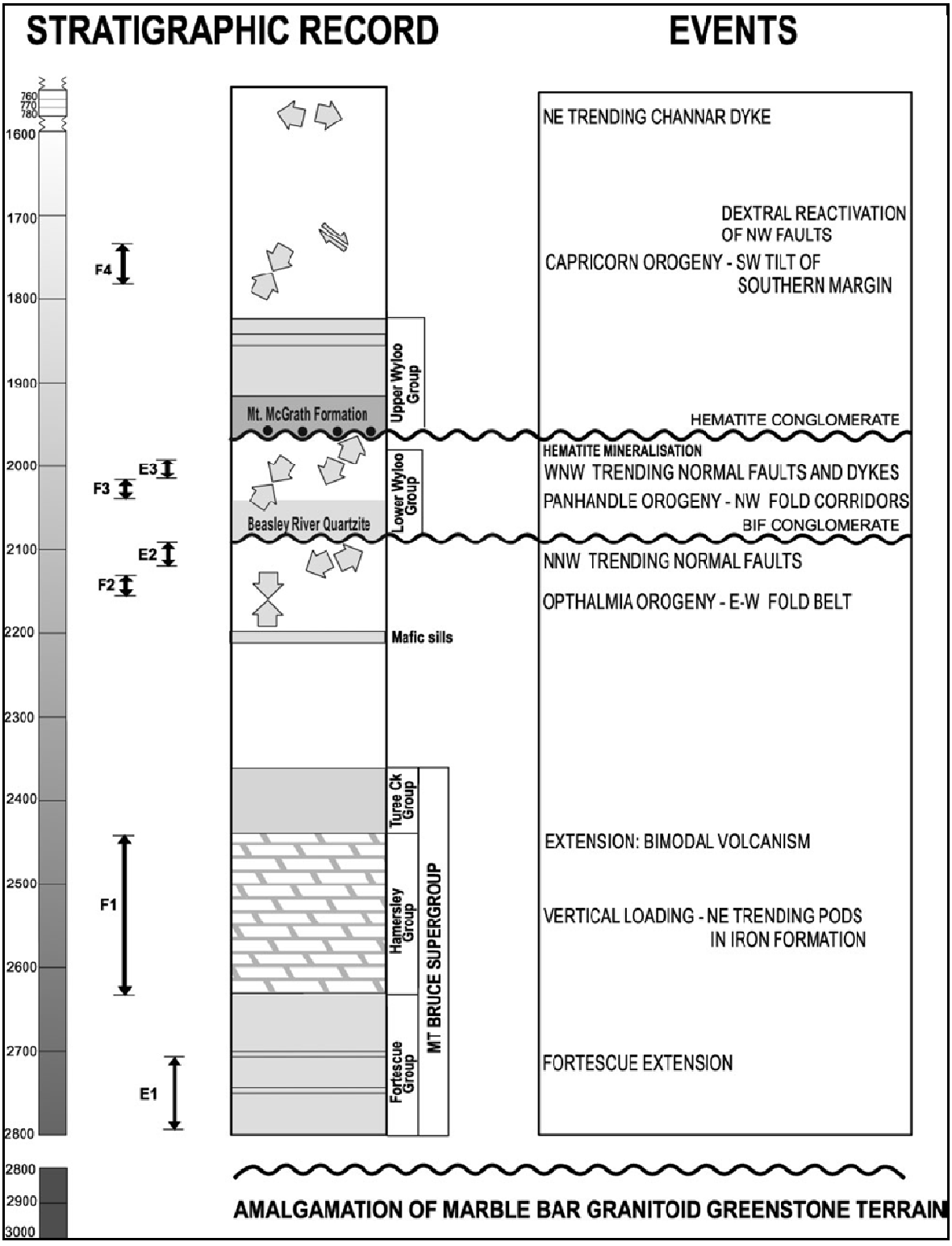

FIGURE 2.7 TECTONOSTATIGRAPHIC COLUMN OF THE HAMERSLEY PROVINCE (FROM DALSTRA, 2006). FOUR REGIONAL FOLDING EVENTS ARE RECOGNISED (F1 TO F4) AND THREE EXTENSIONAL EVENTS (E1 TO E3)

Dating of rocks in the Hamersley Province has put an estimate of the age of the Ophthalmia orogeny at between 2,208 and 2,031 Ma (Muller, Krape, Barley, & Fletcher, 2005). In the southwest of the province, the Ophthalmia orogeny created large dome and basin structures with a NW trend and short, tight, east trending folds were created in the southeast of the province (Tyler and Thorne, 1990). The Panhandle orogeny (F3) preceded the deposition of the upper Wyloo Group (Taylor et al., 2001) and is estimated, from dating of rock in the area, to have occurred between 2,031 and 2,008 Ma (Muller et al., 2005). The Panhandle orogeny created NW trending fold corridors, especially around the Tom Price area. The Capricorn orogeny (F4) occurred after the deposition of the upper Wyloo Group and has a maximum age of around 1,786 Ma (Krapez & McNaughton, 1999) and a minimum age of 1,680 Ma (Krapez, 1999). During the Capricorn orogeny, the southern margin of the Hamersley Province was tilted followed later by reactivation of steep faults at about 1,740 Ma (Dalstra, 2006).

2.4.3 EXTENSION EVENTS

Three major extensional events creating characteristic normal faults are recognised in the Hamersley Province. The first extensional event, the Fortescue extension (E1), took place during the deposition of the Fortescue Group which is believed to have been deposited during continental rifting at about 2,700 Ma (Eriksson, et al., 2002). The Second major extensional event (E2) took place after the Ophthalmia orogeny and before the deposition of the Beasley River Quartzite deposit and is believed to have been formed around 2,100 Ma (Muller et al., 2005). NNW striking step normal faults with offsets of up to 1,100 m (Dalstra, 2006) was formed during this time and is interpreted to have formed scarps due to the varying thicknesses of the conglomerate at the base of the Beasley River deposit. The third major extensional event (E3) took place after the Panhandle orogeny and before the deposition of the Mount McGrath Formation. This event created steep NW striking normal faults with offsets as large as 2,100 m (Dalstra, 2006) and reactivation of E2 faults creating a horst and graben system along the southern margin of the Hamersley Province. Also, NW trending dolerite dykes were preferentially intruded along these faults toward the end of this event, dated at around 2,008 Ma (Muller et al., 2005).

2.4.4 STRUCTURAL CONTROLS ON MINERALISATION

Folding at RTIO mines ranges from little or no folding to intense folding and is not believed to have an effect upon ore genesis. There is, however, a clear spatial relationship between extensional mid-sized normal faults in the Hamersley Province and high grade hematite ore deposits indicating that these faults most likely influence this type of ore formation. There is a clear relationship of high grade hematite ore at Tom Price mine and the Southern Batter fault that intersects the orebody. At Paraburdoo, high grade hematite ore is associated with reactivated ENE dipping normal faults (Dalstra, 2006), specifically to the 18E fault at 4E and 4W deposits (Dalstra, 1997). Faulting associated with high grade mineralisation at Mount Whaleback is less obvious. Recently, Webb et al. (2004 and 2006) has found Mount McRae shale beneath the Mount Whaleback orebody, and close to Mount Whaleback fault, to have been affected by carbonate mineralisation indicating a possible hypogene origin for the high grade ore deposit.

It also appears that faults linking the Wittenoom Formation to the high grade hematite ore bodies, in Tom Price style ore deposits, may be the cause of the mineralisation with the Wittenoom Formation supplying the initial carbonate hypogene fluids. A decollement fault on the top layer of the Wittenoom Formation has been suggested (Hagan, 1996; and Dalstra, 1996) to be connected to these mineralising faults. On top of this detachment fault the bedding is folded. Below, it has been suggested that the Wittenoom Formation has instead been shortened by pressure solution and cleavage formation with a shortening of approximately 18% (Dalstra, 1996).

A structural study of Section 6 deposit, a martite-goethite ore deposit, at Mount Tom Price has shown that Section 6 formed in a basin depression, surrounded by F1 and F3 folds (Behn, 1994). This ore deposit has been interpreted to have formed by supergene processes after the folding occurred, and so it appears that the supergene processes were focused into these basin depressions.

2.5 CLIMATE AND HYDROGEOLOGY OF THE HAMERSLEY PROVINCE

The Hamersley Province is classified as desert to grasslands where climate ranges from hot all year round to hot with dry summers (October to April) and mild winters (May to September) (BOM, 2005). The annual rainfall is low (<350 mm) making the province an arid to semi-arid region. Rainfall generally occurs in the winter or during periodic summer cyclones.

During the summer, maximum temperatures reach over 40^{o}C and rainfall ranges from 0 to 200 mm per month depending on summer cyclones. Winter brings temperatures down to less than 10^{o}C and up to around 27^{o}C during the day. Winter rainfall ranges from 5 to 50 mm per month.

The hydrology of the Pilbara is mainly provided from the summer cyclones that reach the area. These have created a series of rivers and creeks, many of these seasonal as evaporation is high with values commonly higher than 3000 mm per year, much more than the annual rainfall (Johnson & Wright, 2001).

The Hamersley Province is an elevated region that has a complex drainage pattern characterised by periodic river flow and occasional flooding events depending on rainfall. Modern drainage systems have formed many gorges throughout the Hamersley Ranges. Alluvial and colluvial valleys fill the areas between the ranges and the hills.

Groundwater occurs from rainfall discharge and runoff into basement rock outcrops. The main aquifers fall into three groups (Johnson and Wright, 2001): unconsolidated sedimentary aquifers in alluvium and colluvium; chemically deposited aquifers in calcrete and pisolite; and fractured rock aquifers, which can form major or local aquifers, in fractured BIF, dolomite and sandstone.

Mining has the potential to contaminate regional water resources such as through acid mine drainage and from the long term impact of mine voids creating a potential hypersaline solution. Understanding the demand for water, ecological water requirements and the impact of development on groundwater systems are important to the future of the Hamersley Province.

2.6 LAND-USE OF THE HAMERSLEY PROVINCE

The population of the entire 500,000 km^2 Pilbara Region is less than 40,000. Most people live in towns including Port Hedland, Karratha, Newman, Tom Price and Marble Bar. Currently, there are four aboriginal settlements in the region with a total population of 240 (Dames & Moore, 2000). Most of the economy is supplied by mining, especially iron ore mining in the Hamersley Province which is transported by rail to Port Hedland, Port Lambert or Dampier where it is shipped overseas for production. Other mining is also common in the Pilbara. Gold is mined at Marble Bar and there are many oil and gas rigs off the coast of the Pilbara. Farming is also an important aspect to the Pilbara with much of the Pilbara being utilised for pastural activities. Tourism is also present, especially at the national parks such as the Karijini National Park in the Hamersley Province where natural gorges provide beautiful scenery, swimming holes, tramping and camping areas for tourists (Figure 2.8).

FIGURE 2.8 WATERFALL AT HAMERSLEY GORGE, KARIJINI NATIONAL PARK

3 ROCK MASS CLASSIFICATION SYSTEMS

3.1 OVERVIEW

Rock mass character describes how rocks behave *en masse*. This then determines how whole slopes behave and can, therefore, be used in determining slope stability in areas such as natural slopes, road cuttings and open pit mines. Rock mass character can be defined by using rock mass classification schemes. There are many rock mass classification schemes that have been defined and re-defined in the literature, the most popular being the Modified Tunnelling Quality Index (hereafter called the Q-system) and the Rock Mass Rating system (RMR). The Slope Mass Rating (SMR) system is a variation of the RMR classification and has been chosen to be used in this study as it has been improved for defining slope stability. The first half of this chapter provides an overview of slope stability in open pit mining. The second half of this chapter provides an overview of rock mass classification techniques, describing in greater detail RMR and SMR classification techniques.

3.2 SLOPE STABILITY IN OPEN PIT MINING

3.2.1 INTRODUCTION

Open pit mining involves the removal of ore as the pit walls are formed, stepping down from the ground surface with each bench that is mined. Slope angle, height and berm width of the open pit walls are determined by a number of factors including geomechanical characteristics of the rock being mined but is ultimately determined by economic need. Economic justification is determined by stripping ratio which is the ratio of waste rock that is removed (or “stripped”) to the ore that can be mined. Slope angle and berm width are steepened and shortened respectively to optimise this ratio, however, possible slope instability issues requires flattening this slope angle to ensure slope stability so that ore can continue to be mined and the open pit mine can continue to operate safely.

Many parameters affect the slope stability in open pit mines. These include (Stacey, 1993):

- Intact rock strength and defect strength
- Geological structure
- Rock stresses and groundwater conditions
- Pit geometry
- Vibrations (due to blasting or seismic activity)
- Climate
- Time

3.2.2 ROCK MASS STRENGTH

Determining the strength of a rock mass is difficult because of its inherent uncertainty and variability throughout the rock mass but rock mass strength ultimately determines whether a rock mass is likely to fail or not. The strength of the rock mass is determined by three main factors including intact rock strength, strength of the rock masses discontinuities and confining stress.

Intact rock strength is relatively easy to determine in the laboratory such as by the use of Uniaxial Compressive Strength (UCS) testing or triaxial testing. In the field, it is generally estimated from field descriptions (such as is used in RMR and SMR as discussed in Section 4.4.1) or determined using index testing such as point load testing or the Schmidt Hammer rebound test. Pure uniaxial compressive strength is rare in slope situations and tensile strength for large scale rock masses is very small and can usually be assumed to be negligible. Shear strength, on the other hand, is much more important for rock masses, especially along discontinuities.

For a planar discontinuity, the Mohr-Coulomb shear strength criteria states:

$$T = C + \Sigma_N \tan\Phi \qquad (3.1)$$

where τ is peak shear strength, σ_n is effective normal stress, C is cohesion and ϕ is friction angle of the discontinuity. Cohesion can also represent fracturing through intact rock as well as cohesion along the defect.

Barton and Bandis (1990) developed an empirical shear failure criterion which includes roughness of the rock mass to better illustrate shear strength within discontinuities which states:

$$\mathbf{T_F = \Sigma_N \, TAN[JRC \, LOG_{10} \, (JCS/ \, \Sigma_N) + \Phi_B} \qquad \mathbf{(3.2)}$$

where τ_f is the shear strength along the contact at surface, JRC is 'joint roughness coefficient', JCS is 'joint wall compressive strength' and ϕ_b is basic friction angle. The determination of JCS, however, is difficult and quantifying the roughness of a discontinuity surface remains a major problem when assessing shear strength.

Barton and Choubey (1977) revised this equation from the study of direct shear tests, to:

$$\mathbf{T_F = \Sigma_N \, TAN[JRC \, LOG_{10} \, (JCS/ \, \Sigma_N) + \Phi_R} \qquad \mathbf{(3.3)}$$

where ϕ_r is the residual friction angle which can be estimated from:

$$\mathbf{\Phi_R = (\Phi_B - 20) + 20 \, (R/R)} \qquad \mathbf{(3.4)}$$

where r is the Schmidt Hammer rebound number of wet and weathered surfaces and R is the Schmidt Hammer rebound number of dry, unweathered and even surfaces.

The Hoek-Brown failure criterion is a simple equation to determine the actual mechanisms of failure within a rock mass. The Hoek-Brown criterion states:

$$\mathbf{\Sigma_1 = \Sigma_3 + M \, \Sigma_C \, \Sigma_3 + S \, \Sigma_C^2} \qquad \mathbf{(3.5)}$$

where σ_1 and σ_3 are the major and minor stress axes, respectively, σ_c is Uniaxial Compressive Strength and m and s are the rock type and shape factors.

However, the equation (3.1) is generally used as it accurately calculates shear strength in low stress conditions such as near the surface where normal stress is 0 to 2 MPa.

Confining stress is also an important attribute to rock mass strength. Vertical stress (σ_v) can be calculated from:

$$\Sigma_V = \Gamma Z \qquad (3.6)$$

where γ is the unit weight of overlying rock and z is the depth below the surface.

Horizontal confining stress is harder to estimate and, normally, the ratio of average horizontal stress (σ_h) to vertical stress is represented by k where:

$$\Sigma_H = K \Sigma_V = K \Gamma Z \qquad (3.7)$$

Measurements of horizontal stress around the world show that k tends to decrease with depth. Sheorey (1994) developed a model of the elasto-static thermal stress of earth and provided an equation to estimate k, where z is measured in meters and E_h is the average deformation modulus of the upper part of the earth's crust in the horizontal direction and is measured in GPa, where:

$$K = 0.25 + 7 E_H (0.001 + 1/Z) \qquad (3.8)$$

Due to the complicated nature of confining stresses and the effect on underground mining activities, it has been suggested that where confining stress is important to stability (such as in underground mining), the confining pressures should be measured on site (Hoek, 2007).

3.2.3 STRUCTURE

Investigating the geological structure of the rock mass is important in determining the main discontinuities of a rock mass and, hence, in determining the overall strength of the rock mass and the likely failure mechanisms.

Geological structure includes rock type and discontinuities. Geological discontinuities that effect slope stability in the RTIO open pit mines include bedding planes and faults and on a smaller scale, joints. The most problematic of discontinuities of this area are the bedding planes, which generally dip into the pits and are weakest where shale bands are located and/or alteration has taken place.

The geometry and orientation of the discontinuities are very important when dealing with the stability of a slope. The discontinuity surface is generally assumed to be planer or a combination of planes and is otherwise poorly understood. Geological structures are generally mapped in order to better understand the potential problem areas. Scanline mapping or window mapping are the two most used mapping technique for this purpose. The rock mass is generally divided into structural domains that are assumed to behave uniformly.

The most effective technique for studying the geological structure's effect on slope stability includes dealing with the structures through likely failure modes. This includes looking at the orientation of the structures to determine the likely (if any) failure mode. Failure modes are further discussed in Section 3.2.9.

3.2.4 STRESS CONDITIONS

When dealing with slope stability, stresses within the rock masses need to be addressed. There are three major stresses that influence an undisturbed rock mass:

- Gravitational stress (from weight of overlying rock)
- Tectonic stress
- Residual stress

As the rock mass is excavated, the stresses change and redistribute throughout the rock mass. Typically in an open pit mine stress increases at the toe of the slope and decreases towards the crest. The consequence is possible stress induced failures at the slope toe and/or tensile failure at the crest. It is likely that stress is also concentrated at discontinuities within the rock mass and can again cause possible instability issues as the stress changes with excavation along these planes of weaknesses.

3.2.5 DISCONTINUITY ORIENTATION

Orientation of discontinuities to load direction is another important factor to rock mass strength. Failure is more likely when discontinuities are oriented in directions that favour slip. Greater understanding about orientations and their affect on failure is discussed in Section 3.2.9.

3.2.6 GROUNDWATER

Groundwater conditions highly affect the stress state of slopes. Water pressures reduce the effective stress of a permeable rock mass. This leads to a reduction of shear strength on the failure surface. The presence of water can also reduce the intact rock strength of certain rock types and can also potentially cause erosion within the rock mass.

Groundwater is generally only applicable below the water table and for this reason does not affect many of the areas classified in this study. However, many areas in the RTIO mines do mine below the water table at times and it is important to understand that in the presence of water pressure, the stability of the slopes has the potential to decrease dramatically. It is, therefore, an important factor to include when dealing with slope stability conditions and an important mitigation factor in these cases is to drain the water from the slope.

3.2.7 VIBRATIONS

Excavation involving vibrations from blasting has the ability to damage lesser strength rock masses. Such circumstances mean that understanding the stability of the remaining wall rock is much more difficult. It is for this reason that knowledge of excavation methods should be included in classifications when predicting slope stability.

It is generally recognised that the blasting vibrations decrease with distance from the explosive charge and, therefore, blast damage can be expected to decrease with depth and slope surfaces can be expected to contain the majority of the blast damage. Blasting is well known to cause back-break and damage along a slope face which can cause a decrease of the slope angle. Such damage is less important to large slope instability issues. However, it is likely that blasting without precautionary controls can concentrate damage into already weak zones such as structural defects. At RTIO mines, the blast damage can concentrate into the shale bands creating internal structural damage of these zones and a possible weakening of the already weak defect. Smooth blasting is a method that has been developed to counter these effects and involves simultaneous detonation of a row of lightly charged holes to create a clean surface between the final wall rock and rock yet to be blasted to reduce blast damage in the remaining wall.

Vibrations caused by seismic events also have the ability to induce slope failures. These have the potential to cause very large scale slope failures.

3.2.8 SCALE

Increasing scale of rock masses decreases the strength of the rock mass as shown in Figure 3.1. As scale increases, the discontinuity sets in the rock mass becomes more important to the strength of the rock mass. At a small scale, such as at laboratory specimen scale, the rock mass strength may solely be effected by the intact strength of the rock material while at a large volume the joint sets may appear close and numerous and, therefore, the rock mass can be treated as a homogenous, closely jointed material. Roughness also seems to be dependent on scale with roughness having a decreasing effect on the rock mass strength as the scale increases. The basic friction angle, however, does not change with scale.

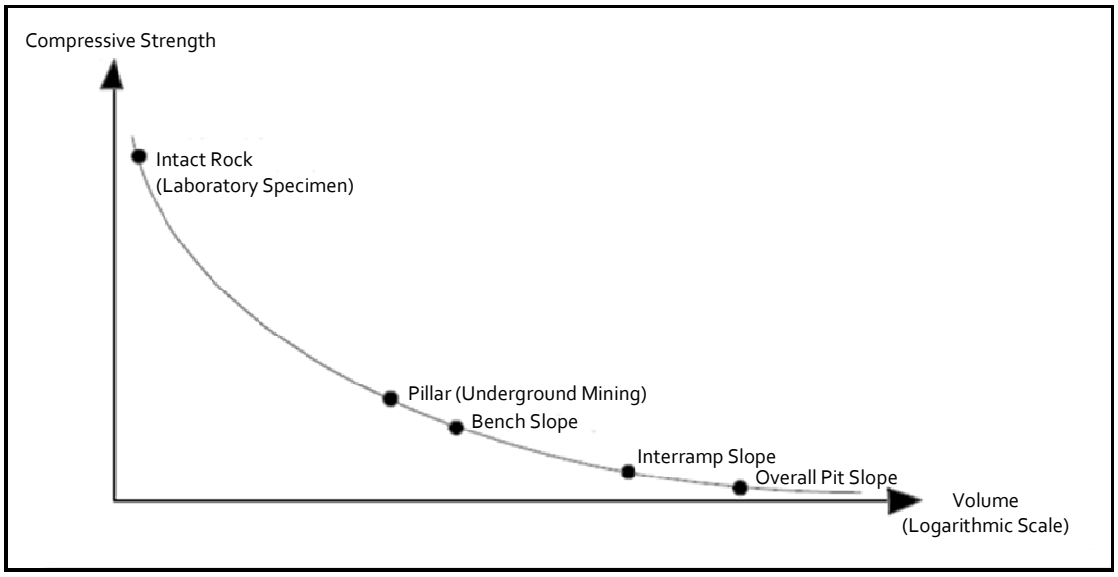

FIGURE 3.1 RELATIONSHIP BETWEEN ROCK MASS STRENGTH AND SCALE OF THE ROCK MASS (SJOBERG, 1996)

Determining the overall strength of a large scale rock mass remains difficult, with few detailed case studies on large scale slope strengths available. The most common approach to this problem include rock mass classification (as described below), large scale testing, mathematical modelling and back analysis of failures (Krauland et al., 1986).

Back analysis is a useful method at determining rock mass strength of failed material. It requires the assessment of failure conditions such as geometry of the failure, groundwater conditions,

and other contributing factors to assess the conditions at failure. It assumes limit equilibrium where driving forces causing failure are equal to resisting forces limiting failure. However, it requires failure to have taken place and for factors affecting the failure mechanisms to be able to be measured.

Large scale testing is a much more difficult method requiring hydraulic jacks and is rarely an economic or practical solution.

Mathematical modelling is very useful but not always a practical field instrument especially when dealing with complex slope environments.

Rock mass classification, on the other hand, is a very useful and practical technique and is discussed in much more detail below. Although it can over-simplify the problem, when used alongside the Hoek-Brown failure criterion, it is especially useful at assigning failure classes and giving practical engineering advice.

3.2.9 ROCK MASS FAILURE MODES

The failure mode of a rock mass depends on the rock mass geomechanical characteristics and the orientation of defects to the slope orientation. There are three main failure modes that are well known to appear in slopes. These are planar failure, circular failure and block flow (Coates, 1965).

Planar failure is by far the most common failure mode that occurs in the RTIO mines. Planar failure includes rock slopes that have failed on discontinuities and form blocks which are kinematically free to move. The failure surface can be formed by a single defect or by several connecting defects and/or releasing planes (refer to Figure 3.2, Figure 3.3 and Figure 3.4).

There are two main types of planar failure; simple planar failure and wedge failure. The major elements of simple planar failure are shown in Figure 3.2. It forms along a single defect dipping down slope into a daylighting surface which forms a shear plane. A releasing plane at the back of the slope is also often required. The major elements of wedge failure are shown in Figure 3.6. It is formed by two intersecting planes where the intersection plunges down slope into a daylighting surface.

In the RTIO mines, it is common for a bedding plane, especially along a shale bed, to create discontinuity surface along which simple planar failure can occur. These generally do not from larger than bench scale failures. However, they have the potential to form bigger failures.

Circular failure occurs in soils and heavily fractured rock masses along both discontinuities and intact rock (Figure 3.5). It does not rely on the orientation of discontinuities within the rock mass but rather on the strength of the rock and the conditions of the discontinuities. It can combine with planar failure and has the ability to affect very large slopes in open pit mines when stress regimes change, such as due to unloading of the toe, loading of the crest and water infiltration.

Other, smaller scale failure modes include block flow. Block flow includes failures caused by the successive breakdown of slopes. An example of this type of failure mode is toppling (Figure 3.6). Toppling occurs when defects dip steeply back into the rock face. Toppling failure is not a major concern in RTIO mines but block flow caused by joints and bedding planes creating small to medium scale blocks can cause rock fall hazards.

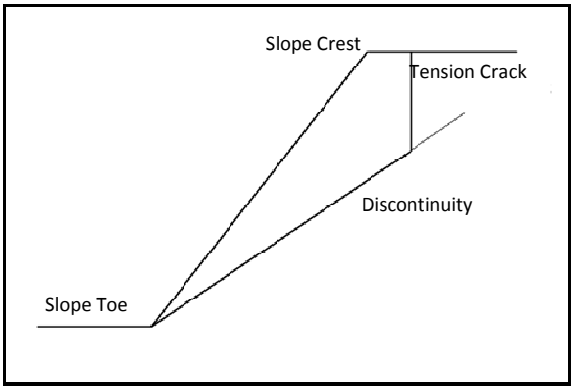

FIGURE 3.2 SIMPLE PLANAR FAILURE (SJOBERG, 1996)

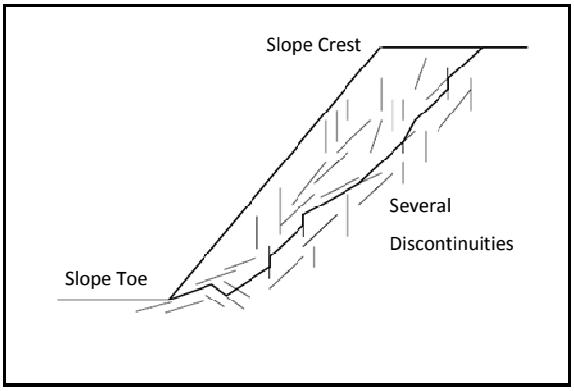

FIGURE 3.3 STEPPED PLANAR FAILURE (SJOBERG, 1996)

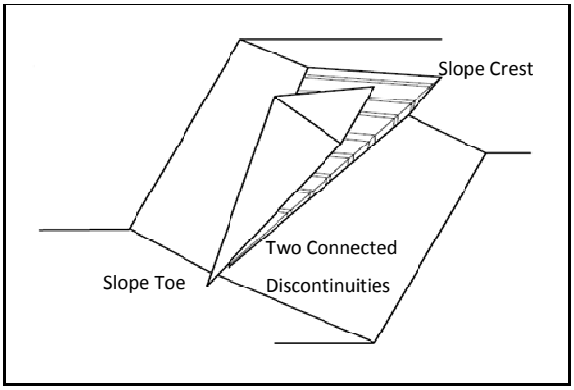

FIGURE 3.4 WEDGE PLANAR FAILURE (SJOBERG, 1996)

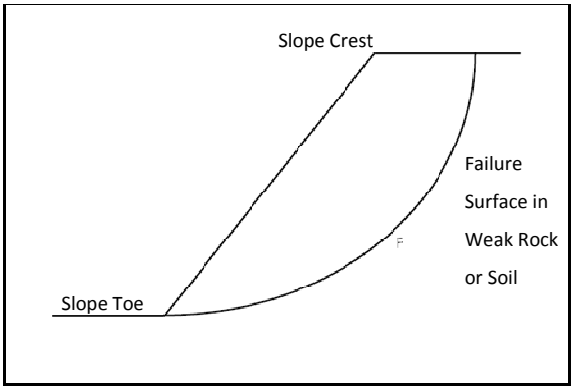

FIGURE 3.5 CIRCULAR FAILURE (SJOBERG, 1996)

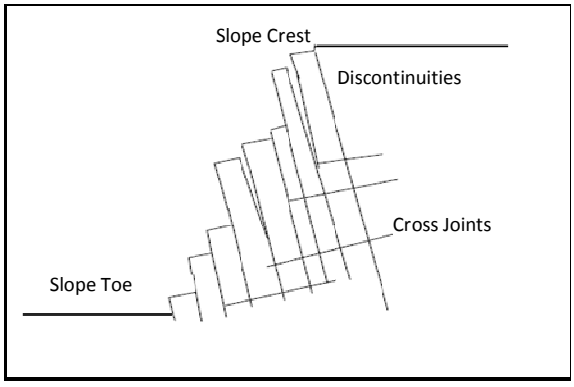

FIGURE 3.6 TOPPLING FAILURE (SJOBERG, 1996)

3.2.10 FACTOR OF SAFETY

The Factor of Safety (FoS) is generally used to determine the likelihood of failure in a wide variety of engineering applications and is based on calculating the resisting forces and the driving forces of a possible failure. It is defined by:

$$\mathbf{FOS = C_0 + \Sigma_N (TAN\Phi) / T \qquad (3.9)}$$

where c_0 is cohesion, σ_n is normal stress, τ is shear stress and ϕ is the friction angle. A FoS of 1 indicates marginal stability. Usually a FoS of ≥1.5 indicates remediation is necessary. In applications with no cohesion, the size of the block of rock becomes irrelevant to the driving force of failure and the FoS can be determined from the friction angle and the orientation of the effective weight vector as defined by:

$$\mathbf{FOS = TAN\ \Phi / TAN\ H \quad (3.10)}$$

where η is the angle between the effective weight vector and the pole to the slide plane. When the weight vector point lies within a friction cone on a stereonet, it will be stable and $\eta < \phi$, and when the weight vector point lies outside the friction cone it will be unstable and $\eta > \phi$.

3.2.11 SUMMARY

Rock mass strength is affected by intact rock strength, the shear strength of rock mass discontinuities and confining stresses. However, rock mass stability is also influenced by many factors including the geological structures that make up the rock mass and by the presence of water within the slope.

All these factors come together in the rock mass classification technique, RMR, which uses the characterisation of rock mass strength parameters and contributing factors to estimate the stability of the slope and likely mitigation techniques that may be needed. It has been discussed here that blasting techniques causing vibrations into the rock mass and the orientation of the structural defects verses the slope orientation are also very important factors in determining the overall rock mass behaviour of open pit mines and therefore have been included here by the use of SMR, a rating technique that is derived from RMR to assess the particular circumstance of slope stability.

As discussed, rock mass classification is the most simple and effective technique in assessing slope stability. Although it is a very simplified field classification technique, it is practical and is able to be used on many different rock mass types and locations without the use of expensive equipment.

3.3 ROCK MASS CLASSIFICATION

3.3.1 INTRODUCTION

Rock mass classification is a tool used in civil and mining projects to characterise and understand the overall mechanical nature of the foundations being worked with so that its behaviour can be estimated and measured precautions can be undertaken. Rock mass classification is an empirical method, designed using case studies and, therefore, care must be taken when applying these methods to new situations.

According to Bieniawski (1973), a rock mass classification should be general so that the same rock mass will be classified the same regardless of how it is being used. This is how RMR was established, with the aim of accurate but general rock mass classification, in order to bring together the conditions that define rock mass behaviour for the purpose of better understanding of the stability of rock masses and defining engineering techniques to mitigate a range of civil and mining situations.

This section will go on to give an overview of the beginnings that have defined the rock mass classification techniques used today and then discuss in detail RMR and SMR which were used in this study.

3.3.2 EARLY ROCK MASS CLASSIFICATION

Rock mass classification techniques firstly came from tunnelling applications with the aim of creating a method to determine the support requirements for specific rock masses. Today many classification systems are used and have been modified for more specific purposes.

Terzaghi (1946) published “Rock Defects and Loads on Tunnel Supports” which uses a descriptive classification scheme to estimate rock loads in tunnels with steel support. Terzaghi divided rock masses into: hard and intact rock, hard stratified rock, massive and moderately

jointed rock, blocky and seamy rock, crushed rock, squeezed rock at moderate depth, squeezed rock at great depth and swelling rock; each with its own description to estimate support needed. This is the earliest rock mass classification technique that is still in use today.

Lauffe (1958) published a classification system that uses the stand up time of an unsupported rock mass within a tunnel to describe the rock mass quality. This classification system has been modified many times since but it was modified by Packer, Rabcewicz and Golser (1974) and incorporated into the New Austrian Tunnelling Method (NATM). The NATM is an extensive method of supporting tunnels that is widely in use today.

In 1967, the Rock Quality Designation (RQD) index was first published (Deere et al., 1967). It uses the percentage of core recovery and the geologist's descriptions to describe the rock mass quality. The procedure for measuring RQD is shown in Figure 3.7. RQD has also been related back to Terzaghi's rock load classification and to support requirements in tunnels. RQD is defined as the percentage of intact rock core that is longer than 10 cm. Palmstrom (1982) suggested that RQD could be estimated at outcrop by estimating the number of joints in clay-free rock. Palmstrom uses the equation:

$$\mathbf{RQD = 115 - 3.3\ J_V} \qquad \mathbf{(3.11)}$$

where J_v is equal to the total number of joints per cubic meter. Today the RQD system is still widely used but it is seldom used alone and is commonly used within other rock mass classification techniques such as RMR and the Q-system.

Wickham, Tiedemann and Skinner (1972) proposed Rock Structure Rating (RSR). RSR is a quantitative system that employs several parameters to describe the rock mass quality and to estimate rock mass support. Importantly, RSR introduced the rating system that went on to be used by many other important rock mass classification techniques. The rating system uses the sum of the weighted values for each parameter to come up with an overall value which describes the rock quality. The weighted values mean that the amount that each parameter is included depends on that parameter's importance to the overall rock mass quality. RSR uses geology, structure, condition and orientation of defects and groundwater effects to determine

the overall rock mass conditions. RSR is not widely used today but marks the beginning of rock mass rating systems which are so important in rock mass classifications today.

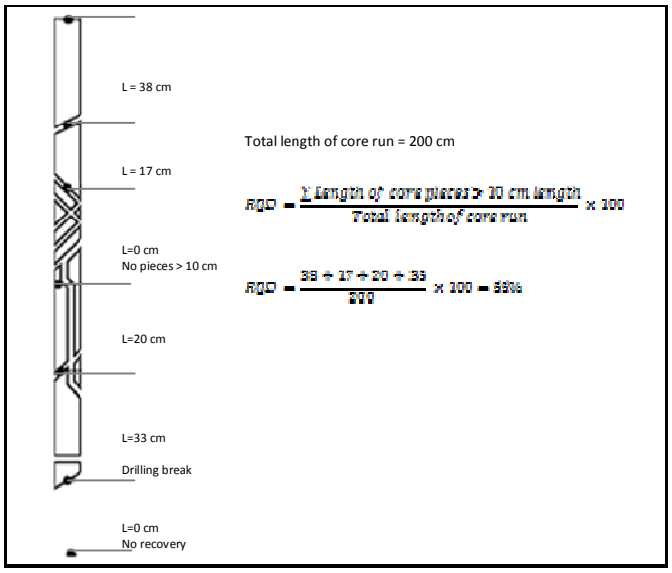

FIGURE 3.7 PROCEDURE FOR THE MEASUREMENT AND THE CALCULATION OF RQD (DEERE, 1989)

3.3.3 IMPORTANT ROCK MASS CLASSIFICATION SYSTEMS

There are many rock mass classification systems in use today, however, for more reliable and homogenous systems, just a few of these systems are commonly used; these include the RMR system and the Q-system. RMR is a system that can be used in many environments and has been modified many times for more specific uses including Geological Strength Index (GSI) and SMR. RMR and its modifications are discussed in detail below. The Q-system is a tunnelling application and, therefore, will only be discussed briefly here. More recent but promising classifications include the Rock Slope Deterioration Assessment (Nicholson & Hencher, 1997), the Slope Stability Probability Classification (Hack, Price, & Rengers, 2002) and the Volcanic Rock Face Safety Rating (Singh & Conolly, 2003).

The Q-system is an empirical rock mass classification system. It was proposed by Barton, Lien and Lunde (1974) for the application of tunnelling procedures. The Q index is defined from:

$$\mathbf{Q = RQD/J_N \ X \ J_R/J_A \ X \ J_W/SRF} \qquad \mathbf{(3.12)}$$

where J_n is the number of joint sets, J_r is the roughness of the most unfavourable joint set, J_a is the alteration along the most unfavourable joint set, J_w is the water inflow and SRF is the stress factor. Q produces a number on a logarithmic scale from 0.001 to 1 000 which describes the rock mass conditions and estimate the support requirements of the tunnel. Each proportion represents a different important factor defining the quality of the rock mass. RQD/J_n represents the block size of the rock mass, J_r/J_a represents the inter-block strength defined by the roughness and friction of the joint walls, and J_w/SRF represents the active stress on the rock mass. The classification of the individual parameters can be found in Table 3.1 and the support measures can be found in Figure 3.8.

A modified Tunnelling Quality Index (Q') (Barton et al., 1974) can be calculated from:

$$\mathbf{Q' = RQD/J_N \ X \ J_R/J_A} \qquad \mathbf{(3.13)}$$

This value of Q' can then be used to estimate GSI from (GSI is discussed in Section 3.3.5):

$$\mathbf{GSI = 9 \ LOG_E \ Q' + 44} \qquad \mathbf{(3.14)}$$

A correlation has also been determined between the Q-system and RMR. Bieniawski (1976) determined from a number a case studies from all over the world that RMR can be correlated to the Q-system by the equation:

$$\mathbf{RMR = 9 \ LN \ Q + 44} \qquad \mathbf{(3.15)}$$

Further correlations have also been made that show a similar relationship.

Description	Value	Notes
1. Rock Quality Designation	**RQD**	
A. Very Poor	0-25	1. Where RQD is reported or measured as ≤ 10 (including 0) a normal value of 10 is used to evaluate Q
B. Poor	25-50	
C. Fair	50-75	
D. Good	75-90	2. RQD intervals of 5, i.e. 100, 95, 90 etc, are sufficiently accurate
E. Excellent	90-100	
2. Joint Set Number	**J_n**	
A. Massive, no or few joints	0.5-1.0	
B. One joint set	2	
C. One joint set plus random	3	
D. Two joint sets	4	
E. Two joint sets plus random	6	
F. Three joint sets	9	1. For intersections use (3.0 x J_n)
G. Three joint sets plus random	12	
H. Four or more joint sets, random, heavily jointed, etc	15	2. For portals use (2.0 x J_n)
J. Crushed rock, earthlike	20	
3. Joint Roughness Number	**J_r**	
a. Rock Wall Contact		
b. Rock Wall Contact Before 10 cm Shear		
A. Discontinuous joints	4	
B. Rough and irregular, undulating	3	
C. Smooth undulating	2	
D. Slickensided undulating	1.5	1. Add 1.0 if the mean spacing of the relevant joint set is greater than 3 m
E. Rough or irregular, planar	1.5	
F. Smooth, planar	1	
G. Slickensided, planar	0.5	2. J_r = 0.5 can be used for planar, slickensided joints having lineations, provided that the lineations are oriented for minimum strength
c. No Rock Wall Contact When Sheared		
H. Zones containing clay minerals thick enough to prevent rock wall contact	1	
J. Sandy, gravely or crushed zone thick enough to prevent rock wall contact	1	
4. Joint Alteration Number	**J_a**	
a. Rock Wall Contact		Φ_r degress (approx.)
A. Tightly healed, hard, non-softening, impermeable filling	0.75	1. Values of Φ_r, the residual friction angle, are intended as an approx. guide to the mineralogical properties of the alteration products, if present
B. Unaltered joint walls, surface staining only	1	25-35
C. Slightly altered joint walls, non-softening mineral coatings, sandy particles, clay free disintegrated rock, etc	2	25-30
D. Slity-, sandy-clay coatings, small clay-fraction (non-softening)	3	20-25
E. Softening or low friction clay mineral coatings and small quantities of swelling clays	4	8-16
b. Rock Wall Contact Before 10 cm Shear		
F. Sandy particles, clay-free, disintegrating rock etc	4	25-30
G. Strongly over-consolidated, non softening clay mineral fillings (continuous <5 mm thick)	6	16-24
H. Medium or low over-consolidated, softening clay mineral fillings (continuous <5 mm thick)	8	12-16
J. Swelling clay fillings (continuous <5 mm) depending on percentage	8-12	6-12

TABLE 3.1 CLASSIFICATION OF INDIVIDUALS USED IN THE Q-SYSTEM (BARTON, LIEN, & LUNDE, 1974)

c. No Rock Wall Contact When Sheared				
K. Zones or bands of disintigrated or crushed	6			
L. Rock and clay	8			
M. Zones or bands of silty- or sandy-clay, small clay fraction, non softening	5			
N. Thick continuous zones or bands of clay	10-13			
5. Joint Water Reduction	**J_w**	Water Pressure (approx.) (kgf/cm^2)		
A. Dry excavation or minor inflow i.e. < 5 l/m locally	1	<1.0		
B. Medium inflow or pressure, occasional outwash of joint filling	0.66	1.0-2.5		
C. Large inflow or high pressure in competent rock with unfilled joints	0.5	2.5-10	1. Factors C to F are crude estimates; increase J_w if drainage installed	
D. Large inflow or high pressure	0.33	2.5-10		
E. Exeptionally high inflow or pressure at blasting, decaying with time	0.2-0.1	>10	2. Special problems caused by ice formation are not considered	
F. Exeptionally high inflow or pressure	0.1-0.05	>10		
6. Stress Reduction Factor	**SRF**			
a. Weakness zones intersecting excavation, which may cause loosening of rock mass when tunnel is excavated				
A. Multiple occurances of weakness zones containing clay or chemically disintegrated rock, very loose surrounding rock (any depth)	10	1. Reduce these values for SRF by 25 - 50% but only if the relevant shear zones influence do not intersect the excavation		
B. Single weakness zones containing clay, or chemically distegrated rock (Excavation <50 m)	5			
C. Single weakeness zones containing clay, or chemically disintegrated rock (Excavations >50 m)	2.5			
D. Multiple shear zones in competant rock (clay free), loose surrounding rock	7.5			
E. Single shear zone in competant rock (clay free) (depth of excavations >50 m)	5			
F. Single shear zones in competant rock (clay free) (depth of excavations >50 m)	2.5			
G. Loose open joints, heavily jointed	5			
b. Competant Rock, Rock Stress Problems		σ_c/σ_1	$\sigma_t\sigma_1$	2. For strongly anisotropic virgin stress field (if measured): when $5 \le \sigma_1/\sigma_3 \le 10$, reduce σ_c to $0.8\sigma_c$ and σ_t to $0.8\sigma_t$. When σ_1/σ_3 >10 reduce σ_c and σ_t to $0.6\sigma_c$ and $0.6\sigma_t$, where σ_c = unconfined compressive strength and σ_t = tensile strength (point load) and σ_1 and σ_3 are the major and minor principle stresses
H. Low stress, near surface	2.5	>200	>13	
J. Medium stress	1	200-10	13-0.66	
K. High stress, very tight structure (usually favourable to stability, maaybe unfavourable to wall stability)	0.5-2	10-4	0.66-0.33	
L. Mild rockburst (massive rock)	5-10	5-2.5	0.33-0.16	
M. Heavy rockburst (massive rock)	10-20	<2.5	<0.16	3. Few cases records available where depth of crown below surface is less than span width. Suggest SRF increase from 2.5 to 5 for such cases
c. Squeezing rock, plastic flow or incompetant rock under influence of high rock pressure				
N. Mild squeezing rock pressure	5-10			
O. Heavy squeezing rock pressure	10-20			
d. Swelling Rock, Chemical Swelling Activity Depending on Presence of Water				
P. Mild swelling rock pressure	5-10			
Q. Heavy swelling rock	10-15			

TABLE 3.1 CLASSIFICATION OF INDIVIDUALS USED IN THE Q-SYSTEM (BARTON, LIEN, & LUNDE, 1974) (CONTINUED)

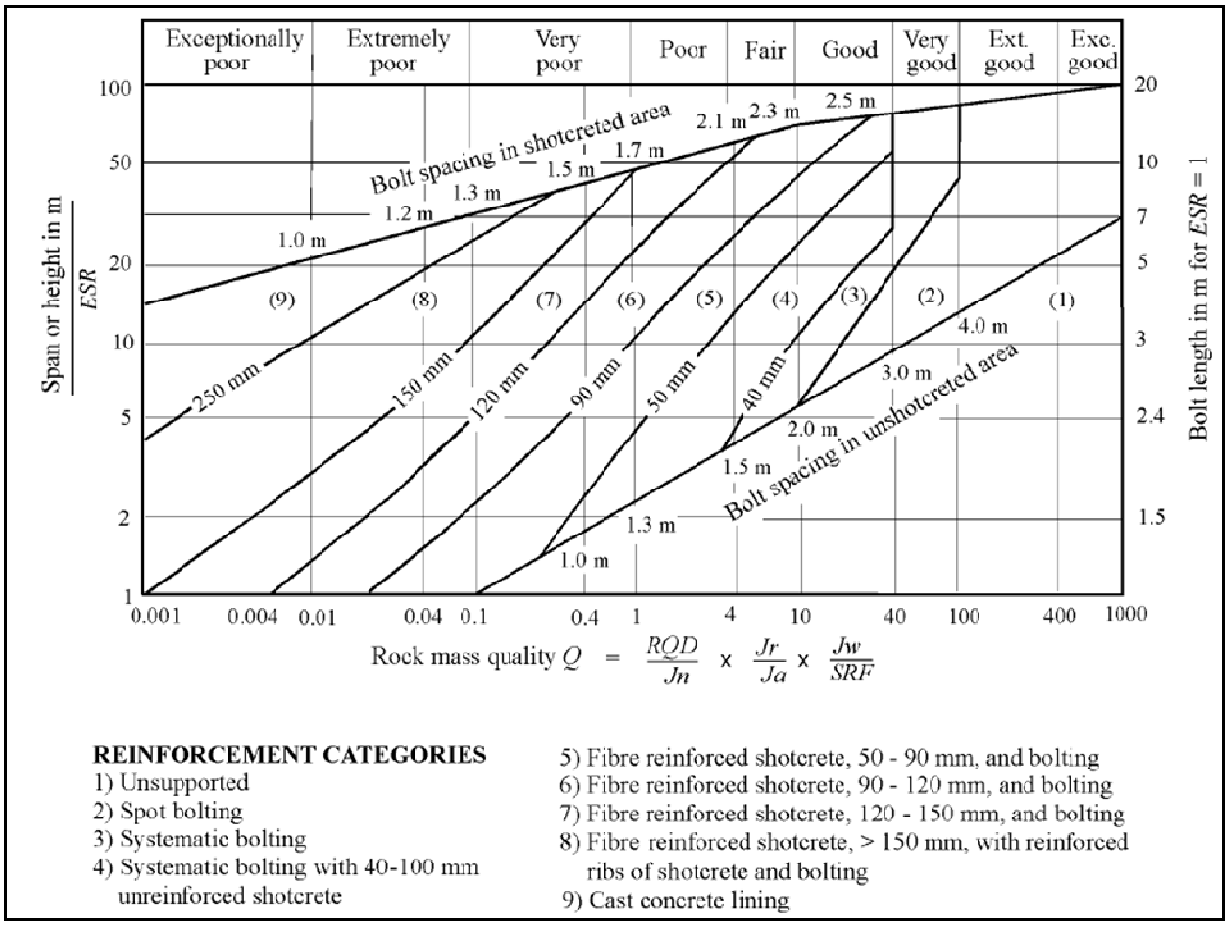

FIGURE 3.8 SUPPORT RECOMMENDATIONS FROM Q-SYSTEM (GRIMSTAD & BARTON, 1993)

3.3.4 ROCK MASS RATING

RMR (also known as the Geomechanics Classification System) is an empirical method of evaluating rock mass strength by investigating five separate rock mass parameters:

- Strength of intact rock
- RQD
- Spacing of discontinuities
- Condition of discontinuities
- Groundwater
- Orientation of discontinuity

Each parameter is assigned with a weighted rating depending on the relative influence each parameter has on overall rock mass stability (refer to Table 3.2 for the complete RMR_{89} chart developed by Bieniawski (1989)). RMR was initially published by Bieniawski in 1973 and has been subsequently modified (Bieniawski & Maschek, 1975 and Bieniawski, 1976 and 1989).

RMR was initially developed to test the stability and support required of underground excavations and has since been further developed and modified to test the strength of rock, the stability of underground tunnel openings, modified to increase the quality of stability prediction for weak and anisotropic rock masses and modified to better deal with the stability of slopes.

Firstly, it is necessary to divide the rock masses into domains of like rock masses with comparable structural properties. Each domain should be thought of as uniform and the properties of the domain should be averaged out and thought of as a whole rock mass. Each 'domain' or 'zone' is then appraised separately.

The RMR parameters are assessed separately using the field descriptions and entered into the field sheet (refer to Table 3.2). The parameters are separated into five ranges with a corresponding rating value for each range. Note that the ratings for the five ranges are different for each parameter. This is because each parameter is weighted so that the parameters that influence the rock mass more severely, have more influence on the overall rock mass rating. Higher ratings mean that the rock mass is in better condition and is, therefore, more stable. Note that RMR_{89} is used in this study to calculate SMR, however, the rating adjustment for joint orientation is neglected when calculating SMR as a new adjustment for discontinuity orientation is used (refer to Section 3.3.6). The adjustment for discontinuity orientation in SMR is favourable as it is quantitative rather than qualitative and is recommended for slopes over RMR_{89} (Bieniawski, 1989).

There are several charts to help determine the rating if one is unsure about which rating to give. These are shown in Figures 3.9, 3.10 and 3.11. These charts show that the ratings can deviate if conditions fall between the ranges given. Figure 3.12 can be used if either the RQD or the spacing of discontinuities data is missing. Using this chart, either the RQD or the discontinuity spacing can be estimated from the other. Laubscher (1977) also proposed that the

discontinuity spacing should reflect the number of joint sets in a rock mass since this otherwise gets ignored.

The five ratings are then added to give a basic RMR. RMR now has many case studies and has proven to be a simple to use formula that can be applied to many different situations such as tunnelling, underground mining, open pit mining, natural slopes, foundations and more. It can be determined by field mapping or borehole data and can be incorporated into many situations as is explained below. RMR was originally developed for civil projects and as a result does tend to be quite conservative for mining measures and can lead to overdesign. However, RMR is just one aspect of evaluating rock mass conditions and does not replace detailed mapping.

A. CLASSIFICATION PARAMETERS AND THEIR RATINGS										
Parameter			Range of values							
1	Strength of intact rock material	Point-load strength index	>10 MPa	4 - 10 MPa	2 - 4 MPa	1 - 2 MPa	For this low range - uniaxial compressive test is preferred		
		Uniaxial comp. strength	>250 MPa	100 - 250 MPa	50 - 100 MPa	25 - 50 MPa	5 - 25 MPa	1 - 5 MPa	< 1 MPa
	Rating		15	12	7	4	2	1	0
2	Drill core Quality *RQD*		90% - 100%	75% - 90%	50% - 75%	25% - 50%	< 25%		
	Rating		20	17	13	8	3		
3	Spacing of discontinuities		> 2 m	0.6 - 2 . m	200 - 600 mm	60 - 200 mm	< 60 mm		
	Rating		20	15	10	8	5		
4	Condition of discontinuities (See E)		Very rough surfaces Not continuous No separation Unweathered wall rock	Slightly rough surfaces Separation < 1 mm Slightly weathered walls	Slightly rough surfaces Separation < 1 mm Highly weathered walls	Slickensided surfaces or Gouge < 5 mm thick or Separation 1-5 mm Continuous	Soft gouge >5 mm thick or Separation > 5 mm Continuous		
	Rating		30	25	20	10	0		
5	Ground water	Inflow per 10 m tunnel length (l/m)	None	< 10	10 - 25	25 - 125	> 125		
		(Joint water press)/ (Major principal σ)	0	< 0.1	0.1, - 0.2	0.2 - 0.5	> 0.5		
		General conditions	Completely dry	Damp	Wet	Dripping	Flowing		
	Rating		15	10	7	4	0		

B. RATING ADJUSTMENT FOR DISCONTINUITY ORIENTATIONS (See F)						
Strike and dip orientations		Very favourable	Favourable	Fair	Unfavourable	Very Unfavourable
Ratings	Tunnels & mines	0	-2	-5	-10	-12
	Foundations	0	-2	-7	-15	-25
	Slopes	0	-5	-25	-50	

C. ROCK MASS CLASSES DETERMINED FROM TOTAL RATINGS					
Rating	100 ← 81	80 ← 61	60 ← 41	40 ← 21	< 21
Class number	I	II	III	IV	V
Description	Very good rock	Good rock	Fair rock	Poor rock	Very poor rock

D. MEANING OF ROCK CLASSES					
Class number	I	II	III	IV	V
Average stand-up time	20 yrs for 15 m span	1 year for 10 m span	1 week for 5 m span	10 hrs for 2.5 m span	30 min for 1 m span
Cohesion of rock mass (kPa)	> 400	300 - 400	200 - 300	100 - 200	< 100
Friction angle of rock mass (deg)	> 45	35 - 45	25 - 35	15 - 25	< 15

E. GUIDELINES FOR CLASSIFICATION OF DISCONTINUITY conditions					
Discontinuity length (persistence) Rating	< 1 m 6	1 - 3 m 4	3 - 10 m 2	10 - 20 m 1	> 20 m 0
Separation (aperture) Rating	None 6	< 0.1 mm 5	0.1 - 1.0 mm 4	1 - 5 mm 1	> 5 mm 0
Roughness Rating	Very rough 6	Rough 5	Slightly rough 3	Smooth 1	Slickensided 0
Infilling (gouge) Rating	None 6	Hard filling < 5 mm 4	Hard filling > 5 mm 2	Soft filling < 5 mm 2	Soft filling > 5 mm 0
Weathering Ratings	Unweathered 6	Slightly weathered 5	Moderately weathered 3	Highly weathered 1	Decomposed 0

F. EFFECT OF DISCONTINUITY STRIKE AND DIP ORIENTATION IN TUNNELLING**			
Strike perpendicular to tunnel axis		Strike parallel to tunnel axis	
Drive with dip - Dip 45 - 90°	Drive with dip - Dip 20 - 45°	Dip 45 - 90°	Dip 20 - 45°
Very favourable	Favourable	Very unfavourable	Fair
Drive against dip - Dip 45-90°	Drive against dip - Dip 20-45°	Dip 0-20 - Irrespective of strike°	
Fair	Unfavourable	Fair	

TABLE 3.2 RMR PARAMETERS (BEINIAWSKI, 1989)

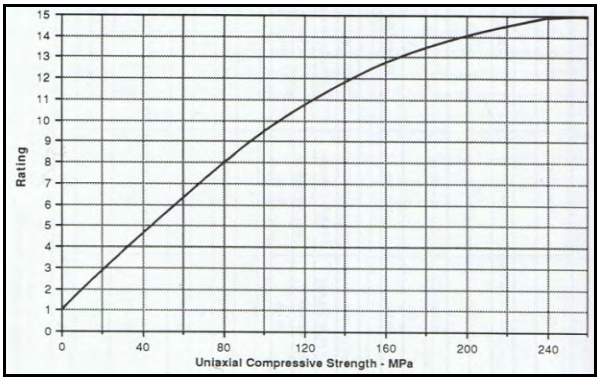

FIGURE 3.9 RMR FOR INTACT ROCK STRENGTH (BIENIAWSKI, 1989)

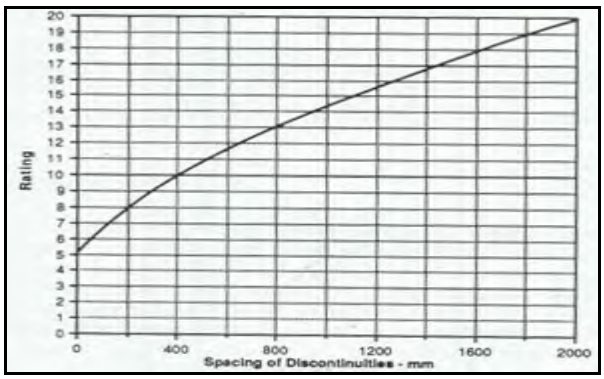

FIGURE 3.10 RMR FOR DISCONTINUITY SPACING (BIENIAWSKI, 1989)

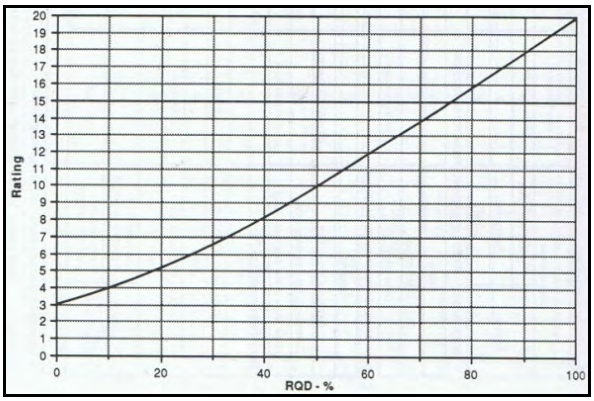

FIGURE 3.11 RMR FOR RQD (BIENIAWSKI, 1989)

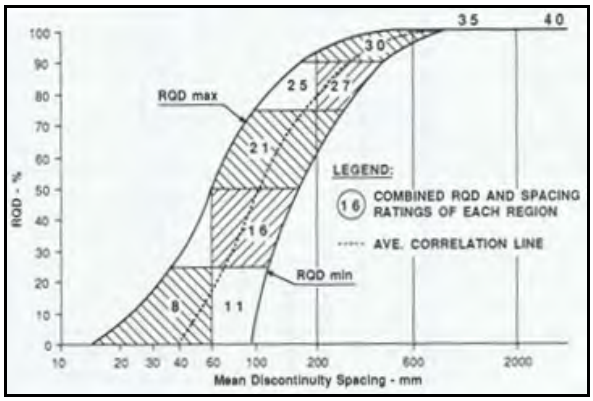

FIGURE 3.12 CORRELATION BETWEEN RQD AND DISCONTINUITY SPACING (BIENIAWSKI, 1989)

3.3.5 MODIFICATIONS TO RMR

RMR has been modified many times over the years since its conception. In this study, RMR_{89} (Bieniawski, 1989) was used. Many new rock mass rating systems that deviate from RMR for more specialist needs have also been proposed. These include systems such as Mining Rock Mass Rating (MRMR), Rock Mass Strength (RMS), Modified Basic RMR (MBR), SMR, Slope Rock Mass Rating (SRMR), Chinese System for SMR (CSMR), Geological Strength Index (GSI), Modified Rock Mass Classification (M-RMR) and Index of Basic Rock Mass Quality (BQ).

MRMR was created by Laubscher (1977, 1984 and 1990) for the purpose of assessing support in underground excavations. It adjusts RMR_{73} (Bieniawski, 1973) to include weathering, field and induced stresses, change in stress, orientation of geological structures and method of excavation.

In 1980, Selby published the method for RMS which modifies RMR to deal more effectively with slopes (Selby, 1980). RMS is based upon eight parameters, three of which are based directly from RMR but all values and ranges are changed. RQD has been removed altogether and joint conditions are divided into separate parameters with width of joints and continuity of joints being separate parameters and weathering and joint orientations also being included. Unfortunately, joint orientation is defined by descriptions of how favourable the orientation is, and do not require measurement or an explanation of the definitions of each range.

MBR was created by Kendorski, Cummings, Bieniawski, & Skinner (1983). It uses the basic RMR and modifies it for mining. It was created from a series of case studies from block caving operations in the USA. It includes blast damage, induced stresses from mining, structural features, distance from the cave front and size of the caving block to the basic RMR parameters. The support recommendations include that for isolated or development drifts and final support of intersection and drifts.

SRMR was proposed by Robertson (1988). SRMR modifies RMR to better evaluate weak rock masses. It comes from a back analysis of failed slopes in a copper mine in British Columbia to better evaluate rock masses with RMR less than 40. In SRMR, groundwater is ignored and intact

rock strength, RQD and discontinuity spacing and condition are modified to better describe the properties specific to weak rock masses.

CSMR is based on SMR (described below) and was introduced by Chen (1995). It applies a discontinuity factor (λ) that describes the conditions of the dominant defect but is only applicable to an 80 m high slope and otherwise has to be adjusted. CSMR is defined as:

$$\mathbf{CSMR = \Xi \ X \ RMR_{1976} - \Lambda \ X \ F_1F_2F_3 + F_4} \qquad \mathbf{(3.16)}$$

Where F_1, F_2, F_3 and F_4 are factors from SMR and are described in Section 3.3.6, ξ is the adjustment for slope height and λ is determined from defect condition descriptions shown in Table 3.3.

λ	Defect Condition
1.0	Faults, long weak seams filled with clay
0.8 to 0.9	Bedding planes, large scale joints with gouge
0.7	Joints, tightly interlocked bedding planes

TABLE 3.3 DISCONTINUITY FACTOR FOR CSMR (CHEN, 1995)

M-RMR was developed by Unal (1996) for better classification of weak, stratified, anisotropic and clay bearing rocks. M-RMR takes the RMR and changes the RMR factors of UCS, RQD and joint condition (JC) by adjusting them for weathering. M-RMR is defined as:

$$\mathbf{M\text{-}RMR = A_B \ A_W \ (F_C \ (I_{UCS} + I_{RQD} + I_{JC}) + I_{JS} + I_{GW} + I_{JO})} \qquad \mathbf{(3.17)}$$

where F_c is the weathering co-efficient and A_b and A_w are adjustments for blasting and major plane of weakness type respectively.

BQ was developed by Lin (1998) through a series of case studies throughout China. It uses numerous numerical analysis techniques, taking the data from case studies to determine an

equation that describes the basic quality of rock masses (which are grouped into five classes of 'strong, intact rock' through to 'soft and fractured rock') but it gives no correlation to any rock mass properties. Also, rock unit weight and average defect spacing, which were found to be important in describing rock mass quality, are not included in the equation. The equation is defined as:

$$\mathbf{BQ = -41.0451 + 1.9212\Sigma_C + 546.1130K_V - 0.0064\Sigma_C^2K_V - 276.9786K_V^2} \qquad \mathbf{(3.18)}$$

where K_v is the insitu seismic velocity divided by the intact seismic velocity and σ_c is the UCS of the intact rock.

In 1994 GSI was proposed and has become is one of the most important schemes to result from RMR. It was introduced by Hoek (1994) and Hoek, Kaiser and Bawden (1995) and focuses upon improving the estimation of rock mass strength from RMR. It initially directly modified RMR to estimate the GSI of the rock mass by adding together the RMR parameters but assuming groundwater to be dry (as this does not affect the rock strength) and joint orientation to be very favourable. Now it has been recommended (Hoek, 2007 ed.) that the GSI is better estimated by the means of the GSI charts. The GSI charts are empirical charts (shown in Figure 3.13 and Figure 3.14) that describe the GSI of a blocky or homogeneous rock mass through descriptive and qualitative means. It is recommended, however, that GSI should not be used if large defect spacing is present but rather be used when discontinuities are close together.

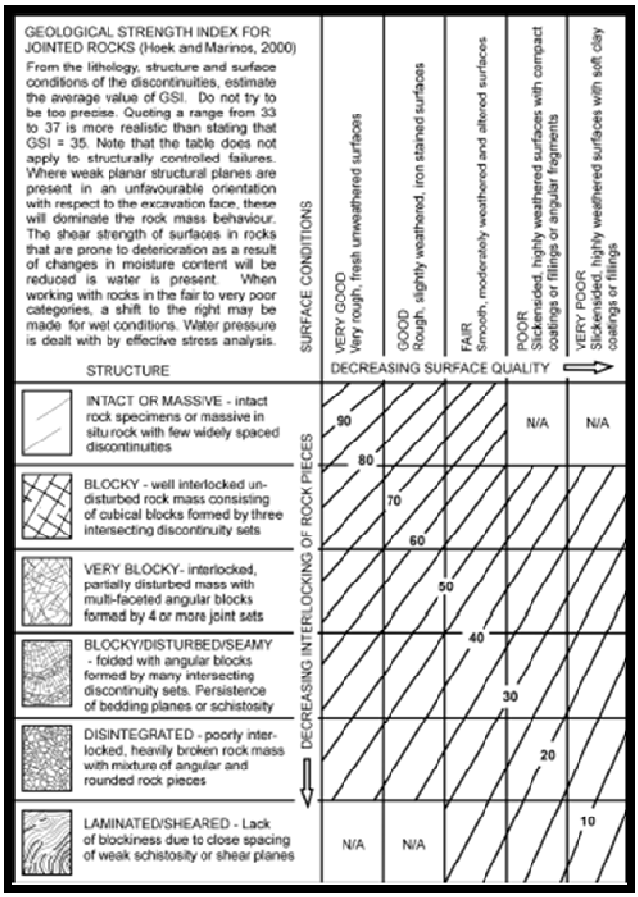

FIGURE 3.13 GSI FOR BLOCKY ROCK MASSES (HOEK, 2007 ED.)

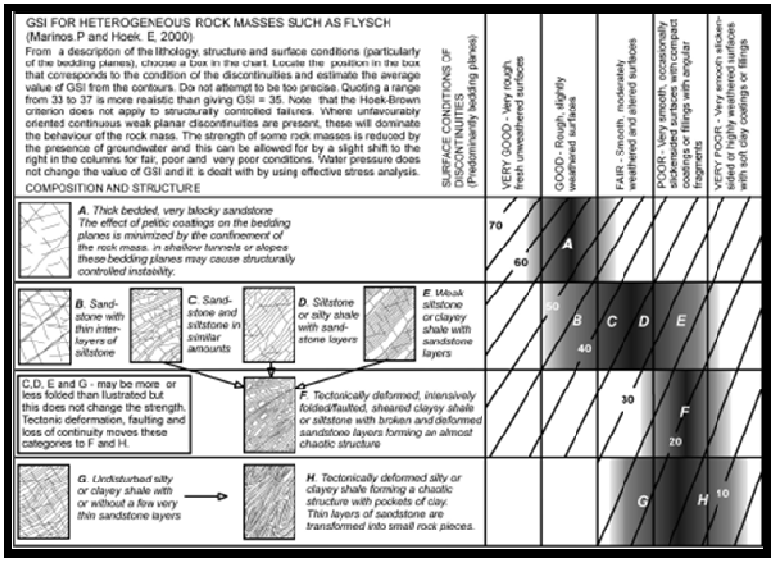

FIGURE 3.14 GSI OF HETEROGENEOUS ROCK MASSES (HOEK, 2007 ED.)

3.3.6 SLOPE MASS RATING

SMR was derived from the popular RMR system. The rock mass parameters that constitute basic RMR include intact rock strength, RQD (measured or estimated), discontinuity spacing and conditions and groundwater.

SMR was modified from RMR by Romana (1985) so that RMR could be applied more successfully to natural and artificial slopes such as in open pit mines. Romana took Bieniawski's basic RMR system and developed new adjustment factors for joint orientation and added blasting effects to get the SMR system which can specifically be used to investigate planar and toppling failure modes.

SMR is defined as:

$$\mathbf{SMR = RMR_{89} + F_1F_2F_3 + F_4} \qquad \mathbf{(3.19)}$$

Table 3.4 shows the RMR parameters used and Table 3.5 and Table 3.6 show the SMR adjustments. The orientation adjustments include three factors. The first factor (F_1) is defined by parallelism between the slope dip direction and the defect dip direction. F_1 ranges from 1.00 when the slope and defect strikes are near parallel to 0.15 when the angle between them is greater than 30^o. F_1 was later found to have a relationship of:

$$\mathbf{F_1 = (1 - SINA)^2} \qquad \mathbf{(3.20)}$$

where A is the angle between the two dip directions.

F_2 is the defect dip factor. In planer failure mode, the rating ranges form 1.00 for dip angles greater than 45^o, to 0.15 for dip angles less than 20^o. F_2 was later found to have the relationship:

$$\mathbf{F_2 = TG^2\ B_J} \qquad \mathbf{(3.21)}$$

where β_j is the joint dip angle. F_2 for toppling is always 1.00.

F_3 is the difference between the slope dip and the joint dip. It is essentially the probability that the defect daylights in the slope face. When the slope dips less than 10^o more than the defect

dips, then the condition is unfavourable. Unfavourable and very unfavourable toppling does not occur in nature as toppling tends to be a much smaller scale event.

F_4 is the adjustment for blasting and is shown in Table 3.6. Natural slopes increase the stability of a slope because the weathering and erosion cuts the slope down to a more stable state. In excavation, pre-splitting and smooth blasting increases the stability of the slope because the method of blasting discourages blast damage into the slope. Normal blasting and mechanical excavation does not affect slope stability but deficient blasting can reduce slope stability and therefore, the SMR is reduced.

Also, Romana (1993) gives more detailed instructions of describing defect spacing and conditions. The conditions of the defects should be undertaken by evaluating the most unstable defect set. However, if there is no dominant set then the average conditions of all the defects should be incorporated. The instructions for evaluating defect spacing and defect conditions more successfully in the field are shown in Table 3.7 and Table 3.8. These tables can be used along with the SMR charts to help determine the SMR parameters more thoroughly.

The description of rock classes, as defined by SMR are given in Table 3.9. The classes are based on the SMR overall rating with above 80 corresponding to very good and completely stable rock mass, 60 to 80 corresponds to good and stable rock mass, 40 to 60 corresponding to normal and partially stable slope conditions, 20 to 40 corresponding to bad and unstable rock mass, and below 20 corresponding to very bad and completely unstable rock mass conditions. The common failure modes and recommended support requirements are also given for each stability class.

The rock parameters used in SMR are the most influential rock mass parameters effecting slope stability in natural and artificial slopes and, therefore, this system has been chosen to predict rock mass conditions for the slopes of the RTIO mines in Western Australia for this research paper. The methods and results, for which, are given in Chapter 4.

Parameter		Range of values						
Strength of intact rock material	Point load strength index	>10 MPa	4 - 10 MPa	2 - 4 MPa	1 - 2 MPa	For low range uniaxial compressive test is preferred		
	Uniaxial compressive	>250 MPa	100 - 250 MPa	50 - 100 MPa	25 - 50 MPa	5 - 25 MPa	1 - 5 MPa	<1 MPa
	Visual description	Extremely strong	Very strong	Strong	Moderate	Weak	V. weak	Soil
	Pocket knife	No peeling	No peeling	No peeling	No peeling	Difficult	Easy	V. easy
	Geological hammer	Only chips after impact	Many blows to fracture	Several blows to fracture	A firm blow to fracture	Can indent	Can Crumble	
Rating		15	12	7	4	2	1	0
Drill core quality RQD		90% - 100%	75% - 90%	50%- 75%	25% - 50%	<25%		
Rating		20	17	13	8	3		
Spacing of discontinuities		>2 m	0.6 - 2 m	200 mm - 600 mm	60 - 200 mm	<60 mm		
Rating		20	15	10	8	5		
Condition of discontinuities		Very rough surfaces. Not continuous. No separation. Unweathered wall rock.	Slightly rough surfaces. Separation <1 mm. Slightly weathered walls.	Slightly rough surfaces. Separation <1 mm. Highly weathered walls.	Slickensided surfaces or gouge <5 mm thick or separation 1 - 5 mm continuous.	Soft gouge >5 mm or Separation >5 mm continuous		
Rating		30	25	20	10	0		
Groundwater in joint		Completely dry	Damp	Wet	Dripping	Flowing		
Rating		15	10	7	4	0		

TABLE 3.4 THE CLASSIFICATION PARAMETERS AND THEIR RATINGS OF RMR SYSTEM (FROM BIENIAWSKI, 1989)

Case		Very Favourable	Favourable	Fair	Unfavourable	Very Unfavourable
Planer	$\lvert\alpha_j - \alpha_s\rvert$	>30°	30° - 20°	20° - 10°	10° - 5°	<5°
Toppling	$\lvert\alpha_j - \alpha_s - 180°\rvert$					
Planer/ Toppling	F_1	0.15	0.4	0.7	0.85	1
Planer	$\lvert\beta_j\rvert$	<20°	20° - 30°	30° - 35°	35° - 45°	>45°
Planer	F_2	0.15	0.4	0.7	0.85	1
Toppling	F_2	1	1	1	1	1
Planer	$\beta_j - \beta_s$	>10°	10° - 0°	0°	0° - (-10°)	<-10°
Toppling	$\beta_j + \beta_s$	<110°	110° - 120°	>120°	-	-
Planer/ Toppling	F_3	0	-6	-25	-50	-60

α_s = slope dip direction
β_s = slope dip
α_j = joint dip direction
β_j = joint dip

TABLE 3.5 ADJUSTMENT RATING FOR DEFECTS (ROMANA, 1993)

Method	Natural Slope	Pre-splitting	Smooth Blasting	Blasting or Mechanical	Deficient Blasting
F_4	15	10	8	0	-8

TABLE 3.6 ADJUSTMENT RATING FOR EXCAVATION METHOD OF SLOPES (ROMANA, 1993)

Description	Spacing (m)	Rock Mass Condition
Very Wide	>2	Solid
Wide	0.6-2	Massive
Moderate	0.2-0.6	Blocky/Seamy
Close	0.06-0.2	Fractured
Very Close	<0.06	Crushed/Shattered

TABLE 3.7 SMR DESCRIPTIONS OF DEFECT SPACING IN ROCK MASSES (ROMANA, 1993)

Roughness/filling		Rating
Very rough		10
Rough		9
Slightly rough		8
Smooth		6
Slickensided/gouge		5
Soft gouge		0
Separation	**Opening (mm)**	**Rating**
Closed	<0.1	9
Moderately open	0.1-1.0	7
Open	1.0-5.0	5
Very open	<5.0	0
Persistence		**Rating**
Not persistent/not continuous		5
Sub-persistent		3
Persistent/ continuous		0
Weathering	**Grade**	**Rating**
Fresh	I	6
Slightly weathered	II	5
Moderately weathering	III	3
Highly weathered	IV	0
Completely weathered	V	0

TABLE 3.8 SMR DESCRIPTIONS OF JOINT CONDITION RATINGS. EACH OF THE ABOVE PARAMETERS CAN BE ADDED TO GET A FINAL RMR RATING FOR JOINT CONDITION (ROMANA, 1993)

Class	SMR	Description	Stabilities	Failure	Support
I	81-100	Very Good	Completely Stable	None	None
II	61-80	Good	Stable	Some Blocks	Occasional
III	41-60	Normal	Partially Stable	Some Joints or Many Wedges	Systematic
IV	21-40	Bad	Unstable	Planer or Big Wedges	Important/Corrective
V	<20	Very Bad	Completely Unstable	Big Planer or Soil Like	Re-excavation

TABLE 3.9 DESCRIPTION OF SMR CLASSES (ROMANA, 1993)

4 GEOTECHNICAL INVESTIGATION

4.1 OVERVIEW

In this study, rock mass conditions throughout RTIO mines were investigated. The purpose of the geotechnical investigation was to:

- Classify the geotechnical characteristics of BIF and shale of the Lower Hamersley Group in RTIO mines as they alter from fresh BIF and shale through to slightly, moderately, highly and extremely altered iron ore and shale and as they change through Recent weathering using SMR parameters and laboratory testing and,
- Use SMR to determine likely stability issues of present and future open cast pits in RTIO mines after using geochemical and/or mineralogical data to decide where stability issues are likely to arise.

The first aim will be discussed and interpreted in this chapter. The second aim will be discussed and interpreted in Chapters 6 and 7, after geochemical and mineralogical data is interpreted and discussed in Chapter 5.

To classify rock mass conditions, the rock mass classification scheme, SMR, was used in specific areas throughout the Hamersley Province. Visual descriptions of slope stability and rock mass character were also undertaken of these chosen areas. Samples were collected, where possible, for further laboratory testing including point load testing and slake durability testing and for later geochemical and mineralogical analysis which will be further discussed in Chapter 5.

Four RTIO mines throughout the Hamersley Province were chosen to be investigated. These mines included Mount Tom Price and Paraburdoo, which dominantly mine in the Brockman Iron Formation; and Marandoo and West Angelas, which dominantly mine in the Marra Mamba Iron Formation of the lower Hamersley Group deposits.

Within each mine, up to three deposits were chosen to be investigated. At Mount Tom Price; Southern Ridge, North Deposit and Section Seven were chosen to be investigated. Field samples of BIF and shale were taken from North Deposit and Section Seven and Southern Ridge was investigated through core samples. At Paraburdoo, 32 East 6 deposit at Eastern Ranges was investigated in the field while 23 East deposit at Eastern Ranges was investigation through core samples. At Marandoo, field samples were taken from Tail Pit and Ridge Pit and some core samples from Tail Pit. At West Angelas Deposit A, core samples were investigated from five separate boreholes.

The rock types chosen to be studied are BIF and shale as these are the two most common rock types in RTIO mines. Throughout the four mines studied, areas of differing alteration and weathering were located and investigated separately by means of a 'window' methodology. 'Window' investigation is a technique where regions of interpreted "uniform" rock mass is classified and studied as one area.

In the Brockman Iron Formation deposits at Mount Tom Price and Paraburdoo, two methods of alteration have taken place (Taylor, et al., 2001). Hypogene alteration has altered deposits such as Southern Ridge, North Deposit and 23 East deposit. This alteration creates a low phosphorus content (low P) ore type. Supergene alteration has created deposits such as Section Seven and 32 East deposits. This creates a high phosphorus content (high P) ore type. For this reason, the Brockman Iron Formation has been analysed in two groups in this study, to account for the different alteration products of low P and high P ore. The Marra Mamba Iron Formation at Marandoo and West Angelas has been altered only by supergene alteration and, therefore, will be analysed in a single group.

4.2 METHODS

4.2.1 PREPARATION

In each area studied, the geology and major structures throughout the area was compiled. If field samples were to be investigated, then the geology and the ore profile were investigated to determine sites where "window" sampling could take place. In areas where core was chosen to

be studied (Southern Ridge, 23 East Deposit and West Angelas), then the core logs were investigated, and sites were selected where “window” sampling could take place.

The aim of choosing the sites, for each rock type, stratigraphy and ore type; was for a range of alteration and weathering states to be encountered. Each area was also assessed for its general lithology, structure and stability.

4.2.2 FIELD ANALYSIS

SMR was undertaken for each area using the field sheet shown in Figure 4.1. This included estimating the intact rock strength, RQD, discontinuity spacing and conditions, groundwater conditions, measuring defect dip and dip direction, slope dip and dip direction and evaluating the blasting method. Once the SMR for each zone had been obtained, this would provide stability classes and descriptions of possible failure modes within each zone (refer to Table 3.9).

Visual observation was undertaken of the studied areas. Current pit wall stability was described for the field samples. This includes describing the failure modes and erosional features that are seen in the pit wall. The RTIO alteration and weathering descriptors for BIF and shale (shown in Figure 4.2 and Figure 4.3) were then used to describe the level of alteration and weathering of each zone.

Within each area, rock samples were collected for point load testing, slake durability testing and later geochemical and mineralogical analysis, where possible. The samples that were collected were given a sample number and recorded alongside some descriptions of the rock specimen, including its spatial location, lithology, colour, grain size and texture.

4.2.3 LABORATORY ANALYSIS

Point load testing and slake durability testing was undertaken where possible. Point load testing was completed at areas being analysed where samples of suitable dimensions could be tested. Ten or more samples were preferred but point load testing was undertaken wherever possible. Slake durability testing was completed on a chosen lot of samples where 10 lumps of roughly round samples of between 40 and 60 grams were collected.

SLOPE MASS RATING

Location:
Pit:
Wall (or Core No):
Sample No:

Parameter		Range of values						
Strength of intact rock material	Point load strength index	>10 MPa	4 - 10 MPa	2 - 4 MPa	1 - 2 MPa	For low range uniaxial compressive test is preferred		
	Uniaxial compressive	>250 MPa	100 - 250 MPa	50 - 100 MPa	25 - 50 MPa	5 – 25 MPa	1 - 5 MPa	<1 MPa
	Visual description	Extremely strong	Very strong	Strong	Moderate	Weak	V. weak	Soil
	Pocket knife	No peeling	No peeling	No peeling	No peeling	Difficult	Easy	V. easy
	Geological hammer	Only chips after impact	Many blows to fracture	Several blows to fracture	A firm blow to fracture	Can indent	Can Crumble	
Rating		15	12	7	4	2	1	0
Drill core quality RQD		90% - 100%	75% - 90%	50%- 75%	25% - 50%	<25%		
Rating		20	17	13	8	3		
Spacing of discontinuities		>2 m	0.6 - 2 m	200 mm - 600 mm	60 - 200 mm	<60 mm		
Rating		20	15	10	8	5		
Condition of discontinuities		Very rough surfaces. Not continuous. No separation. Unweathered wall rock.	Slightly rough surfaces. Separation <1 mm. Slightly weathered walls.	Slightly rough surfaces. Separation <1 mm. Highly weathered walls.	Slickensided surfaces or gouge <5 mm thick or separation 1 - 5 mm continuous.	Soft gouge >5 mm or Separation >5 mm continuous		
Rating		30	25	20	10	0		
Groundwater in joint		Completely dry	Damp	Wet	Dripping	Flowing		
Rating		15	10	7	4	0		

RMR =	

Case		Very Favourable	Favourable	Fair	Unfavourable	Very Unfavourable
Planar	$\lvert\alpha_j - \alpha_s\rvert$	>30°	30° - 20°	20° - 10°	10° - 5°	<5°
Toppling	$\lvert\alpha_j - \alpha_s - 180°\rvert$					
Planar/ Toppling	F_1	0.15	0.4	0.7	0.85	1
Planar	$\lvert\beta_j\rvert$	<20°	20° - 30°	30° - 35°	35° - 45°	>45°
Planar	F_2	0.15	0.4	0.7	0.85	1
Toppling	F_2	1	1	1	1	1
Planar	$\beta_j - \beta_s$	>10°	10° - 0°	0°	0° - (-10°)	<-10°
Toppling	$\beta_j + \beta_s$	<110°	110° - 120°	>120°	-	-
Planar/ Toppling	F_3	0	-6	-25	-50	-60

α_s	slope dip direction		α_j	joint dip direction	
β_s	slope dip		β_j	joint dip	

(F1 x F2 x F3) =	

Method	Natural Slope	Presplitting	Smooth Blasting	Blasting or Mechanical	Deficient Blasting
F_4	15	10	8	0	-8

F4 =	

SMR =	RMR + (F1 x F2 x F3) + F4 =	

FIGURE 4.1 SMR FIELD SHEET USED FOR EACH AREA INVESTIGATED

RTIO ALTERATION DESCRIPTION FOR BIF

FR	Fresh	Rock substance unaffected by alteration.	Iron bands in BIF are magnetic and there is no deterioration of chert.
SA	Slightly altered	Rock substance affected by altered to the extent that partial bleaching or partial discolouration has taken place. The colour and texture of the unaltered rock is recognizable.	Iron bands are non-magnetic and there is no deterioration of chert.
MA	Moderately altered	Rock substance affected by alteration to the extent that discolouration or bleaching extends throughout whole of rock substance and original colour of the unaltered rock is no longer recognizable.	Iron bands are non-magnetic and there may be some change in strength properties. Chert exhibits minor denaturing.
HA	Highly altered	Rock substance affected by alteration to the extant that discolouration or bleaching affects the whole rock substance and signs of chemical or physical decomposition of individual minerals are usually present. Porosity or strength may be increased or decreased when compared to unaltered rock.	Iron bands may be becoming softer, more powdery. Chert bands are particularly denatured but chert still exists.
EA	Extremely altered	Rock substance affected by altered to the extent that the parent rock minerals are absent or entirely replaced.	Iron bands are soft and powdery. Chert has been completely leached away. The rock no longer resembles its parent material and the geotechnical properties of strength and RQD are significantly changed.

RTIO WEATHERING DESCRIPTION FOR BIF

FR	Fresh	Rock substance unaffected by weathering	BIF is green and grey, with no change in strength properties. In essence BIF in it's original form.
SW	Slightly weathered	Rock substance affected by weathering to the extent that partial staining or partial discolouration of the rock substance usually by limonite has taken place. The colour and texture of the fresh rock is recognizable; strength properties are essentially those of the fresh rock substance.	BIF is slightly oxidized, but with no change in the original strength properties of the original material.
MW	Moderately weathered	Rock substance affected by weathering to the extent staining extends throughout whole of the rock substance and the original colour of the fresh rock is no longer recognizable.	BIF is oxidized but without any evidence of vughs.
HW	Highly weathered	Rock substance affected by weathering to the extent that limonite staining or bleaching affects the whole of the rock substance and signs of chemical or physical decomposition of individual minerals are usually evident. Porosity and strength may be increased or decreased when compared to the fresh rock substance, usually as a result of the leaching or deposition of iron. The colour and strength of the original fresh rock substance is no longer recognizable.	BIF will exhibit vughs and can now be considered cangarised. However bedding is still evident.
EW	Extremely weathered	Rock substance affected by weathering to the extent that the rock exhibits soil properties, i.e. it can be remoulded and can be classified according to the Unified Soil Classification System, but the texture of the original rock is still evident.	The BIF exhibits well-developed vughs with complete overprinting of bedding.

FIGURE 4.2 RTIO ALTERATION AND WEATHERING CLASSIFICATIONS FOR BIF IN THE HAMERSLEY PROVINCE

RTIO ALTERATION DESCRIPTIONS FOR SHALE

FR	Fresh	Rock substance unaffected by alteration.	Shale is black.
SA	Slightly altered	Rock substance affected by altered to the extent that partial bleaching or partial discolouration has taken place. The colour and texture of the unaltered rock is recognizable.	Shale will show red reduction spots when pyritic and will become a lighter shade of grey as leaching occurs.
MA	Moderately altered	Rock substance affected by alteration to the extent that discolouration or bleaching extends throughout whole of rock substance and original colour of the unaltered rock is no longer recognizable.	Shale will be leached to a light grey to pink to khaki green in colour.
HA	Highly altered	Rock substance affected by alteration to the extant that discolouration or bleaching affects the whole rock substance and signs of chemical or physical decomposition of individual minerals are usually present. Porosity or strength may be increased or decreased when compared to unaltered rock.	Shale will exhibit a complete leaching of colour. The strength properties may or may not be different to the parent rock. If the shale is within the mineralisation envelope, the shale may be red and ferrunginised with increased strength and density (though not as dense as the surrounding BIF).
EA	Extremely altered	Rock substance affected by altered to the extent that the parent rock minerals are absent or entirely replaced.	Shale will exhibit a complete leaching of colour. The strength properties may or may not be different to the parent rock. If the shale is within the mineralisation envelope, the shale may be red and ferrunginised with highly increased strength and density (though not as dense as the surrounding BIF).

RTIO WEATHERING DESCRIPTIONS FOR SHALE

FR	Fresh	Rock substance unaffected by weathering	Shale is black.
SW	Slightly weathered	Rock substance affected by weathering to the extent that partial staining or partial discolouration of the rock substance usually by limonite has taken place. The colour and texture of the fresh rock is recognizable; strength properties are essentially those of the fresh rock substance.	Shale is slightly oxidized with an orange to red discolouration.
MW	Moderately weathered	Rock substance affected by weathering to the extent staining extends throughout whole of the rock substance and the original colour of the fresh rock is no longer recognizable.	Shale is more strongly oxidized.
HW	Highly weathered	Rock substance affected by weathering to the extent that limonite staining or bleaching affects the whole of the rock substance and signs of chemical or physical decomposition of individual minerals are usually evident. Porosity and strength may be increased or decreased when compared to the fresh rock substance, usually as a result of the leaching or deposition of iron. The colour and strength of the original fresh rock substance is no longer recognizable.	Shale will exhibit vughs and can now be considered cangarised. However bedding is still evident.
EW	Extremely weathered	Rock substance affected by weathering to the extent that the rock exhibits soil properties, i.e. it can be remoulded and can be classified according to the Unified Soil Classification System, but the texture of the original rock is still evident.	The shale exhibits well-developed vughs with complete overprinting of bedding.

FIGURE 4.3 RTIO ALTERATION AND WEATHERING CLASSIFICATION FOR SHALE IN THE HAMERSLEY PROVINCE

4.3 GEOTECHNICAL RESULTS

An overview of the SMR results can be found in Appendix III. Presented below are histograms of a selection of SMR parameters and also point load strength index and calculated GSI for each of the rock groups. The geotechnical results are then interpreted and discussed in the following sections (Sections 4.4, 4.5 and 4.6).

The rock masses have been divided into BIF and shale samples and then again into Brockman Iron Formation 'high P', Brockman Iron Formation 'low P' and Marra Mamba Iron formation samples. This is for the purpose of studying the rock types, ore types and lithologies separately.

4.3.1 LOW P BROCKMAN IRON FORMATION BIF HISTOGRAMS

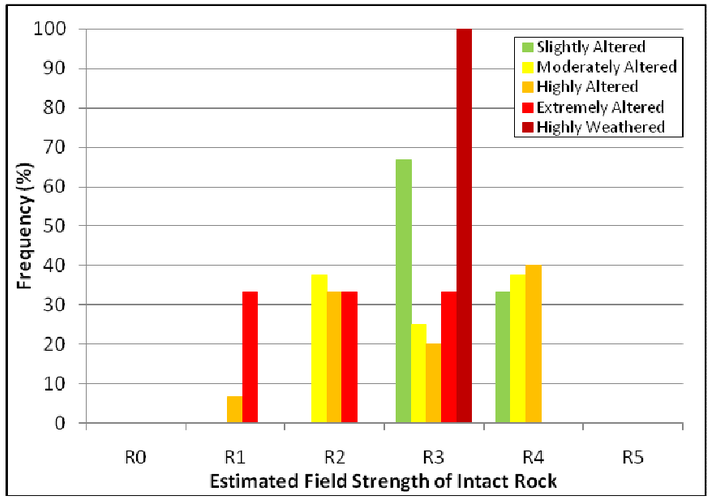

FIGURE 4.4 STRENGTH CLASSIFICATION FOR LOW P BROCKMAN IRON FORMATION BIF

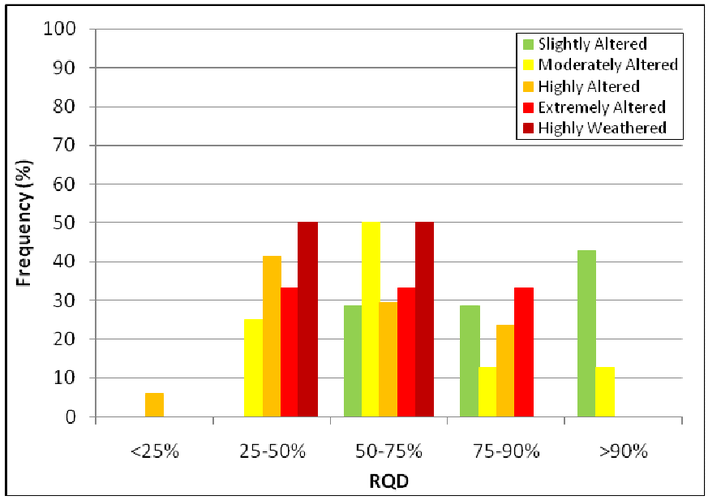

FIGURE 4.5 RQD CLASSIFICATION FOR LOW BROCKMAN IRON FORMATION BIF

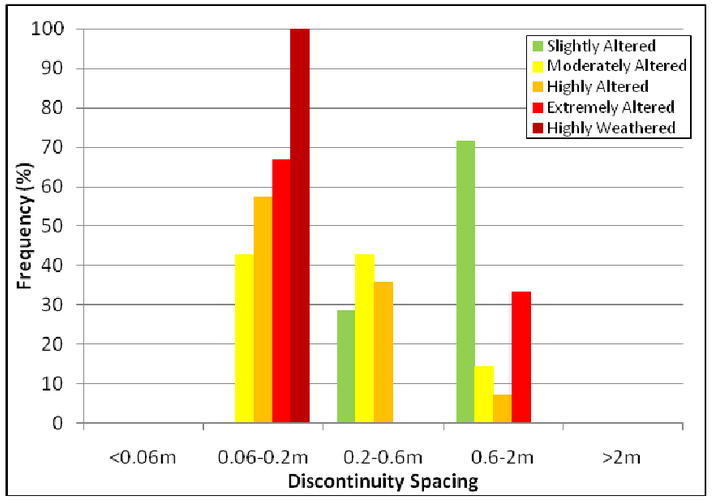

FIGURE 4.6 DISCONTINUITY SPACING CLASSIFICATION FOR LOW P BROCKMAN IRON FORMATION BIF

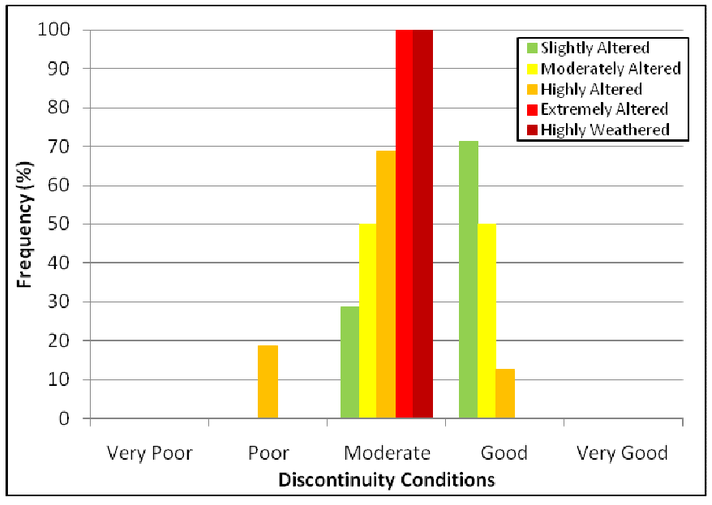

FIGURE 4.7 DISCONTINUITY CONDITION CLASSIFICATION FOR LOW P BROCKMAN IRON FORMATION BIF

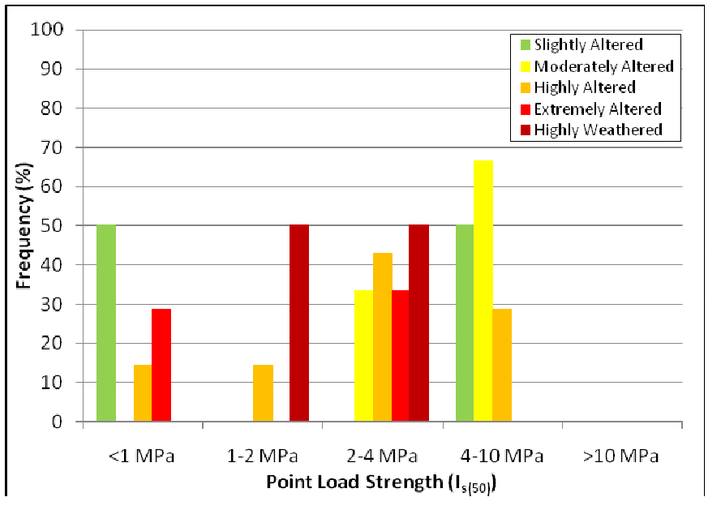

FIGURE 4.8 POINT LOAD TESTING FOR LOW P BROCKMAN IRON FORMATION BIF

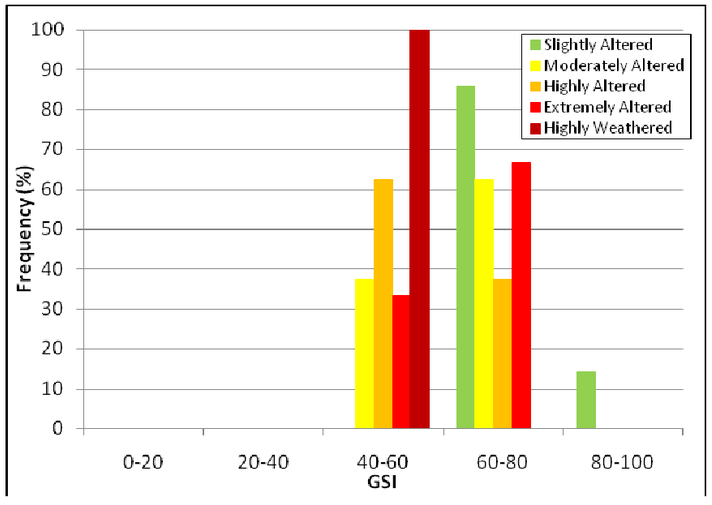

FIGURE 4.9 GSI FOR LOW P BROCKMAN IRON FORMATION BIF

4.3.2 HIGH P BROCKMAN IRON FORMATION BIF HISTOGRAMS

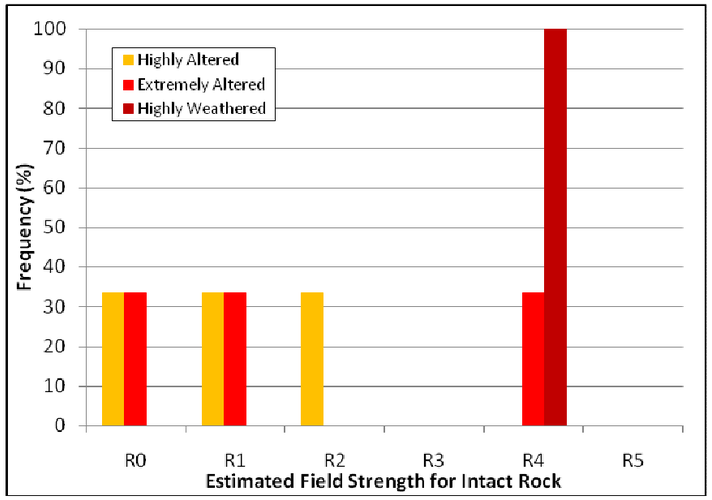

FIGURE 4.10 STRENGTH CLASSIFICATION FOR HIGH P BROCKMAN IRON FORMATION BIF

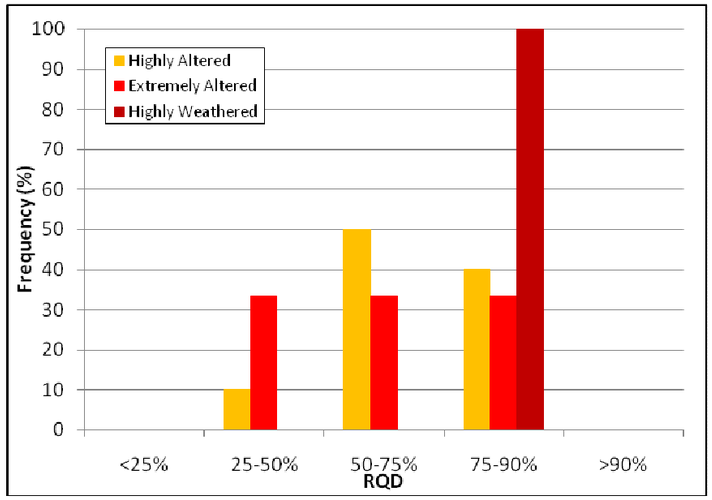

FIGURE 4.11 RQD CLASSIFICATION FOR HIGH P BROCKMAN IRON FORMATION BIF

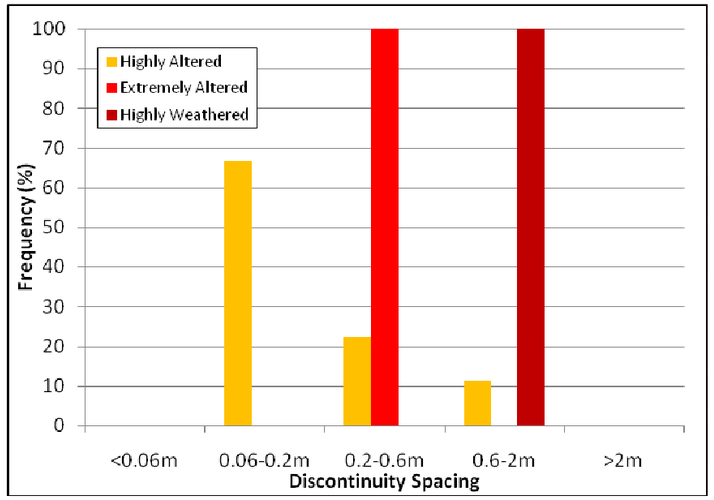

FIGURE 4.12 DISCONTINUITY SPACING CLASSIFICATION FOR HIGH P BROCKMAN IRON FORMATION BIF

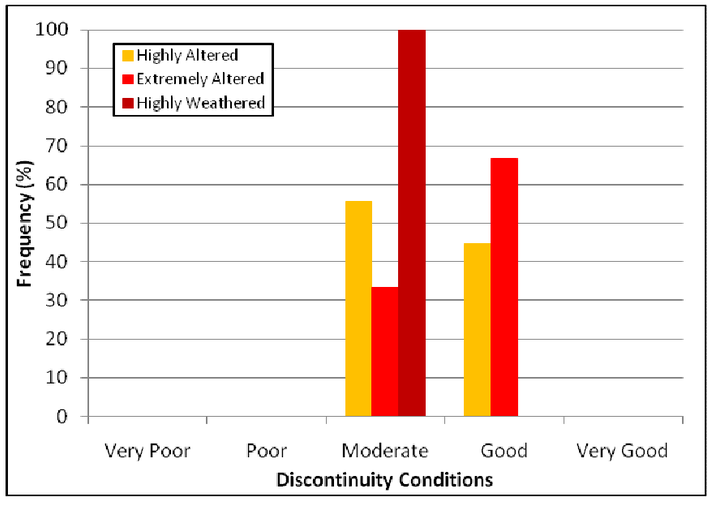

FIGURE 4.13 DISCONTINUITY CONDITION CLASSIFICATION FOR HIGH P BROCKMAN IRON FORMATION BIF

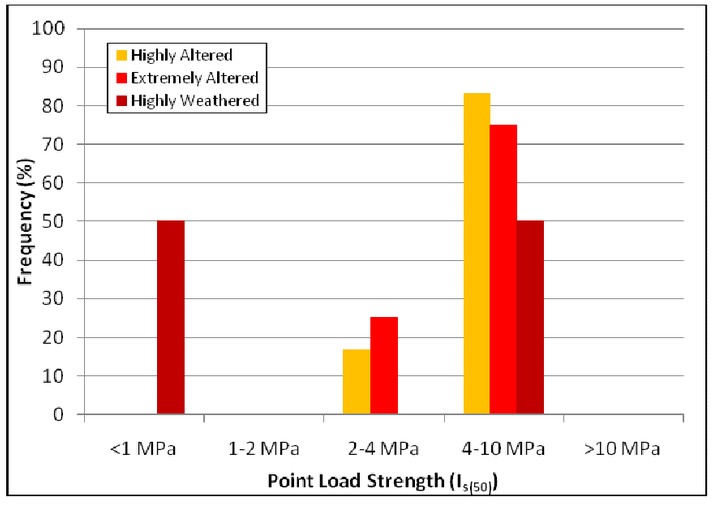

FIGURE 4.14 POINT LOAD TESTING FOR HIGH P BROCKMAN IRON FORMATION BIF

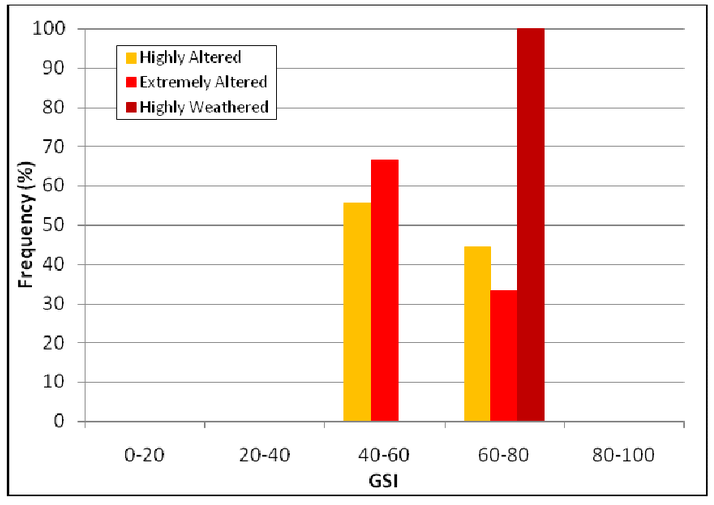

FIGURE 4.15 GSI FOR HIGH P BROCKMAN IRON FORMATION BIF

4.3.3 MARRA MAMBA IRON FORMATION BIF HISTOGRAMS

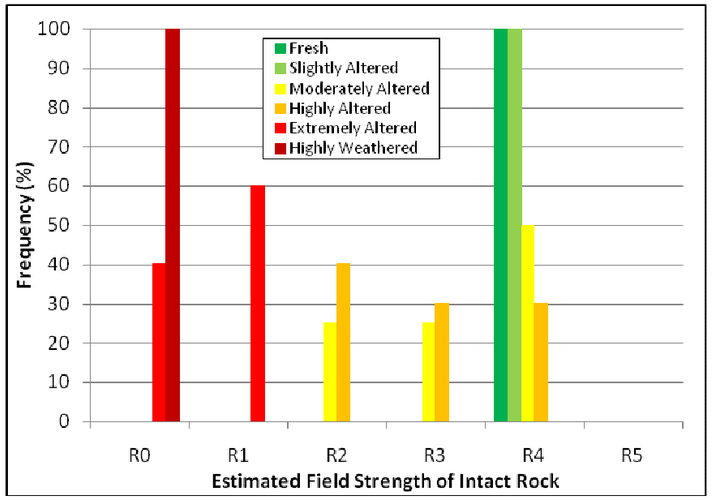

FIGURE 4.16 STRENGTH CLASSIFICATION FOR MARRA MAMBA IRON FORMATION BIF

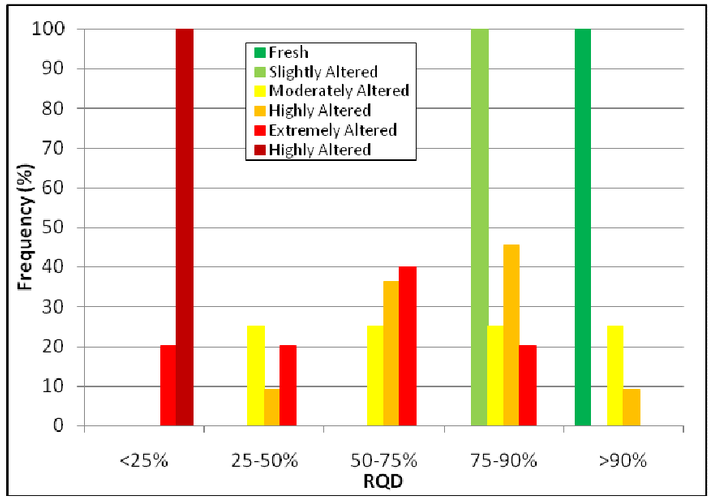

FIGURE 4.17 RQD CLASSIFICATION FOR MARRA MAMBA IRON FORMATION BIF

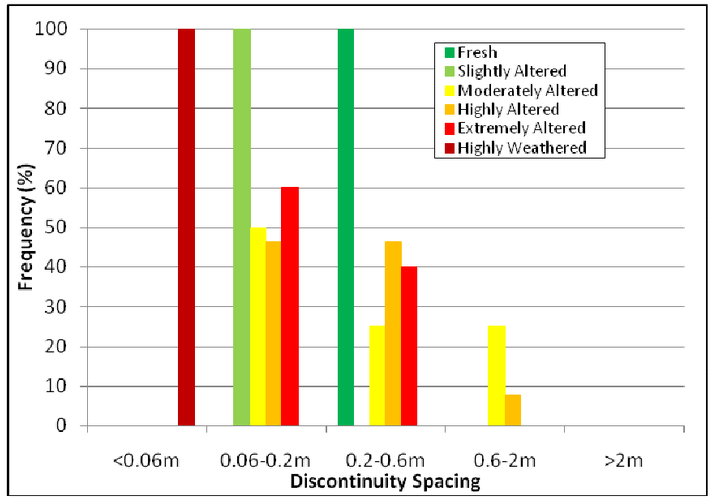

FIGURE 4.18 DISCONTINUITY SPACING CLASSIFICATION FOR MARRA MAMBA IRON FORMATION BIF

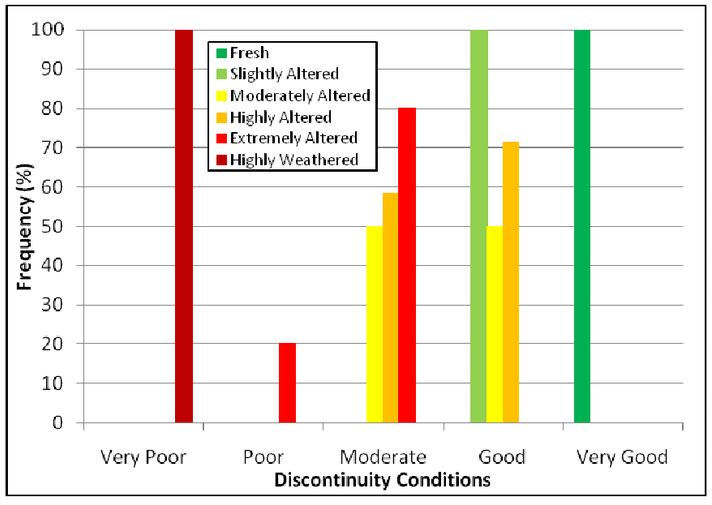

FIGURE 4.19 DISCONTINUITY CONDITION CLASSIFICATION FOR MARRA MAMBA IRON FORMATION BIF

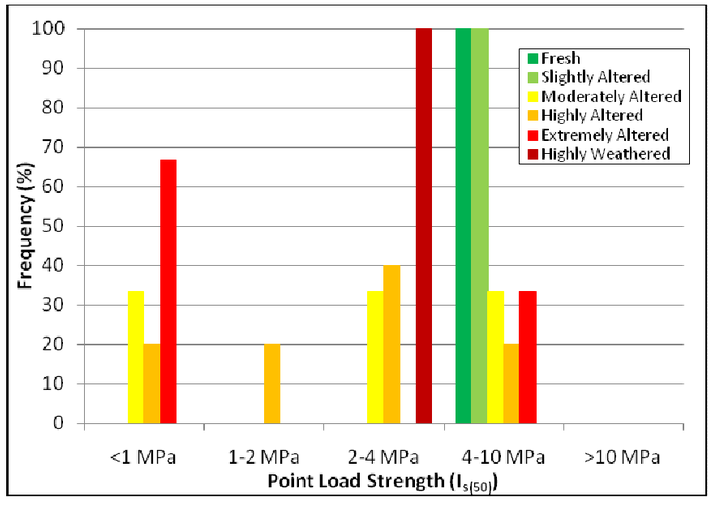

FIGURE 4.20 POINT LOAD TESTING FOR MARRA MAMBA IRON FORMATION BIF

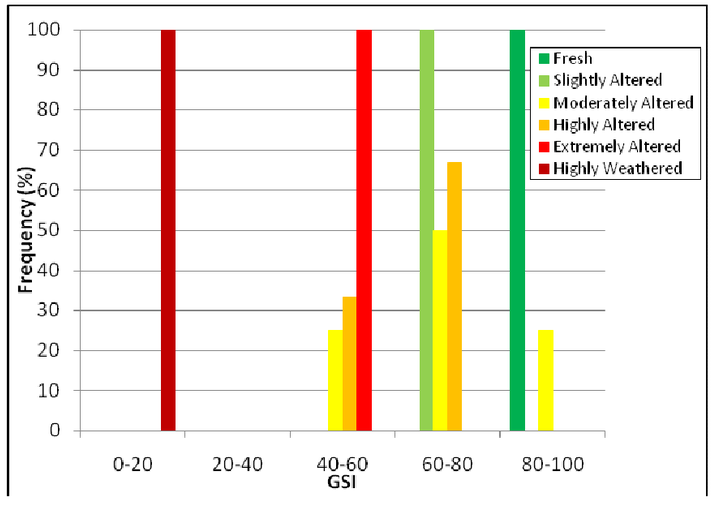

FIGURE 4.21 GSI FOR MARRA MAMBA IRON FORMATION BIF

4.3.4 LOW P BROCKMAN IRON FORMATION SHALE HISTOGRAMS

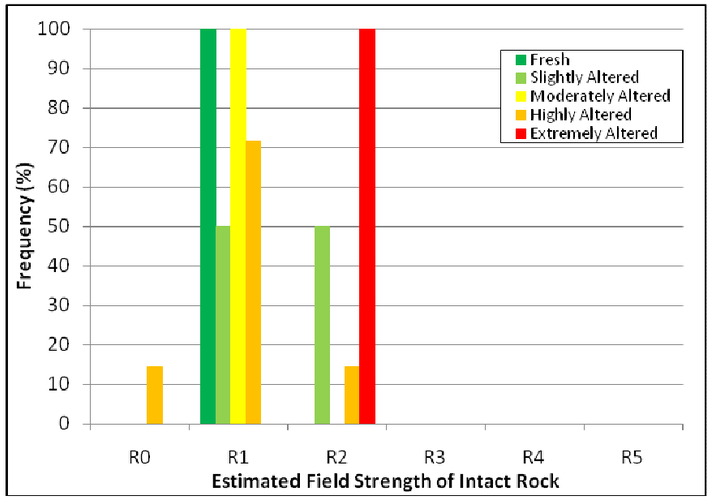

FIGURE 4.22 STRENGTH CLASSIFICATION FOR LOW P BROCKMAN IRON FORMATION SHALE

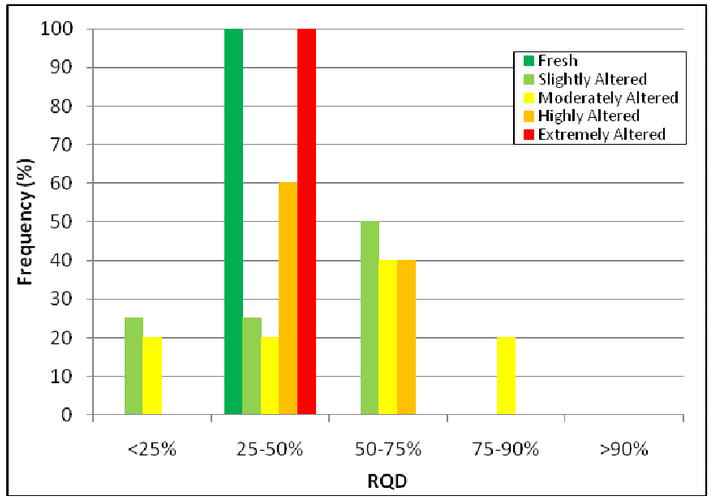

FIGURE 4.23 RQD CLASSIFICATION FOR LOW P BROCKMAN IRON FORMATION SHALE

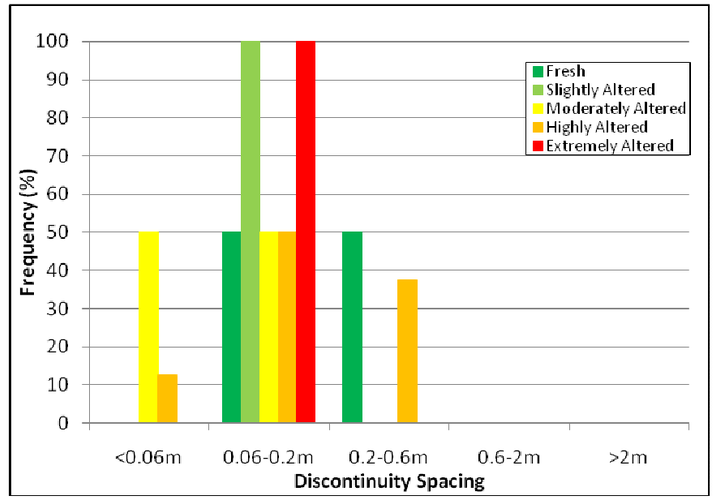

FIGURE 4.24 DISCONTINUITY SPACING CLASSIFICATION FOR LOW P BROCKMAN IRON FORMATION SHALE

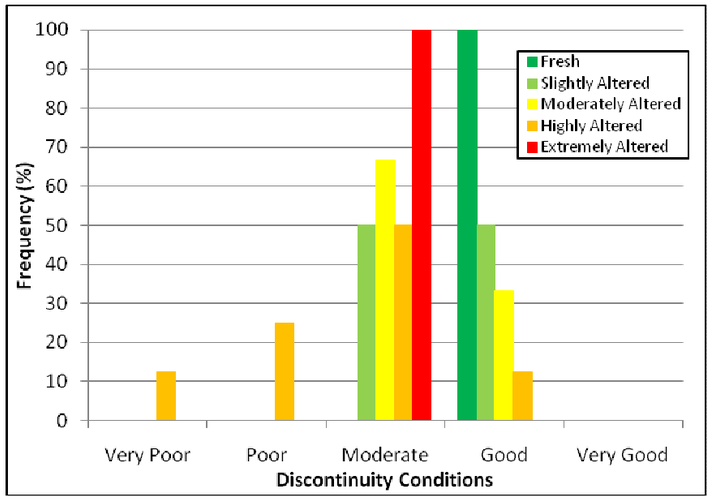

FIGURE 4.25 DISCONTINUITY CONDITION CLASSIFICATION FOR LOW P BROCKMAN IRON FORMATION SHALE

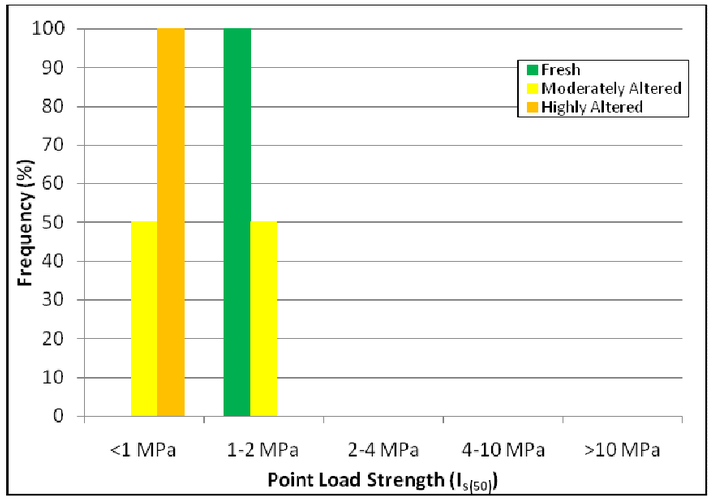

FIGURE 4.26 POINT LOAD TESTING FOR LOW P BROCKMAN IRON FORMATION SHALE

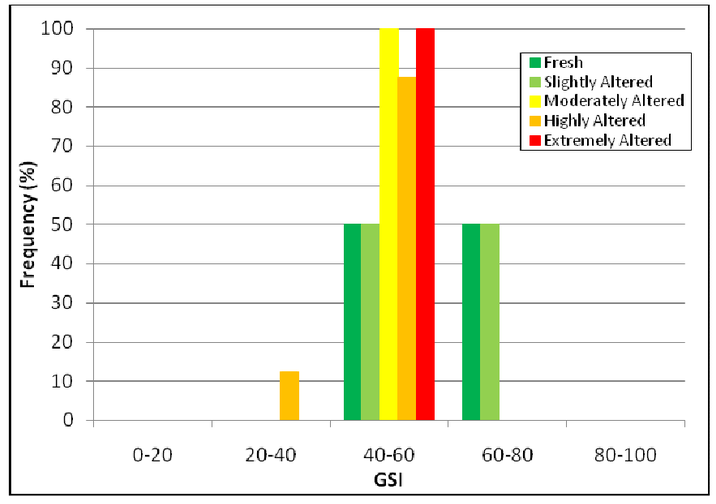

FIGURE 4.27 GSI FOR LOW P BROCKMAN IRON FORMATION SHALE

4.3.5 HIGH P BROCKMAN IRON FORMATION SHALE HISTOGRAMS

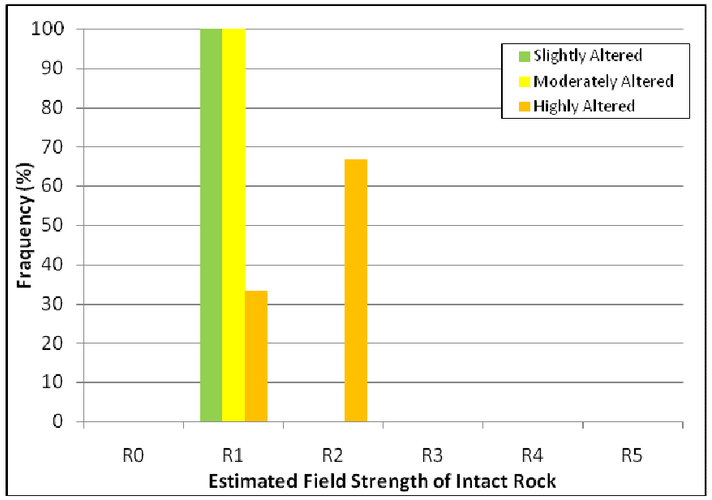

FIGURE 4.28 STRENGTH CLASSIFICATION FOR HIGH P BROCKMAN IRON FORMATION SHALE

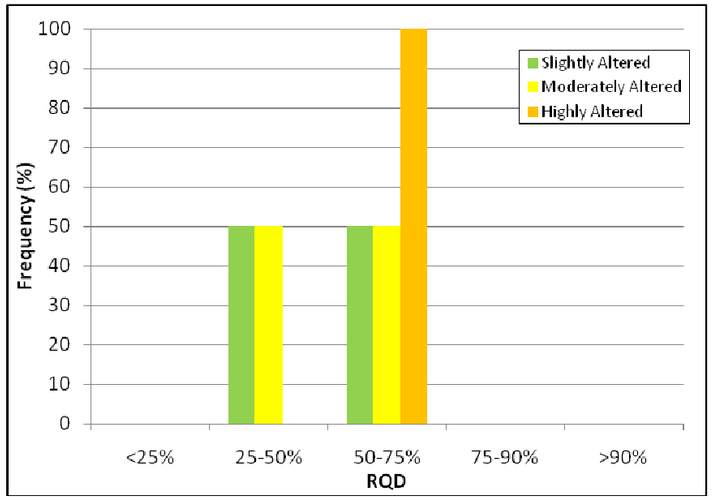

FIGURE 4.29 RQD CLASSIFICATION FOR HIGH P BROCKMAN IRON FORMATION SHALE

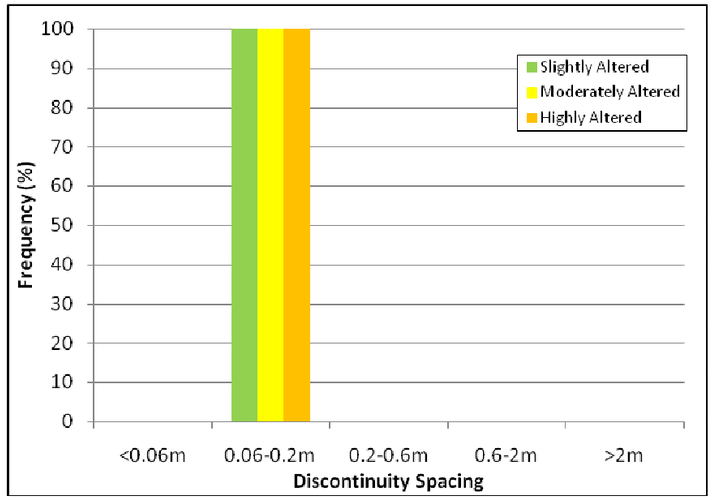

FIGURE 4.30 DISCONTINUITY SPACING CLASSIFICATION FOR HIGH P BROCKMAN IRON FORMATION SHALE

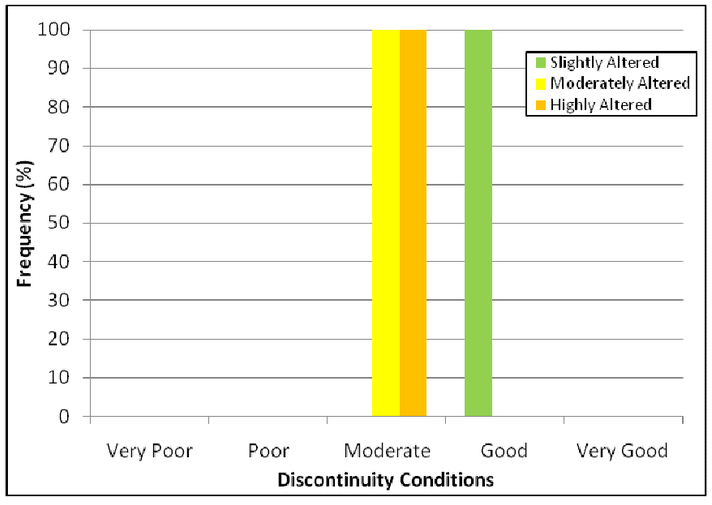

FIGURE 4.31 DISCONTINUITY CONDITION CLASSIFICATION FOR HIGH P BROCKMAN IRON FORMATION SHALE

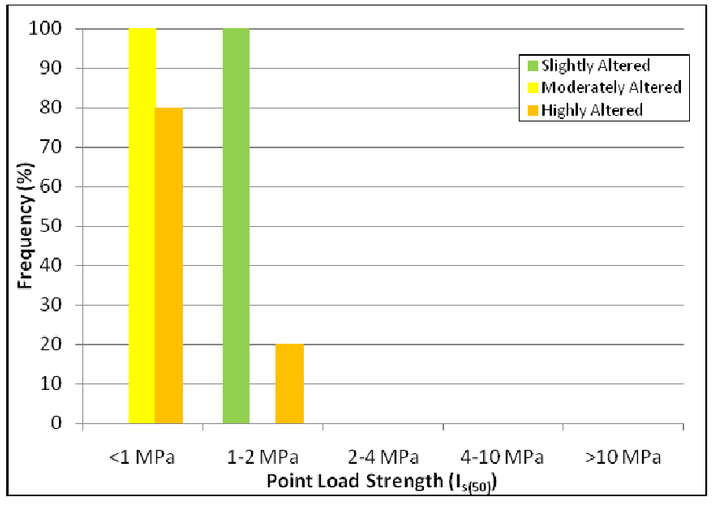

FIGURE 4.32 POINT LOAD TESTING FOR HIGH P BROCKMAN IRON FORMATION SHALE

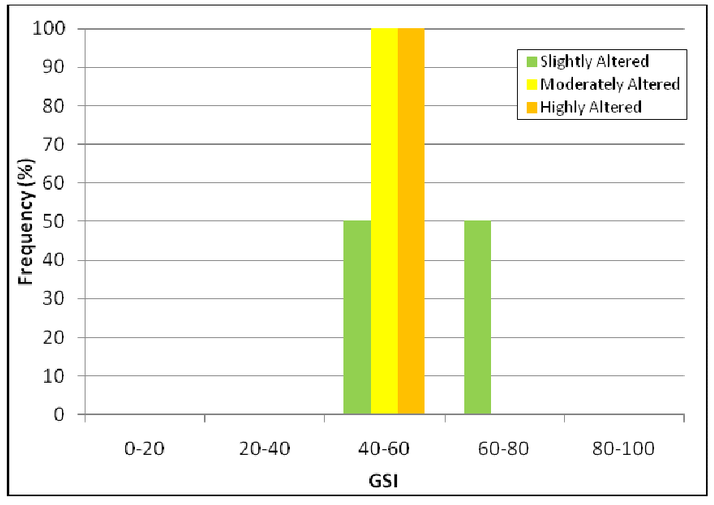

FIGURE 4.33 GSI FOR HIGH P BROCKMAN IRON FORMATION SHALE

4.3.6 MARRA MAMBA IRON FORMATION SHALE HISTOGRAMS

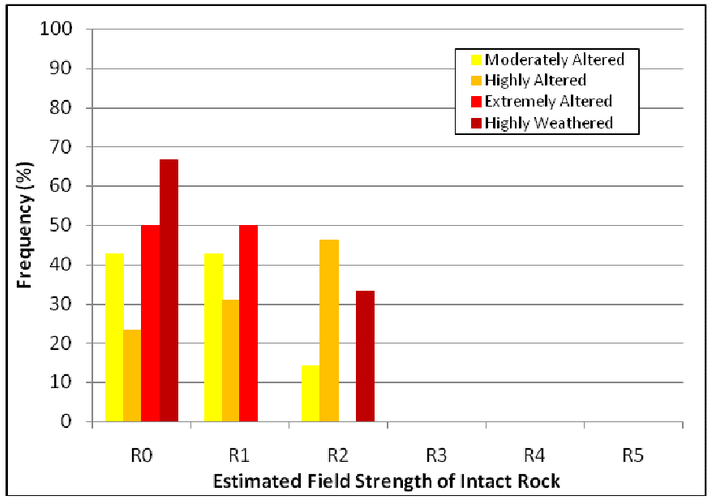

FIGURE 4.34 STRENGTH CLASSIFICATION FOR MARRA MAMBA IRON FORMATION SHALE

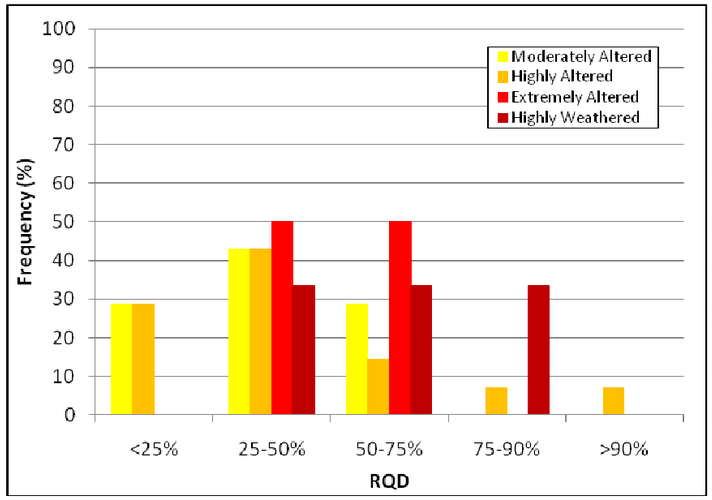

FIGURE 4.35 RQD CLASSIFICATION FOR MARRA MAMBA IRON FORMATION SHALE

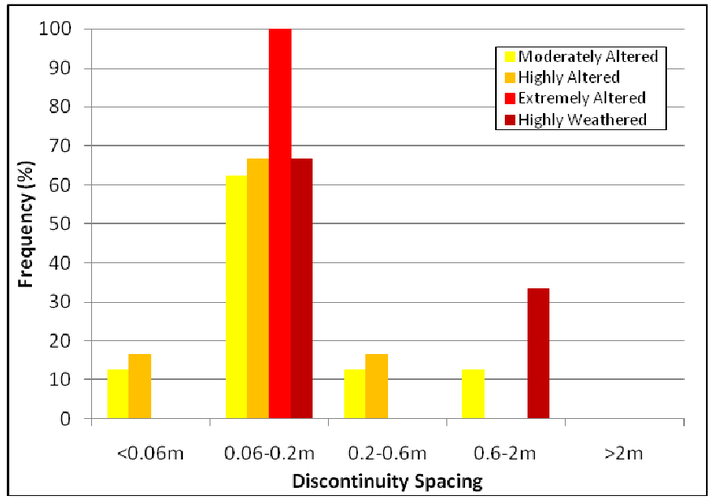

FIGURE 4.36 DISCONTINUITY SPACING CLASSIFICATION FOR MARRA MAMBA IRON FORMATION SHALE

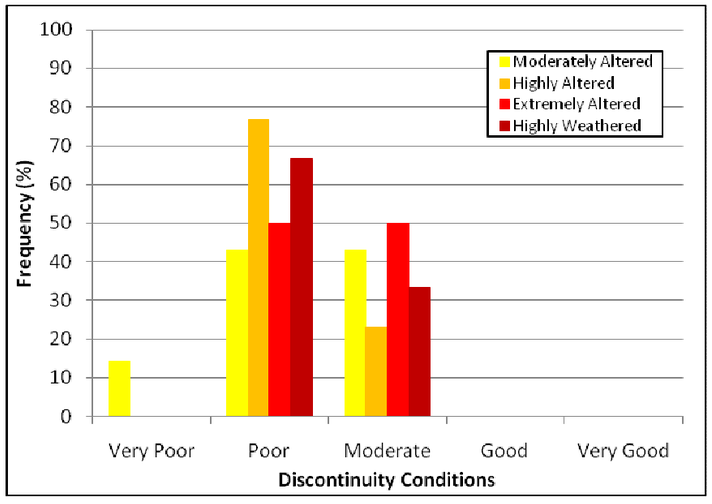

FIGURE 4.37 DISCONTINUITY CONDITION CLASSIFICATION FOR MARRA MAMBA IRON FORMATION SHALE

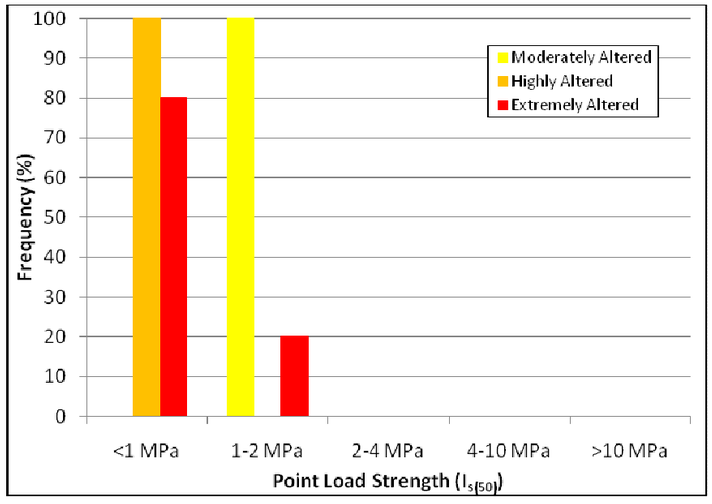

FIGURE 4.38 POINT LOAD TESTING FOR MARRA MAMBA IRON FORMATION SHALE

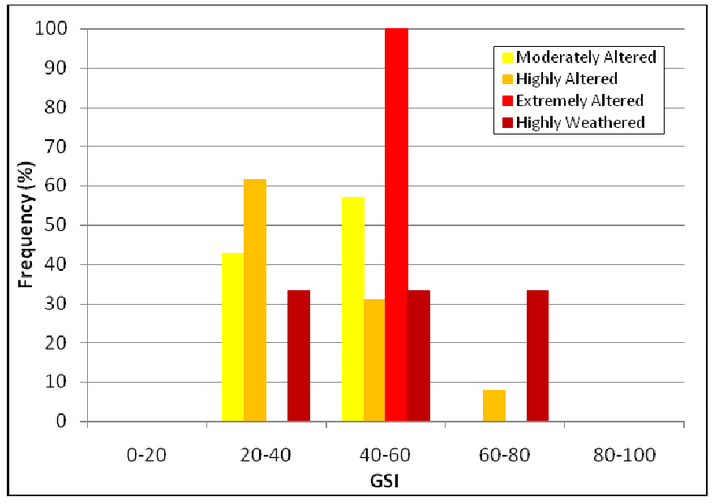

FIGURE 4.39 GSI FOR MARRA MAMBA IRON FORMATION SHALE

4.4 SMR RESULTS

4.4.1 INTACT ROCK STRENGTH

The intact rock strength of each rock type is outlined in the histograms shown previously. The intact rock strength is determined from field descriptions (refer to Figure 4.1). Using a geological hammer or pocket knife, the intact rock strength can be estimated in the field. R0 on the histograms shown previously means that the rock is weak and generally behaves like a soil and has an estimated UCS of <5 MPa. R1 is still weak rock and can be indented with a hammer but peeling with a pocket knife is more difficult. Its estimated UCS is 5 to 25 MPa. R2 is moderately strong rock which requires a firm blow to fracture and has an estimated UCS of 25 to 50 MPa. R3 is strong rock which requires several blows to fracture and has an estimated UCS of 50 to 100 MPa. R4 is very strong rock requiring many blows to fracture and has an estimated UCS of 100 to 250 MPa. And R5 is extremely strong rock which only chips after impact with a geological hammer. It is interpreted to have a large UCS of >250 MPa. R4 and R5 have large error margins when using field descriptions to determine and should be tested in the lab when possible.

The intact rock strength of the BIF is moderately high, ranging from R1 to R4. The low P Brockman Iron Formation BIF studied here has a maximum intact strength at ‘slightly altered’ and decreases in strength with alteration with ‘extremely altered’ BIF having a value of R2. Weathered BIF has an average strength of R3.

The high P Brockman Iron Formation BIF has much lower intact rock strength. No fresh to moderately altered samples were tested here. Highly altered and extremely altered BIF has an average strength of R1 but the strength appears to increase dramatically when weathered with an average strength of R4. Note that the altered rocks here can be compared to the less altered rocks of low P Brockman Iron Formation as they originated from the same material.

Marra Mamba Iron Formation BIF has an average intact rock strength of R4 for fresh and slightly altered BIF. This average rock strength decreases with alteration with extremely altered

rock being dramatically softer with a strength of R1. Highly weathered rock has a very low average strength of R0.

The shale samples have much lower intact strengths of R0 to R2. Low P Brockman Iron shale has an average fresh intact rock strength of R1. Slightly altered shale ranges between R1 and R2 and moderately altered and highly altered has an average strength of R1. Extremely altered shale appears to have increased in strength with a field strength of R2.

In the high P Brockman Iron Formation shale, slightly altered and moderately altered shale have field strengths of R1 and highly altered shale has an increased strength of R2.

The Marra Mamba Iron Formation shale has a moderately altered average strength range of R0 to R1. Highly altered Marra Mamba shale is slightly higher with an average range of R1 to R2 and extremely altered decreases in strength again with an average intact rock strength of R1.

Overall, the fresh to moderately altered BIF is ‘very strong’ to ‘strong’. Intact strength decreases with alteration and highly altered and extremely altered BIF ranges from ‘strong’ to ‘weak’. With weathering, BIF increases in strength in both the low P and high P Brockman Iron Formation deposits, but decreases in strength in the Marra Mamba Iron Formation.

It appears the intact strength of the shale samples changes with increasing alteration in a more complicated fashion. Generally the shale starts as ‘weak’ to ‘moderately strong’ rock and appears to both decrease and increase in intact strength with alteration down to ‘very weak’ rock and up again to ‘moderately strong’ rock. Shale increases in strength with weathering in all three rock types.

4.4.2 **RQD**

RQD is discussed in Section 3.3.2. Generally it is the percentage of intact rock above 10 cm length in drill core (that has not been fractured through the drilling process).

RQD was determined as part of SMR determination and is presented in the histograms above. In both the BIF and shale, RQD ranges greatly.

In the low P Brockman Iron Formation BIF, slightly altered BIF has a very high average RQD of about 90%. The average RQD of moderately altered BIF has decreased with an average of 50% to 75%, and decreases again with further alteration with highly altered BIF having an average RQD of about 50%. Extremely altered BIF, however, has an average RQD of 50% to 75%. And, highly weathered BIF here has an average RQD of about 50%.

In the high P Brockman Iron Formation, fresh BIF has a very high RQD of >90%. As the BIF alters, the average RQD appears to decrease systematically with slightly altered BIF having an average RQD of 75% to 90%, moderately altered BIF having an average RQD of about 75%, highly altered BIF having an average RQD of 50% to 75% and extremely altered BIF having an average RQD of about 50%. Weathering has a very low RQD here of <25%.

Low P Brockman Iron Formation shale has a fresh shale RQD average of 25% to 50%. This increases slightly for slightly altered shale with an average RQD of about 50%. Moderately altered shale has increased in RQD again with an average RQD of 50% to 75%. In highly altered and extremely altered low P Brockman shale, RQD has decreased with an average RQD of about 25% to 50%.

In high P Brockman Iron Formation shale, slightly and moderately altered shale has an average RQD of about 50%. This increases slightly for highly altered shale with an average RQD of 50% to 75%.

Marra Mamba Iron Formation shale has a moderately and highly altered shale average RQD of 25% to 50%. This increases slightly with increased alteration with extremely altered shale having an RQD of about 50%. Highly weathered shale here has an increased average RQD of 50% to 75%.

Overall, the RQD in the BIF in all three rock types appears to mainly decrease with alteration. Weathering in BIF, however, has a very different effect on the different rock types. In low P Brockman Iron Formation BIF, the weathering does not seem to affect the RQD value. In high P Brockman Iron Formation, however, the RQD increases slightly and in the Marra Mamba Iron Formation BIF, RQD has been decreased considerably.

In the shale samples, RQD appears to increase with alteration and weathering in all three rock groups.

4.4.3 SPACING OF DISCONTINUITIES

The average spacing of defects in an outcrop or recovered core is recorded as the "discontinuity spacing" in SMR classification. It is related to RQD and can, hence, be estimated from it (refer to Figure 3.12). The classification falls into 5 separate ranges, from "very wide" at >2 m through to "very close" at <0.06 m (refer to Table 3.7) which can be related to rock mass descriptions of solid rock mass through to massive, blocky/seamy, fractured and crushed/shattered.

An overview of discontinuity spacing throughout the lower Hamersley Group BIF and shale deposits are shown in the histograms above. In BIF, spacing ranges from 'close' to 'wide' and in shale it is mainly 'close' but ranges from 'very close' to 'wide'.

In low P Brockman Iron Formation BIF, the average spacing of slightly altered BIF is 'wide'. Discontinuity spacing decreases as the low P Brockman BIF alters and weathers with moderately altered BIF having a spacing of 'moderate', highly altered BIF having a spacing of 'close' to 'moderate', extremely altered BIF having a average spacing of 'close' and highly weathered BIF having an average spacing of 'close'.

In high P Brockman Iron Formation, moderately altered BIF is described as having an average of 'close' discontinuity spacing while highly altered BIF has an average spacing of 'moderate' and highly weathered high P Brockman BIF having a spacing of 'wide'.

In Marra Mamba Iron Formation, fresh BIF is described as having an average of 'moderate' discontinuity spacing. This decreases to 'close' for slightly altered BIF. In moderately, highly and extremely altered Marra Mamba BIF, however, discontinuity spacing has an average spacing of 'close' through to 'moderate'. In highly weathered Marra Mamba BIF, the discontinuity spacing is 'very close'.

In Low P Brockman Iron Formation shale, fresh shale has discontinuity spacing, on average, of 'close' to 'moderate'. This decreases with alteration with slightly altered shale having an

average spacing of ‘close’, and moderately altered shale having an average spacing of ‘very close’ to ‘close’. Highly altered low P Brockman shale has a range of discontinuity spacing of ‘very close’ through to ‘moderate’ with ‘close’ being the average. And extremely altered Marra Mamba shale is described as having ‘close’ spacing.

In high P Brockman Iron Formation shale, all alteration states have an average discontinuity spacing of ‘close’.

In Marra Mamba Iron Formation shale, moderately, highly and extremely altered shale has an average discontinuity spacing of ‘close’. Highly Weathered Marra Mamba shale has discontinuity spacing ranging from ‘close’ to ‘wide’.

Overall, BIF discontinuity spacing decreases with alteration and can increase or decrease with weathering. The discontinuity spacing of shale, on the other hand, can almost always be described as ‘close’ with minor variations.

4.4.4 CONDITION OF DISCONTINUITIES

Discontinuity conditions is a complex parameter consisting of a general description of the condition of the defects (from ‘very good’ through to ‘good’, ‘moderate’, ‘poor’, and ‘very poor’) from several conditions including discontinuity roughness/filling, separation of the defect, persistence through the rock mass and weathering of the defect walls. Table 3.8 can be used to assist describing these conditions. The SMR rating ranges highly for this parameter, from 0 to 30, suggesting this parameter is very important to the overall rock mass behaviour.

In general ‘very good’ discontinuity conditions can be described as “very rough, non-persistent, closed and unweathered” with decreasing roughness and increasing persistency, openness and weathering with decreasing discontinuity condition until ‘very poor’ conditions are encountered of “soft gouge and >5 mm separation” (refer to Table 3.4).

In low P Brockman Iron Formation BIF, slightly altered rock is described as having ‘good’ rock conditions while moderately altered BIF has, on average, ‘moderate’ to ‘good’ discontinuity

conditions. Highly altered, extremely altered and highly weathered low P Brockman BIF has ‘moderate’ defect conditions.

In high P Brockman Iron Formation BIF, highly altered and extremely altered rock is described as having ‘moderate’ to ‘good’ discontinuity conditions while highly weathered rock has ‘moderate’ conditions.

In Marra Mamba Iron Formation BIF, fresh BIF is described as having ‘very good’ defect conditions. This generally decreases with alteration with slightly altered Marra Mamba BIF being described as having ‘good’ defect conditions, moderately altered and highly altered BIF having, on average, ‘moderate’ to ‘good’ defect conditions and extremely altered BIF as having ‘moderate’ defect conditions. Highly weathered Marra Mamba BIF is described as having ‘very poor’ discontinuity conditions.

In low P Brockman Iron Formation shale, fresh shale is described as having ‘good’ defect conditions. As the alteration increases, the defect conditions decrease with slightly altered low P Brockman shale having an average of ‘moderate’ to ‘good’ conditions, and moderately altered, highly altered and extremely altered shale having ‘moderate’ conditions.

In high P Brockman Iron Formation shale, slightly altered shale is described as having ‘good’ discontinuity conditions while moderate and highly altered high P Brockman shale is described as having ‘moderate’ discontinuity conditions.

In Marra Mamba Iron Formation shale, moderately and highly altered shale is described as having ‘poor’ discontinuity conditions while extremely altered shale is described as having ‘poor’ to ‘moderate’ conditions. Highly weathered Marra Mamba shale is described as having ‘poor’ discontinuity conditions.

Overall, BIF has, on average, ‘very good’ to ‘moderate’ discontinuity conditions with decreasing condition as the rock alters and weathers. The condition tends to decrease to a ‘moderate’ state by the time it is moderately altered and then stays in this condition as it alters further. However, with weathering, Marra Mamba Iron Formation BIF discontinuity conditions become considerably worse with an average rating of ‘very poor’.

A similar relationship is seen in the shale, with decreasing discontinuity condition with alteration from 'good' for fresh and slightly altered shale to 'moderate' and 'poor' as they alter. Marra Mamba shale proves to have worse conditions then the Brockman Iron Formation shale with moderately altered through to highly weathered Marra Mamba shale defect conditions being described as 'poor'.

4.4.5 GROUNDWATER

All of the locations studied are mined above the water table and, therefore, groundwater conditions in all these sites are a possible 'dry' to 'wet' (refer to Table 4.1). Groundwater SMR rating in the study sites were mainly 'completely dry' with a few 'damp' ratings due to staining due to past groundwater flow.

Description	Unfilled Joints		Filled Joints	
	Joint	Flow	Filling	Flow
Completely Dry	Dry	No	Dry	No
Damp	Stained	No	Damp	No
Wet	Damp	No	Wet	Some Drips
Dripping	Wet	Occasional	Outwash	Dripping
Flowing	Wet	Continuous	Washed	Continuous

TABLE 4.1 GROUNDWATER CONDITIONS (ROMANA, 1993)

4.4.6 DEFECT AND SLOPE ORIENTATIONS

The use of defect and slope, dip and dip direction in SMR, is discussed in Section 3.3.6. The dip and dip directions were measured in the field by means of a compass. When core was being investigated, defect alpha and beta angles from core logging was converted to defect dip and dip direction angles using *Rocscience Dips* computer program. Dip and dip direction of slopes were estimated from maps of the mining areas in *Vulcan* 3D computer program. Where slopes have not yet been excavated (Southern Ridge, 23 East Deposit and West Angelas), estimated final slope wall orientations were used.

4.4.7 METHOD OF EXCAVATION

The method of excavation throughout the RTIO open pit mines are mainly excavated by blasting methods and, therefore, incur a SMR value of 0 (refer to Figure 4.1). Pre-splitting and smooth blasting are also used in these mines and have incurred the appropriate SMR value when this has taken place. Some deficient blasting was also encountered in RTIO mines. This was found in many of the areas in Tail Pit, Marandoo. These sites have incurred a SMR value of -8 as deficient blasting contributes negatively to slope stability.

In the analysis of drill core, where the slope has not yet been excavated or finished being excavated (i.e. Southern Ridge, 23 East Deposit and West Angelas), a blasting value of zero was assumed.

4.4.8 GSI

As discussed in Section 3.3.5, GSI is a measure of rock mass strength and is used here to determine how the overall rock mass is affected by alteration and weathering. GSI can be calculated from RMR_{89} using the equation:

$$\mathbf{GSI = RMR_{89}' - 5} \qquad \mathbf{(4.1)}$$

This calculation is from Hoek, Kaiser and Bawden (1995) where the RMR_{89} classification scheme is used to calculate rock mass strength by modifying RMR_{89} by fixing the groundwater as 'dry' (at a rating of 15), adjustment to joint orientation is set at 'very favourable' (at a rating of 0) and by reducing the final product by 5. This equation can be used for $RMR_{89}'>23$; for $RMR_{89}'<23$, Barton, Lein and Lunde's (1974) Q' system (discussed in Section 3.3.3) should be used instead (Hoek at al., 1995).

GSI has been calculated from the SMR results and are presented for each rock group in the histograms above. An overview of GSI is also presented in Figure 4.39 and Figure 4.40.

GSI ranges from 0 to 100 and is presented in the histograms in five groups of 0 – 20 GSI, 20 – 40 GSI, 40 – 60 GSI, 60 – 80 GSI and 80 – 100 GSI values. These groups generally represent 'very poor', 'poor', 'moderate', 'good' and 'very good' overall rock mass strengths respectively.

BIF in the lower Hamersley Group generally has ‘moderate’ to ‘very good’ GSI. But can also have ‘very poor’ GSI. And shale of the lower Hamersley Group Iron Formations usually has between 20 and 80 GSI.

In low P Brockman Iron Formation BIF, slightly and moderately altered BIF has ‘good’ GSI. Highly altered BIF has a decreased GSI down to ‘moderate’ and extremely altered BIF has a slightly higher GSI of ‘good’. Highly weathered low P Brockman BIF has an average GSI of ‘moderate’.

In high P Brockman Iron Formation BIF, highly and extremely altered BIF has an average of ‘moderate’ GSI values. Highly weathered high P Brockman BIF has an average GSI of ‘good’.

In Marra Mamba Iron Formation BIF, fresh BIF has a ‘very good’ GSI value while slightly altered, moderately altered and highly altered BIF all have average GSI values of ‘good’. Extremely altered BIF, however, has a highly decreased GSI value of ‘very poor’. Highly weathered Marra Mamba BIF also has a very low average GSI value of ‘very poor’.

In low P Brockman Iron Formation shale, fresh and slightly altered shale has a GSI of between ‘moderate’ and ‘good’ while moderately altered, highly altered and extremely altered shale has an average GSI of ‘moderate’.

In high P Brockman Iron Formation shale, slightly altered shale has an average GSI of ‘moderate’ to ‘good’ while moderately and highly altered shale have average GSI values of ‘moderate’.

In Marra Mamba Iron Formation BIF, moderately altered shale has an average GSI of ‘moderate’, highly altered shale has a slightly lower average GSI value of ‘poor’ while extremely altered shale has an increased GSI of ‘moderate’. Highly weathered Marra Mamba shale has a high range of GSI values from ‘poor’ through to ‘good’.

Overall, BIF has generally high GSI values, dipping slightly with alteration and may or may not decrease with weathering. An exception to this, however, is the extremely altered and highly weathered Marra Mamba Iron Formation BIF, which decrease in GSI dramatically from the fresher products.

Shale in the lower Hamersley Group is generally 'good' to 'moderate' with slight decreases in GSI in more heavily altered shale. Weathering in the shale, which is only detailed in the Marra Mamba Iron Formation, appears to increase and decrease the GSI of the initial rock mass as shown by the wide range of GSI values.

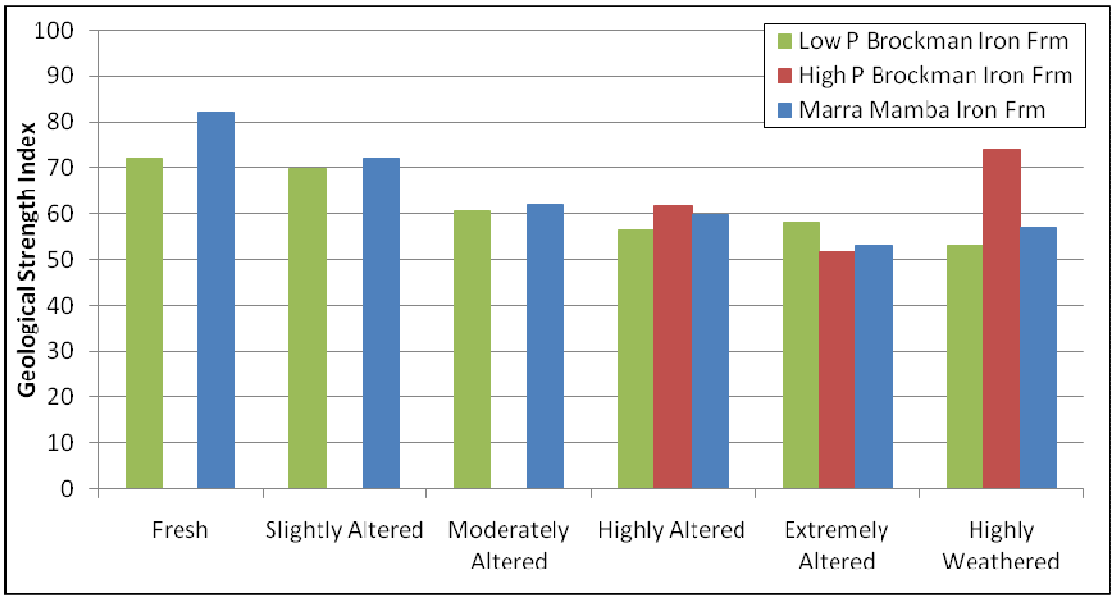

FIGURE 4.40 AN OVERVIEW OF THE GSI RESULTS OF THE LOWER HAMERSLEY GROUP BIF SAMPLES

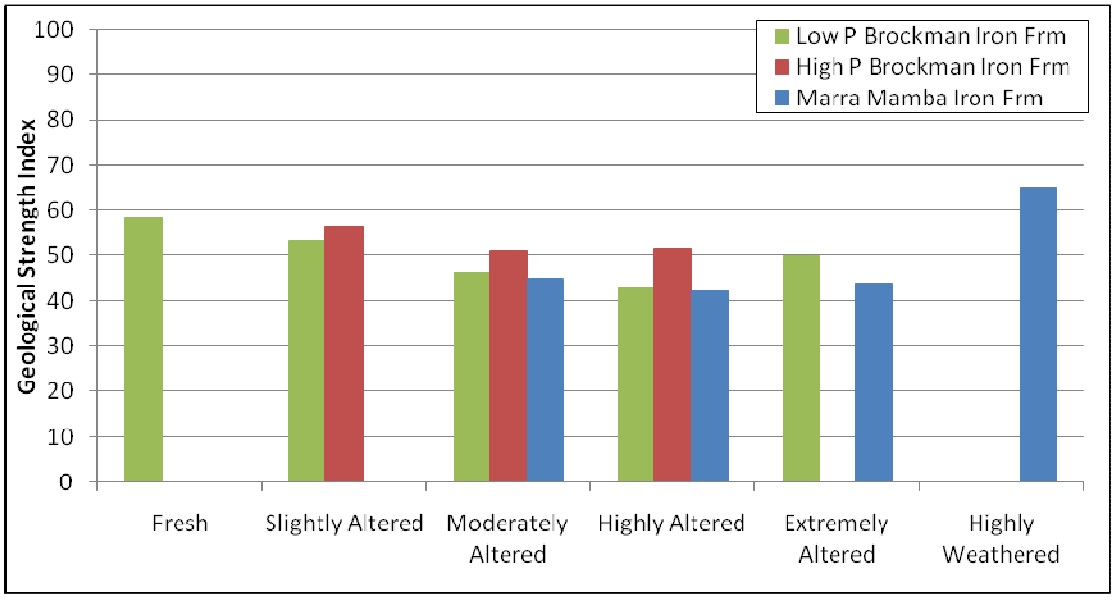

FIGURE 4.41 AN OVERVIEW OF THE GSI RESULTS OF THE LOWER HAMERSLEY GROUP SHALE SAMPLES

4.5 LABORATORY TESTING RESULTS

4.5.1 POINT LOAD TESTING

Point load testing was completed for samples of BIF and shale under ISRM (1985) standards. Axial, diametral and irregular lump testing was completed on 10 or more samples, where possible, on each rock being tested (refer to Appendix IV for point load testing results).

The size corrected Point Load Strength Index ($I_{s(50)}$) was calculated and averaged for each sample (disregarding the highest and lowest results where 10 or more samples were tested). UCS was also estimated from the point load indices using:

$$\mathbf{UCS = 24\ I_{S(50)}} \qquad \mathbf{(4.2)}$$

for BIF samples and:

$$\mathbf{UCS = 15\ I_{S(50)}} \qquad \mathbf{(4.3)}$$

for shale samples.

The multipliers of 24 for BIF and 15 for shale, to calculate UCS from $I_{s(50)}$, were estimated from previous point load testing of Hamersley Group rocks. It should be noted that for low point load indices of <1 MPa, point load testing becomes unreliable and UCS testing is preferred to determine the intact rock strength.

The point load test results are shown in the above histograms for each rock type as $I_{s(50)}$ and is divided into 5 categories of <1 MPa, 1 to 2 MPa, 2 to 4 MPa, 4 to 10 MPa and >10 MPa.

Both BIF and shale in the Hamersley Province proved to have a wide range of point load strength indices with BIF ranging between <1 MPa to 4 – 10 MPa and shale ranging between <1 MPa to 2 MPa.

In low P Brockman Iron Formation BIF, slightly altered BIF ranges from <1 MPa to 4 – 10 MPa. Moderately altered BIF has an average point load index of 4 – 10 MPa. Highly altered BIF has a slightly lower average of 2 – 4 MPa and extremely altered BIF has a slightly lower average again of between <1 MPa and 2 – 4 MPa. Highly weathered low P Brockman BIF has an average point load strength index of between 1 and 4 MPa.

In high P Brockman Iron Formation BIF, highly and extremely altered BIF have an average point load strength index of 4 – 10 MPa while highly weathered BIF has a range of between <1 MPa and 4 – 10 MPa.

In Marra Mamba Iron Formation BIF, fresh and slightly altered BIF has a point load strength index of 4 – 10 MPa. Moderately and highly altered BIF have a lower average point load index of 2 – 4 MPa while extremely altered BIF has a point load index range of between <1 MPa and 4 – 10 MPa. Highly weathered Marra Mamba BIF has a low point load strength index of <1 MPa.

In low P Brockman Iron Formation shale, fresh shale has a point load strength index of between 1 – 2 MPa, moderately altered shale has a point load index of <1 to 2 MPa and highly altered, again, has a decreased point load strength index of <1 MPa.

In high P Brockman Iron Formation shale, slightly altered shale has a point load strength index of 1 – 2 MPa, moderately altered shale has a point load index of <1 MPa and highly altered shale has an average point load strength index of <1 MPa.

In Marra Mamba Iron Formation shale, moderately altered shale has a point load strength of 1 – 2 MPa and highly and extremely altered shale has an average point load strength of <1 MPa.

Overall, lower Hamersley Group BIF has a wide range of point load strength indices over the alteration states but mainly decreases with alteration and either stays similar when weathered or, otherwise, decreases.

Shale in the Lower Hamersley Group has much lower point load strength indices and a smaller range. As alteration increases in the shale, the point load strength indices decrease to low values.

An overview of the average point load testing results (in UCS) of each alteration state, from fresh to extremely altered and highly weathered, is given for each rock type in Figures 4.41 and 4.42.

Figure 4.41 shows the average point load strength (calculated for UCS) for BIF. It clearly shows that BIF decreases in strength with alteration and weathering in all three rock groups. Low P

Brockman Iron Formation BIF reaches a low at extremely altered BIF while both low P and high P Brockman Iron BIF have low strengths at highly altered and highly weathered as well. Marra Mamba Iron Formation BIF has low strengths from moderately altered right through until extremely altered and highly weathered BIF.

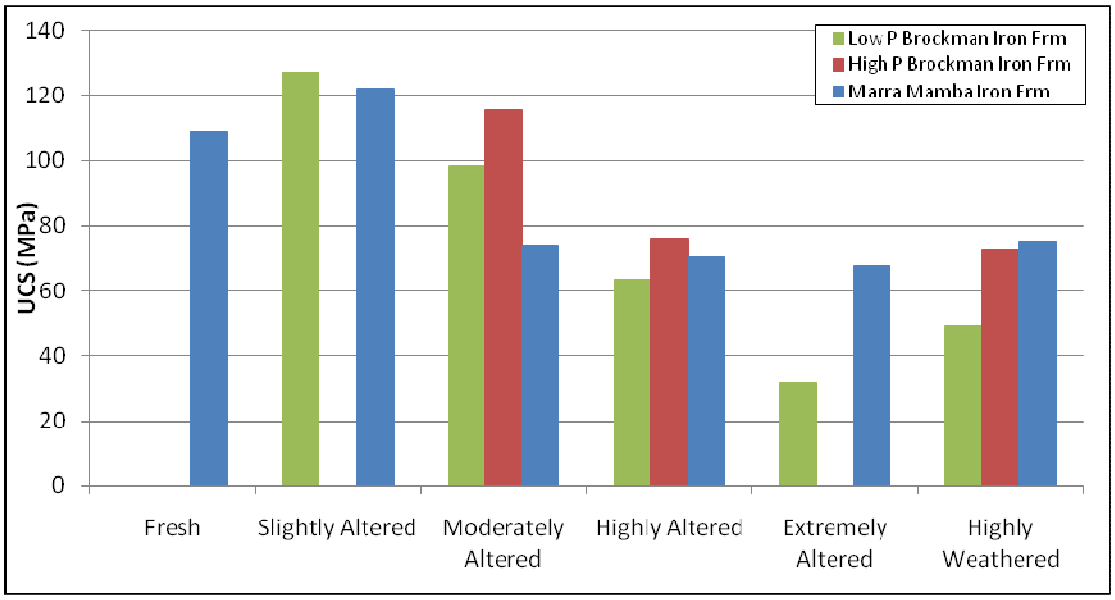

FIGURE 4.42 AN OVERVIEW OF POINT LOAD TESTING RESULTS (UCS) FOR THE LOWER HAMERSLEY GROUP IRON FORMATION BIF SAMPLES

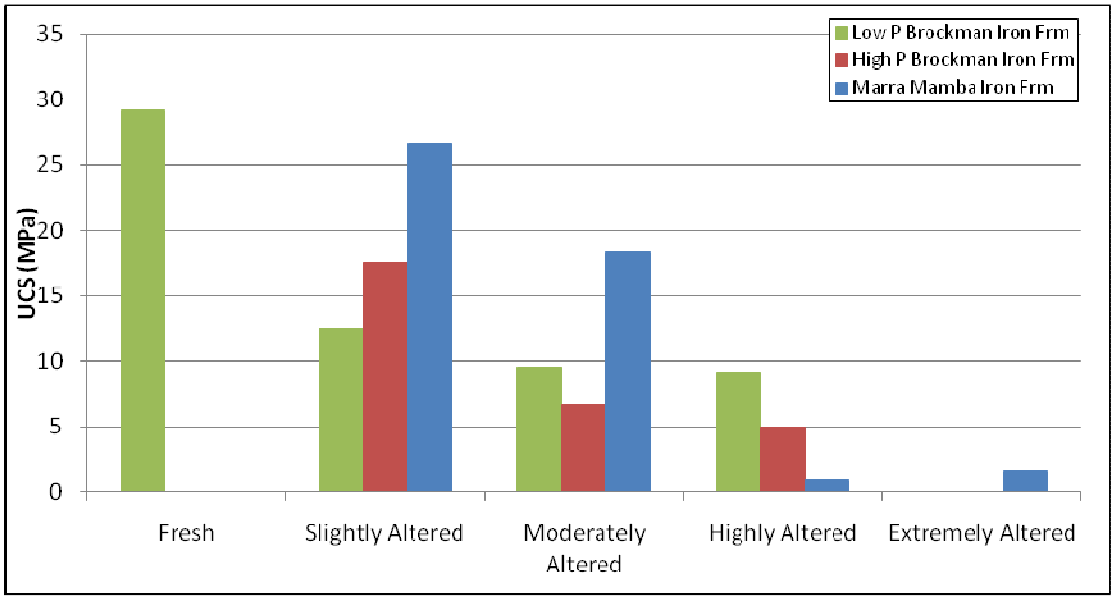

FIGURE 4.43 AN OVERVIEW OF POINT LOAD TESTING RESULTS (UCS) FOR THE LOWER HAMERSLEY GROUP IRON FORMATION SHALE SAMPLES

Figure 4.43 shows an overview of the average point load strength results (calculated for UCS) of shale. It clearly shows how shale decreases in strength with alteration. Low P and high P Brockman Iron Formation shale has reasonably low strength values from moderately altered to highly altered shale while Marra Mamba Iron Formation shale has dramatically low strength values at highly and extremely altered shale.

4.5.2 SLAKE DURABILITY TESTING

Slake durability testing was undertaken on 26 BIF and shale samples from throughout the Hamersley Province. Slake durability testing involves taking 10 roughly spherical rock samples of 40 to 60 grams and putting them into a drum (of weight 'D') of specific dimensions (refer to ISRM, 1981), weighing the sample in the drum (A) and immersing the drum partially in water. The drum is then turned at a constant rate of 20 rpm for 10 minutes. The sample and drum is then taken out of the water, dried and weighed (B). This cycle is repeated to get a second dried sample weight (C). The full procedures can be found in ISRM (1981). The slake durability index (second cycle) (I_{d2}) is calculated as the percentage ratio of final to initial dry sample weight as defined by:

$$\mathbf{I_{d2} = \frac{C-D}{A-D} \times 100\%} \quad \textbf{(4.4)}$$

The full calculations for slake durability testing performed in this study can be located in Appendix VI. An overview of the average slake durability (second cycle) results of BIF and shale are given in Figure 4.43 and Figure 4.45, respectively.

The durability of BIF (as shown in Figure 4.43) is very high. It decreases slightly with moderate and high alteration and more dramatically in extremely altered samples, especially in the high P Brockman Iron Formation BIF. Highly weathered BIF samples also have a slightly lower durability than fresh BIF.

The durability of shale (as shown in Figure 4.45) is high. With slight and moderate alteration, the durability of shale decreases slightly. The durability decreases much more dramatically in the highly altered shale as can be seen in the low P Brockman Iron Formation shale.

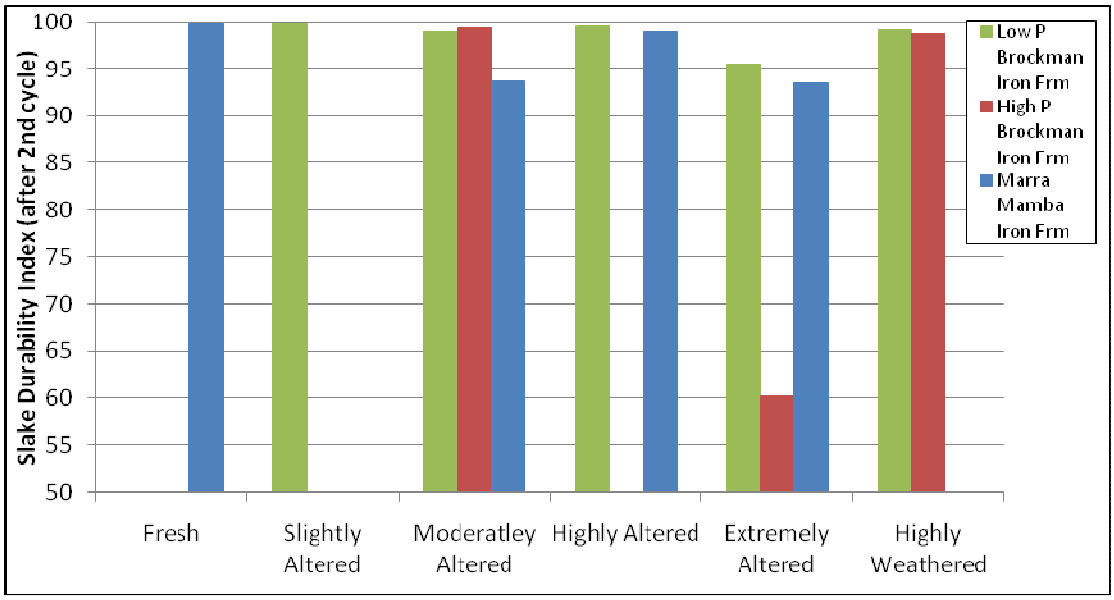

FIGURE 4.44 AN OVERVIEW OF THE SLAKE DURABILITY INDICES CALCULATED AFTER THE SECOND CYCLE FOR THE LOWER HAMERSLEY GROUP IRON FORMATION BIF SAMPLES

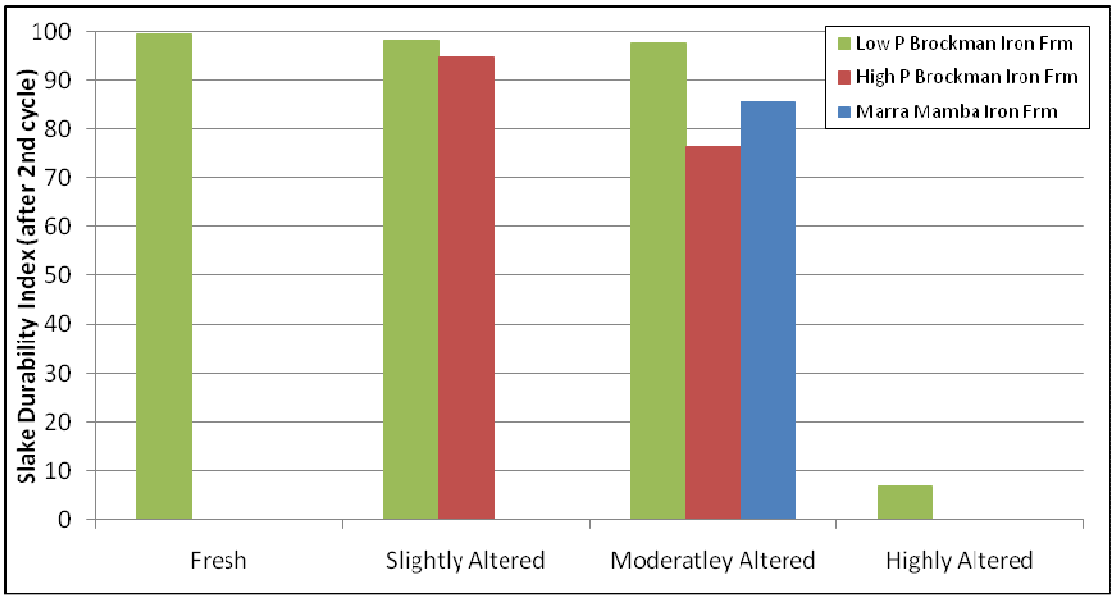

FIGURE 4.45 AN OVERVIEW OF THE SLAKE DURABILITY INDICES CALCULATED AFTER THE SECOND CYCLE FOR THE LOWER HAMERSLEY GROUP IRON FORMATION SHALE SAMPLES

4.6 SYNTHESIS

The geotechnical character that ultimately affects rock slope stability in RTIO open pit mines includes parameters such as intact rock strength, RQD, discontinuity spacing, discontinuity conditions, groundwater conditions, discontinuity orientations against slope orientations, and excavation methods. The geotechnical parameters that are affected by alteration and weathering of the rock mass include intact rock strength (as estimated in the field or determined through laboratory testing such as point load testing), RQD, discontinuity spacing, discontinuity condition, and durability (which estimates erodability). These parameters are estimated and measured here to determine how each geotechnical parameter is affected by alteration and weathering of the lower Hamersley Group Iron Formations BIF and shale samples.

4.6.1 BIF

Intact rock strength was estimated in the field through SMR and was verified by the use of point load strength index through laboratory testing. It showed that intact rock strength of BIF is mostly high but decreases especially in highly and extremely altered BIF of all three rock groups. It also decreases in much of the highly weathered BIF of the lower Hamersley Group Iron deposits.

RQD was estimated in the field and through core logging. It was lowest in highly and extremely altered BIF of the Brockman Iron Formation and in extremely altered and highly weathered BIF of the Marra Mamba Iron Formation. Defect spacing was low in a wide range of lower Hamersley Group BIF, especially in the extremely altered and highly weathered BIF of the low P Brockman Iron Formation and the Marra Mamba Iron Formation. Defect conditions were reasonably moderate to good in all three rock groups with highly altered BIF having the worst defect conditions in the Brockman Iron Formation and extremely altered and highly weathered having “very bad” defect conditions in the Marra Mamba Iron Formation.

GSI, which brings all of the above parameters together in a weighted sum to estimate the overall rock mass strength, shows the overall rock mass character. GSI shows that highly altered

and extremely altered BIF, in all three rock groups, has the lowest GSI with “moderate” and “moderate to good” results. Highly weathered BIF was found to have “very poor” GSI in the Marra Mamba Iron Formation but was found to have “moderate” GSI in low P Brockman Iron Formation and “good” GSI in high P Brockman Iron Formation. An overview of the average GSI ratings of each rock type over each alteration state (Figure 4.40) shows that the GSI of each rock group decreases with alteration with fresh and slightly altered BIF having high average GSI values of above 70 and this decreases to around 60 for moderately and highly altered BIF and between 50 and 60 for extremely altered BIF. Highly weathered BIF ranges between above 70 for high P Brockman Iron BIF and below 60 for low P Brockman Iron Formation and Marra Mamba Iron Formation.

Slake Durability testing, which estimates the effect of erosion on a rock mass, shows BIF is very durable in all three rock groups of the lower Hamersley Group Iron deposits, but can decrease reasonably dramatically in some extremely altered rock masses.

4.6.2 SHALE

From field estimated intact rock strength at RTIO mines, shale has mostly “low” intact rock strength with Marra Mamba Iron Formation shale having “very low” intact strengths. From point load testing results, highly altered shale is shown to be the weakest in all three rock groups along with moderately altered shale of the Brockman Iron Formation and extremely altered shale of the Marra Mamba Iron Formation.

RQD was investigated in the field and through core logging. RQD was similar in all three rock groups with average ranging between 25% and 75%. Defect spacing throughout all three rock groups average “close” with highly weathered shale in Marra Mamba Iron Formation averaging slightly higher. Defect conditions are, on average, “moderate” in the moderately altered to extremely altered shale of the Brockman Iron Formation and “moderate” to “bad” in the moderately altered to extremely altered and highly weathered Marra Mamba Iron Formation shale.

GSI, which estimates the total geological strength from the above parameters, shows that the lowest GSI values are in moderately to extremely altered shale of all three rock groups with an average of “moderate” GSI values for Brockman Iron Formation shale and “moderate” to “bad” in the Marra Mamba Iron Formation. Highly weathered Marra Mamba Iron Formation had much higher GSI than any other shale.

Slake durability of the shale was limited but showed that the durability of shale was quite high but lowest when highly altered.

4.7 CONCLUSIONS

Several general conclusions can be made from the geotechnical investigation of lower Hamersley Group Iron Formation BIF and shale in the RTIO mines of Western Australia. These are:

- Field and laboratory studies of the geotechnical character of BIF and shale throughout the lower Hamersley Group deposits give an understanding of rock mass conditions throughout the RTIO mines as the deposits change with alteration and weathering;
- The geotechnical investigation at RTIO mines show that, in general, BIF and shale decrease in intact rock strength, RQD percentage, defect spacing and defect conditions, as well as decreasing in point load strength index and slake durability index as they alter with the worst conditions when highly and extremely altered conditions are encountered;
- BIF has generally good geotechnical conditions, however, highly altered and extremely altered BIF appears to have “moderate” rock mass conditions;
- Highly weathered low P Brockman Iron Formation BIF and Marra Mamba Iron Formation BIF appears to have, on average, “moderate” rock mass conditions;
- Shale has generally poor geotechnical conditions with moderate to extremely altered shale having overall, “moderate” rock mass conditions in the Brockman Iron Formation shale and “moderate to bad” rock mass conditions in the Marra Mamba Iron Formation shale;
- Weathering in lower Hamersley Group Iron deposits appears to sometimes make the BIF and shale rock masses stronger.

5 GEOCHEMICAL AND MINERALOGICAL INVESTIGATION

5.1 OVERVIEW

In investigating geochemistry and mineralogy, we are essentially investigating the 'fingerprints' and the 'DNA' of the rocks that we are studying. Such detailed investigations give us a unique insight into the rocks history and helps us to understand its complex origin and evolution. In the RTIO mines, in the lower Hamersley Group Iron deposits, areas of BIF and shale have been geochemically and mineralogically altered and weathered through hypogene and supergene alteration and recent weathering processes.

Geochemical and mineralogical investigations of selected areas in RTIO mines have been undertaken in this study with the aim to:

- Classify the geochemical and mineralogical signatures of the lower Hamersley Group Iron Formation BIF and shale deposits, in RTIO mines, as they alter and weather.

Geochemical investigations include major and minor XRF analysis and mineralogical investigations include XRD and microscope analysis.

45 samples were chosen for XRD and XRF analyses to give an average representation of both BIF and shale deposits throughout the lower Hamersley Group deposits, concentrating on areas within and directly adjacent the Brockman Iron Formation and Marra Mamba Iron Formation deposits. The rocks chosen are all commonly found within the pit walls of RTIO open pit mines.

Twelve rock samples were also chosen for microscopic analysis and encompass a range of alteration and weathering states over both the Brockman Iron Formation and the Marra Mamba Iron Formation.

5.2 METHODS

5.2.1 X-RAY FLUORESCENCE ANALYSIS

X-Ray Fluorescence Spectrometry involves using high energy x-rays to excite a material such as a powdered rock sample. This induces more x-rays to be given off the material. The wavelengths emitted are measured and analysed. These wavelengths are characteristic to specific chemicals and, therefore, enable the chemical make-up of the material to be identified. The abundance of each chemical element is determined by the intensity of the wavelengths. This technique is useful for identifying elements atomically heavier then sodium and for proportions from 100% down to a few parts per million.

In this study, a Phillips PW2400 sequential wavelength dispersive X-ray fluorescence spectrometer was used to analyse fresh to highly altered and highly weathered BIF and shale samples from the lower Hamersley Group Iron Formations.

The concentration of major minerals were measured in weight percent (Wt%) of its oxide and minor minerals were measured in parts per million (ppm). The major and minor minerals studied ranged from Boron to Uranium.

5.2.2 X-RAY DIFFRACTION ANALYSIS

X-Ray Diffraction involves using the light scattering effect of x-rays off crystal systems of powdered rock crystals. These x-rays reflect off the sample and scatter in many directions, of which, the angles are measured and analysed. Every crystal system has its own characteristic light scattering properties which are used to detect the minerals present in a rock sample and the magnitude of these wavelengths are used to estimate the proportions of each of the minerals present.

In this study, a Phillips PW 1840/1710 x-ray diffractor was used to determine the crystalline components that make up fresh to weathered lower Hamersley Group BIF and shale deposits.

5.2.3 TRANSMITTED AND REFLECTED MICROSCOPIC ANALYSIS

Transmitted and reflected microscopic analysis was used in this study to give an average representation of lower Hamersley Group Iron Formations BIF and shale in different alteration and weathering states.

Optical microscopy analysis was performed on 30 micrometer polished thin sections of 12 typical rock samples including 4 Brockman Iron Formation BIF samples, 4 Marra Mamba Iron Formation BIF samples and 4 Brockman Iron Formation shale samples.

Transmitted microscopic analysis was performed using a Leica DMXRD polarising microscope. Reflected microscopy was used for the more metallic samples using a Leitz Ortholux POL-BK. Photos were taken using a Leica Q500MC camera and Motic Images v-3.2 digital imaging software.

5.3 RESULTS

5.3.1 XRF AND XRD

Throughout the four areas studied, 24 BIF samples and 21 shale samples were collected and chosen for XRF and XRD analysis. Of these, 16 BIF samples and 13 shale samples (including 5 shale samples from the Mount McRae Shale Formation which lies directly underneath the Dales Gorge member) came from the vicinity of the Brockman Iron Formation and 8 BIF and 9 shale samples come from the vicinity of the Marra Mamba Iron Formation (including 1 BIF and 5 shale samples that come from the West Angelas Shale Member which lies directly above the Mount Newman Member).

The results of XRF major and minor elements analyses are presented in Tables 5.1 and 5.2, respectively. The results of XRD mineral analysis is presented in Table 5.3. An analysis of the XRF and XRD results is given in Section 5.4.

Sample ID	Lithology	SiO_2	TiO_2	Al_2O_3	Fe_2O_3T	MnO	MgO	CaO	Na_2O	K_2O	P_2O_5	LOI	Total
MDO-02	MOUNT NEWMAN BIF	1.59	0.02	0.44	88.95	0.02	<0.05	0.13	0.34	0.06	0.17	7.22	98.94
MDO-12	MOUNT NEWMAN BIF	0.89	0.02	0.59	91.4	0.03	<0.05	<0.1	<0.1	<0.01	0.15	6.32	99.42
PDO-23-04	JOFFRE BIF	1.89	0.04	1.2	92.43	0.03	<0.05	0.08	<0.1	0.01	0.17	3.33	99.17
PDO-23-05	JOFFRE BIF	25.69	0.05	0.85	70.36	0.05	<0.05	0.07	<0.1	0.02	0.04	2.11	99.25
PDO-23-06	JOFFRE BIF	36.69	0.03	0.53	60.52	0.03	<0.05	0.07	<0.1	0.02	0.03	1.18	99.09
PDO-23-11	DALES GORGE BIF	22.09	0.02	0.53	74.11	0.02	<0.05	0.06	<0.1	0.02	0.09	2.47	99.4
PDO-23-12	DALES GORGE BIF	48.26	0.02	<0.2	47.88	0.01	<0.05	0.06	<0.1	0.02	0.11	2.25	98.6
TP-NTD-02	DALES GORGE BIF	0.68	0.03	0.4	96.15	0.02	<0.05	0.06	<0.1	0.01	0.13	2.47	99.96
TP-NTD-03	DALES GORGE BIF	0.30	0.02	<0.2	98.85	0.01	<0.05	0.06	<0.1	0.01	<0.01	0.67	99.92
TP-SSEV-02	DALES GORGE BIF	0.78	0.03	0.52	95.45	0.03	<0.05	0.05	<0.1	<0.01	0.19	2.3	99.33
TP-SSEV-06	DALES GORGE BIF	44.96	0.02	<0.2	52.85	0.02	<0.05	0.05	<0.1	0.03	0.05	1.22	99.19
TP-SSEV-10	DALES GORGE BIF	17.15	1.06	9.36	60.03	<0.01	<0.05	0.05	<0.1	<0.01	0.08	12.16	99.9
TP-SSEV-10	DALES GORGE BIF	39.61	0.91	8.91	40.71	<0.01	<0.05	0.05	<0.1	0.01	0.06	8.99	99.03
TP-STR-01	DALES GORGE BIF	0.34	0.02	0.24	97.66	0.03	<0.05	0.07	<0.1	0.01	0.08	1.31	99.78
TP-STR-11	DALES GORGE BIF	60.60	0.02	<0.2	37.67	0.02	<0.05	0.12	<0.1	<0.01	0.08	0.57	99.07
TP-STR-12	DALES GORGE BIF	4.58	0.03	0.26	93.12	0.14	<0.05	0.06	<0.1	0.01	0.03	0.99	99.23
TP-STR-15	DALES GORGE BIF	59.93	0.01	<0.2	38.67	0.01	<0.05	0.15	<0.1	0.04	0.05	0.47	99.33
TP-STR-17	DALES GORGE BIF	0.68	0.02	0.32	96.14	0.02	<0.05	0.14	0.32	0.07	0.15	1.1	98.95
WA-07-07	WEST ANGELAS SHALE BIF	1.80	0.05	1.52	85.46	0.1	<0.05	0.06	<0.1	<0.01	0.06	10.32	99.36
WA-07-10	MOUNT NEWMAN BIF	0.77	0.02	0.39	93.5	0.05	<0.05	0.13	0.34	0.06	0.12	3.95	99.33
WA-07-12	MOUNT NEWMAN BIF	22.31	0.02	0.38	72.34	0.03	<0.05	0.06	<0.1	0.01	0.09	4.23	99.47
WA-07-14	MOUNT NEWMAN BIF	44.42	0.02	<0.2	52.08	0.01	<0.05	0.06	<0.1	0.01	0.1	2.57	99.26
WA-07-24	MOUNT NEWMAN BIF	32.26	0.03	0.28	63.85	0.01	<0.05	0.14	0.21	0.05	0.13	2.49	99.45
WA-07-25	MOUNT NEWMAN BIF	59.38	0.02	<0.2	30.28	0.04	1.85	3.28	0.15	0.12	0.02	4	99.13
MDO-04	MOUNT NEWMAN SHALE	42.54	0.15	34.41	7.66	<0.01	0.17	0.06	0.18	0.02	0.01	13.91	99.1
MDO-10	MOUNT NEWMAN SHALE	24.71	0.32	8.59	39.34	0.02	1.69	8.47	<0.1	0.14	0.13	15.58	98.99
MDO-13	MOUNT NEWMAN SHALE	43.66	0.46	36.23	4.54	0.03	0.1	0.05	<0.1	<0.01	0.03	14.05	99.15
PDO-23-14	MOUNT MCRAE SHALE	30.16	0.39	10.62	29.74	17.31	<0.05	0.18	0.27	0.44	0.21	10.34	99.65
PDO-32-01	DALES GORGE SHALE	78.56	0.48	14.18	0.32	<0.01	0.1	0.07	<0.1	0.15	0.05	5.72	99.63
PDO-32-05	DALES GORGE SHALE	25.35	0.66	21.65	37.9	0.06	0.2	0.16	0.19	0.73	0.19	12.25	99.33
TP-NTD-10	DALES GORGE SHALE	21.95	0.79	16.76	51.5	0.01	0.24	0.18	<0.1	0.02	0.32	7.67	99.44
TP-NTD-11	DALES GORGE SHALE	29.00	0.97	23.98	33.23	0.01	0.31	0.16	<0.1	0.02	0.44	11.69	99.81
TP-SSEV-03	MOUNT MCRAE SHALE	68.52	0.46	18.67	2.63	<0.01	1.1	0.12	<0.1	3.22	0.05	5.2	99.96
TP-SSEV-07	MOUNT WHALEBACK SHALE	31.65	1.06	26.02	27.26	0.03	0.13	0.07	<0.1	0.02	0.22	13.01	99.46
TP-SSEV-12	MOUNT MCRAE SHALE	48.56	1.38	24.04	15.52	0.02	0.21	0.12	<0.1	0.04	0.09	9.75	99.72
TP-STR-09	MOUNT MCRAE SHALE	68.83	0.41	14.14	3.69	<0.01	1.21	0.12	<0.1	3.14	0.03	7.56	99.12
TP-STR-13	DALES GORGE SHALE	44.71	0.51	15.21	31.11	0.01	0.09	0.15	<0.1	0.05	0.57	6.53	98.94
TP-STR-19	DALES GORGE SHALE	31.93	0.88	21.87	35.06	0.02	0.11	0.06	<0.1	0.02	0.36	9.31	99.61
TP-STR-21	MOUNT MCRAE SHALE	52.08	0.42	12.74	9.47	0.03	13.98	0.21	<0.1	1.25	0.08	9.03	99.28
WA-07-09	MOUNT NEWMAN SHALE	1.99	0.05	3.78	77.99	1.05	0.06	0.16	0.28	0.06	0.37	13.27	99.05
WA-07-16	WEST ANGELAS SHALE	48.73	0.79	18.04	19.63	0.55	0.91	0.13	<0.1	2.42	0.11	7.63	98.95
WA-07-18	WEST ANGELAS SHALE	22.15	0.8	19.07	41.82	1.53	0.6	0.14	0.17	1.42	0.24	12.03	99.95
WA-07-19	WEST ANGELAS SHALE	30.62	1.32	27.57	26.83	0.55	0.15	0.15	0.11	0.07	0.11	12.53	100
WA-50-01	WEST ANGELAS SHALE	16.07	1.16	17.52	52.47	0.02	<0.05	0.16	0.2	0.05	0.1	11.29	99.03

TABLE 5.1 XRF MAJOR RESULTS (%)

Sample	Lithology	V	Cr	Ni	Zn	Zr	Nb	Ba	La	Ce	Nd	Ga	Pb	Rb	Sr	Th	Y	As	Cu	Sc	U
MDO-02	MOUNT NEWMAN BIF	3	9	<3	20	8	3	80	<5	<5	<10	2	<1	<1	3	4	4	16	28	<2	<4
MDO-12	MOUNT NEWMAN BIF	<3	14	<3	23	7	3	80	<5	<5	<10	3	<1	<1	<1	2	6	18	29	<2	<4
PDO-23-04	JOFFRE BIF	6	26	<3	18	13	3	145	<5	<5	<10	6	6	<1	5	<1	11	36	29	<2	<4
PDO-23-05	JOFFRE BIF	8	17	<3	15	16	4	131	<5	<5	<10	4	1	<1	7	<1	11	15	25	<2	<4
PDO-23-06	JOFFRE BIF	7	12	<3	12	11	3	143	<5	<5	<10	3	3	<1	5	<1	13	14	20	<2	<4
PDO-23-11	DALES GORGE BIF	<3	13	<3	20	8	3	140	<5	<5	<10	3	4	<1	7	2	6	18	23	<2	<4
PDO-23-12	DALES GORGE BIF	5	7	<3	10	7	3	92	<5	<5	<10	3	2	1	4	<1	4	11	18	<2	<4
TP-NTD-02	DALES GORGE BIF	7	14	<3	31	10	3	120	<5	<5	<10	4	6	1	2	<1	8	23	33	<2	<4
TP-NTD-03	DALES GORGE BIF	3	10	<3	12	7	3	162	<5	<5	<10	6	5	1	3	<1	4	16	29	<2	<4
TP-SSEV-02	DALES GORGE BIF	10	8	<3	25	11	<2	195	<5	28	<10	4	7	<1	18	<1	21	21	31	<2	<4
TP-SSEV-06	DALES GORGE BIF	3	3	<3	10	6	3	76	<5	<5	<10	<2	3	3	2	<1	11	9	18	<2	<4
TP-SSEV-10A	DALES GORGE BIF	142	51	<3	14	146	21	56	<5	34	19	16	8	<1	6	6	54	79	23	7	<4
TP-SSEV-10B	DALES GORGE BIF	122	40	10	12	133	18	40	<5	17	<10	15	9	<1	7	7	52	36	15	3	<4
TP-STR-01	DALES GORGE BIF	18	11	<3	16	10	4	134	<5	<5	<10	7	6	<1	14	<1	21	25	34	<2	<4
TP-STR-11	DALES GORGE BIF	<3	7	<3	6	8	3	28	<5	<5	<10	4	1	<1	4	<1	15	6	19	<2	<4
TP-STR-12	DALES GORGE BIF	16	13	<3	17	10	<2	204	<5	<5	<10	5	7	<1	8	4	21	24	48	<2	<4
TP-STR-15	DALES GORGE BIF	4	6	<3	7	7	4	53	<5	<5	11	<2	2	<1	4	<1	4	9	16	<2	<4
TP-STR-17	DALES GORGE BIF	43	34	<3	27	10	<2	97	<5	<5	<10	<2	<1	<1	7	<1	15	23	29	<2	<4
WA-07-07	WEST ANGELAS SHALE BIF	15	35	<3	29	11	3	91	<5	<5	<10	4	6	<1	1	2	13	32	39	<2	<4
WA-07-10	MOUNT NEWMAN BIF	5	11	<3	18	8	3	101	<5	<5	36	3	<1	<1	2	1	5	15	37	<2	<4
WA-07-12	MOUNT NEWMAN BIF	<3	9	<3	20	6	3	49	<5	<5	<10	5	3	<1	1	5	6	133	25	<2	<4
WA-07-14	MOUNT NEWMAN BIF	<3	8	<3	15	6	3	57	<5	<5	<10	3	3	<1	2	<1	7	7	18	<2	<4
WA-07-24	MOUNT NEWMANBIF	6	9	<3	14	8	3	61	<5	<5	<10	<2	3	<1	7	<1	10	10	22	<2	<4
WA-07-25	MOUNT NEWMAN BIF	7	6	<3	8	10	3	28	<5	<5	<10	<2	4	6	30	<1	5	3	13	<2	4
MDO-04	MOUNT NEWMAN SHALE	5	11	32	10	26	3	<20	12	9	<10	5	2	<1	7	3	4	<2	9	<2	5
MDO-10	MOUNT NEWMAN SHALE	55	53	10	37	128	10	421	<5	<5	<10	11	3	3	193	17	11	11	23	12	<4
MDO-13	MOUNT NEWMAN SHALE	19	61	40	35	70	6	<20	11	11	<10	9	3	<1	2	6	7	18	11	5	5
PDO-23-14	MOUNT MCRAE SHALE	75	114	674	1681	106	11	2714	21	95	58	18	11	6	68	16	70	455	82	8	9
PDO-32-01	DALES GORGE SHALE	25	51	8	16	218	17	72	81	137	66	21	25	13	61	21	33	3	6	9	7
PDO-32-05	DALES GORGE SHALE	139	101	53	25	212	17	38	9	26	44	23	8	9	6	21	70	22	22	27	<4
TP-NTD-10	DALES GORGE SHALE	164	163	16	55	195	16	140	<5	26	<10	29	60	<1	12	20	51	46	155	19	4
TP-NTD-11	DALES GORGE SHALE	207	203	82	118	325	25	131	21	72	19	40	43	<1	15	27	77	55	211	20	10
TP-SSEV-03	MOUNT MCRAE SHALE	122	140	47	34	105	7	130	81	189	73	21	129	168	11	16	16	138	26	15	<4
TP-SSEV-07	MOUNT WHALEBACK SHALE	249	170	63	163	244	19	51	<5	41	<10	29	23	<1	3	23	45	104	60	34	8
TP-SSEV-12	MOUNT MCRAE SHALE	178	175	<3	38	292	21	23	16	64	31	37	18	<1	26	26	39	50	24	27	7
TP-STR-09	MOUNT MCRAE SHALE	83	81	26	33	157	12	80	37	75	50	20	20	160	10	11	28	30	7	14	6
TP-STR-13	DALES GORGE SHALE	108	127	7	48	152	14	442	85	163	91	27	25	<1	95	18	41	44	53	10	8
TP-STR-19	DALES GORGE SHALE	103	172	48	53	208	22	71	31	81	36	44	12	<1	14	21	52	10	82	20	10
TP-STR-21	MOUNT MCRAE SHALE	101	93	82	135	111	10	83	25	60	30	17	11	72	5	13	23	79	59	14	8
WA-07-09	MOUNT NEWMAN SHALE	13	22	<3	40	18	4	109	<5	87	20	<2	4	<1	4	3	20	18	43	<2	<4
WA-07-16	WEST ANGELAS SHALE	132	103	142	108	160	12	146	48	21	68	23	15	97	7	20	91	39	53	16	7
WA-07-18	WEST ANGELAS SHALE	184	83	169	142	249	13	135	62	53	76	25	27	56	6	21	159	108	74	32	<4
WA-07-19	WEST ANGELAS SHALE	182	199	127	81	241	20	58	30	65	39	36	22	<1	5	22	60	44	61	26	8
WA-50-01	WEST ANGELAS SHALE	171	272	55	28	123	13	74	<5	13	23	17	13	<1	6	8	19	24	55	19	<4
WA-50-10	WEST ANGELAS SHALE	31	39	<3	39	19	3	56	<5	<5	<10	5	3	<1	2	<1	14	21	47	10	<4

TABLE 5.2 XRF MINOR RESULTS (PPM)

Sample ID	Lithology	Quartz	Magnetite	Hematite	Dolomite	Muscovite	Pyrite	Goethite	Kaolinite	Pyrolusite	Manganocalcite
MDO-02	MOUNT NEWMAN BIF	55%	-	-	-	-	-	45%	-	-	-
MDO-12	MOUNT NEWMAN BIF	-	-	65%	-	-	-	35%	-	-	-
PDO-23-04	JOFFRE BIF	-	-	95%	-	-	-	5%	-	-	-
PDO-23-05	JOFFRE BIF	50%	-	50%	-	-	-	-	-	-	-
PDO-23-06	JOFFRE BIF	70%	-	30%	-	-	-	-	-	-	-
PDO-23-11	DALES GORGE BIF	50%	-	50%	-	-	-	-	-	-	-
PDO-23-12	DALES GORGE BIF	90%	-	10%	-	-	-	-	-	-	-
TP-NTD-02	DALES GORGE BIF	-	-	85%	-	-	-	15%	-	-	-
TP-NTD-03	DALES GORGE BIF	-	-	100%	-	-	-	-	-	-	-
TP-SSEV-02	DALES GORGE BIF	-	-	90%	-	-	-	10%	-	-	-
TP-SSEV-06	DALES GORGE BIF	75%	-	25%	-	-	-	-	-	-	-
TP-SSEV-10	DALES GORGE BIF	-	-	-	-	-	-	100%	-	-	-
TP-SSEV-10	DALES GORGE BIF	80%	-	20%	-	-	-	-	-	-	-
TP-STR-01	DALES GORGE BIF	-	-	100%	-	-	-	-	-	-	-
TP-STR-11	DALES GORGE BIF	90%	-	10%	-	-	-	-	-	-	-
TP-STR-12	DALES GORGE BIF	75%	-	25%	-	-	-	-	-	-	-
TP-STR-15	DALES GORGE BIF	90%	-	10%	-	-	-	-	-	-	-
TP-STR-17	DALES GORGE BIF	-	-	100%	-	-	-	-	-	-	-
WA-07-07	WEST ANGELAS SHALE BIF	-	-	-	-	-	-	100%	-	-	-
WA-07-10	MOUNT NEWMAN BIF	-	-	80%	-	-	-	20%	-	-	-
WA-07-12	MOUNT NEWMAN BIF	40%	-	40%	-	-	-	20%	-	-	-
WA-07-14	MOUNT NEWMAN BIF	65%	-	20%	-	-	-	15%	-	-	-
WA-07-24	MOUNT NEWMAN BIF	75%	-	25%	-	-	-	trace	-	-	-
WA-07-25	MOUNT NEWMAN BIF	90%	-	-	10%	-	-	-	-	-	-
MDO-04	MOUNT NEWMAN SHALE	-	-		-	-	-	-	100%	-	-
MDO-10	MOUNT NEWMAN SHALE	-	-		-	-	-	65%	-	-	35%
MDO-13	MOUNT NEWMAN SHALE	-	-		-	-	-	-	100%	-	-
PDO-23-14	MOUNT MCRAE SHALE	60%	-	-	-	-	30%*	-	10%	30%*	-
PDO-32-01	DALES GORGE SHALE	95%	-	-	-	-	-	-	5%	-	-
PDO-32-05	DALES GORGE SHALE	-	-	-	-	-	-	65%	35%	-	-
TP-NTD-10	DALES GORGE SHALE	-	-	75%	-	-	-	-	25%	-	-
TP-NTD-11	DALES GORGE SHALE	-	-	-	-	-	-	55%	45%	-	-
TP-SSEV-03	MOUNT MCRAE SHALE	85%	-	-	-	10%	-	-	5%	-	-
TP-SSEV-07	MOUNT WHALEBACK SHALE	-	-	-	-	-	-	55%	45%	-	-
TP-SSEV-12	MOUNT MCRAE SHALE	60%	-	-	-	-	-	15%	25%	-	-
TP-STR-09	MOUNT MCRAE SHALE	85%	-	-	-	10%	-	-	5%	-	-
TP-STR-13	DALES GORGE SHALE	60%	-	30%	-	-	-	-	10%	-	-
TP-STR-19	DALES GORGE SHALE	40%	-	30%	-	-	-	-	30%	-	-
TP-STR-21	MOUNT MCRAE SHALE	85%	-	-	-	-	-	-	15%	-	-
WA-07-09	MOUNT NEWMAN SHALE	-	-	-	-	-	-	100%	-	-	-
WA-07-16	WEST ANGELAS SHALE	70%	-	-	-	-	-	20%	10%	-	-
WA-07-18	WEST ANGELAS SHALE	-	-	-	-	-	-	80%	20%	-	-
WA-07-19	WEST ANGELAS SHALE	-	-	-	-	-	-	50%	50%	-	-
WA-50-01	WEST ANGELAS SHALE	-	-	55%	-	-	-	35%	10%	-	-
WA-50-10	WEST ANGELAS SHALE	-	-	-	-	-	-	100%	-	-	-

TABLE 5.3 XRD RESULTS

5.3.2 THIN SECTIONS

The thin sections of 12 representative BIF and shale samples were chosen to be analysed. Eight BIF samples were analysed and four shale samples. Of the BIF samples, four were low P (low phosphorus, as discussed in Chapter 2) Dales Gorge Member from the Brockman Iron Formation and the remaining four were Mount Newman Member from the Marra Mamba Iron Formation. The four shale samples included two Mount McRae Shale samples and two Brockman Iron Shale samples. For each of the four samples chosen, one was either fresh or slightly altered, one was moderately altered, one was highly to extremely altered and one was highly to extremely weathered. Microscopic analysis is presented in Figures 5.1 to 5.17.

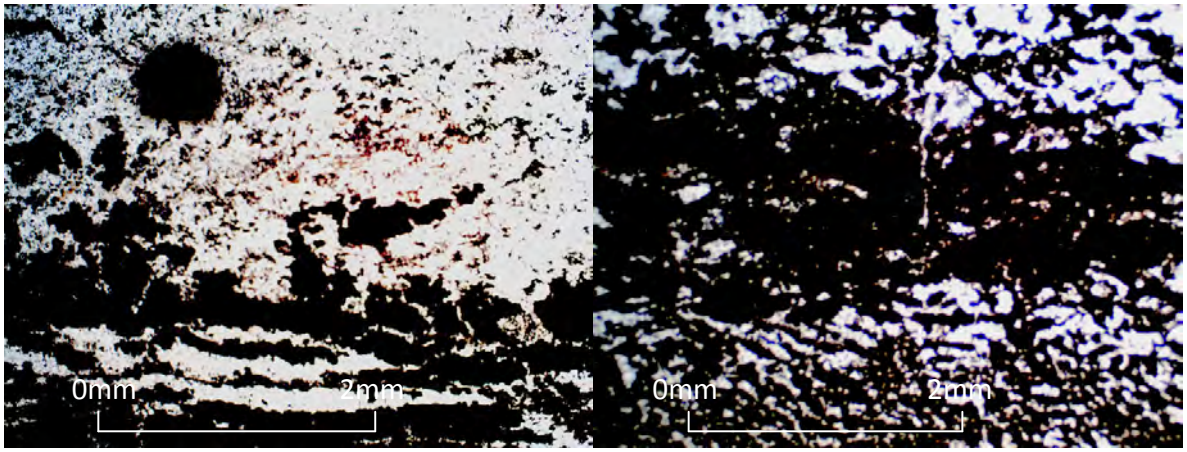

FIGURE 5.1 (LEFT) A TRANSMITTED LIGHT THIN SECTION, MAGNIFIED AT 2.5X, OF AN AVERAGE SLIGHTLY ALTERED DALES GORGE BIF SAMPLE FROM THE LOW P BROCKMAN IRON FORMATION. QUARTZ (CLEAR AREAS) IS VERY ABUNDANT AS IS HEMATITE (BLACK). BEDDING, THROUGHOUT THE SAMPLE, IS PROMINENT.

FIGURE 5.2 (RIGHT) A TRANSMITTED LIGHT THIN SECTION, MAGNIFIED AT 2.5X, OF AN AVERAGE MODERATELY ALTERED DALES GORGE BIF SAMPLE FROM THE LOW P BROCKMAN IRON FORMATION. QUARTZ (CLEAR) AND HEMATITE (BLACK) ARE BOTH ABUNDANT. BEDDING IS PROMINENT.

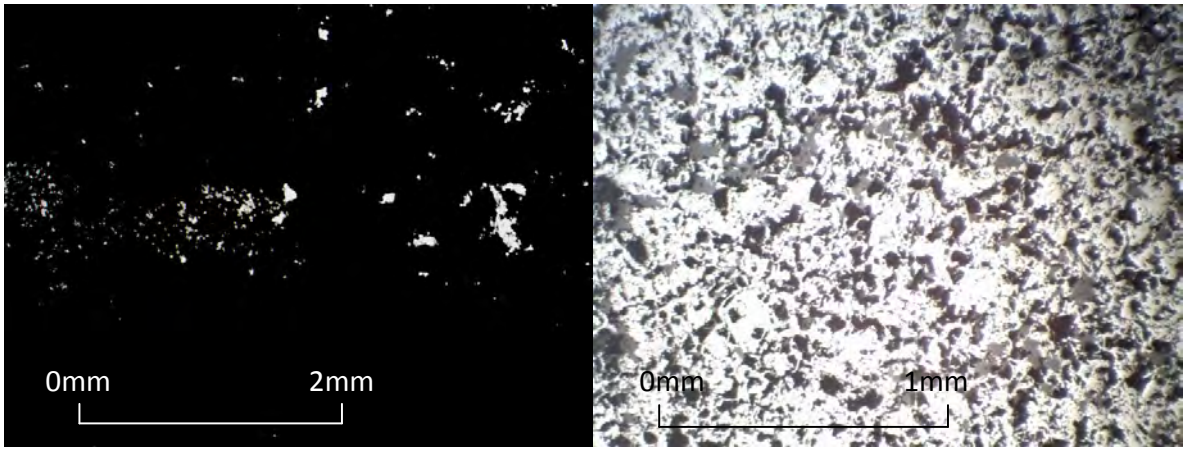

FIGURE 5.3 (LEFT) A TRANSMITTED LIGHT THIN SECTION, MAGNIFIED AT 2.5X, OF AN AVERAGE HIGHLY ALTERED DALES GORGE BIF SAMPLE FROM THE LOW P BROCKMAN IRON FORMATION. THE SAMPLE IS ALMOST ENTIRELY COMPOSED OF HEMATITE (BLACK) WITH SOME VOIDS AND EVEN LESS QUARTZ (CLEAR). BEDDING IS WEAK TO NON-EXISTENT.

FIGURE 5.4 (RIGHT) A REFLECTED LIGHT THIN SECTION, MAGNIFIED AT 3.2X, OF THE SAME HIGHLY ALTERED DALES GORGE BIF SAMPLE FROM LOW P BROCKMAN IRON FORMATION. THE SAMPLE IS COMPOSED OF MAINLY HEMATITE (WHITE) WITH SOME VOIDS AND MINOR QUARTZ (BLACK). SOME MAGNETITE CAN ALSO BE SEEN (GREY) WHICH THE HEMATITE HAS ALTERED FROM.

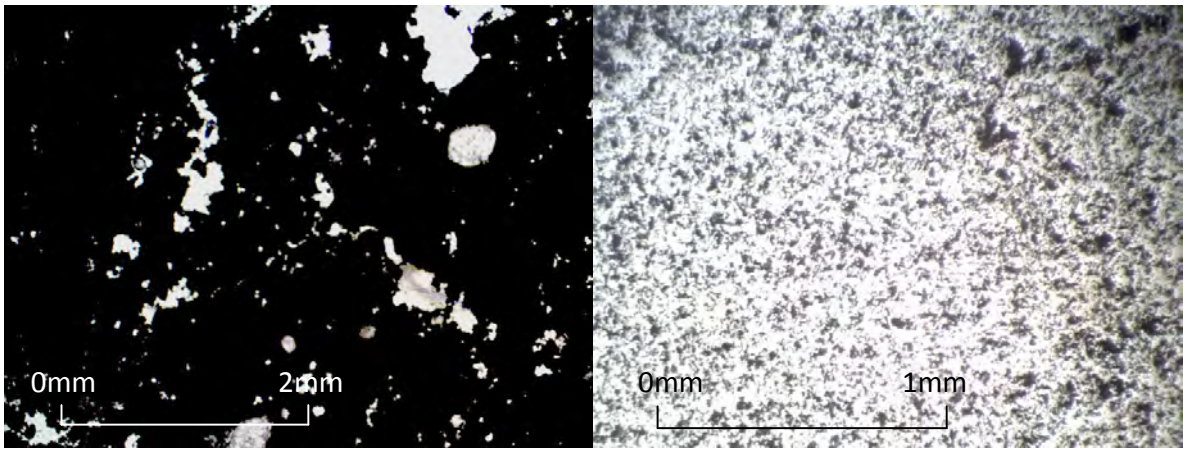

FIGURE 5.5 (LEFT) A TRANSMITTED LIGHT THIN SECTION, MAGNIFIED AT 2.5X, OF AN AVERAGE HIGHLY WEATHERED DALES GORGE BIF SAMPLE FROM THE LOW P BROCKMAN IRON FORMATION. THE SAMPLE IS ENTIRELY COMPOSED OF HEMATITE WITH SOME VOIDS. NO BEDDING IS EVIDENT.

FIGURE 5.6 (RIGHT) A REFLECTED LIGHT THIN SECTION, MAGNIFIED AT 3.2X OF THE SAME HIGHLY WEATHERED DALES GORGE BIF SAMPLE FROM THE LOW P BROCKMAN IRON FORMATION. THE SAMPLE IS ALMOST ENTIRELY COMPOSED OF HEMATITE (WHITE). NO BEDDING IS VISIBLE.

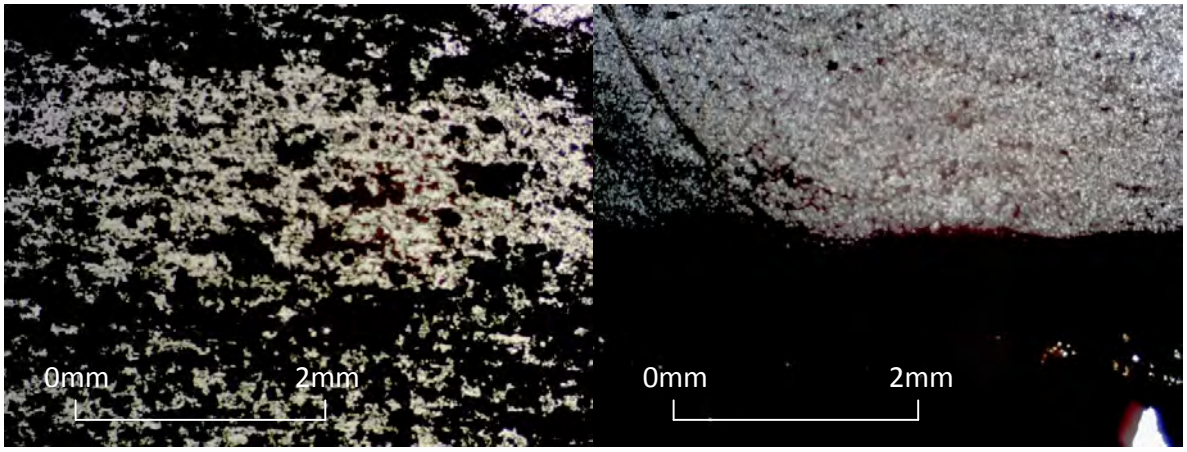

FIGURE 5.7 (LEFT) A TRANSMITTED LIGHT THIN SECTION, MAGNIFIED AT 2.5X, OF A SLIGHTLY ALTERED MOUNT NEWMAN BIF FROM THE MARRA MAMBA IRON FORMATION. THE SAMPLE IS COMPOSED OF MAINLY QUARTZ (CLEAR) WITH HEMATITE (BLACK) AND SOME GOETHITE (DARK RED). BEDDING IS PROMINENT.

FIGURE 5.8 (RIGHT) A TRANSMITTED LIGHT THIN SECTION, MAGNIFIED AT 2.5X, OF A MODERATELY ALTERED MOUNT NEWMAN BIF FROM THE MARRA MAMBA IRON FORMATION. THE SAMPLE IS COMPOSED OF QUARTZ (CLEAR) AND HEMATITE (BLACK) AND SOME GOETHITE (DARK RED). BEDDING IS PROMINENT.

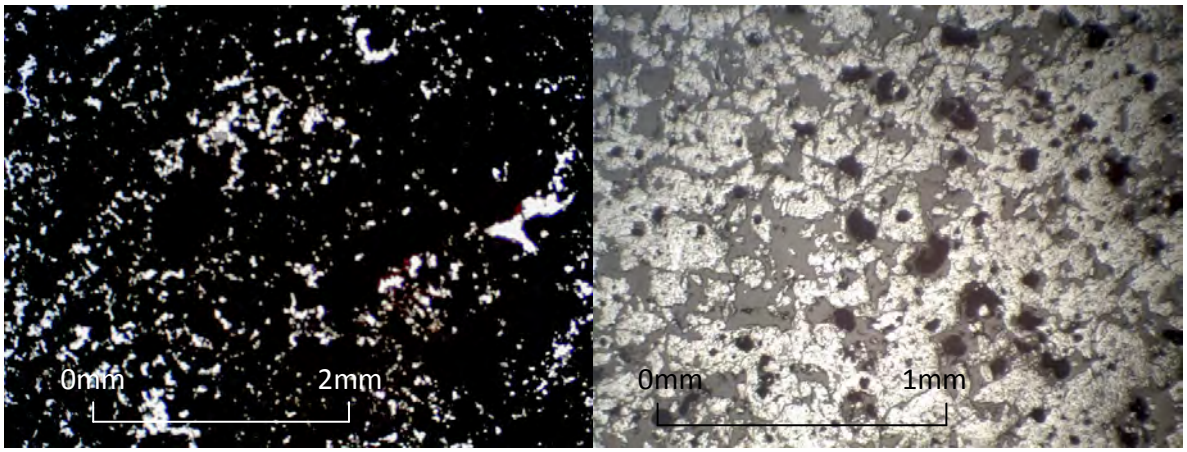

FIGURE 5.9 (LEFT) A TRANSMITTED LIGHT THIN SECTION, MAGNIFIED AT 2.5X, OF HIGHLY ALTERED MOUNT NEWMAN BIF FROM THE MARRA MAMBA IRON FORMATION. THE SAMPLE IS COMPOSED OF HEMATITE (BLACK) AND GOETHITE (DARK RED) WITH SOME VOIDS AND MINOR QUARTZ (CLEAR). BEDDING HAS DISAPPEARED.

FIGURE 5.10 (RIGHT) A REFLECTED LIGHT THIN SECTION, MAGNIFIED AT 3.2X, OF THE SAME HIGHLY ALTERED MOUNT NEWMAN BIF FROM THE MARRA MAMBA IRON FORMATION. THE SAMPLE IS COMPOSED OF HEMATITE (WHITE) AND MUCH GOETHITE (GREY) WITH SOME VOIDS AND QUARTZ (BLACK). NO BEDDING IS VISIBLE.

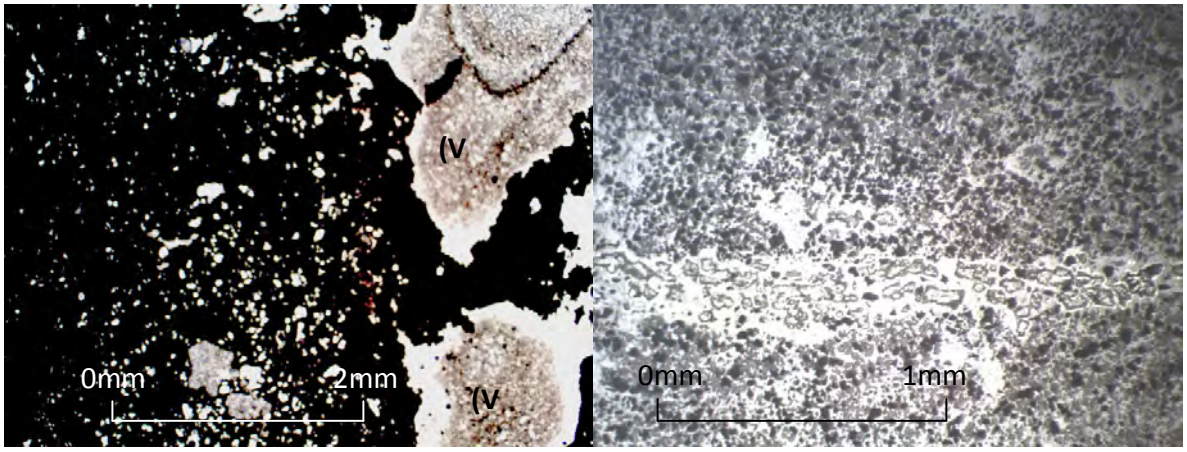

FIGURE 5.11 (LEFT) A TRANSMITTED LIGHT THIN SECTION, MAGNIFIED AT 2.5X, OF HIGHLY WEATHERED MOUNT NEWMAN BIF FROM THE MARRA MAMBA IRON FORMATION. THE SAMPLE IS COMPOSED OF QUARTZ (CLEAR) AND GOETHITE (DARK RED) WITH MANY VOIDS (V). BEDDING HAS DISAPPEARED.

FIGURE 5.12 (RIGHT) A REFLECTED LIGHT THIN SECTION, MAGNIFIED AT 3.2X OF THE SAME HIGHLY WEATHERED MOUNT NEWMAN BIF FROM THE MARRA MAMBA IRON FORMATION. THE SAMPLE IS COMPOSED OF QUARTZ (BLACK) AND GOETHITE (GREY). HEMATITE (WHITE) IS ALSO VISIBLE AND ABUNDANT IN THIS SAMPLE. SOME BEDDING CAN ALSO BE SEEN.

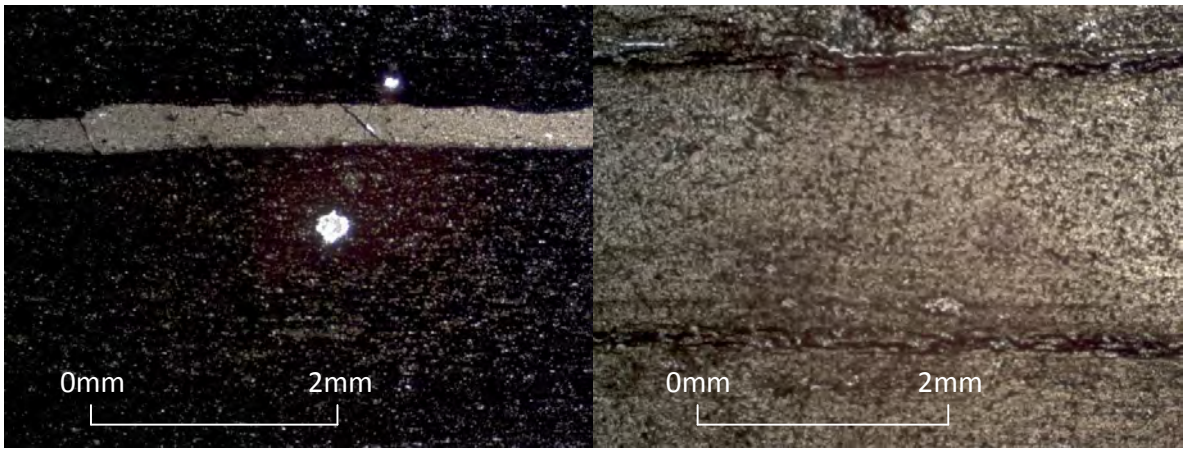

FIGURE 5.13 (ABOVE LEFT) A TRANSMITTED LIGHT THIN SECTION, MAGNIFIED AT 2.5X, OF A FRESH MCRAE SHALE FROM THE LOW P BROCKMAN IRON FORMATION. THE SAMPLE IS MAINLY COMPOSED OF VERY FINE QUARTZ (BLACK) WITH SOME MUSCOVITE AND SOME KAOLINITE. BEDDING IS NOT OBVIOUS BUT ALIGNMENT OF GRAINS IS COMMON.

FIGURE 5.14 (ABOVE RIGHT) A TRANSMITTED LIGHT THIN SECTION, MAGNIFIED AT 2.5X, OF A MODERATELY ALTERED MCRAE SHALE FROM THE HIGH P BROCKMAN IRON FORMATION. THE SAMPLE IS COMPOSED OF MOSTLY QUARTZ WITH SOME HEMATITE AND KAOLINITE. BEDDING IS PROMINENT.

FIGURE 5.15 (LEFT) A TRANSMITTED LIGHT THIN SECTION, MAGNIFIED AT 2.5X, OF A HIGHLY ALTERED DALES GORGE SHALE FROM THE LOW P BROCKMAN IRON FORMATION. THE SAMPLE IS COMPOSED OF QUARTZ, HEMATITE AND KAOLINITE. BEDDING IS PROMINENT.

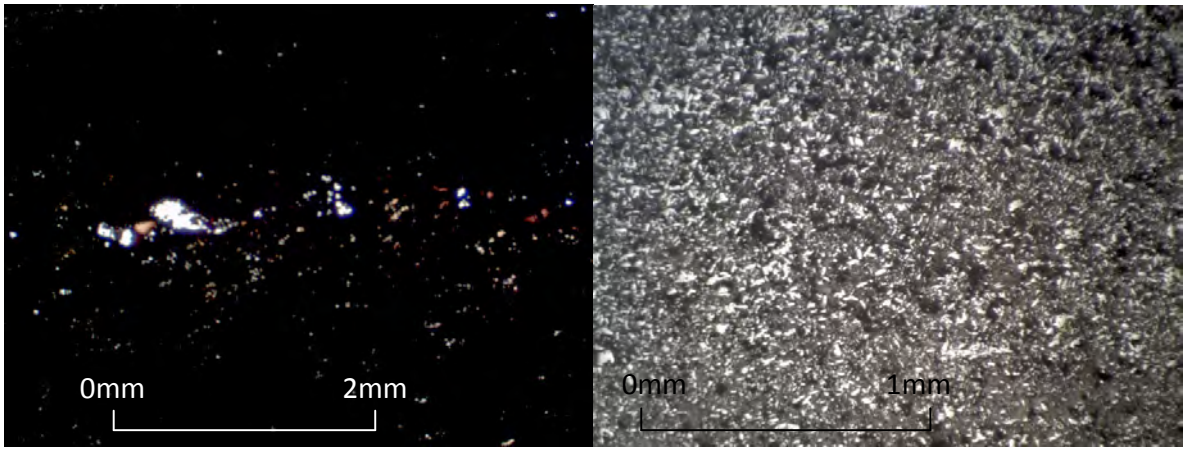

FIGURE 5.16 (LEFT) A TRANSMITTED LIGHT THIN SECTION, MAGNIFIED AT 2.5X, OF A HIGHLY WEATHERED JOFFRE SHALE FROM LOW P BROCKMAN IRON FORMATION. THE SAMPLE IS DOMINANTLY HEMATITE (BLACK) AND GOETHITE (DARK RED) WITH SOME VOIDS AND MINOR QUARTZ (CLEAR). BEDDING IS WEAK.

FIGURE 5.17 (RIGHT) A REFLECTED LIGHT THIN SECTION, MAGNIFIED AT 3.2X, OF THE SAME HIGHLY WEATHERED JOFFRE SHALE FROM LOW P BROCKMAN IRON FORMATION. THE SHALE IS, AGAIN, DOMINANTLY HEMATITE (WHITE) AND GOETHITE (GREY) WITH SOME VOIDS AND MINOR QUARTZ (BLACK). NO BEDDING IS VISIBLE HERE.

5.4 ANALYSIS

5.4.1 CHEMICAL ALTERATION INDEX

Chemical alteration indices are a useful tool in measuring the chemical alteration profile of a particular rock group. The chemical alteration index is calculated using XRF major elements of a group of rocks that are known to increase or decrease as this rock group alters and/or weathers.

A chemical alteration index was equated for each of the rock samples studied here and are shown in Tables 5.4 and 5.5. Chemical alteration indices use key elements in rocks that have been enriched and depleted to analyse the degree of alteration in a specific rock type. The index ranges from 0 to 100, with 0 representing fresh rock and 100 representing completely altered rock, and is constructed from the following equation (Dalstra and Minello, 1999):

$$\mathbf{A = \frac{(Key\ enriched\ elements)100}{(Enriched + Depleted\ elements)}} \qquad \mathbf{(5.1)}$$

The alteration from BIF to ore in the Hamersley Province generally shows an increase in iron, aluminum, titanium and phosphorus and a decrease in silica, magnesium and calcium (Taylor et al., 2001). Using the above equation (5.1), the following *Pilbara Iron* alteration index (A^{PI}) equation was compiled:

$$\mathbf{A^{PI} = \frac{(Fe_2O_3T + Al_2O_3 + TiO_2 + P_2O_5)100}{Fe_2O_3T + Al_2O_3 + TiO_2 + P_2O_5 + SiO_2 + MgO + CaO}} \qquad \mathbf{(5.2)}$$

This equation was applied to the BIF and shale samples studied here using the XRF major element analysis. Table 5.4 and Table 5.5 show the *Pilbara Iron* alteration index with the alteration and weathering descriptions of each rock sample as defined by the RTIO alteration and weathering descriptors for BIF and shale (refer to Figure 4.2 and Figure 4.3).

As shown in Table 5.4 and Table 5.5, the chemical alteration index increases as both the BIF and shale samples become more altered and weathered. The *Pilbara Iron* alteration index does not

differentiate between alteration and weathering but, instead, seems to add the two effects together giving higher values for samples that are both altered and weathered.

The *Pilbara Iron* alteration index, therefore, works well on both the BIF and shale samples of the lower Hamersley Group Iron Formations in describing the extent of the alteration and weathering with values of less than 20 for fresh rock, values between 20 and 40 for slightly altered and/or weathered rock, values between 40 and 60 for moderately altered and/or weathered rock, values between 60 and 80 for highly altered and/or weathered rock and values greater than 80 for extremely altered and/or weathered rock.

Sample ID	Lithology	RTIO Descriptors		Pilbara Iron Alteration Index
WA-07-25	NEWMAN BIF	**FR**	**FR**	**32**
TP-STR-11	DALES GORGE BIF	**SW**	**SA**	**38**
TP-STR-15	DALES GORGE BIF	**SW**	**SA**	**39**
PDO-23-12	DALES GORGE BIF	**SW**	**SA**	**50**
WA-07-14	NEWMAN BIF	**SW**	**SA**	**54**
TP-SSEV-06	DALES GORGE BIF	**MW**	**MA**	**54**
TP-SSEV-10B	DALES GORGE BIF	**EW**	**HA**	**56**
PDO-23-06	JOFFRE BIF	**SW**	**SA**	**62**
WA-07-24	NEWMAN BIF	**MW**	**HA**	**66**
PDO-23-05	JOFFRE BIF	**MW**	**MA**	**73**
WA-07-12	NEWMAN BIF	**MW**	**MA**	**76**
PDO-23-11	DALES GORGE BIF	**MW**	**MA**	**77**
TP-SSEV-10A	DALES GORGE BIF	**EW**	**HA**	**80**
TP-STR-12	DALES GORGE BIF	**MW**	**MA**	**95**
WA-07-07	WEST ANGELAS BIF	**HW**	**HA**	**98**
PDO-23-04	JOFFRE BIF	**HW**	**HA**	**98**
MDO-02	NEWMAN BIF	**HW**	**MA**	**98**
MDO-12	NEWMAN BIF	**SW**	**HA**	**99**
WA-07-10	NEWMAN BIF	**HW**	**EA**	**99**
TP-SSEV-02	DALES GORGE BIF	**MW**	**EA**	**99**
TP-STR-17	DALES GORGE BIF	**MW**	**HA**	**99**
TP-NTD-02	DALES GORGE BIF	**HW**	**HA**	**99**
TP-STR-01	DALES GORGE BIF	**EW**	**HA**	**100**
TP-NTD-03	DALES GORGE BIF	**MW**	**HA**	**100**

TABLE 5.4 THE RTIO ALTERATION AND WEATHERING DESCRIPTIONS OF EACH OF THE BIF SAMPLES TESTED IN THE GEOCHEMICAL INVESTIGATION WITH THE ALTERATION INDEX AS CALCULATED FROM THE XRF MAJOR ELEMENTS ANALYSIS USING THE *PILBARA IRON* ALTERATION INDEX EQUATION (5.2).

Sample ID	Lithology	RTIO Descriptors		Pilbara Iron Alteration Index
PDO-32-01	DALES GORGE SHALE	**SW**	**HA**	**16**
TP-STR-09	MCRAE SHALE	**FR**	**FR**	**21**
TP-SSEV-03	MCRAE SHALE	**SW**	**HA**	**24**
TP-STR-21	MCRAE SHALE	**FR**	**FR**	**26**
WA-07-16	WEST ANGELAS SHALE	**MW**	**HA**	**44**
TP-SSEV-12	MCRAE SHALE	**MW**	**HA**	**46**
MDO-13	NEWMAN SHALE	**SW**	**HA**	**49**
MDO-04	NEWMAN SHALE	**MW**	**MA**	**50**
TP-STR-13	DALES GORGE SHALE	**MW**	**HA**	**51**
PDO-23-14	MCRAE SHALE	**MW**	**MA**	**57**
MDO-10	NEWMAN SHALE	**MW**	**HA**	**58**
TP-SSEV-07	WHALEBACK SHALE	**MW**	**HA**	**63**
WA-07-19	WEST ANGELAS SHALE	**MW**	**HA**	**64**
TP-STR-19	DALES GORGE SHALE	**MW**	**MA**	**64**
TP-NTD-11	DALES GORGE SHALE	**MW**	**HA**	**67**
PDO-32-05	DALES GORGE SHALE	**MW**	**HA**	**70**
WA-07-18	WEST ANGELAS SHALE	**MW**	**HA**	**73**
TP-NTD-10	DALES GORGE SHALE	**MW**	**HA**	**76**
WA-50-01	WEST ANGELAS SHALE	**MW**	**HA**	**81**
WA-07-09	NEWMAN SHALE	**HW**	**EA**	**97**
WA-50-10	WEST ANGELAS SHALE	**MW**	**HA**	**98**

TABLE 5.5 THE RTIO ALTERATION AND WEATHERING DESCRIPTIONS OF EACH OF THE SHALE SAMPLES TESTED IN THE GEOCHEMICAL INVESTIGATION WITH THE ALTERATION INDEX AS CALCULATED FROM THE XRF MAJOR ELEMENT ANALYSIS USING THE *PILBARA IRON* ALTERATION INDEX EQUATION (5.2).

5.4.2 ALUMINIUM VERSES TITANIUM

Ore genesis throughout the Hamersley Province involves removal of gangue minerals and concentration of insoluble elements such as iron, aluminum and titanium (Taylor et al., 2001).

Ewers and Morris (1981), has previously described the correlation between aluminum and titanium in Dales Gorge shale bands and the BIF adjacent to these. They found that rocks that contain more than 0.4% Al_2O_3 also contain significant TiO_2 with a relationship of:

$$\mathbf{AL_2O_3 = 20.5\ TIO_2 + 0.08} \qquad \mathbf{(5.3)}$$

It was also observed by Taylor et al. (2001) that this relationship can be extended to other rocks such as BIF and iron ore and that the values of aluminum and titanium increase as mineralisation increases.

A similar relationship has been observed in the rock samples studied here. Here it has been observed that within the shale samples, this relationship has been approximately followed with fresh shale samples containing lower aluminum and titanium concentrations and higher concentrations in more altered samples (Figure 5.18). Shale samples with secondary goethite and/or hematite and increased kaolinite due to alteration all occur in the upper-right portion of the graph.

There are two sets of outliers within the shale samples. Two samples containing 100% kaolinite are off the trendline altogether with higher aluminum and lower titanium then normal, this can be contributed to the high amount of aluminum found in kaolinite. Also, two samples containing 100% secondary goethite fall in the lower portion of the trendline closer to the BIF samples. This may be partly due to the complete loss of kaolinite.

The BIF samples fall in the very bottom corner of the graph with very low Al_2O_3 and TiO_2 concentrations. The relationship of alteration to Al/Ti is less clear; however, less altered BIF samples generally seem to have less aluminum and are more likely to have little titanium.

5.4.3 PEARCE ELEMENT RATIOS

Pearce Element Ratio (PER) diagrams are a tool used to investigate geochemical data and are useful in applications such as identifying mobile elements in altered environments. PER diagrams are molar ratios that are calculated using a conserved element as the denominator (Pearce, 1968) and ratios these against major mobile elements to examine their true concentrations relative to the denominator (Whitbread, 2002). This reduces background ‘noise’ of raw geochemical data and avoids closure effects caused by plotting percentages by using ratios to examine the data.

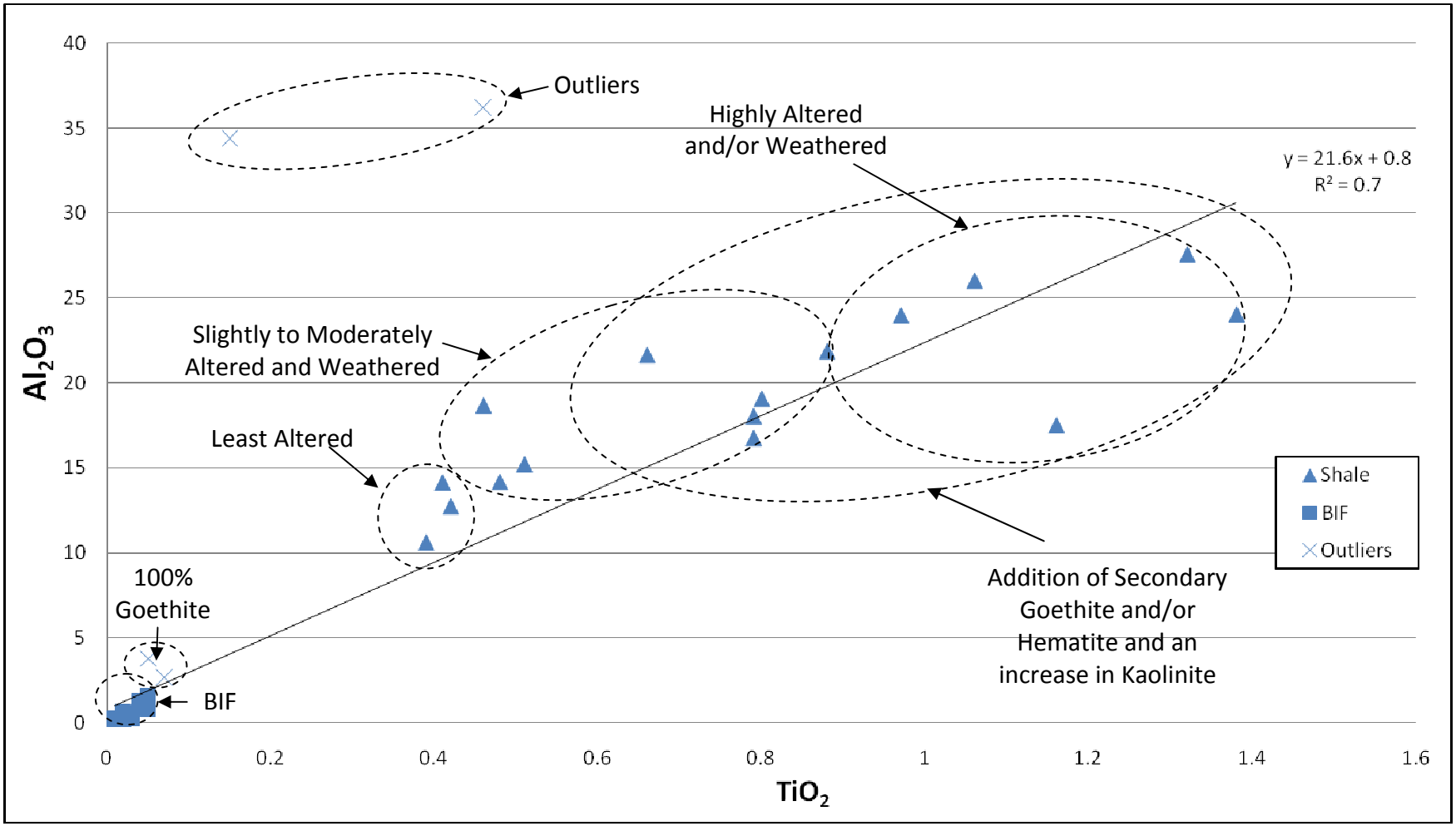

FIGURE 5.18 ALUMINIUM AND TITANIUM CONTENTS OF LOWER HAMERSLEY GROUP IRON FORMATION BIF AND SHALE

By creating a PER diagram, unaltered samples can be represented by a single line and any alteration events cause deviation from that line, creating their own separate line with a different slope that defines it, and can therefore be represented graphically.

Figure 5.19 shows a PER diagram of lower Hamersley Group Iron Formation BIF samples with silica and phosphorus against titanium. Silica and phosphorus were chosen for the BIF PER diagram as the numerators as they are both mobile elements in this environment and are known to increase and/or decrease with alteration and weathering in the lower Hamersley Group BIF. Titanium is known to be a relatively conserved element in this environment (Taylor et al., 2001) and has, therefore, been used as the denominator. Four trendlines have been interpreted on this graph, each representing a different alteration stage.

Only one single fresh BIF was geochemically tested and stands alone to the left of the BIF PER diagram. More fresh BIF samples need to be geochemically testing to determine the slope of fresh BIF on this PER diagram.

The steepest trendline, to the right of the fresh BIF sample, represents slightly altered BIF. These samples have been classified in the field as “slightly” to “moderately” altered and have *Pilbara Iron* alteration indices of less than 62. These rock samples contain high quartz content (70% and above) with the remaining material consisting of hematite.

The next steepest trendline has been interpreted to represent moderately altered BIF. These BIF samples have been described in the field as “slightly” to “moderately” altered and have *Pilbara Iron* alteration indices of 50 to 73. These BIF samples contain between 50% and 90% quartz with the rest of the contents being hematite and one sample containing 15% goethite.

The third steepest trendline has been interpreted as representing highly altered BIF. These BIF samples have been described in the field as “moderately” to “highly” altered and have *Pilbara Iron* alteration indices of between 66 and 95. These BIF samples contain between 40% and 75% quartz, 20% to 50% hematite and up to 15% goethite.

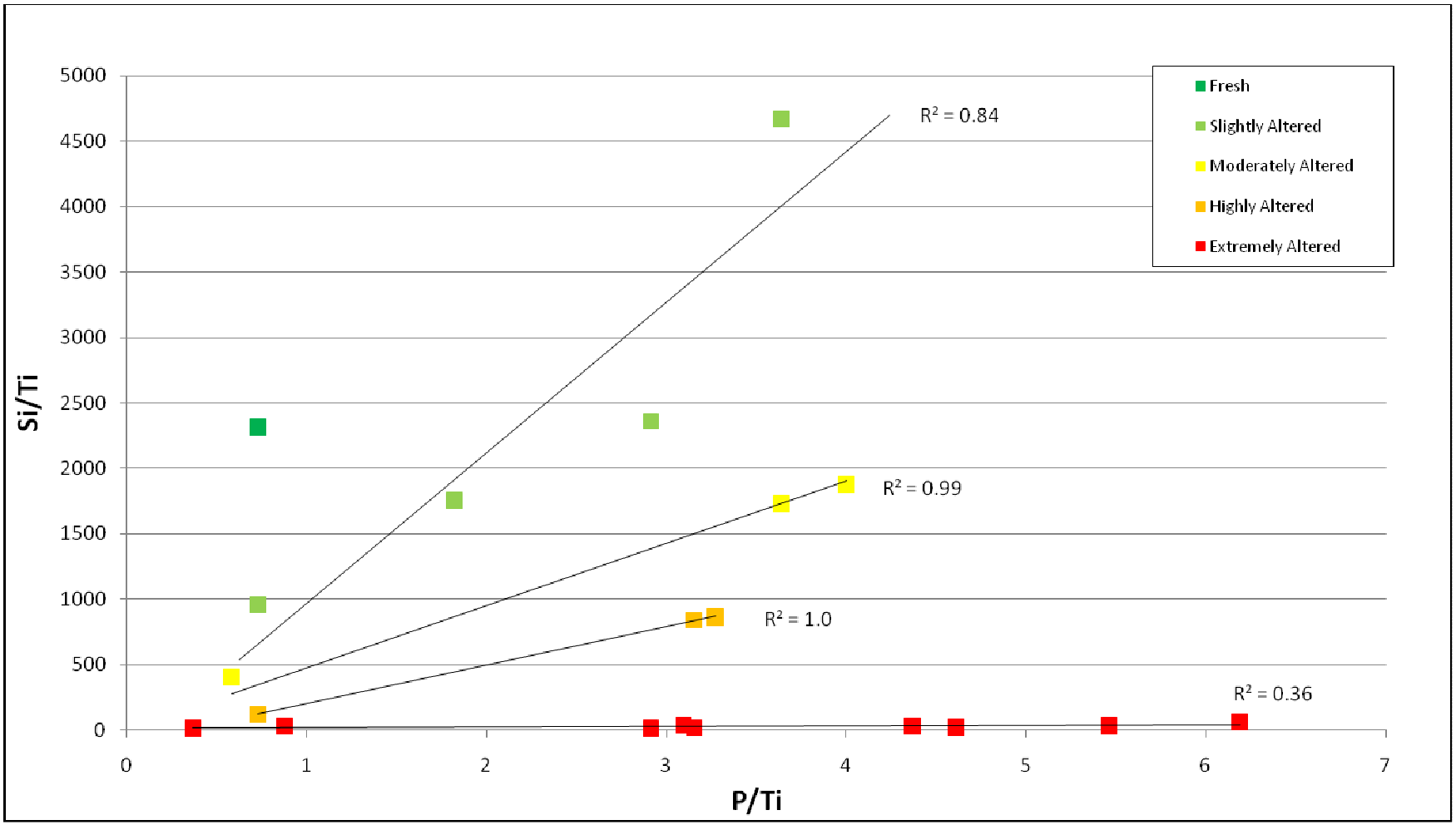

FIGURE 5.19 PER DIAGRAM OF LOWER HAMERSLEY GROUP IRON FORMATION BIF OF SI/TI AND P/TI. FOUR TRENDLINES HAVE BEEN INTERPRETED AND THEIR COEFFICIENTS OF DETERMINATION (R^2) ARE SHOWN.

The flattest trendline has been interpreted to represent extremely altered BIF samples. These samples have been described in the field as “highly” to “extremely” altered and weathered BIF. They have *Pilbara Iron* alteration indices of 98 and above. These BIF samples contain no quartz (with one exception containing 55% quartz) and are composed solely of hematite and/or goethite. The co-efficient of determination (R^2) for this flattest trend line is much lower then the other trendlines interpreted in the PER diagrams with a value of 0.36. Figure 5.20 shows more possible trendlines for these extremely altered BIF samples. More geochemical testing of extremely altered BIF samples is needed to understand this relationship more fully.

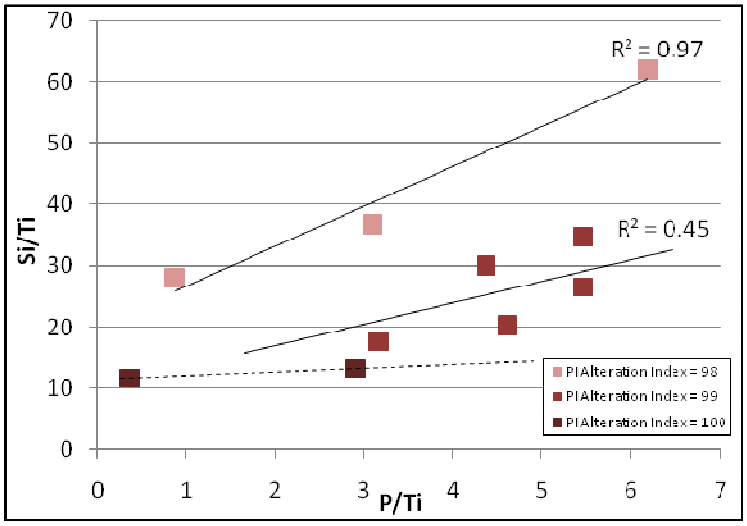

FIGURE 5.20 PER DIAGRAM OF EXTREMELY ALTERED LOWER HAMERSLEY GROUP IRON FORMATION BIF SAMPLES OF SI/TI AND P/TI

Figure 5.21 shows a PER diagram of lower Hamersley Group Iron Formation shale with aluminum and silica against titanium. Silica is, again, a mobile element in this environment, decreasing and/or increasing with alteration and/or weathering. Aluminium has replaced phosphorus as the second numerator as it proves to be better at defining alteration processes in shale in the Hamersley Group deposits. Titanium is, again, used as the denominator as it is a relatively conserved element in this environment. Four trendlines have been interpreted, each representing a different stage of alteration.

The steepest of the four trend lines has been interpreted as representing fresh shale. This trendline contains rock samples that have been interpreted out in the field as “fresh”. These

shale samples contain very high quartz content with some kaolinite and muscovite and have *Pilbara Iron* alteration indices of 21 and 26.

The next steepest trendline has been interpreted as representing slightly altered shale. This trendline contains samples that have been described in the field as “slightly” through to “highly” altered with *Pilbara Iron* alteration indices of between 24 and 58. These rock samples contain high quartz content, increased kaolinite, and some secondary hematite and/or goethite.

The third steepest line has been interpreted as representing highly altered shale. These rock samples have been described in the field as “highly” altered and have *Pilbara Iron* alteration indices between 63 and 76. These rock samples contain high to very high percentages of kaolinite, and low to no quartz. Some of these rock samples also contain high levels of the secondary minerals, hematite or goethite.

The flattest trendline has been interpreted as representing extremely altered shale. These rocks have been described in the field as “highly” altered and/or weathered and have alteration indices of over 80. These rock samples have very high amounts of secondary minerals with greater than 90% values of goethite and/or hematite.

5.4.4 TRACE ELEMENTS

Trace elements are valuable tools for assessing the intricate nature of rock materials. Here they were found to especially be useful in analysing the lower Hamersley Group Iron Formation BIF samples through transition metal diagrams and enrichment-depletion diagrams.

Transition metals are elements that occur from atomic number 21 to 30. Analysing the transition elements of the Hamersley Iron deposits showed that copper and zinc were particularly useful in determining the extent of alteration (including weathering). Copper and zinc are known to be mobile elements, particularly at high temperatures (Seewald and Seyfried, 1990).

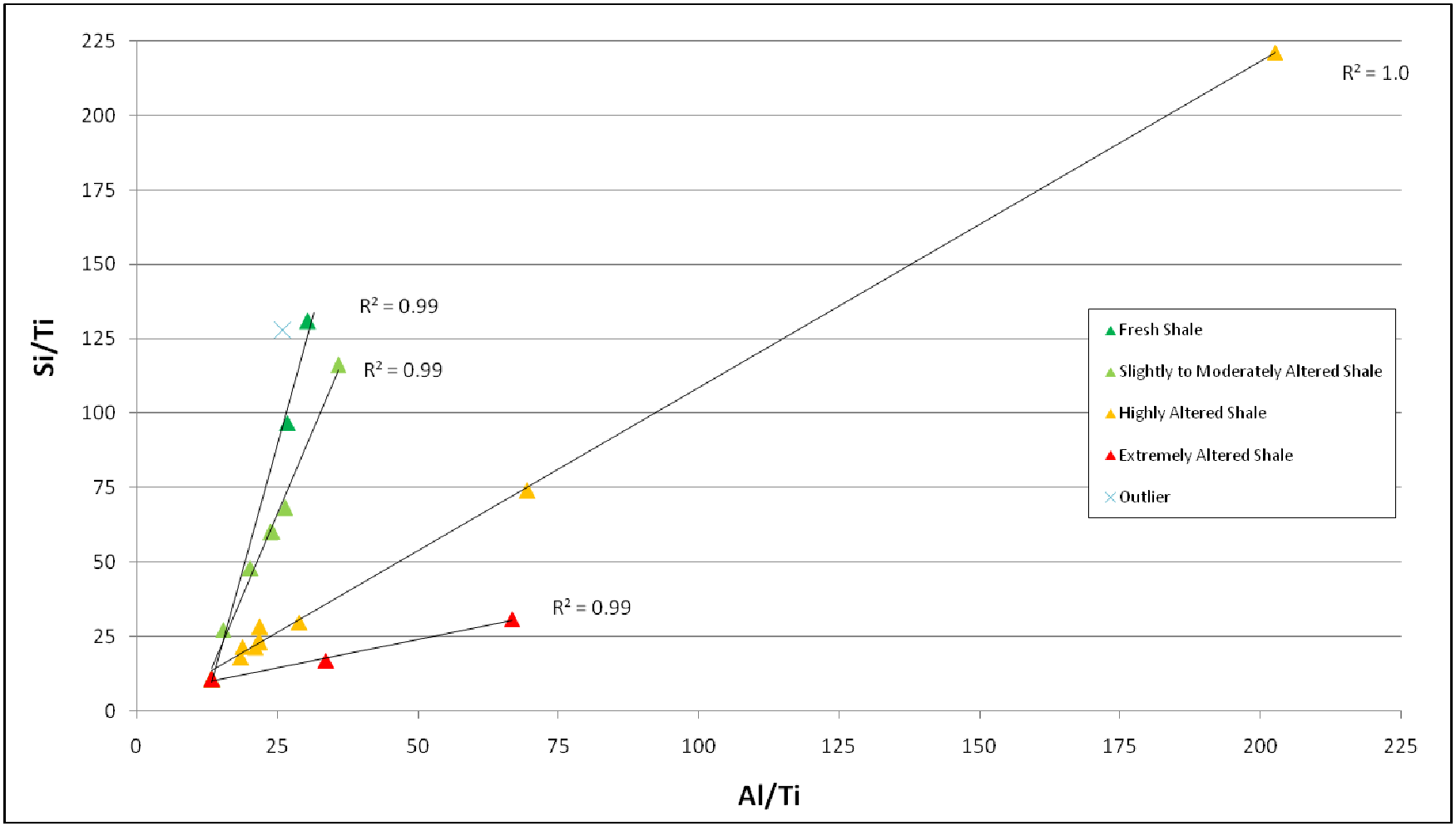

FIGURE 5.21 PER DIAGRAM OF LOWER HAMERSLEY GROUP IRON FORMATION SHALE OF SI/TI AND AL/TI. FOUR TRENDLINES HAVE BEEN INTERPRETED AND THEIR COEFFICIENTS OF DETERMINATION (R^2) ARE SHOWN.

Figure 5.22 shows the relationship between copper and zinc in lower Hamersley Group Iron Formation BIF deposits. The freshest BIF samples fall in the lower-left portion of the graph while the more weathered and altered samples occur in the upper-right portion of the graph, containing increasing copper and zinc with alteration and weathering.

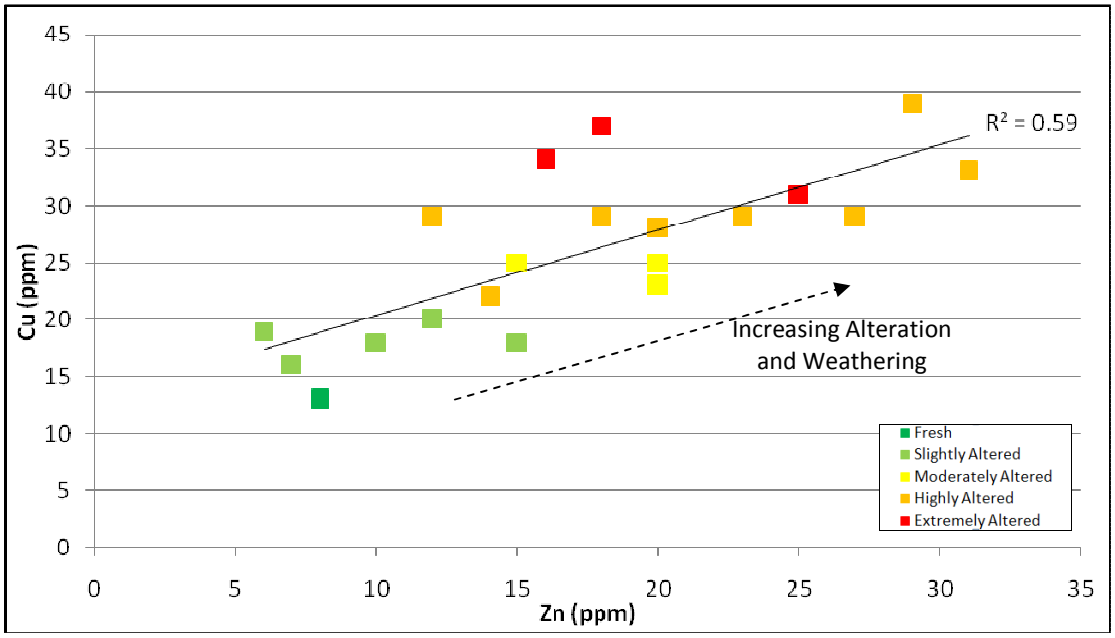

FIGURE 5.22 COPPER AND ZINC ABUNDANCES IN BIF SAMPLES OF THE LOWER HAMERSLEY GROUP IRON FORMATIONS

Enrichment-depletion diagrams show the relative enrichment and depletion of major and minor elements and are useful for displaying the element mobility in areas such as hydrothermal alteration zones. Enrichment-depletion diagrams plot elements (that are plotted in order of atomic number) against their abundance in a rock sample which is ratioed against a primary rock. A fresh (unaltered) Newman BIF was chosen to be the standard for the BIF samples and a carbonaceous Mount McRae Shale (interpreted to be unaltered) was chosen to be the standard for the shale samples in this study. The “fresh” rock samples were assumed to be a similar composition to the parent rocks of the altered BIF and shale samples studied.

Figures 5.23, 5.24, 5.25 and 5.26 show enrichment-depletion diagrams of four types of lower Hamersley Group Iron Formation BIF and Figures 5.27, 5.28, 5.29 and 5.30 show enrichment-depletion diagrams of four types of lower Hamersley Group Iron Formation shale.

The enrichment-depletion graphs show that within the BIF samples, as alteration and weathering increases, Al, P, Ti, Cr, Mn, Fe, Cu, Zn, Ga, As and Y all appear to increase systematically throughout all four BIF groups. At the same time, Na, Si, K, Ca, Rb and Sr all appear to decrease systematically throughout all four BIF groups. Mg, Sc and Ni all appear immobile in this environment and V appears to increase with alteration in low P Dales Gorge BIF but decreases with alteration in Newman BIF while Zr increases in low P Joffre BIF but decreases in the Newman BIF. These may be due to hypogene verses supergene alteration environments but more testing needs to be done to confirm this. Note also that Mg appears immobile, but was identified by Taylor et al. (2001) to be a depleted element in altered environments in a study of high P hematite and magnetite mineralisation at Southern Ridge. It is, however, depleted in the shale samples and this study may be reflecting this, as in this study 'pure' BIF and shale samples have been studied seperately.

The enrichment-depletion graphs show that within the shale samples, as alteration and weathering increases, Na, Al, P, Ca, Sc, Ti, V, Cr, Mn, Fe, Ni, Za, Ga, As, Y, Zr and Nb all appear to increase while Mg, Si, K, Rb and Sr all appear to decrease. Within the Newman shale enrichment-depletion graph, however, which shows moderately weathered to highly weathered shale samples, shows that with weathering a lot of minor elements, especially the lighter elements, become heavily depleted. This includes Sc, Ti, V, Cr, Ni, Ga, As, Y, Zr and Nb. This may potentially be used to discern weathering from alteration in lower Hamersley Group Iron Formation shale, however, more weathered shale samples need to be tested to confirm this.

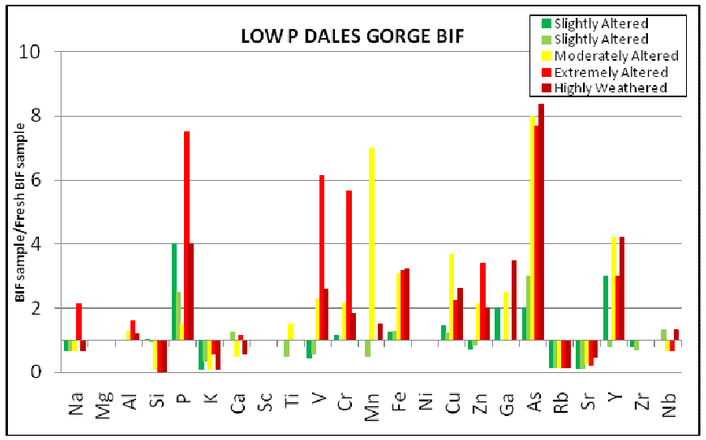

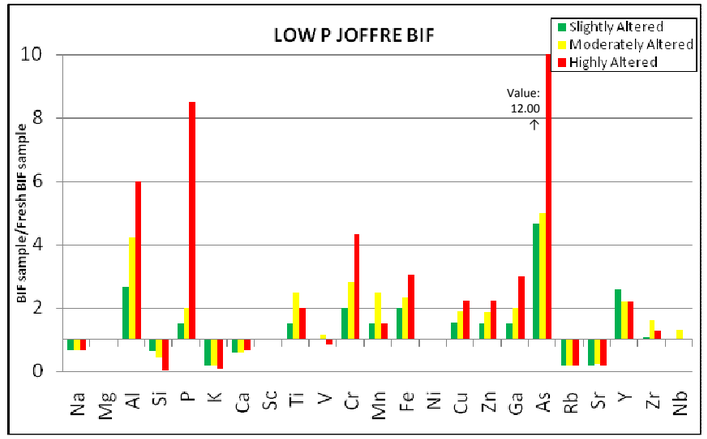

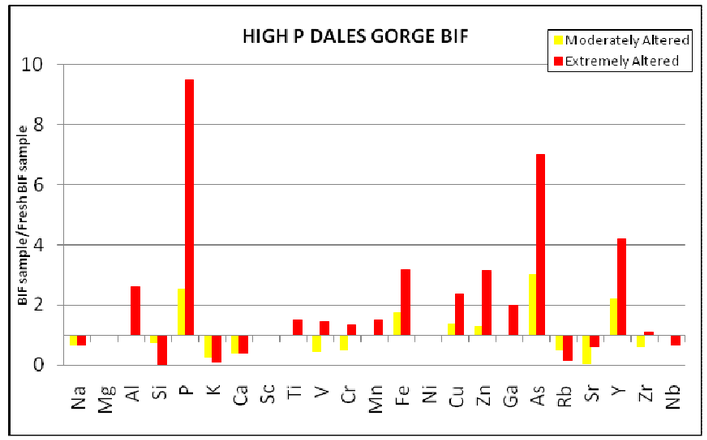

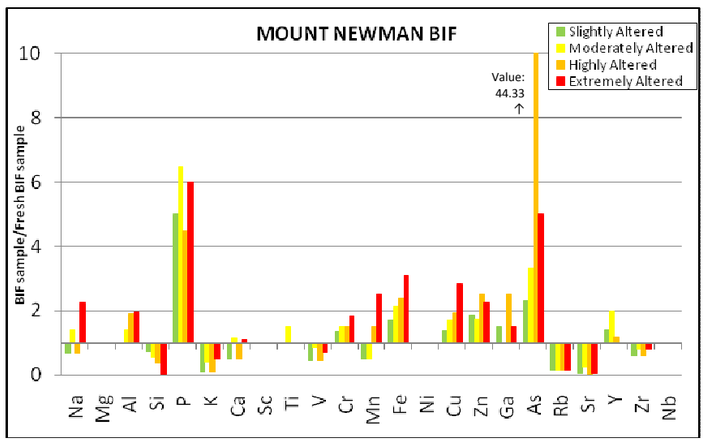

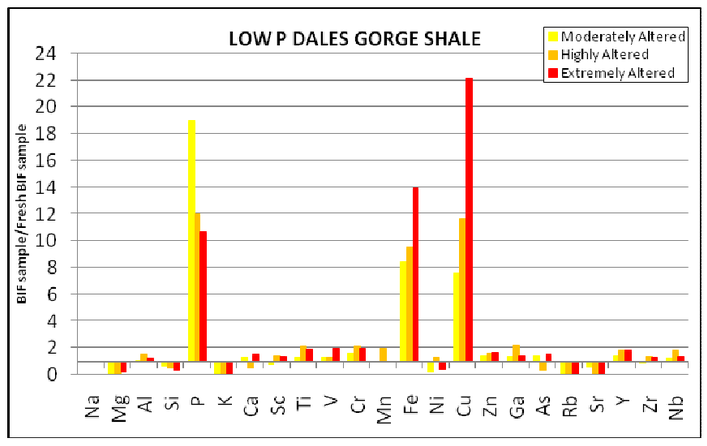

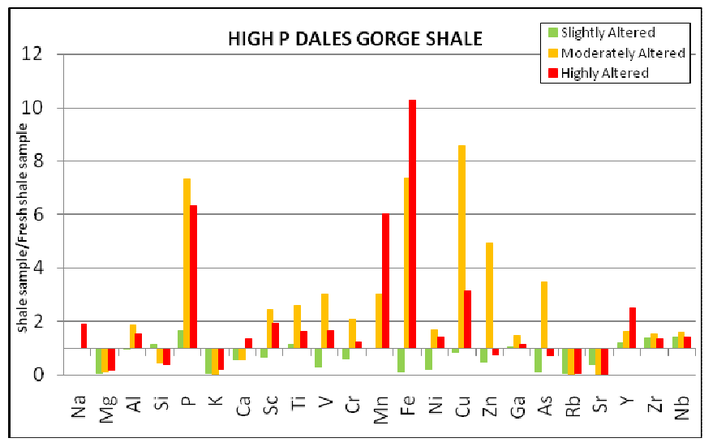

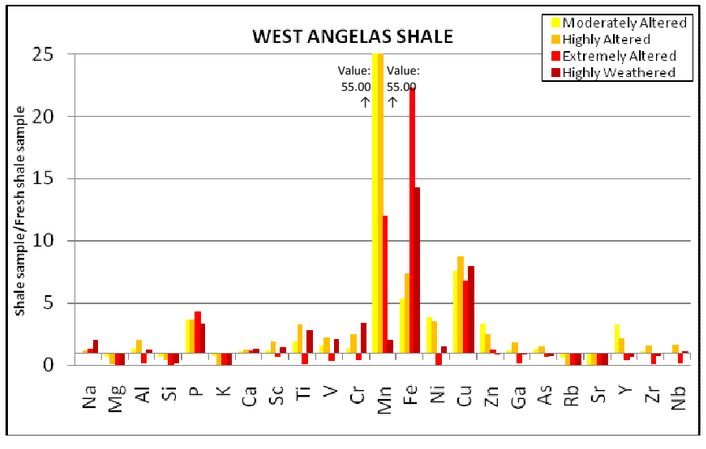

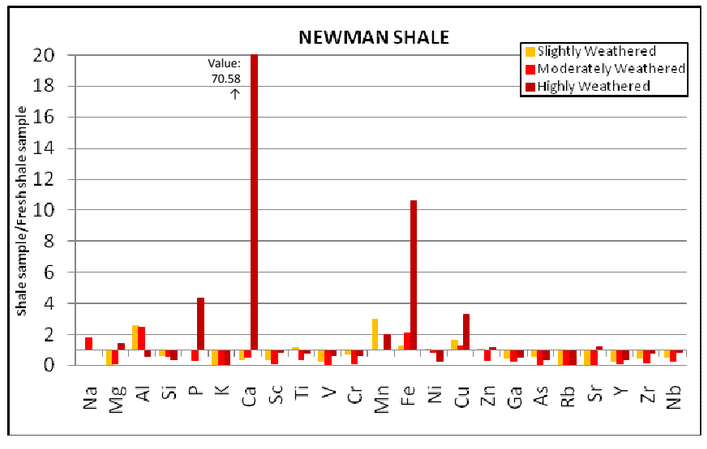

FIGURE 5.30 (TOP LEFT) ENRICHMENT-DEPLETION DIAGRAM OF DALES GORGE BIF FROM THE LOW P BROCKMAN IRON FORMATION
FIGURE 5.30 (TOP MIDDLE) ENRICHMENT-DEPLETION DIAGRAM OF JOFFRE BIF FROM THE LOW P BROCKMAN IRON FORMATION
FIGURE 5.30 (TOP RIGHT) ENRICHMENT-DEPLETION DIAGRAM OF DALES GORGE BIF FROM THE HIGH P BROCKMAN IRON FORMATION
FIGURE 5.30 (MIDDLE LEFT) ENRICHMENT-DEPLETION DIAGRAM OF NEWMAN BIF FROM THE MARRA MAMBA IRON FORMATION
FIGURE 5.30 (MIDDLE) ENRICHMENT-DEPLETION DIAGRAM OF DALES GORGE SHALE FROM THE LOW P BROCKMAN IRON FORMATION
FIGURE 5.30 (MIDDLE RIGHT) ENRICHMENT-DEPLETION DIAGRAM OF DALES GORGE SHALE FROM THE HIGH P BROCKMAN IRON FORMATION
FIGURE 5.30 (BOTTOM LEFT) ENRICHMENT-DEPLETION DIAGRAM OF WEST ANGELAS SHALE FROM THE MARRA MAMBA IRON FORMATION
FIGURE 5.30 (BOTTOM MIDDLE) ENRICHMENT-DEPLETION OF NEWMAN SHALE FROM THE MARRA MAMBA IRON FORMATION

5.4.5 LOSS ON IGNITION

Loss on ignition (LOI) is a geochemical test that consists of igniting the material and measuring the weight loss. This provides an elemental or oxide analysis of the material. According to Taylor et al. (2001), LOI decreases with alteration in BIF samples from Southern Ridge, Tom Price.

The relationship of alteration (using the *Pilbara Iron* alteration index) and LOI in the lower Hamersley Group Iron Formation BIF samples studied here (refer to Figure 5.31) show that the slightly to highly altered BIF increases in LOI with alteration, and therefore does not follow the relationship described by Taylor et al. (2001), with less altered BIF plotting in the lower left of the graph and highly altered BIF plotting in the upper right of the proposed trendline (Figure 5.31). The extremely altered BIF samples, however, behave differently with extremely altered BIF having both very high and very low LOI values. It has been observed that the samples with greater hematite content have much lower LOI with 100% hematite samples plotting in the bottom right of the graph and increasing goethite increases the LOI with 100% goethite sample plotting at the top right of the graph.

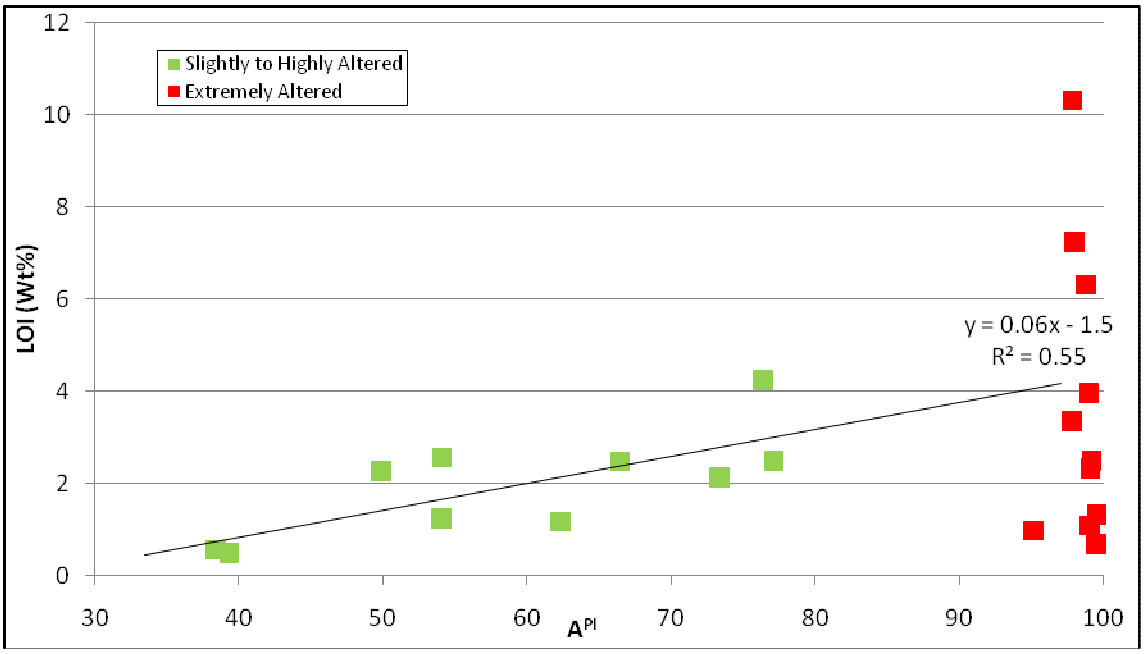

FIGURE 5.31 LOWER HAMERSLEY GROUP IRON FORMATION BIF LOI AND A^{PI}

The relationship of alteration (using the *Pilbara Iron* alteration index) and LOI for the lower Hamersley Group Iron Formation shale can be seen in Figure 5.32 and shows that with alteration, LOI of the shale samples increases with the fresh and slightly altered shale

plotting in the bottom left of the proposed trendline, moderately altered to highly altered plotting further up the trendline and the extremely altered shale plotting at the top right of the trendline.

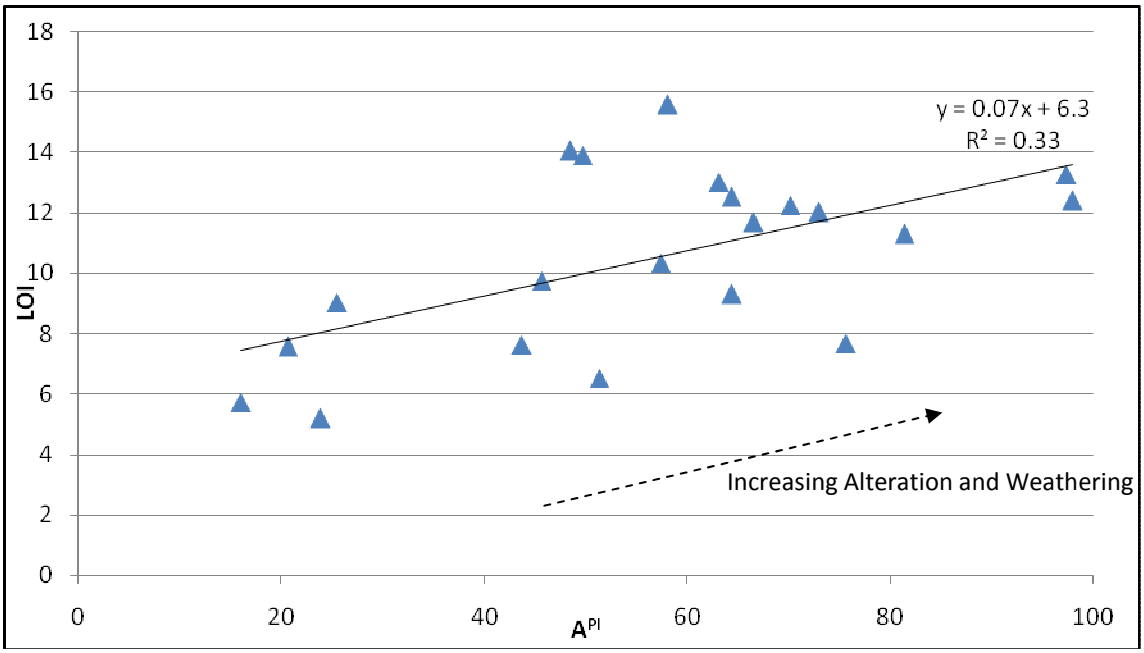

FIGURE 5.32 LOWER HAMERSLEY GROUP IRON FORMATION SHALE LOI AND A^{PI}

5.4.6 RECENT WEATHERING EFFECTS

Much of the chemical alteration and weathering processes in the Hamersley Province are similar to each other and are difficult to discern from one another. In addition to this, the weathering processes are very complex with areas of leaching and/or dehydration and hydration, both of which also occur in the alteration zones. For example, aluminum and titanium are immobile in both altered and weathered environments and a combination of iron leaching and iron concentration is observed in recent weathering zones. Dalstra and Minello (1999) inferred that weathering in the dolerite dykes in the Hamersley Province depletes magnesium. This relationship is not observed in the BIF samples which generally contain very low magnesium concentrations with the exception of the fresh BIF. However, this relationship has been observed in the shale samples studied here. Sodium and titanium also appear to increase with weathering in the lower Hamersley Group Iron Formation deposits (Figure 5.33). More research on weathering processes is needed to understand this geochemical and mineralogical relationship better.

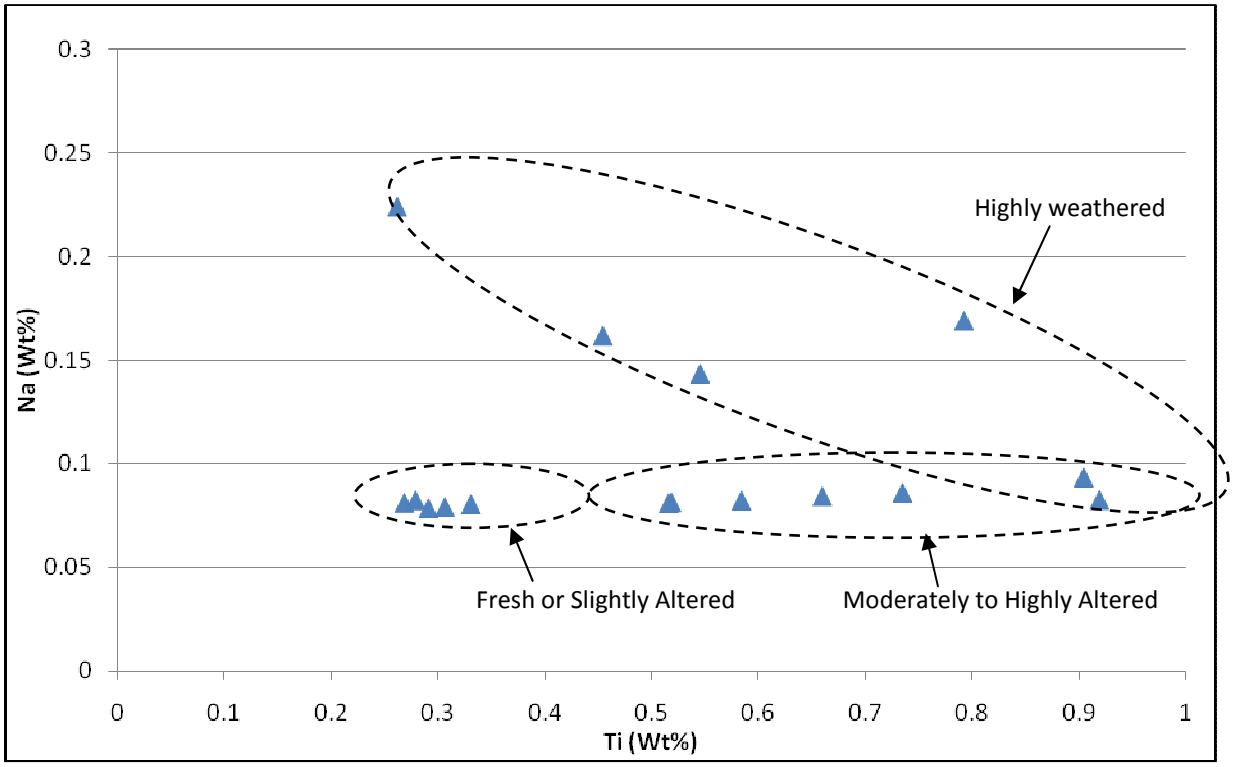

FIGURE 5.33 THE SODIUM AND TITANIUM CONCENTRATIONS FOR LOWER HAMERSLEY GROUP IRON FORMATION SHALE

5.5 CONCLUSIONS

Several conclusions can be made from the geochemical and mineralogical investigation of the lower Hamersley Group BIF and shale deposits. These are:

- The *Pilbara Iron* alteration index is calculated using enriched and depleted elements in the lower Hamersley Group Iron Formation BIF and shale deposits. The element concentrations are determined from geochemical analysis of the BIF and shale samples such as from XRF major element analysis.
- The *Pilbara Iron* alteration index is defined as:

$$A^{PI} = \frac{(Fe_2O_3T + Al_2O_3 + TiO_2 + P_2O_5)100}{Fe_2O_3T + Al_2O_3 + TiO_2 + P_2O_5 + SiO_2 + MgO + CaO}$$

- The *Pilbara Iron* alteration index is the best method for determining the extent of alteration and weathering in both BIF and shale samples of the lower Hamersley Group Iron Formations but is unable to discern between the two processes.
- A *Pilbara Iron* alteration index of less than 20 indicates the rock is fresh, between 20 and 40 indicates the rock is slightly altered and/or weathered, between 40 and 60 indicates the rock is moderately altered and/or weathered, between 60 and 80

indicates the rock is highly altered and/or weathered, and greater than 80 indicates the rock is extremely altered and/or weathered.

- The ratio of aluminium to titanium increases with alteration in the lower Hamersley Group Iron Formation deposits, especially in the shale samples.
- PER diagrams of Si/Ti against P/Ti for lower Hamersley Group BIF deposits and Si/Ti against Al/Ti for the lower Hamersley Group shale deposits can be used to show the alteration stages of the BIF and shale, respectively.
- LOI increases with alteration in both the lower Hamersley Group BIF and shale deposits but increases and decreases dramatically with goethite or hematite mineralisation, respectively, in extremely altered BIF samples.
- Recent weathering effects are generally difficult to discern but may be marked by in increase in Na and Ti or a decrease in Mg in the lower Hamersley Group shale deposits.
- Enrichment-depletion diagrams give a good overall representation of enrichment and depletion processes of the different lower Hamersley Group BIF and shale deposits as they alter and weather and potentially may be used to discern hypogene and supergene alteration processes in BIF and weathering in shale, however, more samples need to be tested to confirm this.

6 THE EFFECT OF ALTERATION AND WEATHERING ON STABILITY IN THE HAMERSLEY PROVINCE

6.1 OVERVIEW

In this chapter, the geotechnical parameters of the lower Hamersley Group BIF and shale studied through field work and laboratory testing and presented in Chapter 4, will be analysed against geochemical parameters of weathering and alteration discussed in Chapter 5. Point load index, slake durability index and the SMR parameters of intact rock strength, RQD, discontinuity spacing, discontinuity conditions and calculated GSI will be analysed against the PI alteration index.

The objective of this chapter is to:

- Link the geochemical and/or mineralogical parameters that occur with alteration and weathering in the lower Hamersley Group BIF and shale, to specific rock mass conditions in RTIO mines.

The PI alteration index was chosen as the parameter for analysing these rocks for alteration and weathering against the geotechnical parameters as it has proven to be the most efficient and successful geochemical or mineralogical parameter. The PI alteration index is calculated from the major elements affected by alteration and weathering in the Hamersley Province, as discussed in Chapter 5. The limitation is that it does not discriminate between alteration and weathering, nor does it discriminate between hypogene and supergene processes.

6.2 GEOTECHNICAL PARAMETERS AND THE PI ALTERATION INDEX

6.2.1 SLOPE MASS RATING PARAMETERS

6.2.1.1 INTACT ROCK STRENGTH

The average intact rock strength rating, as determined by SMR (discussed in Chapter 4), is shown against PI alteration index in Figure 6.1 for the lower Hamersley Group BIF and shale rock masses. The PI alteration index runs along the x-axis in Figures 6.1 to 6.9 and is given in five groups of 0 to 20, 21 to 40, 41 to 60, 61 to 80 and 81 to 100 representing fresh rock, slightly altered and/or weathered rock, moderately altered and/or weathered rock, highly altered and/or weathered rock and extremely altered and/or weathered rock, respectively. The intact rock strength is an estimate of strength completed in the field using the SMR field sheet (Figure 4.1).

Figure 6.1 shows BIF has considerably higher average intact rock strength then shale. It is highest at a PI alteration index of 41 to 60 (moderately altered and/or weathered BIF) and then at a PI alteration index of 21 to 40 (slightly altered and/or weathered BIF). BIF decreases in average intact rock strength rating with increasing alteration with highly altered and/or weathered and extremely altered and/or weathered BIF having successively lower average intact rock strengths. Shale has a highest average intact rock strength at a PI alteration index of 0 to 20 (fresh rock) and 41 to 60 (moderately altered and/or weathered), and decreases slightly for more altered rocks of 61 to 80 and 81 to 100 PI alteration index (highly altered and/or weathered and extremely altered and/or weathered shale).

6.2.1.2 RQD

The average RQD rating, as determined by SMR (discussed in Chapter 4), is shown against PI alteration index in Figure 6.2 for the lower Hamersley Group BIF and shale rock masses. RQD is a measure of the percentage of intact rock pieces over 10 cm in a core run as discussed in Chapter 4.

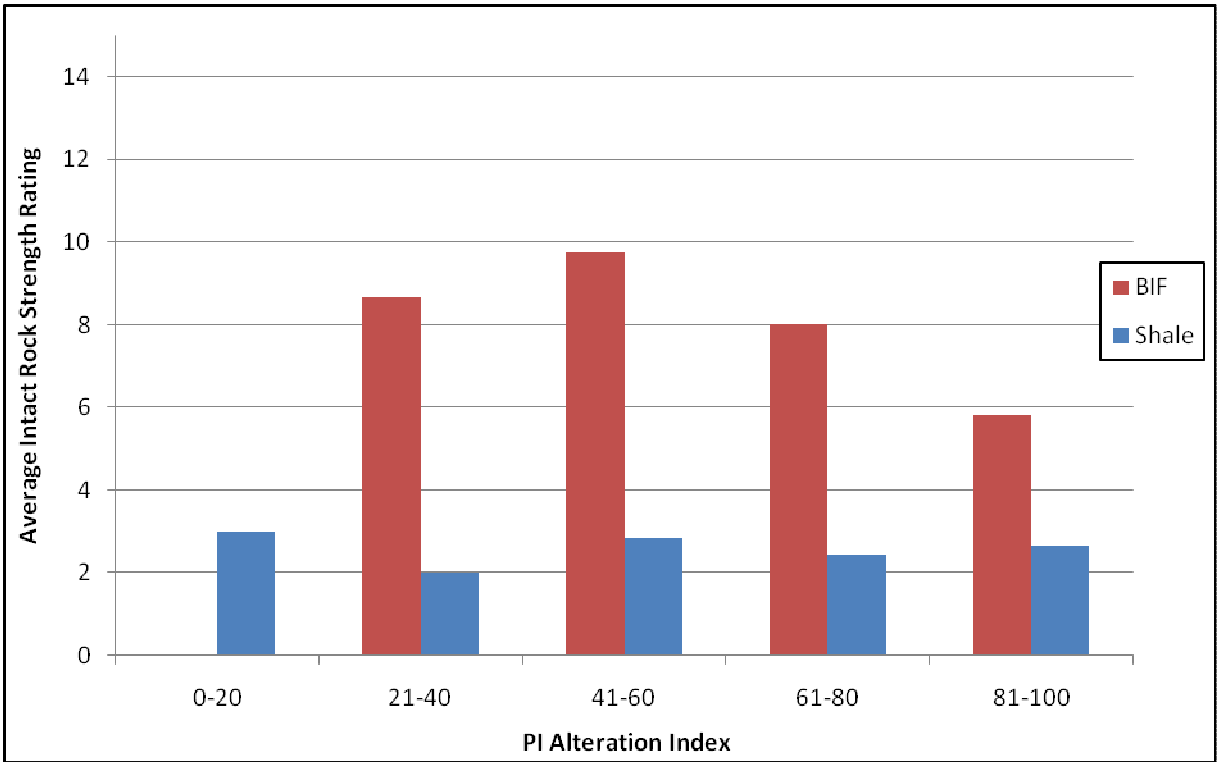

FIGURE 6.1 PI ALTERATION INDEX AGAINST AVERAGE INTACT ROCK STRENGTH RATING FOR LOWER HAMERSLEY GROUP BIF AND SHALE

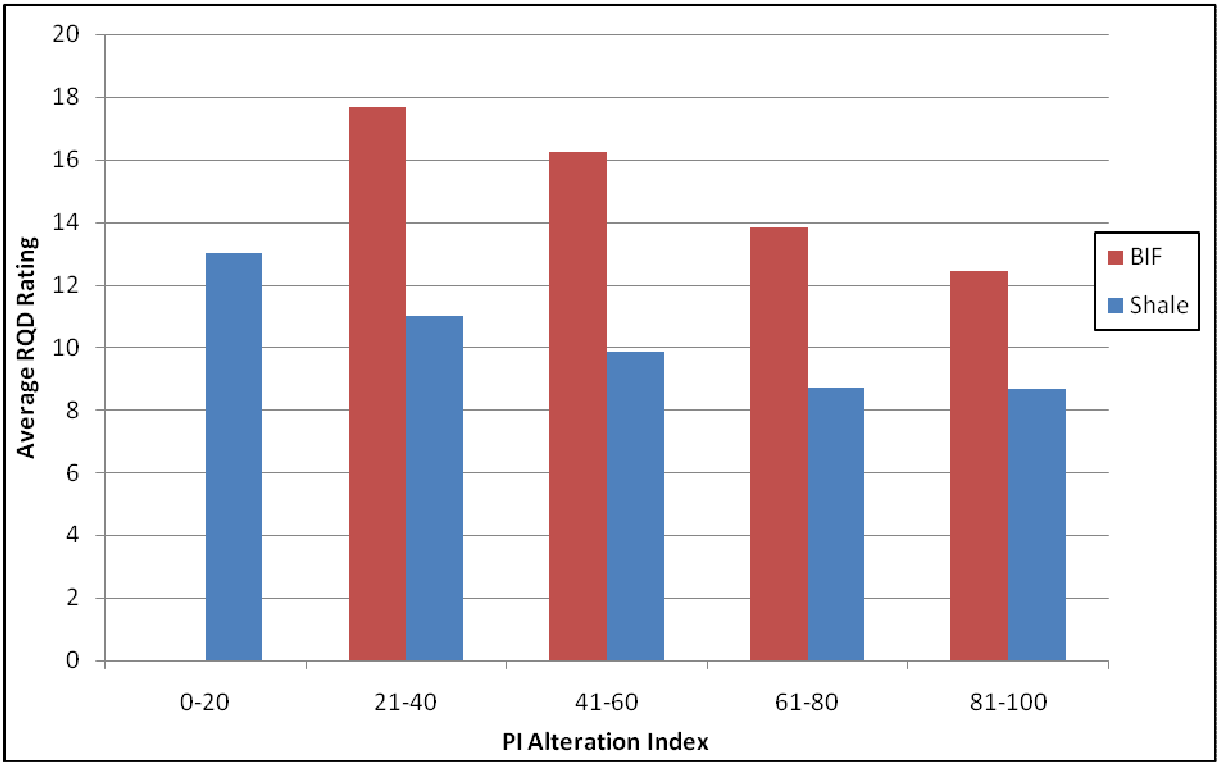

FIGURE 6.2 PI ALTERATION INDEX AGAINST AVERAGE RQD RATING FOR LOWER HAMERSLEY GROUP BIF AND SHALE

Figure 6.2 shows BIF generally has higher average RQD ratings then shale. BIF has its highest average RQD rating at a PI alteration index of 21 to 40 (slightly altered and/or weathered

BIF) and decreases relatively consistently with increased alteration with the lowest average RQD rating at a PI alteration index of 81 to 100 (extremely altered and/or weathered BIF). Shale behaves similarly with its highest average RQD rating at a PI alteration index of 0 to 20 (fresh rock) and constant decrease with alteration with the lowest average RQD rating being at a PI alteration index of 81 to 100 (extremely altered and/or weathered shale).

6.2.1.3 DISCONTINUITY SPACING

The average discontinuity spacing rating, as determined by SMR (as discussed in Chapter 4), is shown against PI alteration index in Figure 6.3 for the lower Hamersley Group BIF and shale rock masses. Discontinuity spacing is a measure of distance between defects in a rock mass and is discussed in Chapter 4.

Figure 6.3 shows BIF generally has a higher average discontinuity spacing rating for most of the PI alteration indices except between 81 and 100 (extremely altered and/or weathered BIF) where the shale has a higher discontinuity spacing rating. BIF has its highest average discontinuity spacing rating at a PI alteration index of 21 to 40 (slightly altered and/or weathered BIF) and decreases with alteration to a low at a PI alteration index of 81 to 100 (extremely altered and/or weathered BIF). Shale, on the other hand, remains relatively constant through the PI alteration Indices except at a PI alteration index of 81 to 100 (extremely altered and/or weathered shale) where the discontinuity spacing increases.

6.2.1.4 DEFECT CONDITIONS

The average discontinuity conditions rating, as determined by SMR (as discussed in Chapter 4), is shown against PI alteration index in Figure 6.4 for lower Hamersley Group BIF and shale rock masses. Discontinuity conditions are the average general condition of discontinuities in a rock mass and includes its roughness or filling, separation of the discontinuity, persistence through the rock mass, and weathering of the discontinuity walls (as described in Chapter 4).

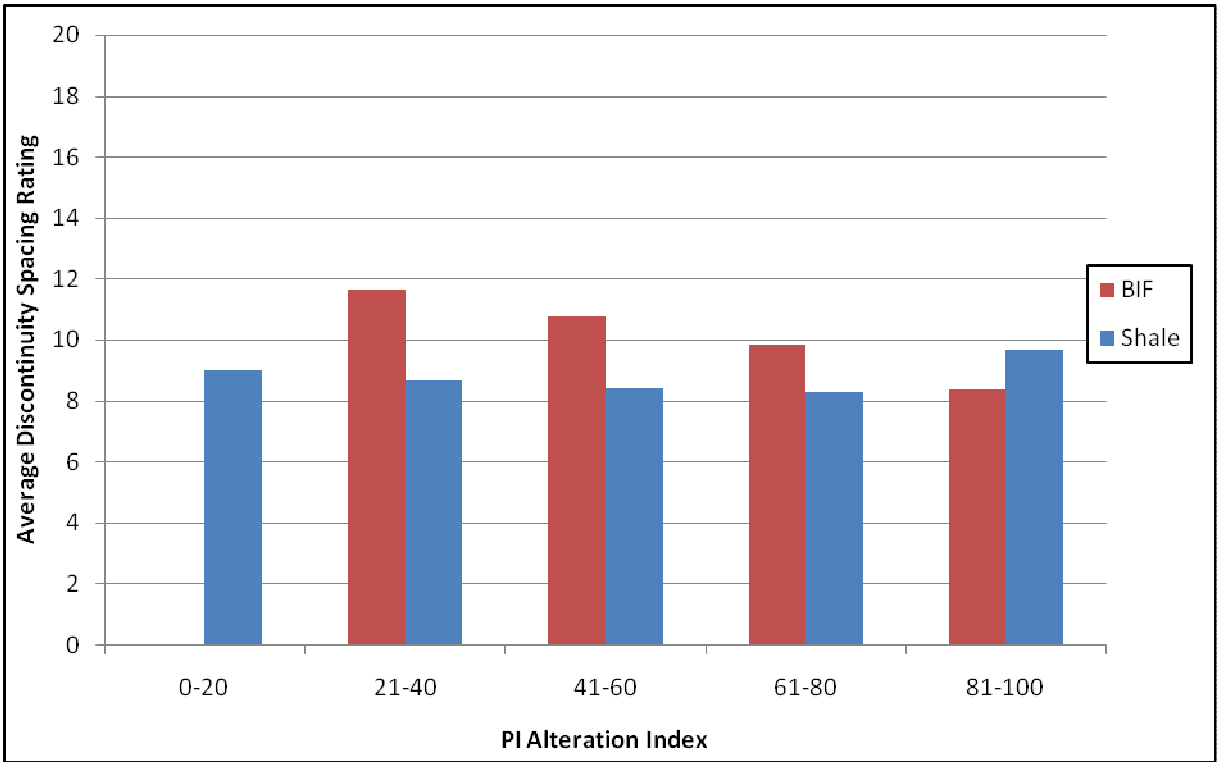

FIGURE 6.3 PI ALTERATION INDEX AGAINST AVERAGE DISCONINTUITY SPACING RATING FOR LOWER HAMERSLEY GROUP BIF AND SHALE

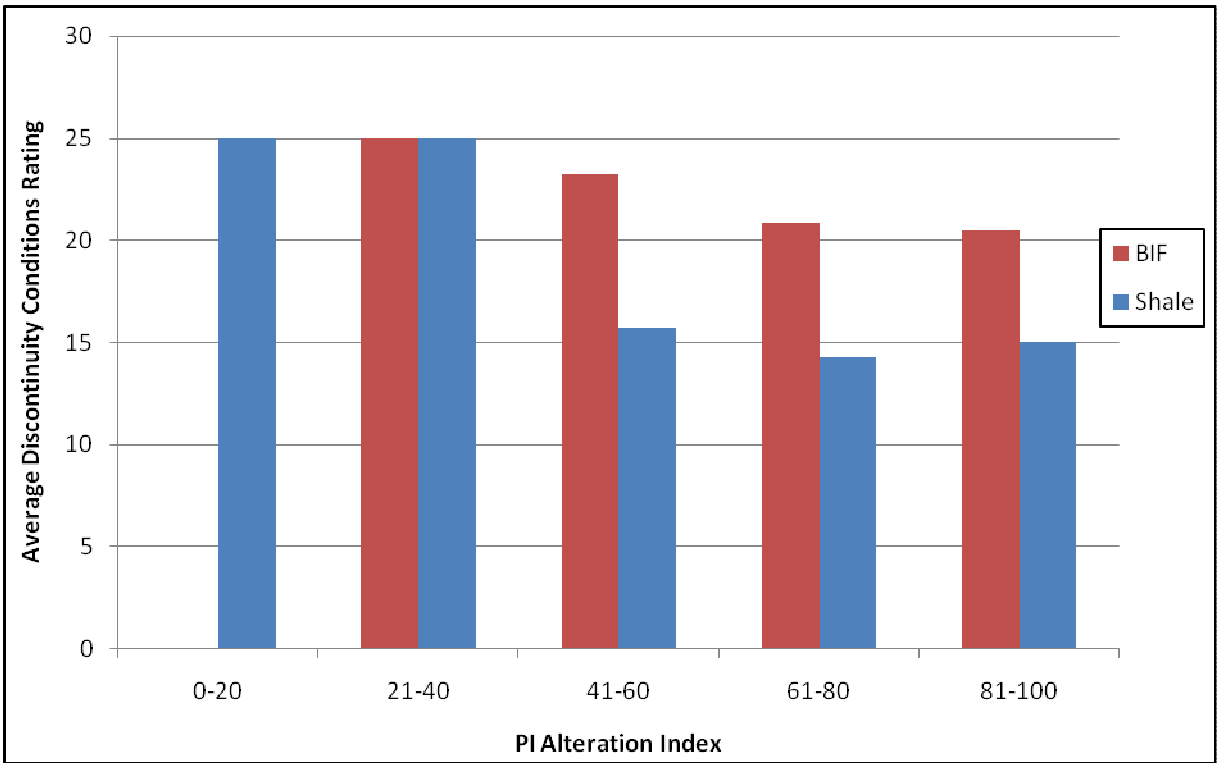

FIGURE 6.4 PI ALTERATION INDEX AGAINST AVERAGE DISCONTINUITY CONDITIONS RATING FOR LOWER HAMERSLEY GROUP BIF AND SHALE

Average Discontinuity condition ratings for low PI alteration indices of 0 to 20 (fresh rock) and 21 to 40 (slightly altered and/or weathered) BIF and shale are high but decreases with increasing alteration. BIF has higher average discontinuity conditions ratings then shale and reaches a low at a PI alteration index of 81 to 100 (extremely altered and/or weathered BIF) while shale reaches a low at a PI alteration index of 61 to 80 (highly altered and/or weathered shale).

6.2.1.5 GEOLOGICAL STRENGTH INDEX

The average Geological Strength Index (GSI), calculated from RMR_{89} (as discussed in chapter 4), is shown against PI alteration index in Figure 6.5 for lower Hamersley Group BIF and shale rock masses. GSI is a measure of overall rock mass strength, as discussed in Chapter 4, measured from intact rock strength rating, RQD rating, discontinuity spacing rating, discontinuity conditions rating and adjustment for orientation. Values of between 0 and 20 GSI indicate very poor rock mass strength, values between 21 and 40 indicate poor rock mass strength, values between 41 and 60 GSI indicate moderate rock mass strength, values between 61 and 80 indicate good rock mass strength and values between 81 and 100 indicate very good rock mass strength.

Figure 6.5 show BIF generally has higher average GSI then shale in the lower Hamersley Group deposits with an average of 'moderate' GSI over all PI alteration index intervals. BIF reaches a high GSI at PI alteration index of 61 to 80 (highly altered and/or weathered BIF) and a low at a PI alteration index of 81 to 100 (extremely altered and/or weathered BIF). Shale has a highest average GSI at a PI alteration index of 21 to 40 (slightly altered and/or weathered shale) with a 'moderate' GSI value and a low at a PI alteration index of 61 to 80 (highly altered and/or weathered shale) with a 'poor' GSI value.

6.2.2 GEOTECHNICAL LABORATORY TESTING

6.2.2.1 POINT LOAD STRENGTH INDEX

The point load strength index is a measure of intact rock strength and verifies the intact rock strength from that estimated in the field. Figure 6.6 shows the PI alteration index of lower Hamersley Group BIF and shale against the point load strength index measured in $I_{s(50)}$ (the average strength for a standard sample size, as discussed in Chapter 4). Figure 6.7 shows the

PI alteration index against the average point load strength index in UCS calculated from UCS = $24.I_{s(50)}$ for BIF and UCS = $15.I_{s(50)}$ for shale, as discussed in Chapter 4.

Figure 6.6 and Figure 6.7 show that BIF has significantly higher intact rock strength then shale. At a PI alteration index of 61 to 80 (highly altered and/or weathered), BIF becomes significantly weaker but increases in intact rock strength slightly with further alteration to a PI alteration index of 81 to 100 (extremely altered and/or weathered BIF). At PI alteration index of 61 to 80 and 81 to 100 (highly altered and/or weathered and extremely altered and/or weathered), the intact rock strength of shale is considerably lowered compared to lower alteration indices.

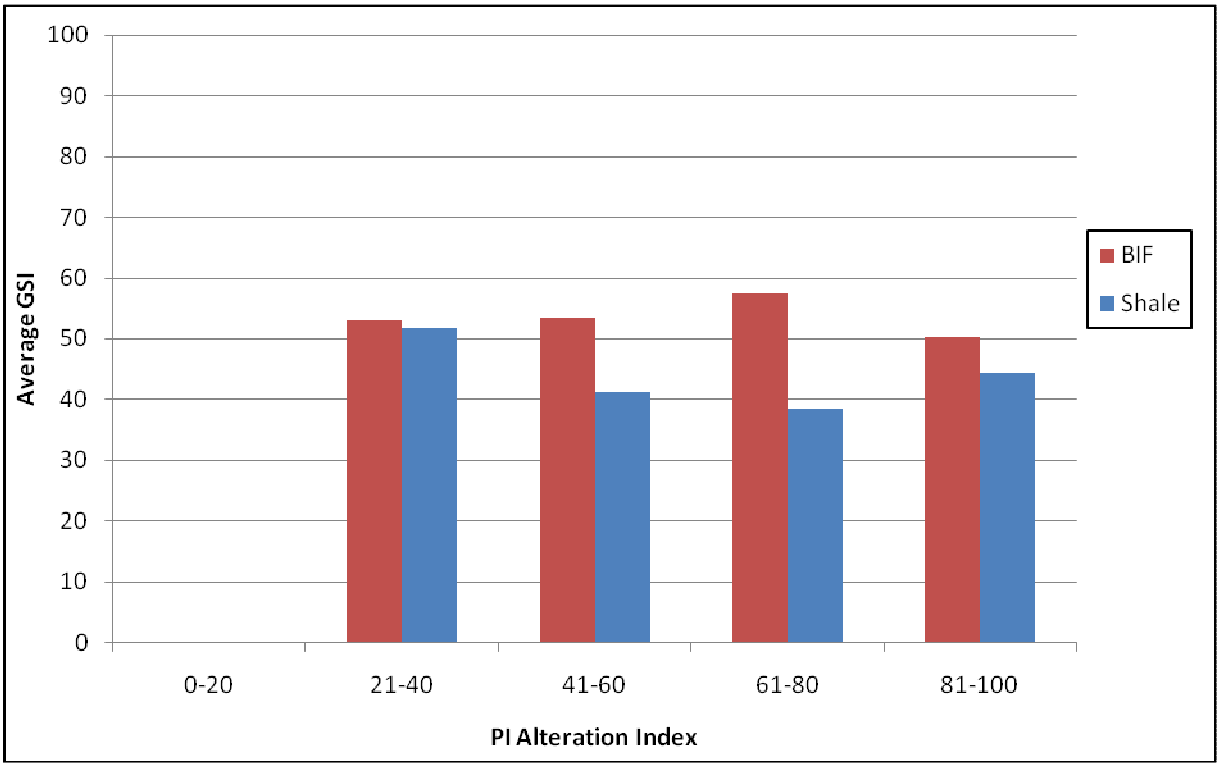

FIGURE 6.5 PI ALTERATION INDEX AGAINST AVERAGE GSI FOR LOWER HAMERSLEY GROUP BIF AND SHALE

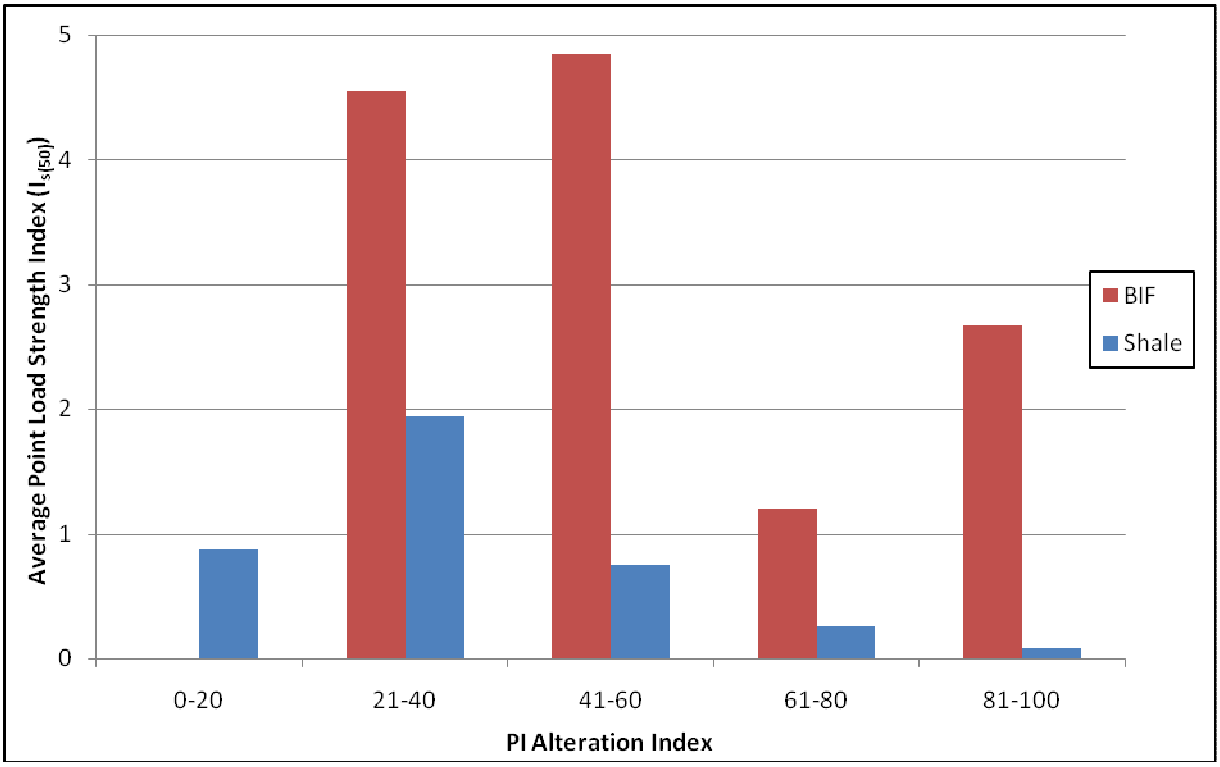

FIGURE 6.6 PI ALTERATION INDEX AGANST POINT LOAD STRENGTH INDEX ($I_{s(50)}$) OF THE LOWER HAMERSLEY GROUP BIF AND SHALE

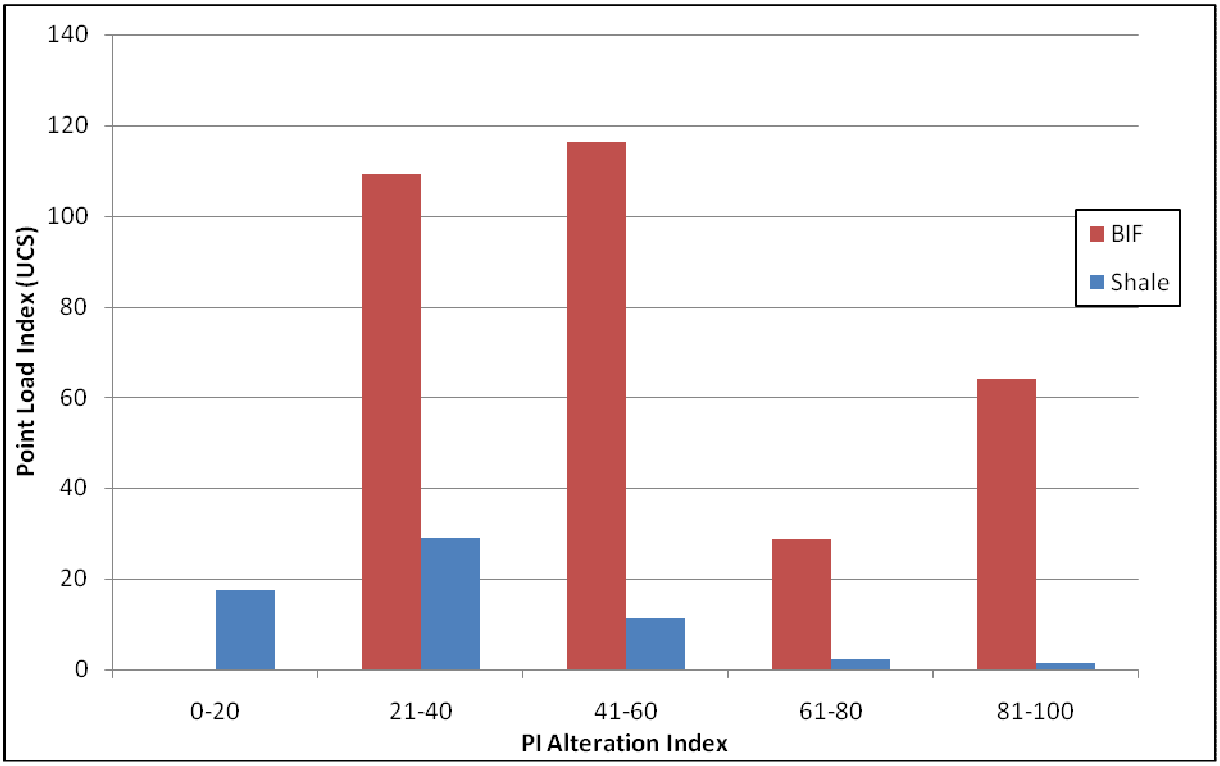

FIGURE 6.7 PI ALTERATION INDEX AGAINST POINT LOAD STRENGTH INDEX (UCS) OF LOWER HAMERSLEY GROUP BIF AND SHALE

Figure 6.7 shows that the equations used by RTIO of 24 for BIF and 15 for shale, multiplied by $I_{s(50)}$, to calculate UCS, shows that the UCS of shale is very low compared to BIF. Figure 6.6 and Figure 6.7 shows that, overall, the lower Hamersley Group shale is considerably weaker then the lower Hamersley Group BIF. Highly altered and/or weathered lower Hamersley Group deposits are also considerably weak particularly in the shale samples.

6.2.2.2 SLAKE DURABILITY INDEX

The slake durability index measures the durability of rocks. Slake durability testing is a good estimate of the effect of weathering or erosion of a rock group and is discussed in further detail in Chapter 4. Figure 6.8 shows the average percentage of rock retained (measured by weight) after the first cycle of slake durability testing (I_{d1}) on lower Hamersley Group BIF and shale against PI alteration index. Figure 6.9 shows the average percentage of rock retained (measured by weight) after the second cycle of slake durability testing (I_{d2}) on lower Hamersley Group BIF and shale against PI alteration index.

Figure 6.8 and Figure 6.9 shows that the durability of both the BIF and shale are high, especially for PI alteration indices of 0 to 20 (fresh rock), 21 to 40 (slightly altered and/or weathered rock) and 41 to 60 (moderately altered and/or weathered rock). Slake durability decreases slightly in the BIF for an increased PI alteration index of 61 to 80 (highly altered and/or weathered BIF) and again for a PI alteration index of 81 to 100 (extremely altered and/or weathered BIF). The durability of shale, however, decreases slightly in shale with a PI alteration index of 41 to 60 (moderately altered and/or weathered shale) and decreases dramatically with an increased PI alteration index of 61 to 80 (highly altered and/or weathered shale). The graphs in Figures 6.8 and 6.9 are reasonably similar showing that the weathering or erosion has slowed down considerably by the second cycle.

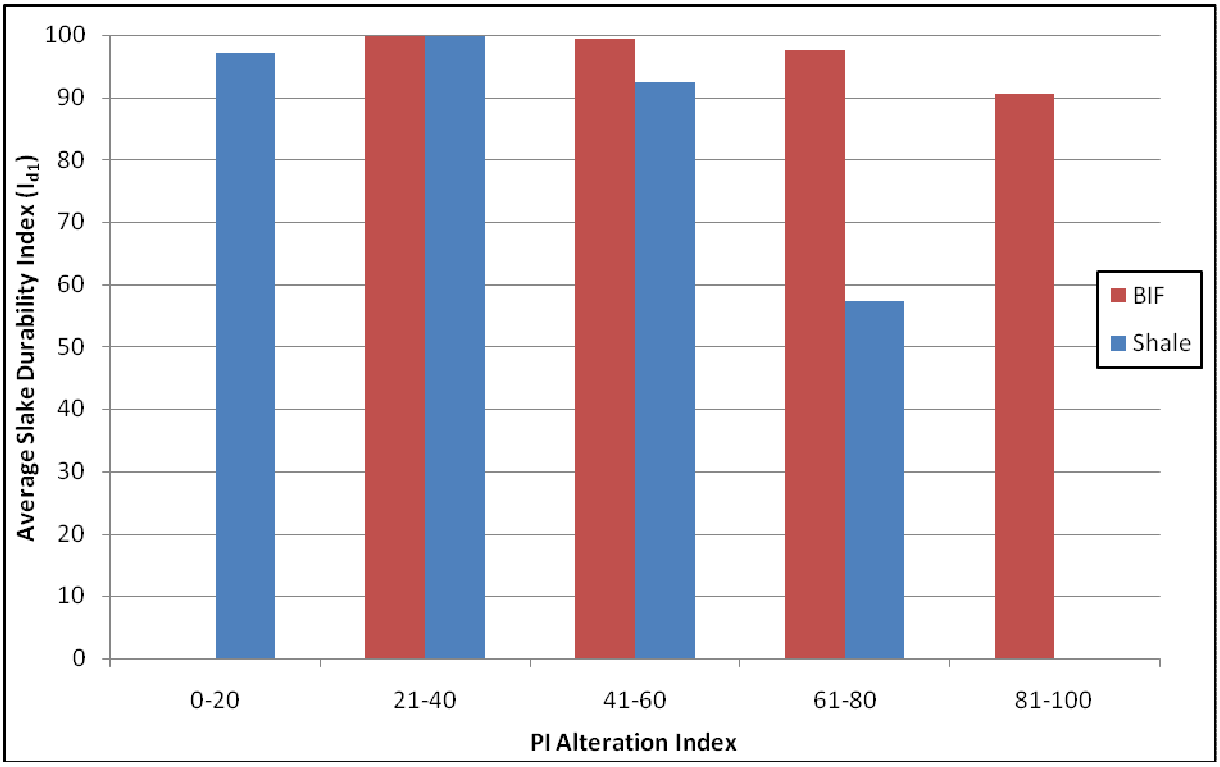

FIGURE 6.8 PI ALTERATION INDEX AGAINST SLAKE DURABILITY INDEX (I_{D1}) FOR THE LOWER HAMERSLEY GROUP BIF AND SHALE

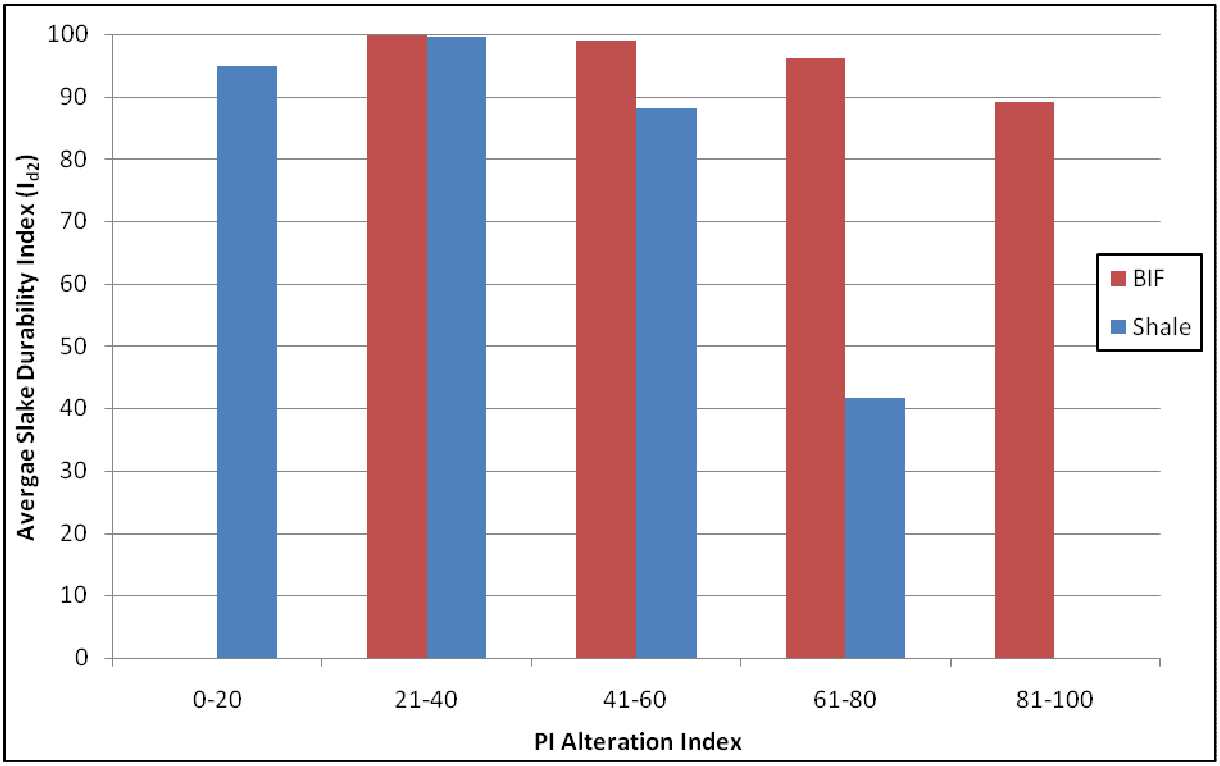

FIGURE 6.9 PI ALTERATION INDEX AGAINST SLAKE DURABILITY INDEX (I_{D2}) FOR THE LOWER HAMERSLEY GOUP BIF AND SHALE

6.3 CONCLUSIONS

Several general conclusions can be made from the discussion of the effect of alteration and weathering by hypogene and supergene alteration and recent weathering of the lower Hamersley Group BIF and shale deposits on stability in the RTIO mines of the Hamersley Province, Western Australia. These are:

- The most favorable geochemical or mineralogical parameter that can be used to measure alteration and/or weathering is the PI alteration index discussed in Chapter 5;
- Using this chemical equation, the alteration and weathering of lower Hamersley Group BIF and shale can be estimated and divided into five groups of fresh rock, slightly altered and/or weathered rock, moderately altered and/or weathered rock, highly altered and/or weathered rock, and extremely altered and/or weathered rock as discussed in Chapter 5;
- By studying the geotechnical characteristics of these groups, it has been found that lower Hamersley Group BIF is likely to have better rock mass conditions then shale;
- BIF generally has 'moderate' GSI values and has geotechnical characteristics that are generally poorer at a PI alteration index of 61 to 80 and 81 to 100 (highly and extremely altered and/or weathered BIF), with highly altered and/or weathered BIF having the lowest point load indices and extremely altered and/or weathered BIF having the lowest slake durability indices, average estimated rock strength, average RQD, and average discontinuity spacing and conditions;
- Shale generally ranges from having 'moderate' to 'poor' GSI values and has geotechnical characteristics that are generally poorer at a PI alteration index of 61 to 80 and 81 to 100 (highly and extremely altered and/or weathered shale), with extremely altered and/or weathered shale having the lowest average intact rock strengths and highly altered and/or weathered shale having the poorer average discontinuity spacing and conditions.

7 IMPLICATIONS FOR HAMERSLEY IRON ORE MINING

7.1 OVERVIEW

It has been determined that the PI alteration index is a useful tool for determining the extent of alteration and weathering of lower Hamersley Group BIF and shale. This can then be used to estimate the rock mass conditions of the samples being analysed, as discussed in Chapter 6. This chapter outlines the use of the PI alteration index to estimate the rock mass conditions of lower Hamersley Group BIF and shale deposits in RTIO open pit mines.

The objective of this chapter is to:

- Use geochemical and/or mineralogical analysis on lower Hamersley Group BIF and shale core samples to predict the extent of alteration and/or weathering and, therefore, use as a predictive tool for open pit slope stability in RTIO mines, Pilbara, Western Australia.

The geochemical PI alteration index was chosen to be used because it is a simple and effective technique. It is hoped, with further research of geochemistry and mineralogy, a more comprehensive insight will be gained into the effect of alteration and weathering on geochemical and mineralogical changes with ore genesis within the Hamersley Province BIF and shale.

The PI alteration index can be calculated from geochemical analysis such as XRF major element analysis. XRF analysis is an economic and time efficient analysis. It can be completed in small intervals along rock masses, such as from boreholes, effectively giving a profile of the extent of alteration and weathering of BIF and shale throughout the Hamersley Province. Potentially, if many boreholes are analysed along a section, a 2-D visual representation of the extent of alteration and weathering could be compiled, and if many boreholes throughout a 3-D area are analysed, a block model of the extent of alteration and weathering could then be compiled.

In this chapter, examples of PI alteration index profiles are given and 2D and 3D visual representation of the extent of alteration and weathering is discussed. Next, the use of PI alteration index profiles as a tool for predicting stability is discussed and three case studies are presented using SMR as the slope mass conditions analysis. Lastly, remedial measures are considered.

7.2 The Extent of Alteration and Weathering with Depth

7.2.1 Alteration Index Profiles

Three areas were studied by borehole, these were at Southern Ridge Deposit at Tom Price, 23 East Deposit at Paraburdoo, and West Angelas Deposit A. Alteration profiles were created using five boreholes from these three study areas and are shown in Figures 7.1 to 7.5. Several samples were taken from each borehole and geochemically tested (refer to Chapter 5). From XRF major element analysis, the PI alteration index was calculated for each sample to give a description of the alteration and/or weathering of each position down the borehole using the alteration descriptions described in section 5.4.1. These alteration descriptions use the PI alteration indices to describe the extent of alteration and/or weathering using:

- *Fresh rock* as rock with a PI alteration of 0 to 20;
- *Slightly altered and/or weathered rock* as rock with a PI alteration index of 21 to 40;
- *Moderately altered and/or weathered rock* as rock with a PI alteration index of 41 to 60;
- *Highly altered and/or weathered rock* as rock with a PI alteration index of 61 to 80 and
- *Extremely altered and/or weathered rock* as rock with a PI alteration index of 81 to 100.

Ideally, many more samples would be taken at small, regular intervals down a borehole being studied. To give a visual representation of the extent of alteration and/or weathering, a colour scheme can be constructed, such as has been used in Figures 7.1 to 7.5.

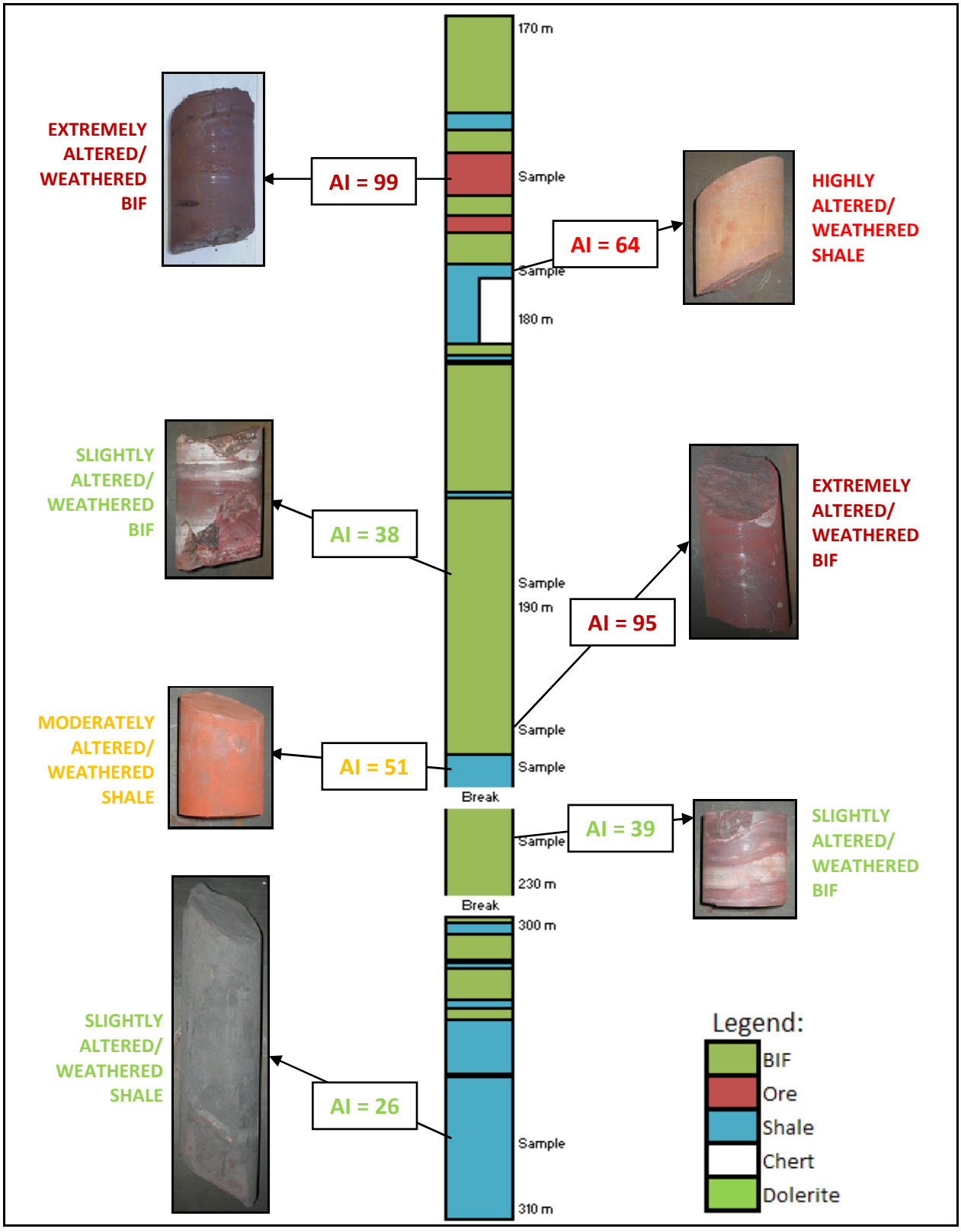

FIGURE 7.1 THE STRATIGRAPHIC COLUMN OF BOREHOLE GC08STR0003 FROM ~170 M TO ~310 M DEPTH AT SOUTHERN RIDGE, TOM PRICE. THE PI ALTERATION INDEX PROFILE OF SEVEN ROCK SAMPLES IS SHOWN.

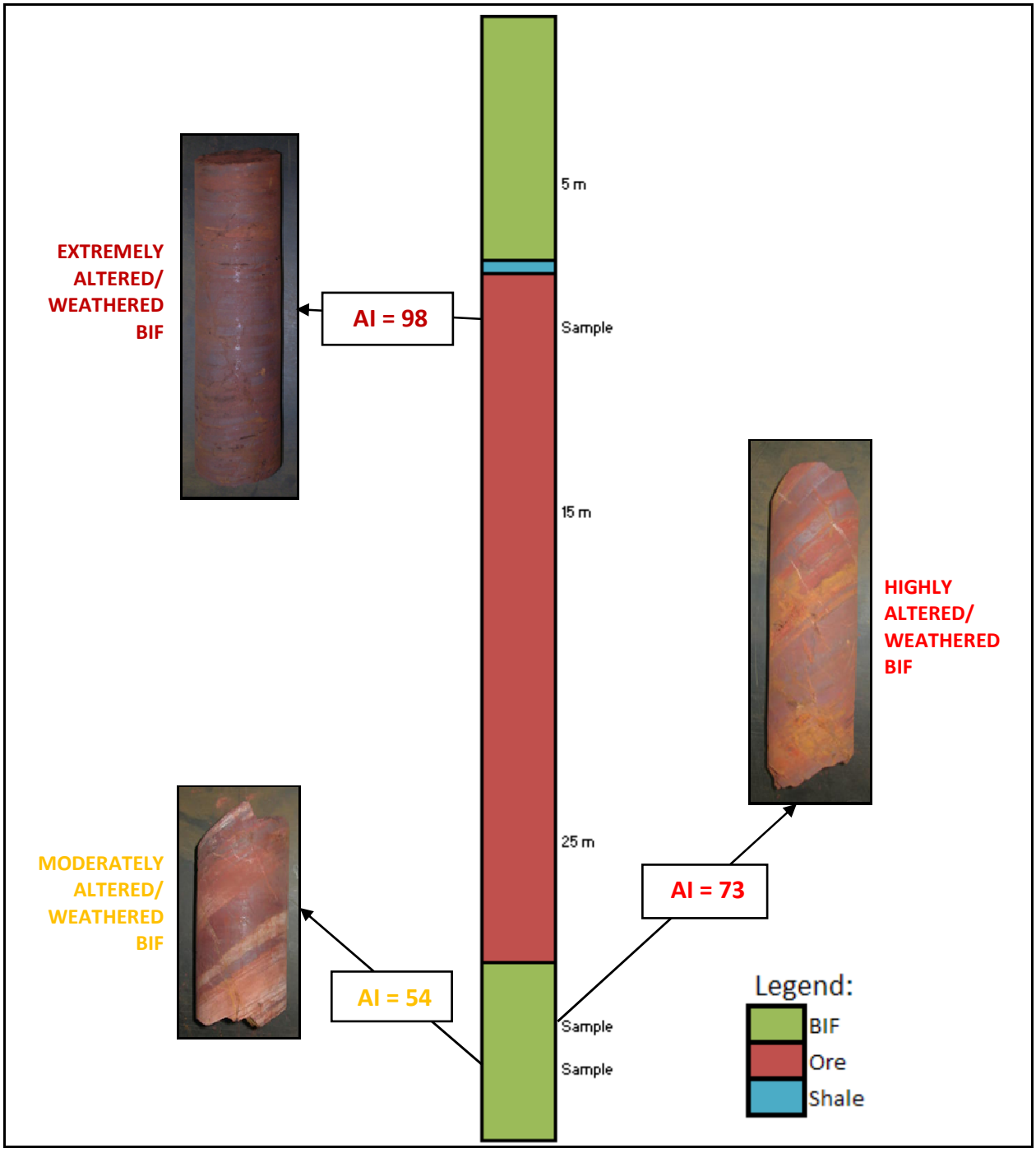

FIGURE 7.2 THE STRATIGRAHIC COLUMN OF BOREHOLE GD0823E0001 FROM 0 M TO ~30 M DEPTH AT EASTERN RANGE, PARABURDOO. THE PI ALTERATION INDEX PROFILE OF THREE ROCK SAMPLES IS SHOWN.

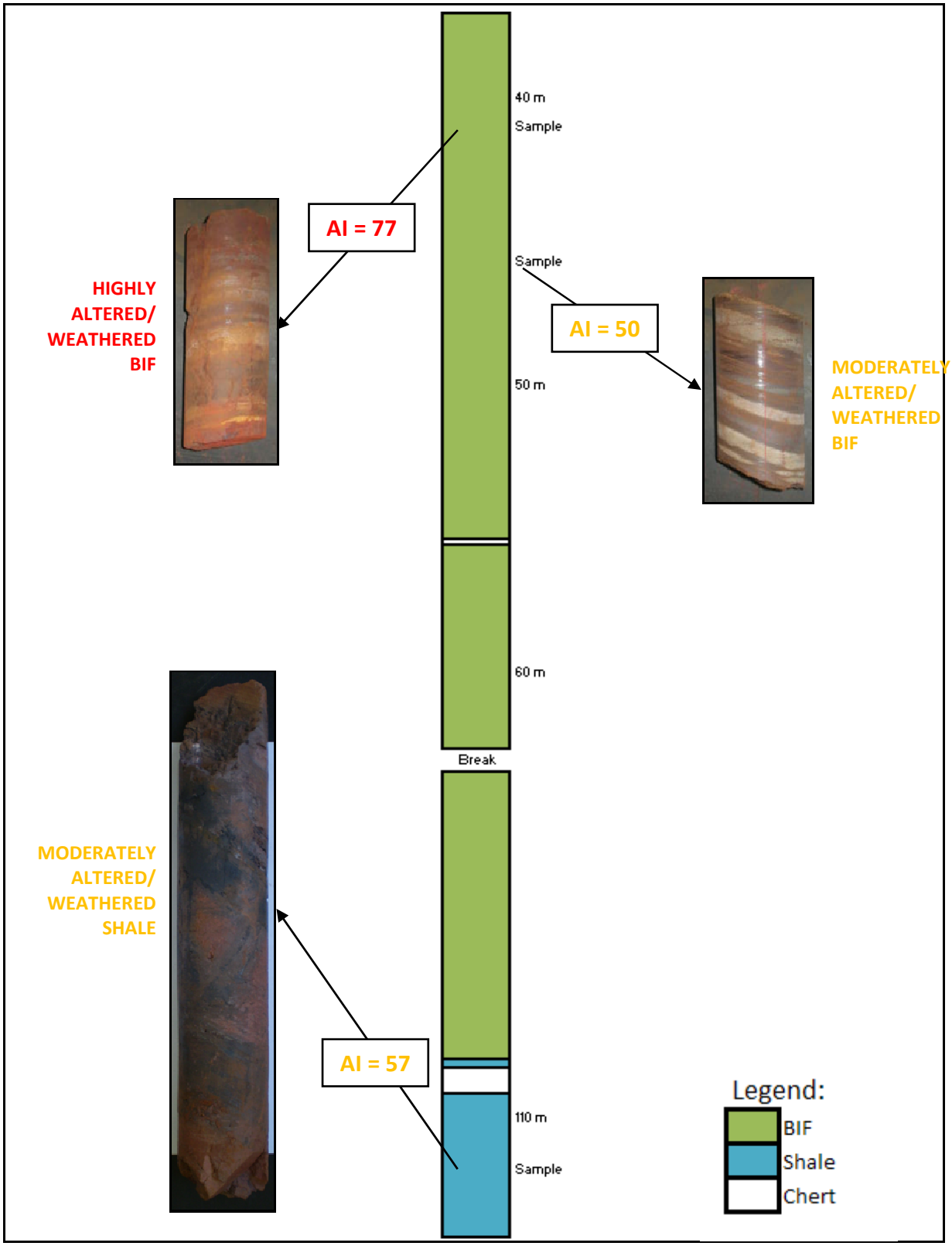

FIGURE 7.3 THE STRATIGRAPHIC COLUMN OF BOREHOLE GD0823E0008 FROM ~37 M TO ~114 M DEPTH AT EASTERN RANGE, PARABURDOO. THE PI ALTERATION INDEX PROFILE OF THREE ROCK SAMPLES IS SHOWN.

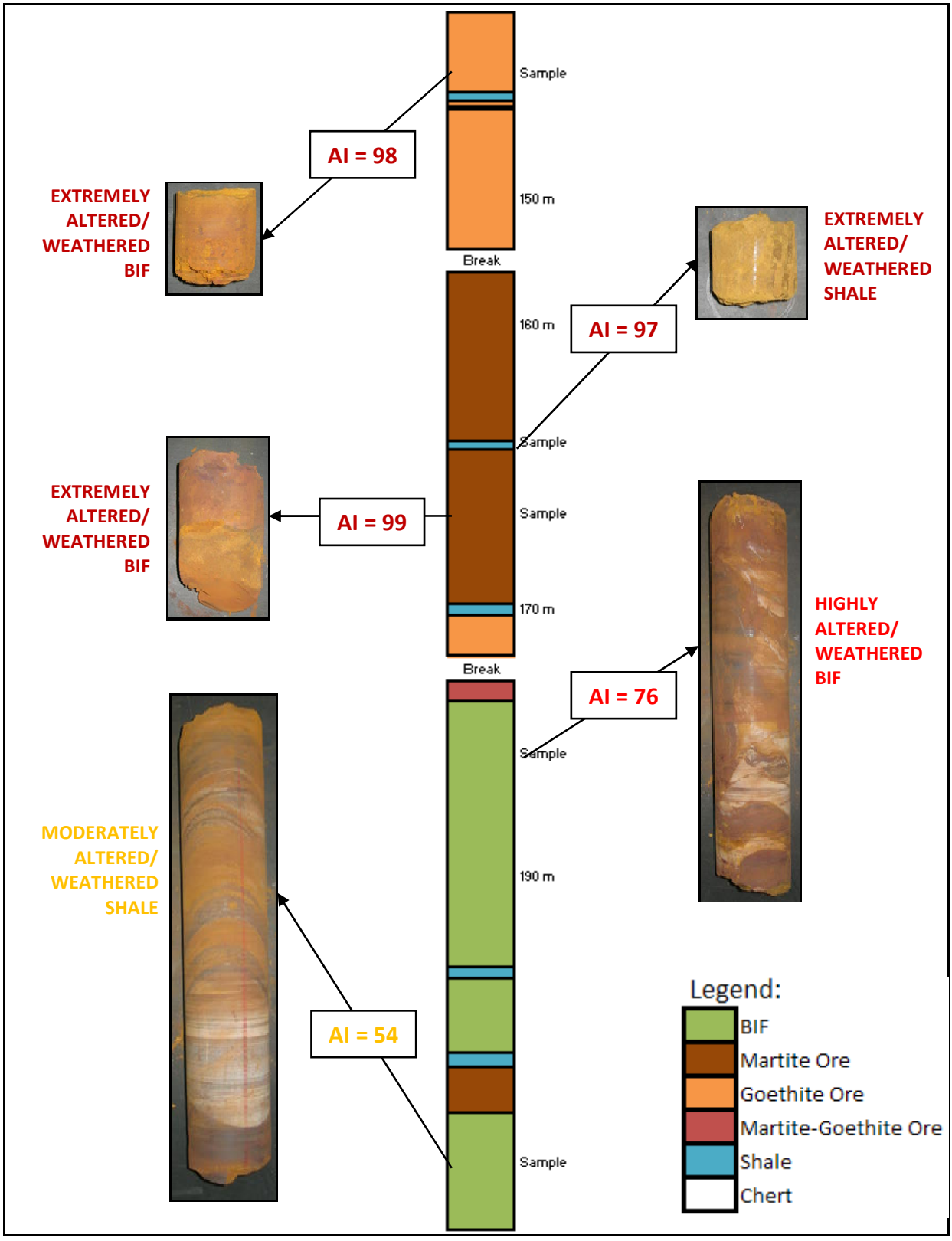

FIGURE 7.4 THE STRATIGRAPHIC COLUMN OF BOREHOLE WAADC0731 FROM ~143 M TO ~202 M DEPTH AT WEST ANGELAS DEPOSIT A. THE PI ALTERATION INDEX PROFILE OF FIVE ROCK SAMPLES IS SHOWN.

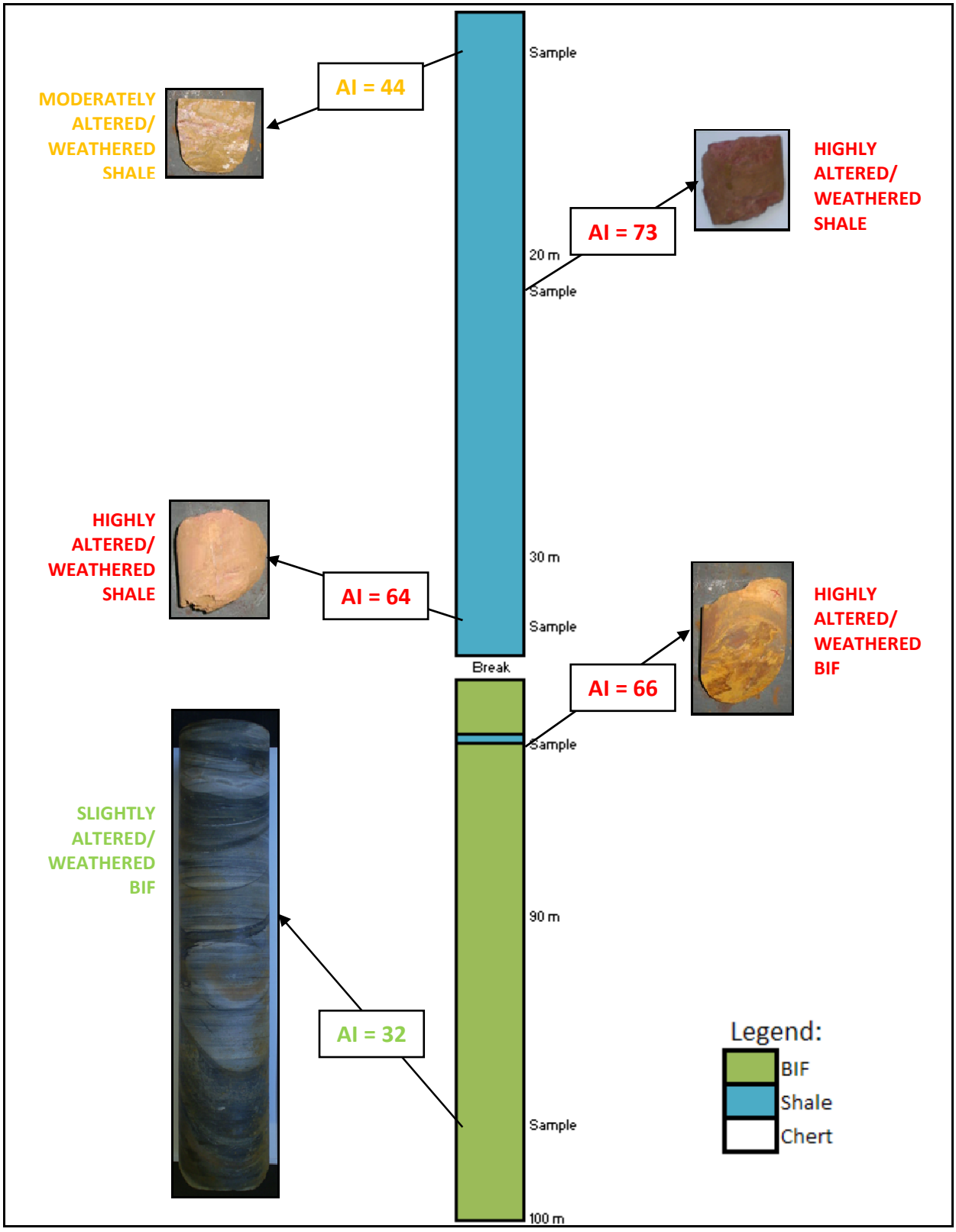

FIGURE 7.5 THE STRATIGRAPHIC COLUMN OF BOREHOLE WAADC0730 FROM 12 M TO 100 M DEPTH AT WEST ANGELAS DEPOSIT A. THE ALTERATION INDEX PROFILE OF FIVE ROCK SAMPLES IS SHOWN.

7.2.2 FURTHER USE

Ideally, many boreholes would be geochemically tested in an area so that cross sections or 3D block diagrams can be compiled to generate 2D or 3D alteration regions. Thereby, geotechnically vulnerable areas, such as highly altered and/or weathered and extremely altered and/or weathered zones can be determined. Figures 7.6a, 7.6b and 7.6c show a schematic representation of the application of using geochemical analysis to identify geotechinically vulnerable areas. Figure 7.6a shows a geological cross section of lower Hamersley Group BIF and shale deposits with a series of boreholes drilled through the geological succession. Using geochemical analysis to determine the PI alteration index profiles down these boreholes is shown in Figure 7.6b where colours are assigned to each alteration description to give a colour profile of the alteration down the boreholes. Finally the alteration regions can be outlined to give a 2D alteration diagram that can potentially be used to identify geotechnically vulnerable areas (Figure 7.6c).

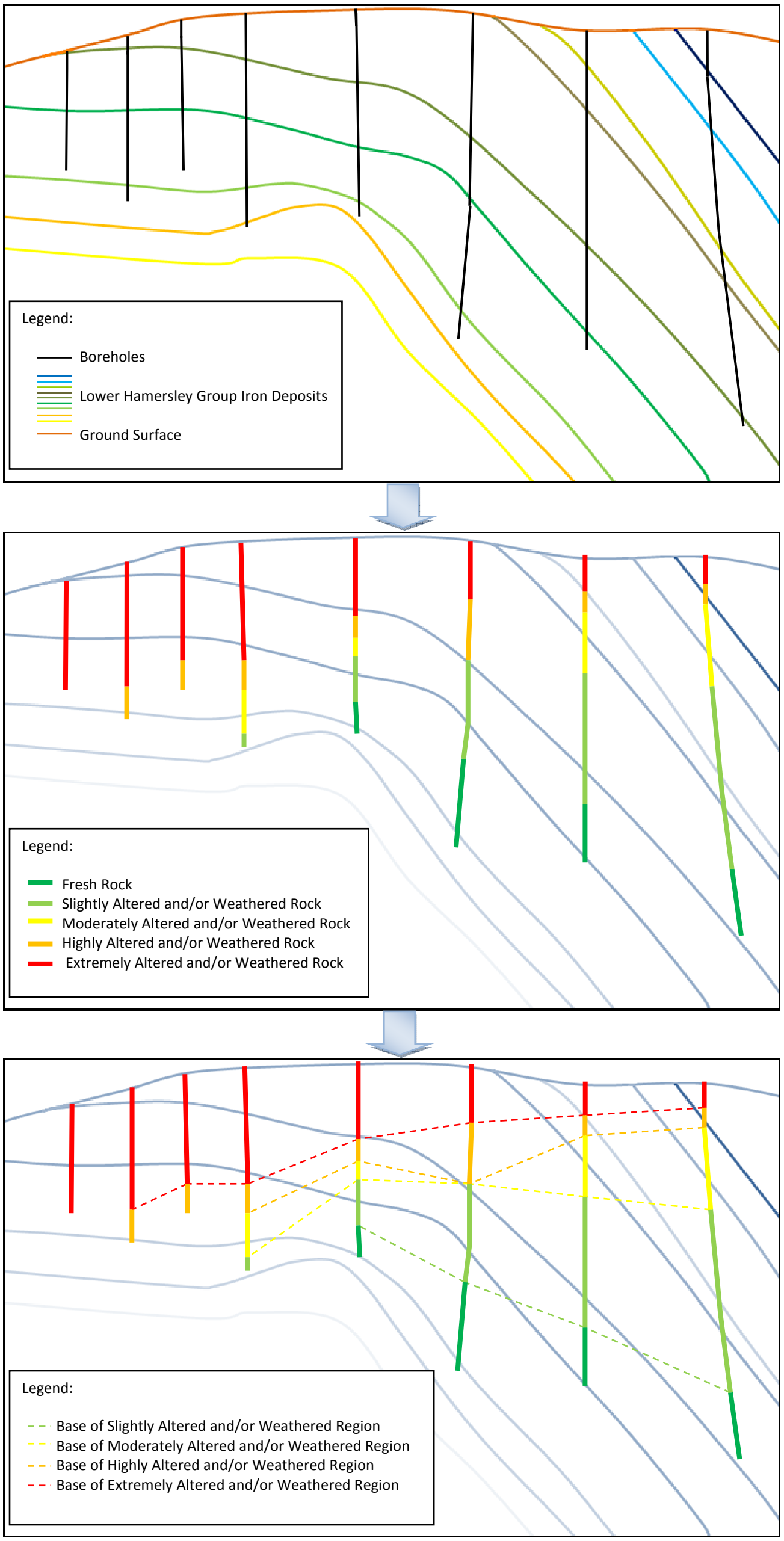

FIGURE 7.6 A SCHEMATIC REPRESENTATION SHOWING THE USE OF PI ALTERATION INDEX PROFILES, CREATED DOWN BOREHOLES, TO SHOW THE ALTERATION ZONES IN A CROSS SECTION. FIGURE 7.6A SHOWS A CROSS SECTION OF A GEOLOGICAL SUCCESSION OF LOWER HAMERSLEY GROUP BIF AND SHALE DEPOSITS WITH EIGHT BOREHOLES DRILLED THROUGH THE SUCCESSION. FIGURE 7.6B SHOWS THE ALTERATION PROFILES DOWN THE INDIVIDUAL BOREHOLES DETERMINED FROM THE PI ALTERATION INDEX AND DIVIDED INTO FIVE GROUPS BASED ON THE ALTERATION DESCRIPTIONS (DISCUSSED IN SECTION 5.4.1). FIGURE 7.6C SHOWS THE ALTERATION REGIONS ACROSS THE GEOLOGICAL CROSS SECTION MADE BY LINKING THE ALTERATION GROUPS. THE DASHED LINES SHOW THE BASE OF THE ALTERATION ZONES WITH THE FRESH REGION UNDER THE BASE OF THE SLIGHTLY ALTERED ZONE.

7.3 IMPLICATIONS FOR SLOPE STABILITY PREDICTIONS

7.3.1 INTRODUCTION

After identifying the extent of alteration and/or weathering of lower Hamersley Group BIF and shale deposits, geotechnically vulnerable areas can be determined. From Chapter 6 these areas have been identified to be highly and extremely altered and/or weathered regions with PI alteration indices of between 61 and 100. After identifying these zones their positions in relation to final walls should be determined and rock mass classification, such as SMR, can be used to assess the stability of the final wall. Three case studies are given below using the five boreholes presented in Section 7.2 and SMR is used to assess the slope stability.

7.3.2 CASE STUDIES

7.3.2.1 SOUTHERN RIDGE

Seven lower Hamersley Group BIF and shale samples were geochemically tested down borehole GC08STR0003 at Southern Ridge, Tom Price. These are shown in Figure 7.1 with the calculated PI alteration indices and corresponding alteration description. Three samples were found to be 'highly' or 'extremely altered' and, as discussed in Chapter 6, are, therefore, geotechnically vulnerable areas and further stability analysis is advised. Rock mass classification, of each area should be undertaken. Here, SMR was completed on the three highly and extremely altered and/or weathered samples (Table 7.1). SMR shows that all three areas should be 'partially stable' to 'stable' as classified by Romana (1993) (refer to Table 7.4).

7.3.2.2 EASTERN RANGES

Three lower Hamersley Group BIF and shale samples were geochemically tested down borehole GD0823E0001 and another three samples down borehole GD0823E0008 at Eastern Ranges, Paraburdoo. These are shown in Figures 7.2 and 7.3 with the calculated PI alteration indices and corresponding alteration descriptions. Two samples from borehole GD0823E0001 and one from borehole GD0823E0008 were found to be 'highly' or 'extremely altered and/or weathered' and are, therefore, geotechnically vulnerable areas. SMR was conducted on these three areas (Table 7.2) which shows that all three samples are 'partially stable' (refer to Table 7.4).

Borehole ID	PI Alteration Index	Alteration Description	SMR Parameters									
			Strength Rating	RQD Rating	Spacing Rating	Condition Rating	Ground-water	F_1	F_2	F_3	Blasting Rating	SMR
GC08STR0003	99	Extremely Altered BIF	4	8	8	20	15	0.15	0.4	-60	0	51
GC08STR0003	64	Highly Altered Shale	2	8	8	20	15	0.15	0.4	-60	0	49
GC08STR0003	95	Extremely Altered BIF	7	13	10	20	15	0.15	0.15	-60	0	64

TABLE 7.1 THE PI ALTERATION INDEX, ALTERATION DESCRIPTION AND SMR OF THE HIGHLY AND EXREMELY ALTERED AND/OR WEATHERED BIF AND SHALE SAMPLES OF THE GEOCHEMICALLY ASSESSED BOREHOLES AT SOUTHERN RIDGE, TOM PRICE

Borehole ID	PI Alteration Index	Alteration Description	SMR Parameters									
			Strength Rating	RQD Rating	Spacing Rating	Condition Rating	Ground-water	F_1	F_2	F_3	Blasting Rating	SMR
GD0823E0001	98	Extremely Altered BIF	7	17	10	20	15	0.15	1	-60	0	60
GD0823E0001	73	Highly Altered BIF	13	13	10	20	15	0.15	1	-60	0	54
GD0823E0008	77	Highly Altered BIF	7	12	7	20	15	1	0.15	-60	0	52

TABLE 7.2 THE PI ALTERATION INDEX, ALTERATION DESCRIPTION AND SMR OF THE HIGHLY AND EXREMELY ALTERED AND/OR WEATHERED BIF AND SHALE SAMPLES OF THE GEOCHEMICALLY ASSESSED BOREHOLES AT EASTERN RANGES, PARABURDOO

Borehole ID	PI Alteration Index	Alteration Description	SMR Parameters									
			Strength Rating	RQD Rating	Spacing Rating	Condition Rating	Ground-water	F_1	F_2	F_3	Blasting Rating	SMR
WAADC0731	98	Extremely Altered BIF	4	17	9	20	15	0.85	1	-6	0	60
WAADC0731	97	Extremely Altered shale	1	3	5	10	15	0.15	0.85	-25	0	31
WAADC0731	99	Extremely Altered BIF	1	11	8	20	15	0.15	0.85	-50	0	48
WAADC0731	76	Highly Altered BIF	12	15	9	25	15	0.15	0.15	-60	0	75
WAADC0730	73	Highly Altered Shale	1	13	10	10	15	0.15	1	-6	0	48
WAADC0730	64	Highly Altered Shale	2	3	8	10	15	0.15	0.7	-60	0	32
WAADC0730	66	Highly Altered BIF	4	11	8	15	15	0.15	0.85	-50	0	47

TABLE 7.3 THE PI ALTERATION INDEX, ALTERATION DESCRIPTION AND SMR OF THE HIGHLY AND EXREMELY ALTERED AND/OR WEATHERED BIF AND SHALE SAMPLES OF THE GEOCHEMICALLY ASSESSED BOREHOLES AT WEST ANGELAS DEPOSIT A

7.3.2.3 WEST ANGELAS

Five lower Hamersley Group BIF and shale samples were geochemically tested down borehole WAADC0731 and another five samples down borehole WAADC0730 at West Angelas Deposit A. These are shown in Figures 7.4 and 7.5 with the calculated PI alteration indices and corresponding alteration description. Four samples from borehole WAADC0731 and three from borehole WAADC0730 were found to be 'highly' or 'extremely altered and/or weathered' and are, therefore, geotechnically vulnerable areas. SMR was conducted on these seven areas (Table 7.3) which shows that five of the samples are 'partially stable' to 'stable', while the two remaining samples are classified as 'unstable' and are likely to experience large planar or wedge failures (refer to Table 7.4).

Class	SMR	Description	Stability	Failures
I	81-100	Very Good	Completely Stable	None
II	61-80	Good	Stable	Some blocks
III	41-60	Normal	Partially Stable	Some Joints or many wedges
IV	21-40	Bad	Unstable	Planar or big wedges
V	0-20	Very Bad	Completely Unstable	Big planar or soil-like

TABLE 7.4 DESCRIPTION OF SMR CLASSES (MODIFIED FROM ROMANA, 1993)

7.3.3 REMEDIAL MEASURES

After an initial assessment is made of the slope conditions using SMR or another rock mass classification tool, at the geotechnically vulnerable areas of 'highly' or 'extremely altered and/or weathered' lower Hamersley Group BIF or shale deposits in the Hamersley Province, the degree of the hazard and risk should be assessed for these future slopes. Hazard assessment includes investigating potential failure modes, shear strength of the intact rock or discontinuities, and investigating groundwater conditions. Slope geometry, including height, inclination and shape, needs to be assessed as these affect stress conditions and potential failure volume. Weather and seismic factors may also need to be addressed during hazard assessment.

Once an initial assessment is made of the slope, remedial options can be considered. These options fall into three basic categories (from Hunt, 2005):

1. Avoid the high risk hazard,
2. Accept the low to moderate risk hazard or,
3. Stabilize the slope.

Avoiding the hazard involves relocating the slope to an area less hazardous and more stable. This is completed where the failure hazard is large and unpredictable.

Accepting the hazard is a satisfactory option when failure is predictable but preventative measures are uneconomical. This occurs in low to moderate risk slopes and monitoring possible slope movements is, instead, employed to provide an early warning system for possible slope failures.

Slope stabilization occurs when failures have occurred or are occurring and the slope is suitable for treatment. For low to medium risk failure, the risk is either eliminated or reduced depending on economics, however, for a high risk failure, the risk should be eliminated.

Slope stabilization methods (from Hunt, 2005) include:

- Altering slope geometry,
- Controlling surface water,
- Controlling groundwater and,
- Provide retention.

Altering slope geometry is a simple and effective technique to decrease driving forces and increase resisting forces of failures, and is especially useful as an early prevention measure when an area has been recognized to be potentially unstable. This is completed by reducing the height of the slope or by reducing the angle of the slope, thus, reducing driving forces of a potential failure. Weight can also be added to the toe if circular failure is likely, thereby, to increasing resisting forces.

Controlling surface water and/or groundwater is another stabilization method. By stopping water from infiltrating the slope or by draining the surface water or groundwater from the slope using drains or trenches etc, decreases the driving forces caused by increased water pressure in the slope.

Retention methods may also be used to stabilize slopes. Retention methods work by increasing resisting forces of a potential failure zone and include the use of rock bolts, cable anchors, shotcrete and constructed walls etc, but are not always economically feasible or necessary.

In RTIO mines, when using PI alteration index profiles down boreholes to predict slope conditions, potential hazards and risks should be first assessed such as by assessing potential failure modes, shear strength and groundwater conditions. Possible treatments for slope stability would likely involve a change in slope design such as height or angle of a slope combined with smooth blasting techniques and adequate drainage measures such as utilizing gravity drains to decrease surface water and/or groundwater in the slope. RTIO does not use systematic support, but incorporates design changes appropriate to the strength of the material.

7.4 CONCLUSIONS

Several conclusions can be made from the implications of using geochemical and/or mineralogical analysis as a predictive tool for slope stability in lower Hamersley Group BIF and shale in RTIO mines in the Hamersley Province, Western Australia. These are:

- PI alteration index can be calculated economically and efficiently from major element analysis in intervals down boreholes of lower Hamersley Group BIF and shale deposits to measure the extent of alteration and/or weathering down the profile of a borehole;
- This creates an alteration and/or weathering profile of a borehole that can be colour coded to show a visual transition of changing alteration and/or weathering down the borehole profile;

- When many boreholes are analysed in this way, 2D section and potentially 3D blocks can be analysed for alteration and/or weathering regions in the RTIO mines in the Hamersley Province;
- From Chapter 6, 'highly altered and/or weathered' and 'extremely altered and/or weathered' regions in the lower Hamersley Group BIF and shale deposits are the most geotechnically vulnerable areas, therefore, 'highly altered and/or weathered' and 'extremely altered and/or weathered' regions should be located down the borehole profiles and outlined in the 2D sections or 3D block models;
- Slope stability assessment is required of these areas, this can be completed using a rock mass classification system such as SMR;
- If slope stability analysis shows that the slope is potentially unstable, hazard and risk analysis of these areas should be completed;
- Hazard and risk analysis involves assessment of slope geometry, shear strength of the rock mass and ground water conditions;
- Remedial options include avoiding the high risk hazard by relocation, accepting the low to moderate risk hazard and monitoring the slope, or stabilizing the slope;
- Common slope stabilization methods include altering slope geometry, controlling surface water and groundwater, and providing retention of potentially unstable rock masses.

8 SUMMARY AND CONCLUSIONS

8.1 OVERVIEW

The aim of this investigation was to develop a method of estimating the slope stability conditions of open-cast pit slopes within the RTIO mines throughout the Hamersley Province by analysing the geochemistry and/or mineralogy of the rock. This study provides a geotechnical investigation into the rock mass conditions of the lower Hamersley Group Iron Formation deposits throughout four RTIO mines in the Hamersley Province, Western Australia with the objective to document, analyse and classify pit slope stability. This was followed by a geochemical and mineralogical investigation of selected rock samples collected from these four mine sites with the objective to document, analyse and classify the geochemical and mineralogical characteristics of altered and/or weathered BIF and shale samples from the lower Hamersley Group Iron Deposits. Next, the geochemical characteristics of altered and/or weathered BIF and shale were linked to specific rock mass conditions in the Hamersley Province. Lastly, the use of this relationship as a predictive tool for open pit slope stability in the Hamersley Province was demonstrated.

In this chapter, each stage in this investigation is outlined and key conclusions are given. This is followed by recommended future research for using geochemistry as a predictive tool for slope stability.

8.2 GEOTECHNICAL INVESTIGATION

8.2.1 METHODS

A geotechnical investigation was undertaken on four RTIO mines on lower Hamersley Group BIF and shale deposits in the Hamersley Province, Western Australia. The geotechnical investigation included the use of the rock mass classification system, SMR, which involves field estimates of intact rock strength, RQD, discontinuity spacing, discontinuity conditions, groundwater, discontinuity and slope orientations and blasting method to semi-quantitatively assess the

stability of the rock mass. Laboratory testing was also performed including point load testing and slake durability testing. The extent of alteration and weathering of the rock groups were estimated in the field by RTIO alteration and weathering descriptions.

8.2.2 RESULTS

8.2.2.1 INTACT ROCK STRENGTH

The intact rock strength of lower Hamersley Group BIF and shale was estimated in the field through rock mass classification and measured in the laboratory by point load testing. The intact rock strength of BIF is high but decreases in highly altered and extremely altered rock and some highly weathered BIF. Shale had low to very low intact rock strength with the lowest intact rock strength in highly altered shale.

8.2.2.2 RQD

The RQD of lower Hamersley Group BIF and shale was estimated in the field though rock mass classification. The RQD of BIF had a range of values over alteration and weathering conditions with the lowest RQD values in highly altered, extremely altered and highly weathered conditions. The RQD of shale was relatively constant at about 50% over all alteration and weathering conditions.

8.2.2.3 DISCONTINUITY SPACING AND CONDITIONS

The defect spacing and conditions of lower Hamersley Group BIF and shale was estimated in the field from rock mass classification. Defect spacing of BIF was low especially in extremely altered and high weathered BIF. Defect conditions of BIF were moderate to good with decreasing conditions in highly altered, extremely altered and highly weathered BIF with decreasing roughness and increasing persistency, openness and weathering. The defect spacing of shale was, on average, low with slightly higher spacing in highly weathered shale. Defect conditions in shale were good to poor with the worst conditions in moderately, highly and extremely altered and highly weathered shale.

8.2.2.4 GEOLOGICAL STRENGTH INDEX

The Geological Strength Index (GSI) of lower Hamersley Group BIF and shale was assessed from measured parameters from rock mass classification and is an indication of rock mass shear strength. The GSI of BIF indicated generally high rock mass shear strength, especially in fresh and slightly altered conditions, with the lowest rock mass shear strengths in highly altered conditions. The GSI of shale indicated generally good to moderate rock mass shear strength but decreases slightly in highly altered shale and increases in highly weathered conditions.

8.2.2.5 DURABILITY

The durability of lower Hamersley Group BIF and shale was measured in the laboratory from slake durability testing giving a slake durability index. Slake durability testing showed that BIF is very durable and only decreases in some extremely altered rock masses. Slake durability testing of shale showed that shale is also very durable but durability decreases in highly altered conditions.

8.3 GEOCHEMICAL AND MINERALOGICAL INVESTIGATION

8.3.1 METHODS

A geochemical and mineralogical investigation was undertaken on selected samples throughout the lower Hamersley Group BIF and shale deposits in RTIO mines in the Hamersley Province, Western Australia. The geochemical investigation included XRF major and minor element analysis and the mineralogical investigation included XRD mineral analysis and microscopic analysis. Geochemical and mineralogical data and their relationship to alteration and weathering in the Hamersley Province were then investigated using several methods outlined below.

8.3.2 RESULTS

8.3.2.1 CHEMICAL ALTERATION INDEX

Chemical alteration indices use the enrichment and depletion of major elements, as a specific rock type chemically changes with alteration and/or weathering, to measure the extent of alteration and/or weathering. It produces a number from 0 to 100 with 0 representing fresh

rock and 100 representing extremely altered rock. A chemical alteration index for lower Hamersley Group BIF and shale deposits was created here and named the '*Pilbara Iron* alteration index' (PI alteration index) using the main major increasing and decreasing elements during alteration in the Hamersley Province. This alteration index was calculated from XRF major element analysis for the selected rock samples studied here. It proved to work well for both the BIF and the shale samples. It did not distinguish between alteration and weathering but, instead, measured the total effect of both.

8.3.2.2 ALUMINUM VERSES TITANIUM

It has been found from past research that aluminum in shale in Hamersley Iron Formation deposits, proportionately increases with titanium with increasing alteration and in a recent study it has been suggested that this relationship can be extended to BIF and iron ore. Here it has been found that lower Hamersley Group shale follows this relationship well. BIF does not follow this relationship as well and has only very low Al/Ti ratios. Total replacement by kaolinite or goethite in the shale can also alter this relationship.

8.3.2.3 PEARCE ELEMENT RATIOS

PER diagrams are created from molar ratios of two major mobile elements with a common denominator of a relatively conserved element in the environment being studied; and is presented on a scatter graph. By creating a PER diagram for a specific rock type, alteration events can be identified from the slopes of trendlines created. Here it has been found that a PER diagram of Si/Ti against P/Ti for lower Hamersley Group BIF can be used to show the alteration stages of BIF successively flatter trendline slopes for slightly altered, moderately altered, highly altered and extremely altered BIF, respectively. A PER diagram of Si/Ti against Al/Ti for lower Hamersley Group shale deposits can be used to show the alteration stages of shale with fresh shale creating a trendline with a steep slope and successively flatter trendline slopes for slightly to moderately altered, highly altered and extremely altered shale.

8.3.2.4 TRACE ELEMENTS

The trace elements were found to be reasonably useful at analysing lower Hamersley Group BIF as copper and zinc both increase with alteration and weathering in the BIF. Also, enrichment-depletion diagrams, showing the overall enrichment and depletion of geochemically tested elements, of lower Hamersley Group BIF and shale in different alteration and weathering conditions, shows a good visual representation of the overall chemical enrichment and depletion that occurs with alteration and weathering in the Hamersley Province. Specifically, it has been observed that common groups of elements are enriched and depleted in hypogene and supergene environments in BIF deposits and weathering in shale deposits seem to create an intense depletion of many elements. This may potentially be used to decipher between these processes, however, more study is needed.

8.3.2.5 LOSS ON IGNITION

LOI provides an oxide analysis of a rock material. LOI analysis in the lower Hamersley Group BIF and shale shows that both BIF and shale generally increases in LOI with alteration. In the extremely altered BIF samples, however, this relationship breaks down and increasing goethite increases LOI while increasing hematite decreases LOI.

8.3.2.6 RECENT WEATHERING

Weathering in the Hamersley Province is complex and is difficult to discern geochemically or mineralogically in lower Hamersley Group BIF and shale deposits from alteration processes. In shale deposits it appears that sodium and titanium increases with weathering and magnesium decreases, however, a more comprehensive study of weathering of Hamersley Group deposits is recommended.

8.4 THE EFFECT OF ALTERATION AND WEATHERING ON STABILITY IN HAMERSLEY IRON ORE MINING

8.4.1 OUTLINE

The extent of alteration and weathering on lower Hamersley Group Iron Formation BIF and shale deposits can be estimated from the PI alteration index. The PI alteration indices are calculated from the geochemically tested, selected rock samples in this study; and are linked to rock mass conditions defined by parameters of the rock mass classification system, SMR, including intact rock strength, RQD, discontinuity spacing, discontinuity conditions and calculated GSI; and also by laboratory testing including point load testing and slake durability testing.

8.4.2 ROCK MASS CONDITIONS AND THE PI ALTERATION INDEX

Rock mass classification and geotechnical laboratory testing shows that BIF in the lower Hamersley Group deposits, has better rock mass conditions then shale with an average of moderate SMR parameters while shale averages moderate to poor values. BIF with a PI alteration index of between 61 and 80 generally has the lowest point load strength indices while BIF with a PI alteration index of between 81 and 100 has the lowest average RQD ratings, average discontinuity spacing and condition ratings and slake durability indices. Shale with a PI alteration index of between 61 and 80 has the lowest discontinuity spacing ratings and condition ratings while shale with a PI alteration index of between 81 and 100 has the lowest intact rock strength. Therefore, overall BIF and shale has weakest rock mass conditions at a PI alteration index of 61 to 100 (highly and extremely altered and/or weathered rock) with shale generally having worse conditions than BIF.

8.5 IMPLICATIONS FOR HAMERSLEY PROVINCE IRON ORE MINING

8.5.1 OUTLINE

The PI alteration index can be calculated from geochemical analysis of major elements in lower Hamersley Group BIF and shale in the Hamersley Province, simply and effectively, estimating the extent of alteration and/or weathering.

8.5.2 ALTERATION INDEX PROFILES

The PI alteration index can be measured down boreholes and colour coded based on the extent of alteration and/or weathering as indicated from the PI alteration index. Potentially, the PI alteration index should be measured in intervals down as many boreholes as possible along a section or in a 3D area and the extent of alteration linked up over these areas to create a cross section or a block diagram of the regions of the extent of alteration and/or weathering. This can then be used to locate geotechnically vulnerable areas in lower Hamersley Group BIF and shale deposits of highly and extremely altered and/or weathered areas.

8.5.3 SLOPE STABILITY PREDICTIONS

Where the geotechnically vulnerable areas of highly and extremely altered and/or weathered lower Hamersley Group BIF and shale have been located, slope stability analysis will need to take place. Slope stability analysis can be undertaken using rock mass classification, such as SMR which estimates the potential slope stability and gives an indication of the extent of support required. In areas of potential instability, remedial measures will be required.

8.5.4 REMEDIAL MEASURES

Potential remedial measures include relocation of the slope for high risk hazards, for low to moderate risk hazards the risk may be accepted and monitoring of the slope during its life will be required; otherwise stabilization of the slope will be required. Stabilization methods most commonly include altering slope geometry, such as decreasing the height of the slope or increasing the slope angle or load on the toe of the slope; controlling surface water and/or ground water in the slope such as by draining the slope; or retention of unstable areas on the slope can be employed, for example by the use of bolts, shotcrete or thin spray-on liners.

8.6 KEY CONCLUSIONS

- Geotechnical investigation at RTIO mines show that BIF and shale generally worsen in intact rock strength, RQD, defect spacing and conditions, and durability with alteration;
- The PI alteration index is the most promising geochemical and/or mineralogical method for determining the extent of alteration and/or weathering in lower Hamersley Group BIF and shale deposits, as it is a simple but effective method and uses the concentrations of major enriched and depleted elements in the BIF and shale;
- The PI index is defined as:

$$A^{PI} = \frac{(Fe_2O_3T + Al_2O_3 + TiO_2 + P_2O_5)100}{Fe_2O_3T + Al_2O_3 + TiO_2 + P_2O_5 + SiO_2 + MgO + CaO}$$

- A PI alteration index of ≤20 indicates fresh rock, between 21 and 40 indicates slightly altered rock, between 41 and 60 indicates moderately altered rock, between 61 and 80 indicates highly altered rock and between 81 and 100 indicates extremely altered rock;
- Enrichment-depletion diagrams give a good overall representation of enrichment and depletion of major and minor elements in lower Hamersley Group BIF and shale as they alter and weather, and may potentially be used to discern between hypogene and supergene and Recent weathering, however, more study is required to effectively use these;
- The PI alteration index of lower Hamersley Group BIF and shale samples shows that BIF has, on average, moderate rock mass conditions with lowest geotechnical characteristics at highly and extremely altered and/or weathered PI alteration indices (61 to 80 and 81 to 100) while shale has moderate to poor rock mass conditions with lowest geotechnical to characteristics at highly and extremely altered and/or weathered PI alteration indices (61 to 80 and 81 to 100);
- The PI alteration index can be calculated economically and efficiently down boreholes in the Hamersley Province to create alteration profiles which can be linked to other boreholes in section or in block models to locate regions of highly and extremely altered

and/or weathered lower Hamersley Group BIF and shale that can be further analysed for slope stability, such as from the rock mass classification technique, SMR;

- Hazard and risk analysis should be undertaken of potentially unstable slopes and relocation, monitoring or slope stabilization by altering pit slope geometry, controlling surface or ground water, or providing retention, should take place.

8.7 RECOMMENDATIONS FOR FUTURE RESEARCH

Further research to better understand the relationship of slope stability to alteration and weathering is recommended. This may include a more comprehensive study of the three rock types studied here with more samples tested over the alteration and weathering extents. Along with this, a more comprehensive study of the major and minor geochemistry by enrichment and depletion diagrams may give same helpful insight into the geochemical changes caused by hypogene, supergene and weathering processes of the lower Hamersley Group BIF and shale deposits.

The next stage of this investigation is to test this theory out in practice by calculating the PI alteration indices down a series of boreholes in a future or a present mine, and record the predicted stability zones against the actual stability zones.

REFERENCES

Barley, M. E., Pickard, A. L., & Sylvester, P. J. (1997). Emplacement of a Large Igneous Province as a Possible Cause of Banded Iron Formation 2.45 Billion Years Ago. *Nature* , 55-58.

Barley, M. E., Pickard, A. L., Hagemann, S. G., & Folkert, S. L. (1999). Hydrothermal Origin for the 2 Billion Year Old Mount Tom Price Giant Iron Ore Deposit, Hamersley Province, Western Australia. *Mineralium Deposita* , 784-789.

Barton, N. R., & Choubey, V. (1977). The Shear Strength of Rock Joints in Theory and Practice. *Rock Mechanics* , 1-54.

Barton, N., & Bandis, S. (1990). Review of Predictive Capabilities of JRC-JCS Model in Engineering Practice. *Proceedings of the International Symposium on Rock Joints* (pp. 83-94). Rotterdam: A. A. Balkema.

Barton, N., Lien, R., & Lunde, J. (1974). Engineering Classification of Rock Masses for the Design of Tunnel Support. *Rock Mechanics and Rock Engineering* , 183-236.

Behn, M. (1994). The Role of Structures in the Development of Iron Ore: Examples From Mount Tom Price and Section Six Deposits, Tom Price, Western Australia. *UWA: MSc Thesis*.

Bieniawski, Z. T. (1989). *Engineering Rock Mass Classifications*. New York: Wiley.

Bieniawski, Z. T. (1973). Engineering classification of jointed rock masses. *Trans. South Afr. Inst. of Civ. Eng.* , V 15, pp 335 - 344.

Bieniawski, Z. T. (1976). Rock mass classification in rock engineering. *Proc. Symp. on Exploration for Rock Eng.* (pp. 1, pp 97 - 106). Rotterdam: Balkema.

Bieniawski, Z. T., & Maschek, R. K. (1975). Monitoring the Behaviour of Rock Tunnels during Excavations. *Civ. Eng. South Afr.* , 17, pp 256 - 264.

BOM. (2005). *Climate Map For Climate Classification.* Retrieved August 5, 2009, from Bureau of Meteorology: http://www.bom.gov.au/cgi-bin/climate/cgi_bin_scripts/clim_classification.cgi

Brown, E. T. (1981). Suggested Method for Determining Water Content, Porosity, Density Absorbtion and Related Properties and Swelling and Slake Durability Index Properties. In *Rock Characterisation, Testing and Monitoring* (pp. 81-94). Oxford: Pergamon Press.

Chen, Z. (1995). Recent Developments in Slope Stability Analysis. *Proceedings of the 8th International Congress ISRM*, (pp. 1041-1048). Tokyo.

Clout, J. M. (2006). Iron Formation-Hosted Iron Ores in the Hamersley Province. *Applied Earth Sciences (Trans. Inst. Min. Metall. B)* , 115-125.

Clout, J. M. (2003). Upgrading Processes in BIF-derived Iron Ore Deposits: Implications for Ore Genesis and Downstream Mineral Processing. *Applied Earth Sciences (Tans. Inst. Min. Metall. B)* , B89-B95.

Coates, D. F. (1965). *Rock Mechanics Principles.* Ottawa: Department of Mines and Technical Surveys.

Dalstra, H. (1996). *Dissolution of Wittenoom Dolomite Underneath Structural Corridors in the Hamersley Range.* Dampier: Hamersley Iron PTY Limited.

Dalstra, H. J. (2006). Structural Controls of Bedded Iron Ore in the Hamersley Province, Western Australia - An Example From the Paraburdoo Ranges. *Applied Earth Sciences (Trans. Inst. Min. Metall. B)* , 139-145.

Dalstra, H., & Minello, J. (1999). *Alteration in Dolerite Dykes and Basalts from the Hamersley Basin; Significance for Exploration for Tom Price Style Hematite Deposits.* Dampier: Resources Task Force.

Dames, & Moore. (2000). *Central Pilbara Infrastructure Planning Study.* Perth: Department of Resources Development.

Deere, D. U. (1989). *Rock Quality Designation (RQD) after 20 years.* Vicksburg: Waterways Experiment Station.

Deere, D. U., Hendron, A. J., Patton, F. D., & Cording, E. J. (1967). Design of Surface and Near Surface Construction in Rock. *Proceedings of the 8th U.S. Symposium on Rock Mechanics* (pp. 237-302). New York: AIME.

Eriksson, P. G., Condie, K. C., Van der Westhuizen, W., Van der Merwe, R., De Bruiyn, H., Nelson, D. R., et al. (2002). Late Archaean Superplume Events: A Kraapvaal-Pilbara Perspective. *Journal of Geodynamics* , 207-247.

Franklin, J. A. (1985). Suggested Method for Determining Point Load Strength. *International Journal of Rock Mechanics and Mining Sciences and Geomechanics* , 51-60.

Grimstad, E., & Barton, N. (1993). Updating the Q-System for NMT. *Proceedings of International Symposium on Sprayed Concrete*, Fagernes, Norway (p. 20). Oslo: Norwegian Concrete Association.

Hack, R., Price, D., & Rengers, N. (2002). A New Approach to Rock Slope Stability - A Probability Calculation. *Bulletin of Engineering Geology and the Environment* , 167-184.

Hagan, T. (1996). *Tom Price Structure. Investigation of the Relationship Between Faulting in the Mount Tom Price Deposit and in the Underlying Basement Terrain*. Dampier: Hamersley Iron PTY Limited.

Hagemann, S. G., Barley, M. E., & Folkert, S. L. (1999). A Hydrothermal Origin for the Giant BIF-Hosted Tom Price Iron Ore Deposit. In C. J. Stanely, *Mineral Deposits, Precesses to Processing* (pp. 41-44). Rotterdam: Balkema.

Harmsworth, R. A., Kneeshaw, M., Morris, R. C., Robinson, C. J., & Shrivastava, P. K. (1990). BIF-Derived Iron Ores of the Hamersley Province. In F. E. Hughes, *Geology of the Mineral Deposits of Australia and Papua New Guinea* (pp. 617-642). Melbourne: The Australasian Institute for Mining and Metallurgy.

Hoek, E. (2007 ed.). *Practical Rock Engineering*. Retrieved June 12, 2009, from RocScience: http://www.rocscience.com/hoek/PracticalRockEngineering.asp

Hoek, E. (1994). Strength of Rock and Rock Masses. *News J ISRM* , 187-223.

Hoek, E., Kraiser, P. K., & Bawden, W. f. (1995). *Support on Underground Excavations in Hard Rock*. Rotterdam: Balkema.

Horwitz, R. C. (1987). The Unconformity in the Kelly Belt, East Pilbara Craton (Australia). *Royal Society of Western Australia* , 49-53.

Hunt, R. E. (2005). Assesment of Slopes. In R. E. Hunt, *Geotechnical Engineering Investigation Handbook* (pp. 755-813). Boca Raton: Taylor and Francis Group.

Johnson, S. L., & Wright, A. J. (2001). *Central Pilbara Groundwater Study, Water and Rivers Commisson*. Perth: Hydrogeological Record Series Report HG.

Kendorski, F., Cummings, R., Bieniawski, Z. T., & Skinner, E. (1983). Rock Mass Classification for Block Caving Mine Drift Support. *Proceedings of the 5th International Congress on Rock Mechanics* (pp. B51-B63). Melbourne: ISRM.

Krapez, B. (1999). Stratigraphic Record of an Atlantic-Type Global Tectonic Cycle in the Palaeoproterozoic Ashburton Province of Western Australia. *Australian Journal of Earth Sciences* , 71-87.

Krapez, B., & McNaughton, N. J. (1999). SHRIMP Zircon U-Pb Age and Tectonic Significance of the Palaeoproterozoic Boolaloo Granodiorite in the Ashburton Province, Western Australia. *Australian Journal of Earth Sciences* , 283-287.

Krauland, N., Soder, P. E., & Agmalm, G. (1986). Hallfasthetsbestamning med bergklassificering - nagra erfarenheter och fragor fran Bolidens gruvor. *Bergmekanikdagen 1986 - Papers presented at Rock Mechanics Meeting* (pp. 221-237). Stolkholm: Swedish Rock Mechanics Research Foundation.

Laubscher, D. H. (1984). Design Aspects and Effectiveness of Support Systems in Different Mining Conditions. *Transactions of the Institution of Mining and Metallurgy* , A70-A82.

Laubscher, D. H. (1977). Geomechanics Classification of Jointed Rock Masses - Mining Applications. *Transactions of the Institution of Mining and Metallurgy* (pp. A1-A8). London: The Institution.

Laubscher, D. H., & Page, C. (1990). The Design of Rock Support in High Stress or Weak Rock Environments. *Proceedings of the 92nd Canadian Institute of Mining and Metallurgy* .

Lauffer, H. (1958). Gebirgskassifizierung fur den Stollenbau. *Geol Bauwesen* , 46-51.

Lin, Y. (1998). An introduction of the Chinese Standard for Engineering Classification of Rock Masses. In *Advances in Rock Mechanics* (pp. 317-327). World Scientific Publishing.

Martin, D. M., Li, Z. X., Nemchin, A. A., & Powell, C. M. (1998). A Pre 2.2 Ga Age for Giant Hematite Ores of the Hamersley Province, Australia. *Economic Geology* , 184-209.

Morris, R. C. (1980). A textural and Mineralogical Study of the Relationship of Iron Ore to Banded Iron Formation in the Hamersley Iron Province of Western Australia. *Economic Geology* , 184-209.

Morris, R. C. (1985). Genesis of Iron Ore in Banded Iron-Formation by Supergene and Supergene-Metamorphic Processes - A Conceptual Model. In K. H. Wolff, *Handbook of Stratabound and Strataform Ore Deposits* (pp. 73-235). Amsterdam: Elsevier.

Morris, R. C. (1993). Genetic Modeling for Banded Iron-Formation of the Hamersley Group, Pilbara Craton, Western Australia. *Precambrian Research* , 243-286.

Muller, S. G., Krape, B., Barley, M. E., & Fletcher, I. R. (2005). Giant Iron-Ore Deposits of the Hamersley Province Related to the Breakup of Peleoprotoerozoic Australia: New Insights From In Situ SHRIMP Dating of Baddeleyite From Mafic Intrusions. *Geology* , 577-580.

Nicholson, D. T., & Hencher, S. R. (1997). Assessing the Potential for Deterioration of Engineering Rockslopes. *Proceedings of the IAEG Symposium*, (pp. 911-917). Athens.

Oliver, N. H., & Dickens, G. R. (1999). Hematite Ores of Australia Formed by Syntectonic Heated Meteoric Fluids. In C. J. Stanley, *Mineral Deposits, Processes to Processing* (pp. 889-892). Rotterdam: Balkema.

Pacher, F., Rabcewics, L., & Golser, J. (1974). Zum der seitigen Stand der Gebirsklassifizierung in Stollen-und Tunnelbau. *Proceedings of the 22nd Geomechanics Colloquium*, (pp. 51-58). Salzburg.

Palmstrom, A. (1975). *Characterising the Degree of Jointing and Rock Mass Quality*. Oslo: Berdal.

Palmstrom, A. (1982). The Volumetric Joint Count - a Useful and Simple Measure of the Degree of Rock Jointing. *Proceedings of 4th International Congress* (pp. 221-228). Dehli: International Association of Engineering Geologists.

Pearce, T. H. (1968). A Contribution to the Theory of Variation Diagrams. *Contributions to Mineralogy and Petrology* , 142-157.

Powell, C. M., Oliver, N. H., Li, Z. X., Martin, D. M., & Ronaszeki. (1999). Synorogenic Hydrothermal Origin for Giant Hamersley Iron Oxide Ore Bodies. *Geology* , 175-178.

Rio Tinto Iron Ore. (2009). *Mining*. Retrieved August 11, 2009, from Rio Tinto Iron Ore: http://www.riotintoironore.com/ENG/operations/497_mining.asp

Robertson, A. (1988). Estimating Weak Rock Strength. *Proceedings of the SME Annual Meeting,* (pp. 1-5). Pheonix.

Romana, M. (1985). New Adjustment Ratings for Application of Bieniawski Classification to Slopes. *Proc. Int. Symp. Rock Mech. in Excav. Min. Civ. Works* (pp. pp 59 - 68). Mexico city: ISRM.

Romana, M. R. (1993). A Geomechanical Classification for Slopes: Slope Mass Rating. In J. A. Hudson, *Comprehensive Rock Engineering: Principles, Practice and Projects.* Oxford: Pergamon Press.

Seewald, J. S., & Seyfried, W. E. (1990). The Effect of Temperature on Metal Mobility in Subseafloor Hydrothermal Systems: Constraints from Basalt Alteration Expiriments. *Earth and Planertary Sciences Letters* , 388-403.

Selby, M. J. (1980). A Rock Mass Strength Classification for Geomorphic Purposes: With Tests from Antarctica and New Zealand. *Zeit Geomorph* , 31-51.

Sheorey, P. R. (1994). A Theory for In Situ Stresses in Isotropic and Transversely Isotropic Rock. *International Journal of Rock Mechanics and Mining Sciences and Geomechanics* , 23-34.

Singh, A., & Conolly, M. (2003). VRFSR - An Empirical Method for determining Volcanic Rock Excavation Safety on Construction Sites. *Journal of the Institution of Engineers (India)* , 176-191.

Sjoberg, J. (1996). *Large Scale Slope Stability in Open Pit Mining - A Review*. Lulea: Tekniska Hogskolan I Lulea.

Stacey, P. F. (1993). Pit Slope Designs for the 21st Century. In *Innovative Mine Design for the 21st Century* (pp. 3-11). Rotterdam: A. A. Balkema.

Taylor, D., Dalstra, H. J., Harding, A. E., Broadbent, G. C., & Barley, M. E. (2001). Genesis of High Grade Hematite Orebodies of the Hamersley Province, Western Australia. *Economic Geology* , 837-873.

Terzaghi, K. (1946). Rock Defects and Loads on Tunnel Supports. In K. Terzaghi, R. V. Proctor, & T. L. White, *Rock Tunnelling with Steel Supports* (pp. 17-99). Youngstown: Commercial Shearing and Stamping Company.

Thorne, W. S., Hagemann, S. G., & Barley, M. E. (2006). Hydrothermal Alteration Zonation and Fluid Chemistry of the Sounthern Ridge and North Deposits at Mount Tom Price. *Applied Earth Science (Trans. Inst. Min. Metall. B)* , 152-160.

Thorne, W. S., Hagemann, S. G., & Barley, M. (2004). Petrographic and Geochemical Evidence for Hydrothermal Evolution of North Deposit, Mount Tom Price, Western Australia. *Mineralium Deposita* , 766-783.

Trendall, A. F. (1983). The Hamersley Basin. In A. F. Trendall, & R. C. Morris, *Iron-Formation: Facts and Problems* (pp. 69-129). Amsterdam: Elsevier.

Tyler, I. M., & Thorne, A. M. (1990). The Northern Margin of the Capricorn Orogen, Western Australia - An Example of an Early Protoerzoic Collision Zone. *Journal of Structural Geology* , 685-701.

Unal, E. (1996). Modified Rock Mass Classification: M-RMR System. In *Milestones in Rock Engineering*, the Bieniawski Jubilee Collection (pp. 203-223). Rotterdam: Balkema.

Webb, A. D., Dickens, G. R., & Oliver, N. H. (2006). Carbonate Alteration of the Upper Mount McRae Shale at Mount Whaleback, Western Australia - Impications for Iron Ore Genesis. *Applied Earth Science (Trans. Inst. Min. Matall. B)* , 161-166.

Webb, A. D., Dickens, G. R., & Oliver, N. H. (2004). Carbonate Alteration of the Upper Mount McRae Shale Beneath the Martite-Microplaty Hematite Ore Deposit at Mount Whaleback, Western Australia. *Mineralium Deposita* , 632-645.

Webb, A. D., Dickens, G. R., & Oliver, N. H. (2003). From Banded Iron Formation to Iron Ore: Geochemical and Mineralogical Constraints from across the Hamersley Province, Western Australia. *Chemical Geology* , 215-251.

Whitbread, M. A. (2002). Ratio Analysis of Bulk Geochemical Data: Tracking Ore-Related Cryptic Alteration by Modelling Mineral Changes. In R. I. (ed), *Regolith and Landscapes in Eastern Australia* (pp. 133-135). Canberra: CRC LEME.

Wickham, G. E., Tiedemann, H. R., & Skinner, E. H. (1972). Support Determination Based on Geologic Preditions. *Proceedings of the Rapid Excavations and Tunnelling Conference* (pp. 43-64). New York: AIME.

APPENDIX I: **SAMPLE LOCATIONS**

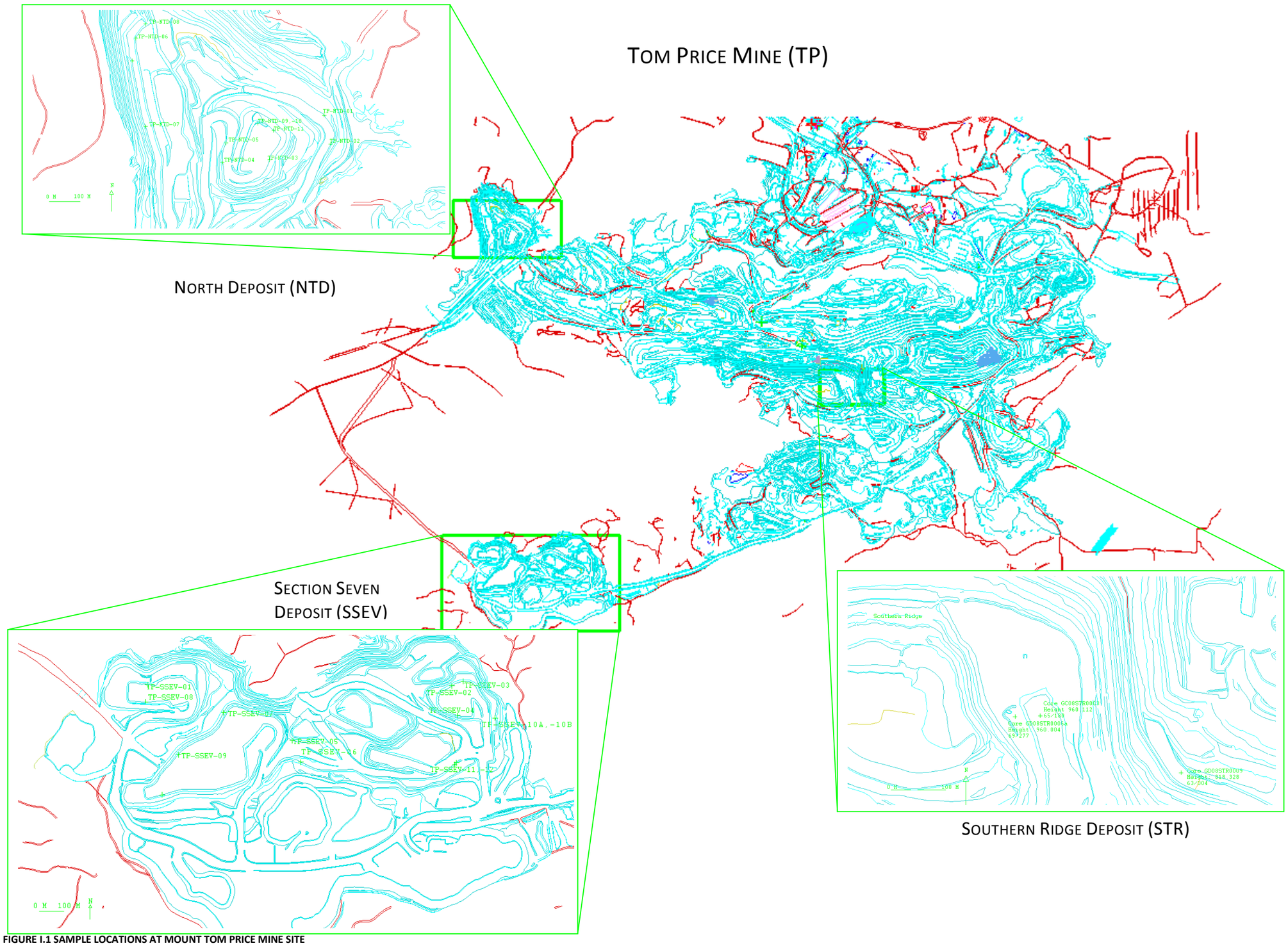

FIGURE I.1 SAMPLE LOCATIONS AT MOUNT TOM PRICE MINE SITE

PARABURDOO MINE (PDO), EASTERN RANGE

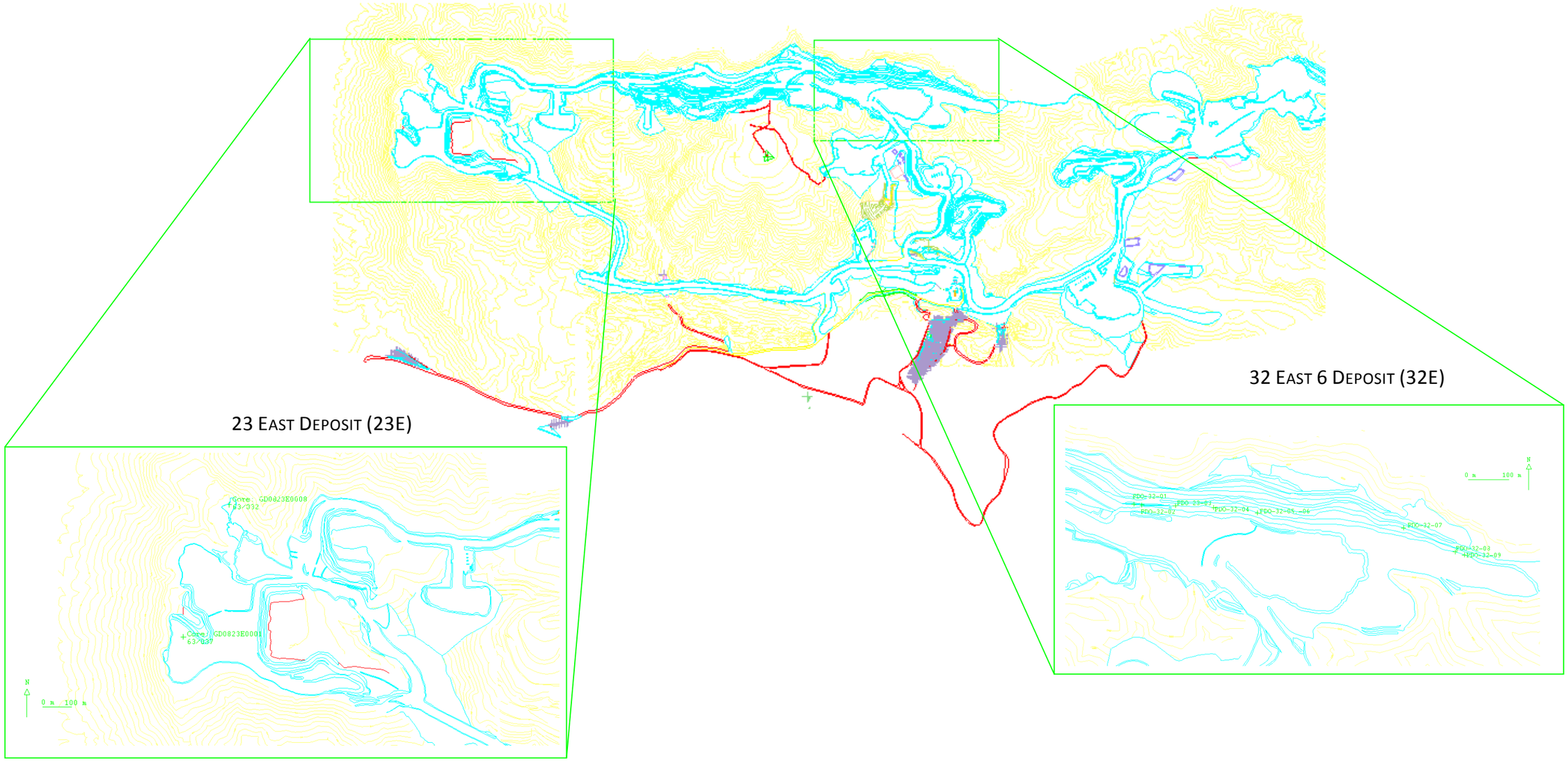

FIGURE I.2 SAMPLE LOACTIONS AT PARABURDOO MINE SITE, EASTERN RANGES

MARANDOO MINE (MDO)

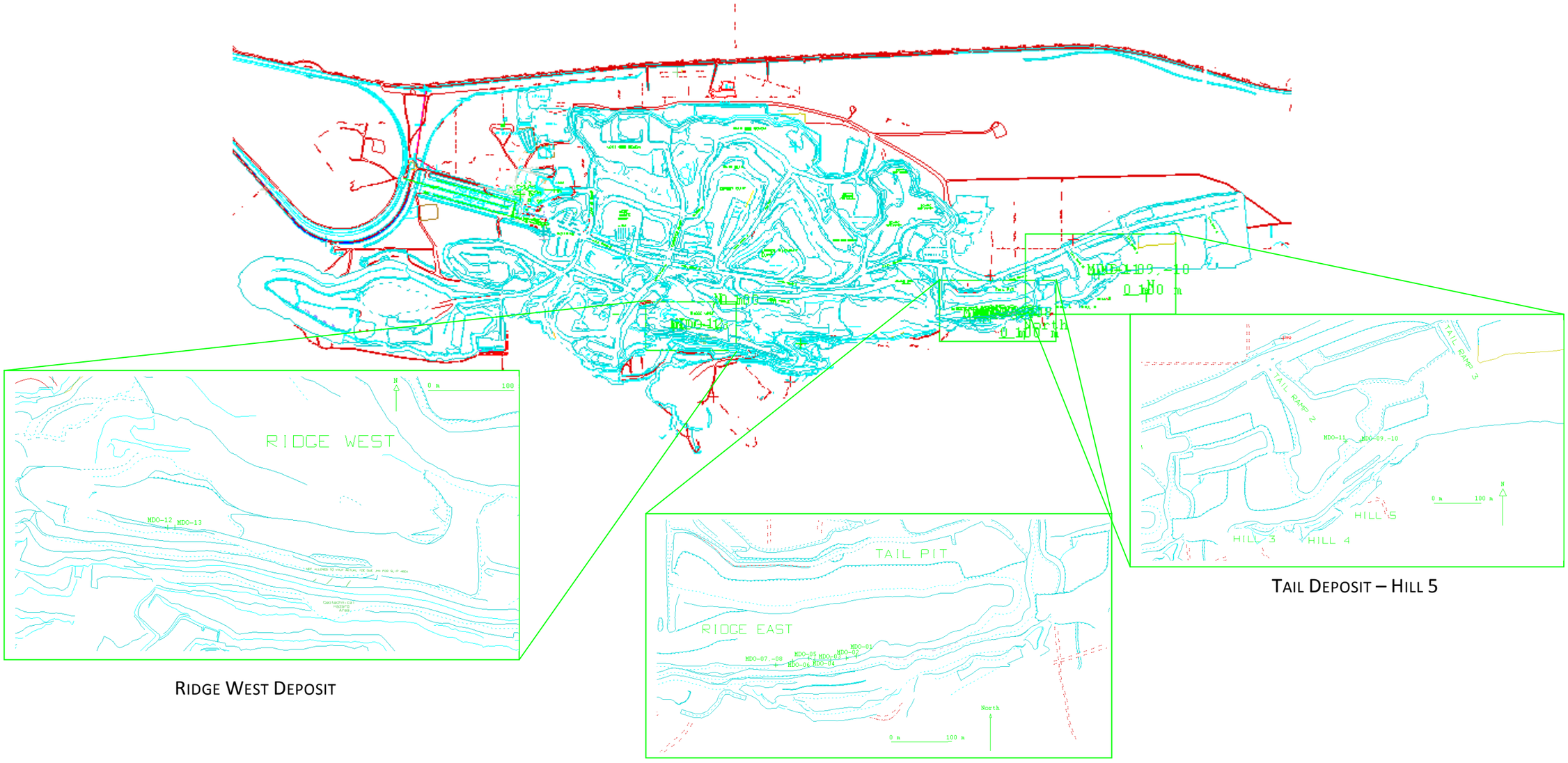

RIDGE WEST DEPOSIT

TAIL DEPOSIT – HILL 1

TAIL DEPOSIT – HILL 5

FIGURE I.3 SAMPLE LOACTIONS AT MARANDOO MINE SITE

WEST ANGELAS MINE (WA), DEPOSIT A

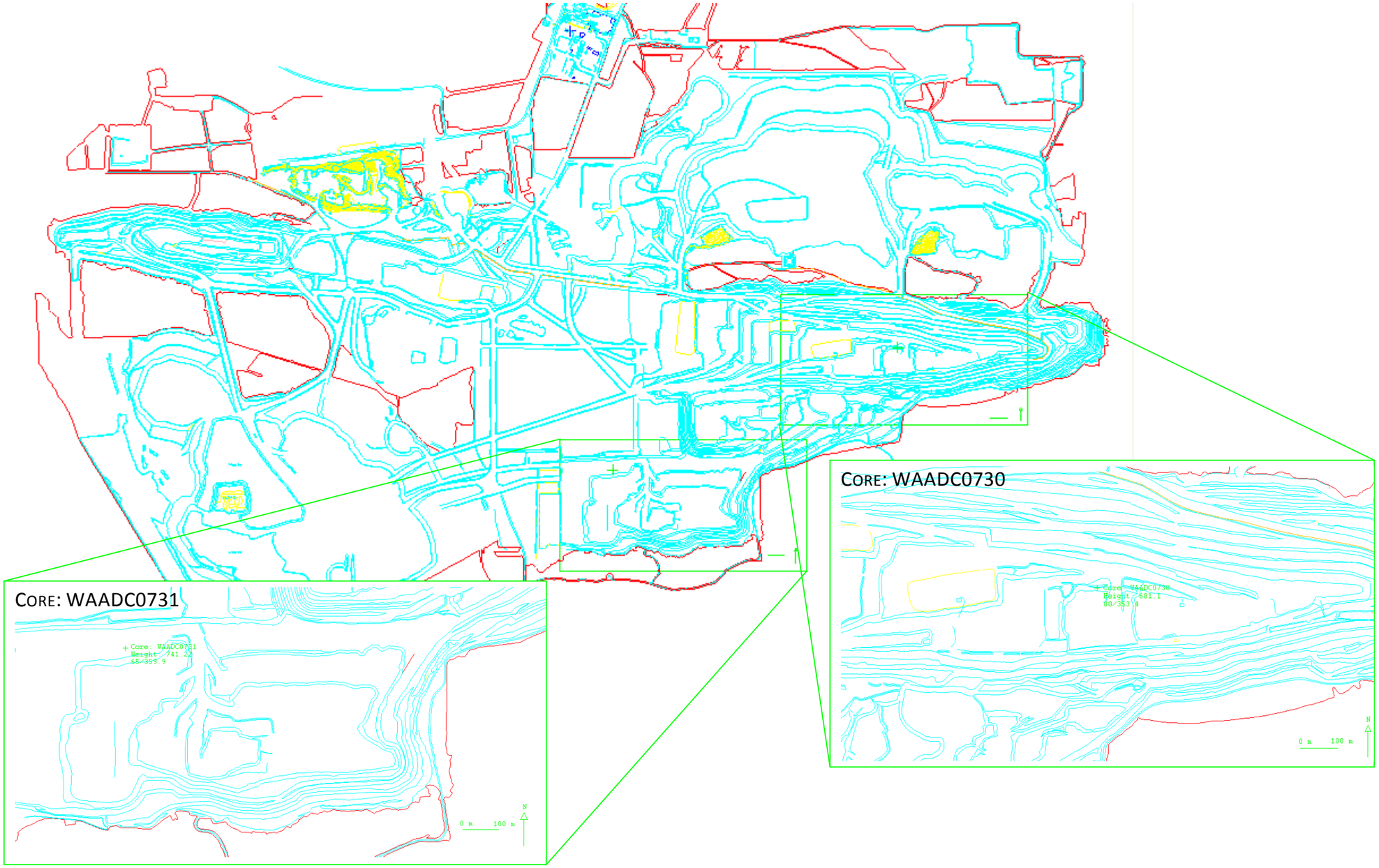

FIGURE I.4 MAP OF SAMPLE LOACTIONS AT WEST ANGELAS, DEPOSIT A MINE SITE

APPENDIX II: **VISUAL DESCRIPTIONS OF FIELD SAMPLE LOCATIONS**

Sample No	Rock Type:	Extent of Weathering:	Extent of Alteration:	Failure Types:	Erosional Features:	Structure:	Overall Stability Estimate:
TP-NTD-01	SHALE	Moderately	Highly	Past planar failures; some spalling		Dipping out of wall	Good
TP-NTD-02	BIF	Highly	Highly	Block flows (up to 0.5 m2)	Minor cavities	Dipping into wall	Good
TP-NTD-03	BIF	Moderately	Highly	Past Planar failure; some block flow and spalling		Dipping out of wall	Moderate
TP-NTD-04	BIF	Slightly	Highly	Some wedge failures (up to 1m2) and block flow		Highly jointed	Moderate
TP-NTD-05	SHALE	Slightly	Highly	Spalling and block flow		Dipping north	Moderate
TP-NTD-06	BIF	Moderately	Highly	Minor block flows (up to 1m2); major spalling	Some cavities	Thin bedding; dipping south	Moderate
TP-NTD-07	BIF	Highly	Moderately	Some planar failures (up to 10 m across); block flows; toppling due to joints	Some cavities	Dipping out of wall; moderate folding	Poor
TP-NTD-08	SHALE	Moderately	Highly	Small wedge failures; block flow (up to 0.5 m)		Thinly bedded; jointed; dipping into wall	Good
TP-NTD-09	BIF	Moderately	Highly	Spalling	Rilling	Dipping down wall face	Good
TP-NTD-10	SHALE	Moderately	Highly	Spalling	Rilling	Dipping down wall face	Good
TP-NTD-11	SHALE	Moderately	Highly	Spalling	Rilling	Dipping down wall face	Good
TP - SSEV - 01	BIF	Moderately	Highly	Lots of spalling	Some cavities	Gently folding; dipping out of wall	Good
TP - SSEV - 02	BIF	Moderately	Extremely	Some spalling	Some rilling	Dipping to west; folded	Good
TP - SSEV - 03	SHALE	Moderately	Highly	Some spalling	Some rilling	Dipping to west; folded	Good
TP - SSEV - 04	BIF	Moderately	Highly	Some block flow (up to 10 cm2); some spalling	Minor cavities; some gullying	Very gentle folding	Good
TP - SSEV - 05	BIF	Moderately	Highly	Minor spalling	Small cavities and gullying	Dipping into wall	Very Good
TP - SSEV - 06	BIF	Moderately	Highly	Minor spalling	Small cavities and gullying	Dipping into wall	Very Good
TP - SSEV - 07	BIF	Moderately	Highly	Small planar failures; minor block flow and spalling	Some gullying	Moderately folded (up to 10 m)	Good to Moderate
TP - SSEV - 08	BIF	Moderately	Highly	Some small planar failures (up to 2 m); block flow and spalling	Some rilling	Dipping out of wall	Moderate
TP - SSEV - 09	BIF	Moderately	Highly	Some block flow and spalling		Faulting and breccia zones	Moderate
TP - SSEV - 10a	BIF	Extremely	Highly	Many (up to 1 m2) blocks	Some cavities	Blocky and vughy	Moderate
TP - SSEV - 10b	BIF	Extremely	Highly	Many (up to 1 m2) blocks	Some cavities	Blocky and vughy	Moderate
TP - SSEV - 11	BIF	Moderately	Highly	Many block flows (up to 1 m2)	Minor cavities	Moderately folded	Moderate
TP - SSEV - 12	SHALE	Moderately	Highly	Some planar failures	Minor cavities	Moderately folded	Moderate
PDO - 32 - 01	SHALE	Moderately	Highly	Planar slide (about 25 m across); Much block flow		Very gentle folding	Very Poor
PDO - 32 - 02	BIF	Moderately	Extremely	Block flow and spalling		Very gentle folding	Poor
PDO - 32 - 03	BIF	Moderately	Highly	Spalling; some block flow		Gently dipping out of wall	Good
PDO - 32 - 04	BIF	Highly	Highly	Small planer failures (up to 1 m2); Much block flow		Steep bedding	Poor
PDO - 32 - 05	SHALE	Moderately	Highly	Some block flow and spalling		Dipping out of wall	Moderate
PDO - 32 - 06	BIF	Moderately	Highly	Some block flow and spalling		Dipping out of wall	Moderate
PDO - 32 - 07	BIF	Highly	Highly	Lots of spalling; some small blocks	Some small cavities	Small joints; dipping out of wall	Good
PDO - 32 - 08	BIF	Highly	Extremely	Spalling; some block flow (up to 0.5 m2)		Fault zone	Good
PDO - 32 - 09	BIF	Moderately	Extremely	Spalling; some small blocks		Faulting and steep bedding	Good
MDO - 01	BIF	Moderately	Extremely	Some planar failure; lots of block flow		Steep bedding	Moderate to Poor
MDO - 02	BIF	Highly	Highly	Minor planar failure; lots of spalling		Steeply dipping	Moderate
MDO - 03	BIF	Moderately	Highly	Lots of spalling and small blocks		Very steeply dipping	Moderate to Good
MDO - 04	SHALE	Moderately	Moderately	Spalling and block flows		Dipping out of wall	Poor
MDO - 05	SHALE	Moderately	Highly	Large block flows and spalling		Moderate folding (up to 20m)	Poor
MDO - 06	BIF	Highly	Highly	Block flow and spalling		Very steeply dipping	Moderate
MDO - 07	BIF	Highly	Highly	Minor spalling	Some small cavities	Steeply dipping	Good
MDO - 08	SHALE	Moderately	Highly	Minor spalling	Some small cavities	Steeply dipping	Good
MDO - 09	BIF	Slightly	Highly	Some small planar failures; many block flows (up to 1 m2)	Some small cavities	Jointing; dipping out of wall	Poor to Moderate
MDO - 10	SHALE	Moderately	Highly	Some small planar failures; many block flows (up to 1 m2)	Some small cavities	Jointing; dipping out of wall	Poor to Moderate
MDO - 11	BIF	Moderately	Highly	Planar failure (about 10 m across); block flow (up to 1 m2)	Moderate cavities	Jointing; dipping out of wall	Poor
MDO - 12	BIF	Slightly	Highly	Many block flows (up to 1 m2); lot of spalling		Jointing; dipping out of wall	Poor
MDO - 13	SHALE	Slightly	Highly	Many block flows (up to 1 m2); lot of spalling		Jointing; dipping out of wall	Poor

TABLE II.1 VISUAL DESCRIPTIONS OF STABILITY OF FIELD SAMPLE LOCATIONS (FOR WEATHERING AND ALTERATION DESCRIPTIONS REFER TO FIGURES 4.2 AND 4.3; OVERALL STABILITY IS ESTIMATED FROM FIGURE 3.11 (ROMANA, 1993) WHERE FAILURE TYPES AND STABILITY CONDITIONS ARE RELATED TO A DESCRIPTION)

APPENDIX III: **SMR CALCULATIONS**

Sample ID	Strength Rating	RQD Rating	Spacing Rating	Condition Rating	Ground -water Rating	Adjust -ment for Joint Ori -entations	RMR_{89}	RMR_{89} for SMR Calculat -ion	RMR_{89}'	GSI	Joint to Slope Direction (F_1)	Joint Dip (F_2)	Joint to Slope Dip (F_3)	$F_1 \times F_2 \times F_3$	Blasting Rating (F_4)	SMR
TP-STR-01	6	8	8	20	15	-5	52	57	57	52	0.15	1	-50	-7.5	0	50
TP-STR-02	2	10	9	20	15	-5	51	56	56	51	0.15	1	-60	-9	0	47
TP-STR-03	10	10	8	20	15	-50	13	63	63	58	1	0.7	-60	-42	0	21
TP-STR-04	10	10	9	25	15	-5	64	69	69	64	0.7	0.15	-60	-6.3	0	63
TP-STR-05	2	3	5	20	15	-5	40	45	45	40	0.15	0.15	-60	-1.35	0	44
TP-STR-06	12	8	8	20	15	-5	58	63	63	58	0.15	0.85	-60	-7.65	0	55
TP-STR-07	12	8	8	25	15	-5	63	68	68	63	0.15	1	-60	-9	0	59
TP-STR-08	2	8	8	20	15	-5	48	53	53	48	0.15	0.85	-60	-7.65	0	45
TP-STR-09	2	8	8	25	15	-5	53	58	58	53	0.15	1	-60	-9	0	49
TP-STR-10	7	13	10	25	15	-5	65	70	70	65	0.15	0.15	-60	-1.35	0	69
TP-STR-11	7	13	10	25	15	-5	65	70	70	65	0.15	0.15	-60	-1.35	0	69
TP-STR-12	7	13	10	20	15	-5	60	65	65	60	0.15	0.15	-60	-1.35	0	64
TP-STR-13	2	13	10	20	15	0	60	60	60	55	0.7	1	0	0	0	60
TP-STR-14	2	13	10	20	15	0	60	60	60	55	0.7	1	0	0	0	60
TP-STR-15	7	20	15	20	15	-5	72	77	77	72	0.15	0.4	-60	-3.6	0	73
TP-STR-16	7	20	15	20	15	-5	72	77	77	72	0.15	0.4	-60	-3.6	0	73
TP-STR-17	4	8	8	20	15	-5	50	55	55	50	0.15	0.4	-60	-3.6	0	51
TP-STR-18	4	8	8	20	15	-5	50	55	55	50	0.15	0.15	-60	-1.35	0	54
TP-STR-19	2	8	8	20	15	-5	48	53	53	48	0.15	0.4	-60	-3.6	0	49
TP-STR-20	12	20	15	20	15	-5	77	82	82	77	0.15	0.15	-60	-1.35	0	81
TP-STR-21	2	17	10	25	15	-5	64	69	69	64	0.4	0.15	-60	-3.6	0	65
TP-STR-22	2	5	6	20	15	0	48	48	48	43	0.7	1	0	0	0	48
TP-STR-23	12	17	10	20	15	-5	69	74	74	69	0.15	1	-25	-3.75	0	70
TP-STR-24	12	20	15	25	15	-5	82	87	87	82	0.15	0.4	-60	-3.6	0	83
TP-STR-25	3	8	8	15	15	-5	44	49	49	44	0.15	1	-50	-7.5	0	42
TP-STR-26	12	18	10	25	15	-5	75	80	80	75	0.15	1	-50	-7.5	0	73
TP-STR-27	12	10	10	20	15	-5	62	67	67	62	0.15	0.85	-60	-7.65	0	59
TP-STR-28	7	13	10	20	15	-5	60	65	65	60	0.15	0.85	-60	-7.65	0	57

TABLE III.1 SMR RESULTS OF SOUTHERN RIDGE (DETAILS FOR THE CALCULATION OF RMR_{89}, GSI AND SMR ARE FOUND IN CHAPTERS 3 AND 4; 'RMR_{89} FOR SMR CALCULATION' IS RMR_{89} WITHOUT THE ADJUSTMENT FOR JOINT ORIENTATIONS AS DISCUSSED IN SECTION 3.3.6; RMR_{89}' IS RMR MODIFIED FOR THE CALCULATION OF GSI WITH GROUNDWATER RATING = 15 AND ADJUSTMENT FOR JOINT ORIENTATIONS = 0; COLOURS OF RATINGS REPRESENT THE ASSOCIATED CONDITIONS WITH 0 TO 20 = VERY POOR, 21 TO 40 = POOR, 41 TO 60 = MODERATE, 61 TO 80 = GOOD, AND 81 TO 100 = VERY GOOD)

Sample ID	Strength Rating	RQD Rating	Spacing Rating	Condition Rating	Ground -water Rating	Adjust -ment for Joint Ori -entations	RMR_{89}	RMR_{89} for SMR Calculat -ion	RMR_{89}'	GSI	Joint to Slope Direction (F_1)	Joint Dip (F_2)	Joint to Slope Dip (F_3)	$F_1 \times F_2 \times F_3$	Blasting Rating (F_4)	SMR
TP-NTD-01	4	8	8	20	13	-5	48	53	55	50	0.7	0.85	-6	-3.57	0	49
TP-NTD-02	12	17	10	20	10	-5	64	69	74	69	0.15	0.7	-60	-6.3	0	63
TP-NTD-03	4	8	5	25	13	-5	50	55	57	52	0.15	0.7	-60	-6.3	0	49
TP-NTD-04	4	13	13	25	10	-5	60	65	70	65	0.15	0.4	-60	-3.6	0	61
TP-NTD-06	2	10	8	15	10	-5	40	45	50	45	0.15	0.85	-60	-7.65	0	37
TP-NTD-07	7	10	8	20	10	-5	50	55	60	55	0.15	0.7	-60	-6.3	0	49
TP-NTD-08	2	8	5	23	13	-5	46	51	53	48	0.15	0.4	-60	-3.6	8	55
TP-NTD-09	12	17	10	5	15	-25	34	59	59	54	0.85	0.4	-50	-17	0	42
TP-NTD-10	4	8	8	20	15	0	55	55	55	50	0.85	0.4	-50	-17	0	38
TP-NTD-11	2	8	8	0	15	0	33	33	33	28	0.85	0.4	-50	-17	0	16
TP-SSEV-01	7	13	8	20	13	-5	56	61	63	58	0.4	0.4	-60	-9.6	0	51
TP-SSEV-02	2	15	8	20	15	-5	55	60	60	55	0.15	0.15	-60	-1.35	8	67
TP-SSEV-03	2	8	8	25	15	-5	53	58	58	53	0.15	0.15	-60	-1.35	0	57
TP-SSEV-04	2	13	8	23	15	-5	56	61	61	56	0.15	0.4	-60	-3.6	0	57
TP-SSEV-05	2	17	13	25	10	-5	62	67	72	67	0.85	0.15	-60	-7.65	0	59
TP-SSEV-06	5	17	12	23	12	-5	64	69	72	67	0.15	0.15	-60	-1.35	8	76
TP-SSEV-07	2	8	8	20	15	-5	48	53	53	48	0.15	0.15	-60	-1.35	8	60
TP-SSEV-08	6	13	10	20	13	-5	57	62	64	59	0.7	0.4	-60	-16.8	0	45
TP-SSEV-09	7	17	8	23	12	-5	62	67	70	65	0.4	0.7	-60	-16.8	0	50
TP-SSEV-10a	12	17	15	20	10	-5	69	74	79	74	0.85	0.15	-60	-7.65	0	66
TP-SSEV-10b	12	17	15	20	10	-5	69	74	79	74	0.85	0.15	-60	-7.65	0	66
TP-SSEV-11	5	13	8	20	10	-5	51	56	61	56	0.4	0.4	-60	-9.6	0	46
TP-SSEV-12	3	10	8	20	10	-5	46	51	56	51	0.4	0.4	-60	-9.6	0	41

TABLE III.2 SMR RESULTS OF NORTH DEPOSIT AND SECTION SEVEN (DETAILS FOR THE CALCULATION OF RMR_{89}, GSI AND SMR ARE FOUND IN CHAPTERS 3 AND 4; 'RMR_{89} FOR SMR CALCULATION' IS RMR_{89} WITHOUT THE ADJUSTMENT FOR JOINT ORIENTATIONS AS DISCUSSED IN SECTION 3.3.6; RMR_{89}' IS RMR MODIFIED FOR THE CALCULATION OF GSI WITH GROUNDWATER RATING = 15 AND ADJUSTMENT FOR JOINT ORIENTATIONS = 0; COLOURS OF RATINGS REPRESENT THE ASSOCIATED CONDITIONS WITH 0 TO 20 = VERY POOR, 21 TO 40 = POOR, 41 TO 60 = MODERATE, 61 TO 80 = GOOD, AND 81 TO 100 = VERY GOOD)

Sample ID	Strength Rating	RQD Rating	Spacing Rating	Condition Rating	Ground -water Rating	Adjust -ment for Joint Ori -entations	RMR_{89}	RMR_{89} for SMR Calculat -ion	RMR_{89}'	GSI	Joint to Slope Direction (F_1)	Joint Dip (F_2)	Joint to Slope Dip (F_3)	$F_1 \times F_2 \times F_3$	Blasting Rating (F_4)	SMR
PDO-4E-01	4	10	8	23	15	0	60	60	60	55	0.15	1	-6	-0.9	0	59
PDO-4E-02	4	8	8	20	15	-5	50	55	55	50	0.4	0.7	-60	8	8	71
PDO-4E-03	5	17	8	25	15	-5	65	70	70	65	0.15	1	-50	-7.5	0	63
PDO-4E-04	4	10	8	20	15	-5	52	57	57	52	0.15	0.85	-60	-7.65	8	57
PDO-4E-05	4	9	9	20	15	-5	52	57	57	52	0.15	0.85	-60	-7.65	8	57
PDO-4E-06	4	15	9	20	15	-25	38	63	63	58	0.4	0.85	-50	-17	0	46
PDO-23-01	4	8	9	20	15	-5	51	56	56	51	0.15	0.4	-60	-3.6	0	52
PDO-23-02	5	10	9	20	15	-5	54	59	59	54	0.15	0.4	-60	-3.6	0	55
PDO-23-03	4	8	8	25	15	-5	55	60	60	55	0.15	0.15	-60	-1.35	0	59
PDO-23-04	7	17	10	20	15	-5	64	69	69	64	0.15	1	-60	-9	0	60
PDO-23-05	5	13	10	20	15	-5	58	63	63	58	0.15	1	-60	-9	0	54
PDO-23-06	8	15	10	25	15	-5	68	73	73	68	0.15	0.85	-60	-7.65	0	65
PDO-23-07	7	13	8	20	10	-5	53	58	63	58	0.15	0.4	-60	-3.6	0	54
PDO-23-08	2	13	16	20	13	-5	59	64	66	61	0.15	0.15	-60	-1.35	0	63
PDO-23-09	2	13	9	15	15	-5	49	54	54	49	0.15	0.15	-60	-1.35	0	53
PDO-23-10	8	18	8	20	15	-5	64	69	69	64	0.15	0.15	-60	-1.35	0	68
PDO-23-11	7	12	7	20	15	-5	56	61	61	56	1	0.15	-60	-9	0	52
PDO-23-12	10	14	8	25	15	-5	67	72	72	67	0.15	0.4	-60	-3.6	0	68
PDO-23-13	1	8	6	15	15	-5	40	45	45	40	0.15	0.4	-60	-3.6	0	41
PDO-23-14	4	12	8	25	15	-5	59	64	64	59	0.15	0.15	-60	-1.35	0	63
PDO-32-01	3	13	9	25	15	-50	15	65	65	60	1	0.7	-60	-42	0	23
PDO-32-02	4	8	8	15	15	-50	0	50	50	45	1	0.7	-60	-42	0	8
PDO-32-03	5	15	9	25	15	-25	44	69	69	64	1	0.4	-60	-24	0	45
PDO-32-04	0	10	8	23	15	-5	51	56	56	51	1	0.15	-60	-9	0	47
PDO-32-05	4	13	8	20	15	-50	10	60	60	55	1	0.85	-60	-51	0	9
PDO-32-06	2	8	8	20	15	-50	3	53	53	48	1	0.85	-60	-51	0	2
PDO-32-07	6	17	10	20	15	-50	18	68	68	63	1	0.85	-50	-42.5	0	26
PDO-32-08	12	15	9	15	15	0	66	66	66	61	0.4	1	0	0	0	66
PDO-32-09	3	13	10	15	15	0	56	56	56	51	0.15	1	0	0	0	56

TABLE III.3 SMR RESULTS OF PARABURDOO (DETAILS FOR THE CALCULATION OF RMR_{89}, GSI AND SMR ARE FOUND IN CHAPTERS 3 AND 4; 'RMR_{89} FOR SMR CALCULATION' IS RMR_{89} WITHOUT THE ADJUSTMENT FOR JOINT ORIENTATIONS AS DISCUSSED IN SECTION 3.3.6; RMR_{89}' IS RMR MODIFIED FOR THE CALCULATION OF GSI WITH GROUNDWATER RATING = 15 AND ADJUSTMENT FOR JOINT ORIENTATIONS = 0; COLOURS OF RATINGS REPRESENT THE ASSOCIATED CONDITIONS WITH 0 TO 20 = VERY POOR, 21 TO 40 = POOR, 41 TO 60 = MODERATE, 61 TO 80 = GOOD, AND 81 TO 100 = VERY GOOD)

Sample ID	Strength Rating	RQD Rating	Spacing Rating	Condition Rating	Ground -water Rating	Adjust -ment for Joint Ori -entations	RMR_{89}	RMR_{89} for SMR Calculat -ion	RMR_{89}'	GSI	Joint to Slope Directio n (F_1)	Joint Dip (F_2)	Joint to Slope Dip (F_3)	$F_1 \times F_2 \times F_3$	Blasting Rating (F_4)	SMR
MDO-01	5	12	8	20	10	-50	**5**	55	60	55	1	1	-50	-50	0	**5**
MDO-02	4	8	8	20	10	-5	45	50	55	50	0.7	1	-6	-4.2	0	46
MDO-03	2	15	10	20	10	0	57	57	62	57	0.85	1	0	0	0	57
MDO-04	4	8	8	15	15	0	50	50	50	45	0.7	1	0	0	0	50
MDO-05	4	5	8	15	15	-25	22	47	47	42	0.7	0.7	-60	-29.4	0	**18**
MDO-06	5	15	8	20	10	0	58	58	63	58	1	1	0	0	0	58
MDO-07	5	18	15	20	10	0	68	68	73	68	0.7	1	0	0	0	68
MDO-08	4	8	8	10	15	0	45	45	45	40	0.7	1	0	0	0	45
MDO-09	7	13	8	20	10	-5	53	58	63	58	0.15	0.85	-60	-7.65	-8	42
MDO-10	3	5	8	10	15	-5	36	41	41	36	0.15	0.85	-60	-7.65	-8	25
MDO-11	4	13	8	20	10	-5	50	55	60	55	0.15	0.85	-60	-7.65	-8	39
MDO-12	13	15	8	20	10	-25	41	66	71	66	0.7	0.7	-60	-29.4	-8	29
MDO-13	3	8	8	15	15	-25	24	49	49	44	0.7	0.7	-60	-29.4	-8	**12**
MDO-14	7	8	8	22	10	0	55	55	60	55	-	-	-	-	-	-
MDO-15	10	14	9	22	10	0	65	65	70	65	-	-	-	-	-	-
MDO-16	3	8	8	25	15	0	59	59	59	54	-	-	-	-	-	-
WA-50-01	5	15	15	20	15	0	70	70	70	65	-	-	-	-	-	-
WA-50-02	2	9	15	15	15	0	56	56	56	51	-	-	-	-	-	-
WA-50-03	2	5	5	15	15	0	42	42	42	37	-	-	-	-	-	-
WA-50-04	12	19	15	25	15	0	**86**	**86**	**86**	**81**	-	-	-	-	-	-
WA-50-05	2	17	10	20	15	0	64	64	64	59	-	-	-	-	-	-
WA-50-06	1	3	8	15	15	0	42	42	42	37	-	-	-	-	-	-
WA-50-07	12	17	9	27	15	0	80	80	80	75	-	-	-	-	-	-
WA-50-08	3	10	9	20	15	0	57	57	57	52	-	-	-	-	-	-
WA-50-09	2	8	8	15	15	0	48	48	48	43	-	-	-	-	-	-
WA-50-10	2	8	9	15	15	0	49	49	49	44	-	-	-	-	-	-
WA-50-11	12	17	12	22	15	0	78	78	78	73	-	-	-	-	-	-
WA-50-12	10	15	10	20	15	0	70	70	70	65	-	-	-	-	-	-
WA-50-13	5	13	9	20	15	0	62	62	62	57	-	-	-	-	-	-

TABLE III.4 SMR RESULTS FOR MARANDOO AND WEST ANGELAS (DETAILS FOR THE CALCULATION OF RMR_{89}, GSI AND SMR ARE FOUND IN CHAPTERS 3 AND 4; 'RMR_{89} FOR SMR CALCULATION' IS RMR_{89} WITHOUT THE ADJUSTMENT FOR JOINT ORIENTATIONS AS DISCUSSED IN SECTION 3.3.6; RMR_{89}' IS RMR MODIFIED FOR THE CALCULATION OF GSI WITH GROUNDWATER RATING = 15 AND ADJUSTMENT FOR JOINT ORIENTATIONS = 0; COLOURS OF RATINGS REPRESENT THE ASSOCIATED CONDITIONS WITH 0 TO 20 = VERY POOR, 21 TO 40 = POOR, 41 TO 60 = MODERATE, 61 TO 80 = GOOD, AND 81 TO 100 = VERY GOOD)

Sample ID	Strength Rating	RQD Rating	Spacing Rating	Condition Rating	Ground -water Rating	Adjust -ment for Joint Ori -entations	RMR_{89}	RMR_{89} for SMR Calcuat ion	RMR_{89}'	GSI	Joint to Slope Direction (F_1)	Joint Dip (F_2)	Joint to Slope Dip (F_3)	$F_1 \times F_2 \times F_3$	Blasting Rating (F_4)	SMR
WA-07-01	4	20	12	20	15	-5	66	71	71	66	0.15	0.85	-50	-6.375	0	65
WA-07-02	1	15	8	10	15	-5	44	49	49	44	0.15	0.85	-50	-6.375	0	43
WA-07-03	2	6	8	10	15	-5	36	41	41	36	0.15	0.15	-60	-1.35	0	40
WA-07-04	4	17	9	20	15	-5	60	65	65	60	0.15	0.85	-25	-3.1875	0	62
WA-07-05	1	9	6	10	15	-5	36	41	41	36	0.4	0.85	-50	-17	0	24
WA-07-06	1	5	10	15	15	0	46	46	46	41	0.4	1	0	0	0	46
WA-07-07	4	17	9	20	15	-5	60	65	65	60	0.85	1	-6	-5.1	0	60
WA-07-08	4	8	7	10	15	-5	39	44	44	39	0.85	1	-6	-5.1	0	39
WA-07-09	1	3	5	10	15	-5	29	34	34	29	0.15	0.85	-25	-3.1875	0	31
WA-07-10	1	11	8	20	15	-5	50	55	55	50	0.15	0.85	-50	-6.375	0	49
WA-07-11	0	3	5	0	15	0	23	23	23	18	0.15	1	0	0	0	23
WA-07-12	12	15	9	25	15	-5	71	76	76	71	0.15	0.15	-60	-1.35	0	75
WA-07-13	1	3	5	10	15	-5	29	34	34	29	0.15	0.85	-50	-6.375	0	28
WA-07-14	12	17	8	25	15	-5	72	77	77	72	0.15	0.85	-50	-6.375	0	71
WA-07-15	2	13	8	10	15	-5	43	48	48	43	0.15	0.7	-60	-6.3	0	42
WA-07-16	1	13	9	5	15	0	43	43	43	38	0.15	1	0	0	0	43
WA-07-17	1	10	8	10	15	-5	39	44	44	39	0.15	1	-25	-3.75	0	40
WA-07-18	1	13	10	10	15	-5	44	49	49	44	0.15	1	-6	-0.9	0	48
WA-07-19	2	3	8	10	15	-5	33	38	38	33	0.15	0.7	-60	-6.3	0	32
WA-07-20	1	10	8	15	15	-5	44	49	49	44	0.15	0.7	-60	-6.3	0	43
WA-07-21	0	8	7	5	15	0	35	35	35	30	0.15	1	-6	-0.9	0	34
WA-07-22	4	8	7	10	15	0	44	44	44	39	0.15	1	-6	-0.9	0	43
WA-07-24	4	11	8	15	15	-5	48	53	53	48	0.15	0.85	-50	-6.375	0	47
WA-07-25	12	20	10	30	15	-5	82	87	87	82	0.4	1	-6	-2.4	0	85

TABLE III.5 SMR RESULTS FOR WEST ANGELAS (CONTINUED) (DETAILS FOR THE CALCULATION OF RMR_{89}, GSI AND SMR ARE FOUND IN CHAPTERS 3 AND 4; 'RMR_{89} FOR SMR CALCULATION' IS RMR_{89} WITHOUT THE ADJUSTMENT FOR JOINT ORIENTATIONS AS DISCUSSED IN SECTION 3.3.6; RMR_{89}' IS RMR MODIFIED FOR THE CALCULATION OF GSI WITH GROUNDWATER RATING = 15 AND ADJUSTMENT FOR JOINT ORIENTATIONS = 0; COLOURS OF RATINGS REPRESENT THE ASSOCIATED CONDITIONS WITH 0 TO 20 = VERY POOR, 21 TO 40 = POOR, 41 TO 60 = MODERATE, 61 TO 80 = GOOD, AND 81 TO 100 = VERY GOOD)

APPENDIX IV: POINT LOAD AND SLAKE DURABILITY SAMPLE DESCRIPTIONS

SAMPLE ID	MINE SITE	DEPOSIT	CORE ID (core samples) or AREA (field samples)	HEIGHT meters depth (core samples) or RL (field samples)	ROCK TYPE	LITHOLOGY	EXTENT OF WEATHER -ING (RTIO standards)	EXTENT OF ALTERAT -ION (RTIO standards)	COLOUR	GRAIN SIZE	STRUCTURE	GEOTECHNICAL TESTING
TP - STR - 01	Tom Price	Southern Ridge	GD08STR0009	72.9-74.6	CANGA	Dales Gorge	Extremely	Highly	Yellow-Red-Blue	FINE	BEDDING	Slake Durability
TP - STR - 08	Tom Price	Southern Ridge	GD08STR0009	112.7-112.8	SHALE	Footwall Zone	Moderately	Highly	Yellow-White	VERY FINE	LAMINATIONS	Point Load
TP - STR - 09	Tom Price	Southern Ridge	GD08STR0009	171.2-171.5	SHALE	Mount McRae Shale	Fresh	Fresh	Black	VERY FINE	LAMINATIONS	Point Load
TP - STR - 13	Tom Price	Southern Ridge	GC08STR0003	195.45-195.6	SHALE	Dales Gorge	Moderately	Moderately	Red-Orange	VERY FINE	MASSIVE	Point Load
TP - STR - 16	Tom Price	Southern Ridge	GC08STR0003	228.6-228.8	BIF	Dales Gorge	Moderately	Fresh	Blue-White	VERY FINE	BEDDING	Slake Durability
TP - STR - 21	Tom Price	Southern Ridge	GC08STR0003	307.6-307.7	SHALE	Mount McRae Shale	Fresh	Fresh	Black	VERY FINE	BEDDING	Slake Durability
TP - NTD - 02	Tom Price	North Deposit	SOUTH	695 RL	BIF	Dales Gorge	Highly	Highly	Blue-Red	FINE	SOME BEDDING	Point Load
TP - NTD - 03	Tom Price	North Deposit	SOUTH	625 RL	BIF	Dales Gorge	Moderately	Highly	Blue	MED	MASSIVE	Point Load
TP - NTD - 04	Tom Price	North Deposit	SOUTH	635 RL	BIF	Dales Gorge	Slightly	Highly	Blue	FINE	SOME BEDDING	Point Load
TP - NTD - 05	Tom Price	North Deposit	CENTRE	685 RL	SHALE	Whaleback Shale	Slightly	Highly	White	VERY FINE		Point Load
TP - NTD - 06	Tom Price	North Deposit	NW	685 RL	BIF	Joffre	Moderately	Highly	White-Blue-Red	FINE	BEDDING	Point Load
TP - NTD - 07	Tom Price	North Deposit	WEST	705 RL	BIF	Joffre	Highly	Moderately	White-Blue-Red	FINE	BEDDING	Point Load
TP - NTD - 10	Tom Price	North Deposit	CENTRE	625 RL	SHALE	Dales Gorge	Moderately	Highly	White	VERY FINE	LAMINATIONS	Point Load and Slake Duability
TP - SSEV - 01	Tom Price	Section Seven	WEST	660 RL	BIF	Joffre	Moderately	Highly	White-Blue	VERY FINE	BEDDING	Point Load
TP - SSEV - 02	Tom Price	Section Seven	NE MAIN	670 RL	ORE	Dales Gorge	Moderately	Extremely	Blue	FINE		Slake Durability
TP - SSEV - 03	Tom Price	Section Seven	NE MAIN	670 RL	SHALE	Mount McRae Shale	Moderately	Highly	White	VERY FINE		Point Load
TP - SSEV - 04	Tom Price	Section Seven	NE MAIN	670 RL	BIF	Dales Gorge	Moderately	Highly	Blue	FINE - MED	BEDDING	Point Load
TP - SSEV - 05	Tom Price	Section Seven	CENTRE	690 RL	BIF	Dales Gorge	Moderately	Highly	Blue	FINE - MED	LAMINAR BEDDING	Point Load
TP - SSEV - 06	Tom Price	Section Seven	CENTRE	700 RL	BIF	Dales Gorge	Moderately	Moderately	White-Blue	FINE - VERY FINE	BEDDING	Point Load and Slake Duability
TP - SSEV - 07	Tom Price	Section Seven	CENTRE	680 RL	SHALE	Whaleback Shale	Moderately	Highly	White-Purple	VERY FINE	SOME BEDDING	Point Load and Slake Duability
TP - SSEV - 09	Tom Price	Section Seven	CENTRE	680 RL	BIF	Dales Gorge	Moderately	Highly	Blue	FINE	BEDDING	Point Load
TP - SSEV - 10a	Tom Price	Section Seven	NE MAIN	690 RL	BIF	Dales Gorge	Extremely	Highly	Red	FINE - GRANULAR		Point Load and Slake Duability
TP - SSEV - 10b	Tom Price	Section Seven	NE MAIN	690 RL	CANGA	Dales Gorge	Extremely	Highly	Red	FINE - GRANULAR		Point Load and Slake Duability
TP - SSEV - 11	Tom Price	Section Seven	SE MAIN	685 RL	BIF	Footwall Zone	Moderately	Highly	Blue	FINE	BEDDING	Point Load
PDO - 4E - 01	Paraburdoo	4 East Main	TOP EAST	380 RL	BIF	Joffre	Moderately	Moderately	Red-Blue	FINE	BEDDING	Point Load
PDO - 4E - 02	Paraburdoo	4 East Main	SOUTH	305 RL	ORE	Joffre	Fresh	Extremely	Blue	MED	MASSIVE	Point Load
PDO - 4E - 03	Paraburdoo	4 East Main	NE	305 RL	BIF	Joffre	Slightly	Moderately	Red-Blue	FINE	BEDDING	Point Load
PDO - 4E - 04	Paraburdoo	4 East Main	SOUTH	315 RL	BIF	Joffre	Slightly	Highly	Blue	MED	SOME BEDDING	Point Load
PDO - 4E - 05	Paraburdoo	4 East Main	HAUL RD	337 RL	BIF	Yandicoogina Shale	Moderately	Moderately	Red	FINE	MACRO BEDDING	Point Load
PDO - 4E - 06	Paraburdoo	4 East Main	LOOK OUT	410 RL	BIF	Joffre	Moderately	Highly	Red-White-Blue	FINE	BEDDING	Point Load
PDO - 23 - 02	Paraburdoo	23 East	GD0823E0001	5.5-6.4	BIF	Joffre	Extremely	Highly	Yellow-Red-Blue	FINE	SOME BEDDING	Point Load
PDO - 23 - 03	Paraburdoo	23 East	GD0823E0001	6.6-7.2	SHALE	Joffre	Highly	Highly	Red	VERY FINE	SOME BEDDING	Point Load

PDO - 23 - 04	Paraburdoo	23 East	GD0823E0001	8.2-8.6	BIF	Joffre	Highly	Highly	Yellow-Red-Blue	FINE	BEDDING	Point Load
PDO - 23 - 06	Paraburdoo	23 East	GD0823E0001	31.7-34.7	BIF	Joffre	Slightly	Slightly	White-Blue	FINE - VERY FINE	BEDDING	Point Load
PDO - 23 - 07	Paraburdoo	23 East	GD0823E0008	2.5-3.6	BIF	Whaleback Shale	Highly	Highly	Blue-Red-White	FINE	BEDDING	Point Load
PDO - 23 - 08	Paraburdoo	23 East	GD0823E0008	13.4-13.9	BIF	Whaleback Shale	Highly	Extremely	Red-Blue	FINE	SOME BEDDING	Point Load
PDO - 23 - 09	Paraburdoo	23 East	GD0823E0008	14.5-15	SHALE	Whaleback Shale	Highly	Highly	Pink-White	VERY FINE	LAMINATIONS	Point Load
PDO - 23 - 10	Paraburdoo	23 East	GD0823E0008	17.0-17.3	BIF	Whaleback Shale	Highly	Extremely	Red-Blue	VERY FINE	SOME BEDDING	Point Load
PDO - 23 - 11	Paraburdoo	23 East	GD0823E0008	41.3-44.1	BIF	Dales Gorge	Moderately	Moderately	White-Red-Blue	FINE	BEDDING	Point Load
PDO - 23 - 12	Paraburdoo	23 East	GD0823E0008	45.6-46.6	BIF	Dales Gorge	Slightly	Slightly	White-Red-Blue	FINE	BEDDING	Point Load
PDO - 23 - 14	Paraburdoo	23 East	GD0823E0008	111.8-112.6	SHALE	Footwall Zone	Moderately	Moderately	Black-Red	VERY FINE	SOME BEDDING	Point Load and Slake Duability
PDO - 32 - 01	Paraburdoo	32 East 6	PT 12	610 RL	SHALE	Dales Gorge	Moderately	Highly	Pink-White	VERY FINE	LAMIATIONS	Point Load and Slake Duability
PDO - 32 - 02	Paraburdoo	32 East 6	PT 12	610 RL	BIF	Dales Gorge	Moderately	Extremely	Blue	FINE	BEDDING	Point Load
PDO - 32 - 03	Paraburdoo	32 East 6	PT 13	610 RL	BIF	Dales Gorge	Moderately	Highly	Blue	FINE	BEDDING	Point Load
PDO - 32 - 04	Paraburdoo	32 East 6	PT 61	610 RL	BIF	Dales Gorge	Highly	Highly	Blue	FINE	MASSIVE	Point Load
PDO - 32 - 06	Paraburdoo	32 East 6	PT 59	610 RL	BIF	Dales Gorge	Moderately	Highly	Blue	FINE	BEDDING	Point Load
PDO - 32 - 07	Paraburdoo	32 East 6	PT 27	620 RL	BIF	Dales Gorge	Highly	Highly	Blue	FINE	MASSIVE	Point Load
PDO - 32 - 08	Paraburdoo	32 East 6	PT 23	610 RL	BIF	Dales Gorge	Highly	Extremely	Blue	VERY FINE	BEDDING	Point Load
PDO - 32 - 09	Paraburdoo	32 East 6	PT 23	610 RL	BIF	Dales Gorge	Moderately	Extremely	Orange	MED	SOME BEDDING	Point Load
MDO - 01	Marandoo	Tail	HILL 1	720 RL	BIF	Mount Newman	Moderately	Extremely	Blue	FINE - MED	BEDDING	Point Load
MDO - 02	Marandoo	Tail	HILL 1	720 RL	BIF	Mount Newman	Highly	Highly	Blue-Red-Yellow	MED	BEDDING	Point Load and Slake Duability
MDO - 04	Marandoo	Tail	HILL 1	720 RL	SHALE	Mount Newman	Moderately	Moderately	Yellow	FINE		Slake Durability
MDO - 06	Marandoo	Tail	HILL 1	720 RL	BIF	Mount Newman	Highly	Highly	Blue	FINE - MED	BEDDING	Point Load
MDO - 07	Marandoo	Tail	HILL 1	720 RL	BIF	Mount Newman	Highly	Highly	Grey	VERY FINE		Point Load
MDO - 09	Marandoo	Tail	HILL 5	720 RL	BIF	Mount Newman	Fresh	Highly	Blue	FINE	BEDDING	Point Load
MDO - 10	Marandoo	Tail	HILL 5	720 RL	SHALE	Mount Newman	Moderately	Highly	Red	VERY FINE	LAMINATIONS	Slake Durability
MDO - 11	Marandoo	Tail	HILL 5	720 RL	BIF	Mount Newman	Moderately	Highly	Yellow-Blue	FINE	SOME BEDDING	Point Load
MDO - 12	Marandoo	Ridge	WEST	710 RL	BIF	Mount Newman	Slightly	Highly	Blue	FINE - MED	BEDDING	Point Load
MDO - 13	Marandoo	Ridge	WEST	710 RL	SHALE	Mount Newman	Slightly	Highly	Pink-White	VERY FINE	LAMINATIONS	Slake Durability
MDO - 14	Marandoo	Tail	GT06MDO_01	1-1.5	BIF	Mount Newman	Highly	Highly	Red-Blue	VERY FINE	SOME BEDDING	Point Load
MDO - 16	Marandoo	Tail	GT06MDO_01	13.2-13.9	ORE	Mount Newman	Moderately	Extremely	Yellow-Blue	MED	SOME BEDDING	Point Load
WA - 07 - 07	West Angelas	Deposit A	WAADC0731	145.6-145.8	ORE	West Angelas Shale	Highly	Highly	Brown-Yellow	FINE	BEDDING	Slake Durability
WA - 07 - 10	West Angelas	Deposit A	WAADC0731	166.6;167.4	ORE	Mount Newman	Highly	Extremely	Red-Brown	FINE	SOME BEDDING	Slake Durability
WA - 07 - 16	West Angelas	Deposit A	WAADC0730	13.3;14.8	SHALE	West Angelas Shale	Moderately	Highly	Light Brown	VERY FINE	MASSIVE	Slake Durability
WA - 07 - 24	West Angelas	Deposit A	WAADC0730	84.2-84.5	BIF	Mount Newman	Moderately	Highly	Yellow-Red-Blue	FINE	BEDDING	Slake Durability
WA - 07 - 25	West Angelas	Deposit A	WAADC0730	96.9-97.1	BIF	Mount Newman	Fresh	Fresh	Green-Grey	FINE	BEDDING	Slake Durability

TABLE IV-1 POINT LOAD AND SLAKE DURABILITY SAMPLE DESCRIPTIONS

APPENDIX V: **POINT LOAD TESTING RESULTS**

Sample No	Rock Type	Test Type	Defect Orientation	Failure Mode	Mean $I_{s(50)}$ (MPa)	Mean Estimated UCS (MPa)
TP-STR-01	BIF	Diametral	L	IR	2.71	64.97
TP-STR-08	SHALE	Axial	L	IR	0.57	<15.00
TP-STR-09	SHALE	Axial	L	IR	1.94	29.10
TP-STR-13	SHALE	Axial	L	IR	1.14	17.10

TABLE V.1 POINT LOAD TESTING RESULTS FOR SOUTHERN RIDGE ROCK SAMPLES

Sample No	Rock Type	Test Type	Defect Orientation	Failure Mode	Mean $I_{s(50)}$ (MPa)	Mean Estimated UCS (MPa)
TP-NTD-02	BIF	Irregular lump	L	IR	4.72	113.25
TP-NTD-05	BIF	Irregular lump	L	IR	5.91	141.96
TP-NTD-06	BIF	Irregular lump	L	IR	2.25	54.02
TP-NTD-07	BIF	Irregular lump	L	IR	4.77	114.43
TP-NTD-08	SHALE	Irregular lump	L	IR	0.12	<15.00
TP-NTD-10	SHALE	Irregular lump	L	IR	0.24	<15.00

TABLE V.2 POINT LOAD TESTING RESULTS FOR NORTH DEPOSIT ROCK SAMPLES

Sample No	Rock Type	Test Type	Defect Orientation	Failure Mode	Mean $I_{s(50)}$ (MPa)	Mean Estimated UCS (MPa)
TP-SSEV-01	BIF	Irregular lump	L	IR	6.30	151.21
TP-SSEV-03	SHALE	Irregular lump	L	IR	0.46	<15.00
TP-SSEV-04	BIF	Irregular lump	L	IR	3.30	79.24
TP-SSEV-05	BIF	Irregular lump	L	IR	5.44	130.44
TP-SSEV-06	BIF	Irregular lump	L	IR	4.18	100.24
TP-SSEV-07	SHALE	Irregular lump	L	IR	0.31	<15.00
TP-SSEV-09	BIF	Irregular lump	L	IR	5.14	123.40
TP-SSEV-10	CANGA	Irregular lump	L	IR	0.90	<24.00
TP-SSEV-11	BIF	Irregular lump	L	IR	4.16	99.81

TABLE V.3 POINT LOAD TESTING RESULTS FOR SECTION SEVEN ROCK SAMPLES

Sample No	Rock Type	Test Type	Defect Orientation	Failure Mode	Mean $I_{s(50)}$ (MPa)	Mean Estimated UCS (MPa)
PDO-4E-01	BIF	Irregular lump	L	IR	4.02	96.59
PDO-4E-02	BIF	Irregular lump	L	IR	2.63	63.15
PDO-4E-04	BIF	Irregular lump	L	IR	2.12	50.95
PDO-4E-05	BIF	Irregular lump	L	IR	5.45	130.80
PDO-4E-06	BIF	Irregular lump	L	IR	1.99	47.70

TABLE V.4 POINT LOAD TESTING RESULTS FOR 4 EAST DEPOSIT ROCK SAMPLES

Sample No	Rock Type	Test Type	Defect Orientation	Failure Mode	Mean $I_{s(50)}$ (MPa)	Mean Estimated UCS (MPa)
PDO-23-02	SHALE	Axial	L	IR	1.87	28.05
PDO-23-03	SHALE	Axial	L	IR	0.66	<15.00
PDO-23-04	BIF	Axial	L	IR	1.45	34.80
PDO-23-05	BIF	Axial	L	IR	3.47	83.39
PDO-23-06	BIF	Axial	L	IR	0.80	<24.00
PDO-23-07	BIF	Axial	L	IR	2.15	51.50
PDO-23-08	BIF	Axial	L	IR	0.78	<24.00
PDO-23-09	SHALE	Axial	L	IR	0.17	<15.00
PDO-23-10	BIF	Axial	L	IR	0.60	<24.00
PDO-23-11	BIF	Axial	L	IR	2.48	59.60
PDO-23-12	BIF	Axial	L	IR	5.28	126.81
PDO-23-14	SHALE	Axial	L	IR	0.84	<15.00

TABLE V.5 POINT LOAD TESTING RESULTS FOR 23 EAST DEPOSIT ROCK SAMPLES

Sample No	Rock Type	Test Type	Defect Orientation	Failure Mode	Mean $I_{s(50)}$ (MPa)	Mean Estimated UCS (MPa)
PDO-32-01	SHALE	Irregular lump	L	IR	0.87	<15.00
PDO-32-02	BIF	Irregular lump	L	IR	4.00	96.02
PDO-32-03	BIF	Irregular lump	L	IR	4.09	98.20
PDO-32-04	BIF	Irregular lump	L	IR	4.02	96.53
PDO-32-06	BIF	Irregular lump	L	IR	3.82	91.79
PDO-32-07	BIF	Irregular lump	L	IR	1.75	41.95
PDO-32-08	BIF	Irregular lump	-	IR	0.71	<24.00
PDO-32-09	BIF	Irregular lump	//	IR	6.34	152.24

TABLE V.6 POINT LOAD TESTING RESULTS FOR 32 EAST 6 DEPOSIT ROCK SAMPLES

Sample No	Rock Type	Test Type	Defect Orientation	Failure Mode	Mean $I_{s(50)}$ (MPa)	Mean Estimated UCS (MPa)
MDO-01	BIF	Irregular lump	L	IR	7.34	176.12
MDO-02	BIF	Irregular lump	L	IR	5.33	127.91
MDO-06	BIF	Irregular lump	L	IR	3.50	83.95
MDO-07	BIF	Irregular lump	L	IR	3.12	74.80
MDO-09	BIF	Irregular lump	L	IR	4.81	115.46
MDO-10	SHALE	Irregular lump	L	IR	1.22	18.30
MDO-11	BIF	Irregular lump	L	IR	2.78	66.81
MDO-12	BIF	Irregular lump	L	IR	3.83	91.99
MDO-14	BIF	Axial	L	IR	1.55	37.12
MDO-16	ORE	Axial	L	IR	0.55	<24.00

TABLE V.7 POINT LOAD TESTING RESULTS FOR MARANDOO ROCK SAMPLES

Sample No	Rock Type	Test Type	Defect Orientation	Failure Mode	Mean $I_{s(50)}$ (MPa)	Mean Estimated UCS (MPa)
WA-50-10	SHALE	Axial	L	IR	0.15	<15.00
WA-07-07	ORE	Axial	L	IR	0.07	<24.00
WA-07-09	SHALE	Axial	L	IR	0.03	<15.00
WA-07-10	ORE	Axial	L	DEFECT	0.60	<24.00
WA-07-12	BIF	Axial	L	IR	0.62	<24.00
WA-07-13	SHALE	Axial	L	IR	0.01	<15.00
WA-07-14	BIF	Axial	L	IR	5.09	122.20
WA-07-16	SHALE	Axial	L	IR	0.11	<15.00
WA-07-18	SHALE	Axial	L	IR	0.07	<15.00
WA-07-19	SHALE	Axial	L	IR	0.40	<15.00
WA-07-23	BIF	Axial	L	IR	1.33	31.83
WA-07-25	BIF	Axial	L	IR	4.55	109.10

TABLE V.8 POINT LOAD TESTING RESULTS FOR WEST ANGELAS ROCK SAMPLES

Symbols and Abbreviation List:

Defect Orientation:
L – Test completed perpendicular to defect
// - Test completed parallel to defect
- - No defect in specimen

Failure Mode:
IR = Intact rock

For details on point load testing methods refer to Section 4.5 or ISRM (1985) ‘Suggested Method for Determining Point Load Strength’

APPENDIX VI: SLAKE DURABILITY TESTING CALCULATIONS

ID	ROCK TYPE	EXTENT OF WEATHER -ING (RTIO standards)	EXTENT OF ALTERAT -ION (RTIO standards)	(A) Mass Dry Drum + Sample Before	(B) Mass Dry Drum + Sample After 1st Cycle	(C) Mass Dry Drum + Sample After 2nd Cycle	(D) Mass Dry Drum (without Lid)	(B-D)	(A-D)	(C-D)	(B-D) /(A-D)	(C-D) /(A-D)	Slake Durability (I_{d1})	Slake Durability (I_{d2})
TP - STR - 01	BIF	Extremely	Highly	1906.0	1903.3	1901.5	1374.9	528.4	531.1	526.6	0.9949	0.9915	99.49	99.15
TP - STR - 11	BIF	Slightly	Slightly	1938.8	1938.5	1938.2	1408.7	529.8	530.1	529.5	0.9994	0.9989	99.94	99.89
TP - STR - 13	SHALE	Moderately	Moderately	1885.7	1879.3	1874.6	1398.5	480.8	487.2	476.1	0.9869	0.9772	98.69	97.72
TP - STR - 16	BIF	Slight	Slightly	1862.0	1861.7	1861.6	1370.0	491.7	492.0	491.6	0.9994	0.9992	99.94	99.92
TP - STR - 21	SHALE	Fresh	Fresh	1933.9	1932.7	1931.7	1399.0	533.7	534.9	532.7	0.9978	0.9959	99.78	99.59
TP - NTD - 02	BIF	Highly	Highly	1940.7	1939.1	1938.2	1398.7	540.4	542.0	539.5	0.9970	0.9954	99.70	99.54
TP - NTD - 03	BIF	Moderately	Highly	1874.9	1862.2	1852.3	1369.5	492.7	505.4	482.8	0.9749	0.9553	97.49	95.53
TP - NTD - 10	SHALE	Moderately	Highly	1909.7	1526.4	1411.2	1375.1	151.3	534.6	36.1	0.2830	0.0675	28.30	6.75
TP - SSEV - 02	BIF	Moderately	Extremely	1899.7	1717.1	1704.3	1408.9	308.2	490.8	295.4	0.6280	0.6019	62.80	60.19
TP - SSEV - 06	BIF	Moderately	Moderately	1878.7	1876.9	1875.2	1374.5	502.4	504.2	500.7	0.9964	0.9931	99.64	99.31
TP - SSEV - 07	SHALE	Moderately	Moderately	1946.3	1874.6	1819.5	1408.7	465.9	537.6	410.8	0.8666	0.7641	86.66	76.41
TP - SSEV - 10	BIF	Extremely	Highly	1895.4	1890.6	1888.8	1367.7	522.9	527.7	521.1	0.9909	0.9875	99.09	98.75
PDO - 23 - 04	BIF	Highly	Highly	1914.5	1913.0	1911.7	1374.4	538.6	540.1	537.3	0.9972	0.9948	99.72	99.48
PDO - 23 - 05	BIF	Moderately	Moderately	1847.4	1844.4	1842.4	1369.7	474.7	477.7	472.7	0.9937	0.9895	99.37	98.95
PDO - 23 - 06	BIF	Slightly	Slightly	1854.3	1852.8	1851.1	1374.3	478.5	480.0	476.8	0.9969	0.9933	99.69	99.33
PDO - 23 - 14	SHALE	Moderately	Moderately	1906.8	1901.5	1897.1	1374.9	526.6	531.9	522.2	0.9900	0.9818	99.00	98.18
PDO - 32 - 01	SHALE	Moderately	Highly	1909.2	1894.8	1882.8	1399.2	495.6	510.0	483.6	0.9718	0.9482	97.18	94.82
MDO - 02	BIF	Highly	Highly	1883.2	1880.8	1879.0	1375.2	505.6	508.0	503.8	0.9953	0.9917	99.53	99.17
MDO - 04	SHALE	Moderately	Moderately	1896.8	1882.4	1868.9	1370.3	512.1	526.5	498.6	0.9726	0.9470	97.26	94.70
MDO - 10	SHALE	Moderately	Highly	1922.7	1920.7	1919.7	1399.1	521.6	523.6	520.6	0.9962	0.9943	99.62	99.43
MDO - 12	BIF	Slightly	Highly	1887.9	1884.0	1882.1	1408.5	475.5	479.4	473.6	0.9919	0.9879	99.19	98.79
MDO - 13	SHALE	Slightly	Highly	1909.1	1906.5	1905.5	1398.7	507.8	510.4	506.8	0.9949	0.9929	99.49	99.29
WA - 07 - 07	BIF	Highly	Highly	1881.0	1861.8	1855.1	1408.7	453.1	472.3	446.4	0.9593	0.9452	95.93	94.52
WA - 07 - 10	BIF	Highly	Extremely	1921.2	1893.4	1882.6	1409.0	484.4	512.2	473.6	0.9457	0.9246	94.57	92.46
WA - 07 - 16	SHALE	Moderately	Highly	1930.9	1753.7	1660.8	1399.1	354.6	531.8	261.7	0.6668	0.4921	66.68	49.21
WA - 07 - 24	BIF	Moderately	Highly	1890.3	1869.3	1857.3	1370.4	498.9	519.9	486.9	0.9596	0.9365	95.96	93.65
WA - 07 - 25	BIF	Fresh	Fresh	1892.6	1891.8	1891.5	1370.2	521.6	522.4	521.3	0.9985	0.9979	99.85	99.79

TABLE VI.1 SLAKE DURABILITY TESTING CALCULATIONS

APPENDIX VII: SLAKE DURABILITY TESTING PHOTOS

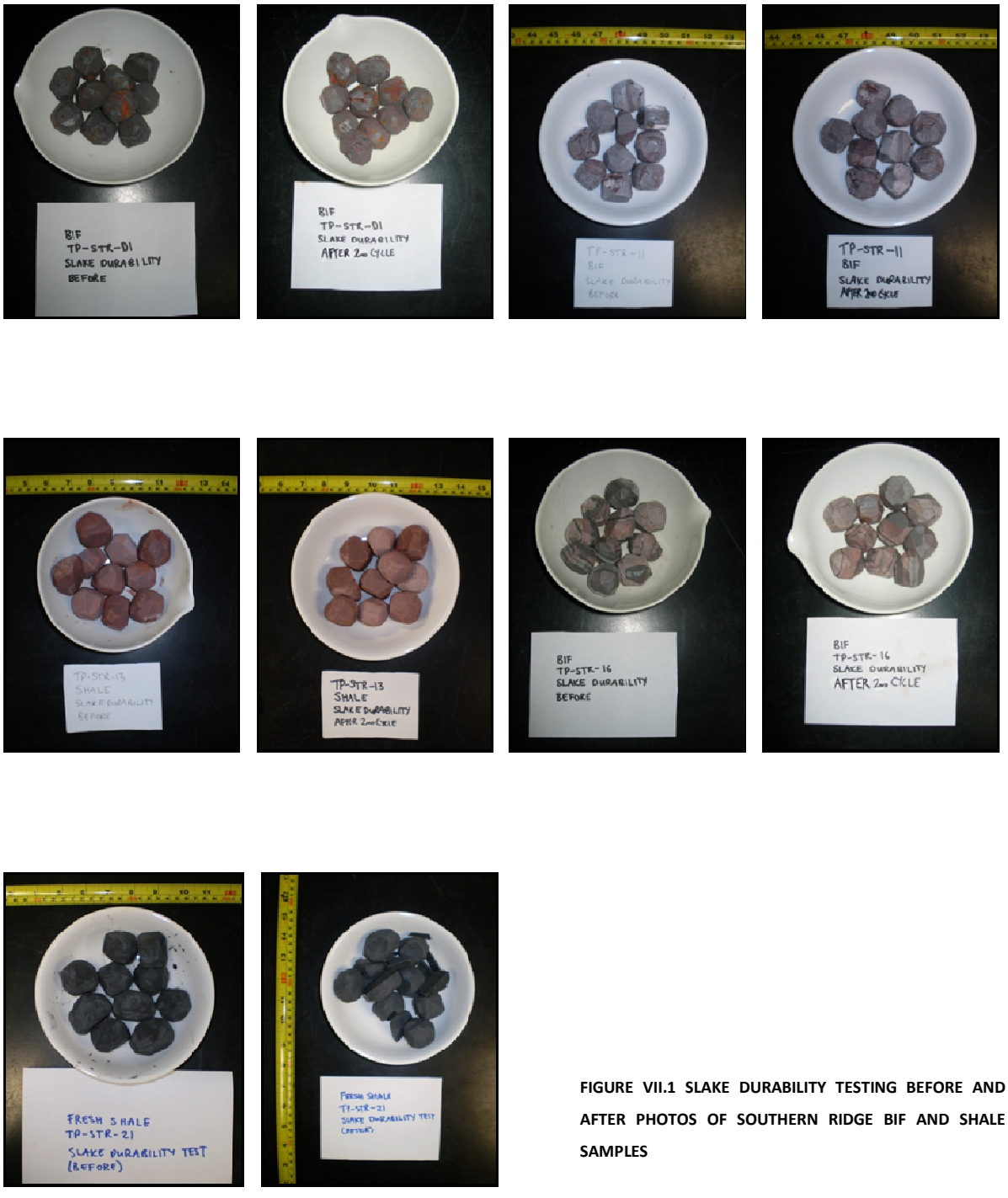

FIGURE VII.1 SLAKE DURABILITY TESTING BEFORE AND AFTER PHOTOS OF SOUTHERN RIDGE BIF AND SHALE SAMPLES

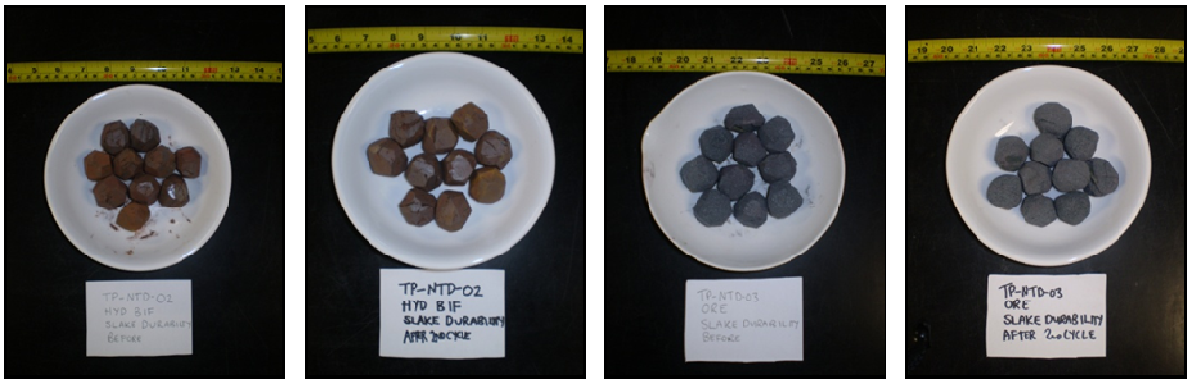

FIGURE VII.3 (ABOVE AND LEFT) SLAKE DURABILITY TESTING BEFORE AND AFTER PHOTOS OF NORTH DEPOSIT BIF AND SHALE SAMPLES

FIGURE VII.3 (BELOW) SLAKE DURABILITY TESTING BEFORE AND AFTER PHOTOS OF SECTION SEVEN BIF AND SHALE SAMPLES

FIGURE VII.4 SLAKE DURABILITY TESTING BEFORE AND AFTER PHOTOS OF PARABURDOO (23 EAST AND 32 EAST) BIF AND SHALE SAMPLES

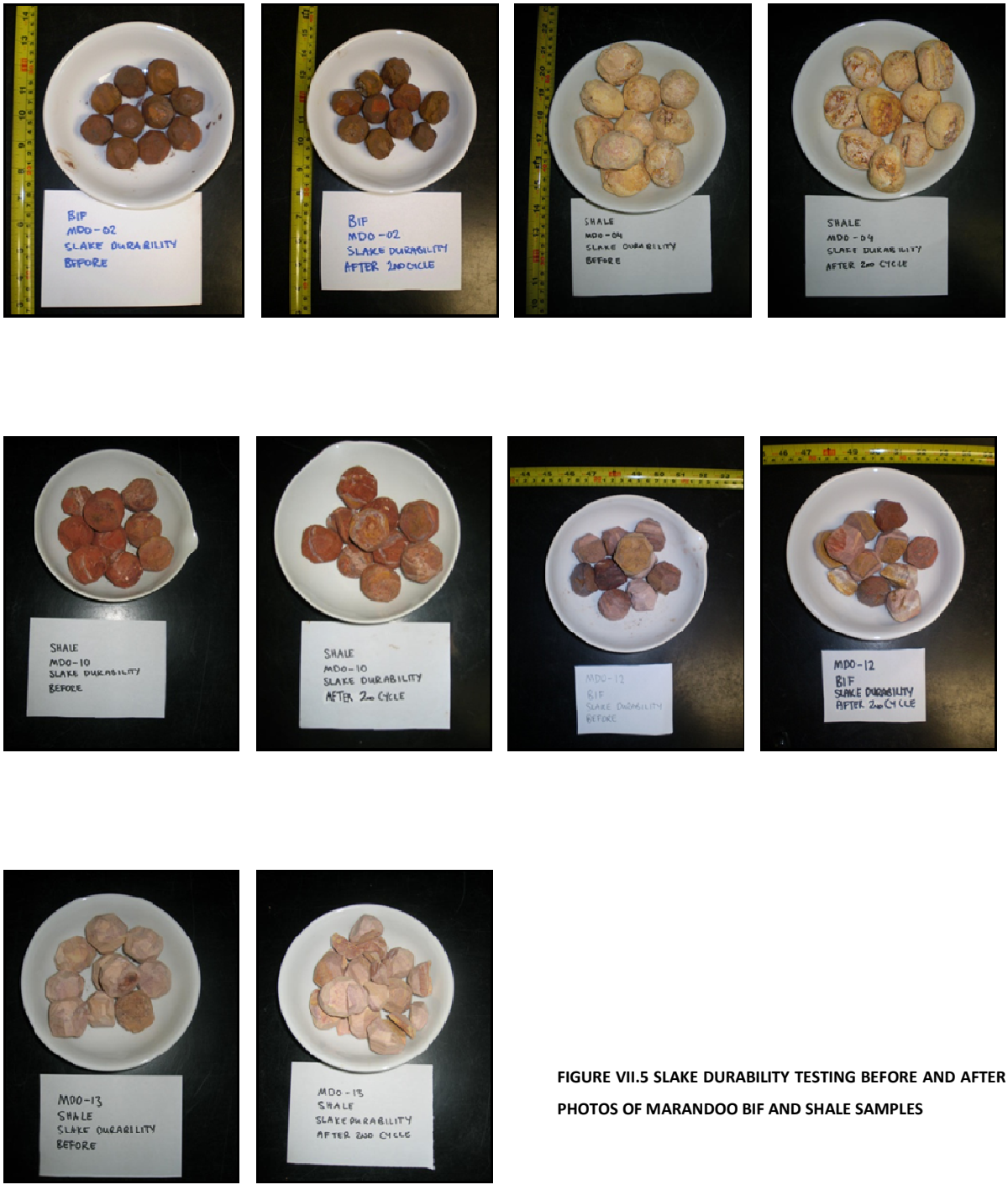

FIGURE VII.5 SLAKE DURABILITY TESTING BEFORE AND AFTER PHOTOS OF MARANDOO BIF AND SHALE SAMPLES

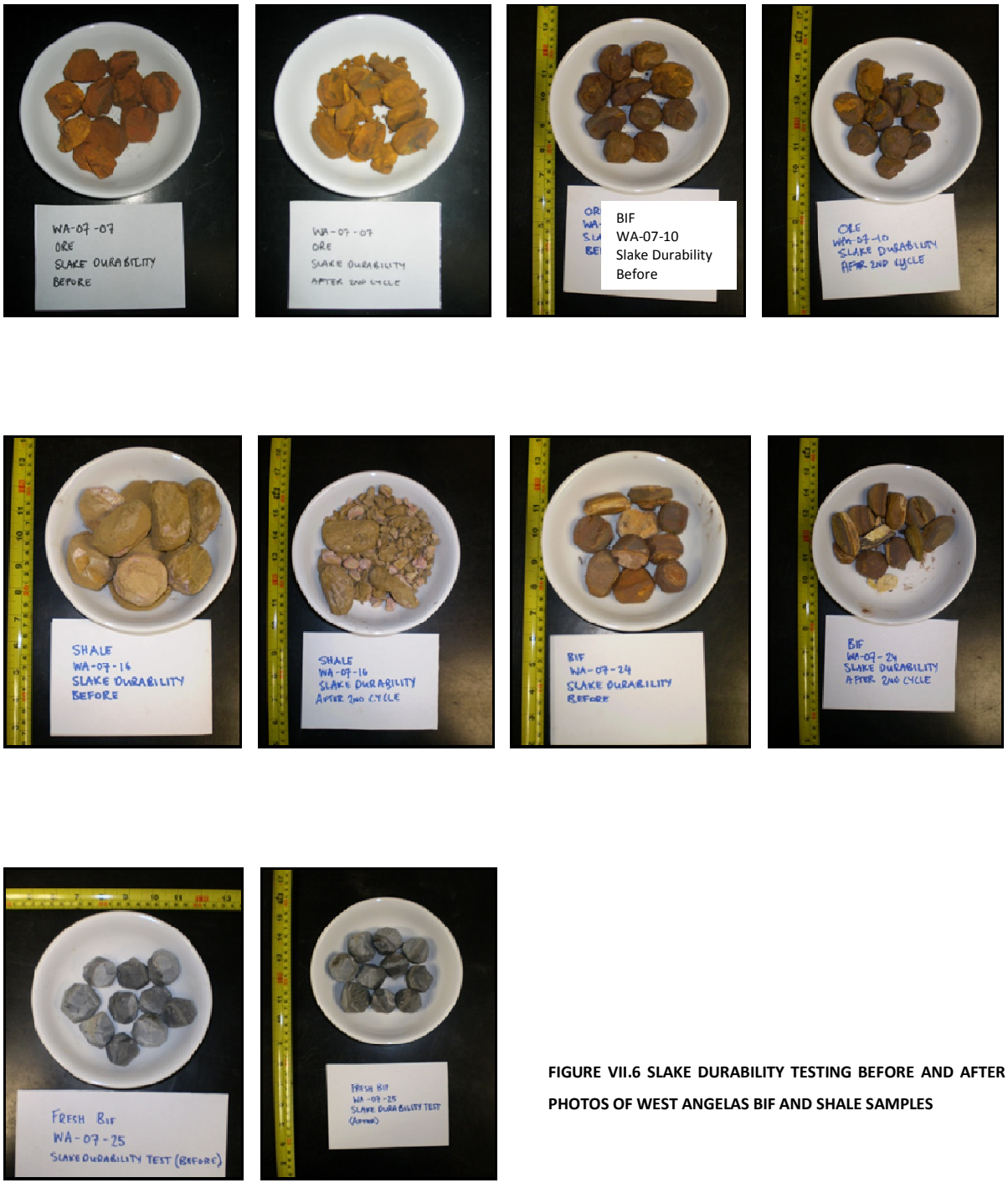

FIGURE VII.6 SLAKE DURABILITY TESTING BEFORE AND AFTER PHOTOS OF WEST ANGELAS BIF AND SHALE SAMPLES

APPENDIX VIII: **XRF/XRD AND MICROSCOPE SAMPLE DESCRIPTIONS**

SAMPLE ID	MINE SITE	DEPOSIT	CORE # (core samples) or AREA (field samples)	HEIGHT meters depth (core samples) or RL (field samples)	ROCK TYPE	LITHOLOGY	EXTENT OF WEATHER -ING (RTIO standards)	EXTENT OF ALTERAT -ION (RTIO standards)	COLOUR	GRAIN SIZE	STRUCTURE	GEOCHEMICAL/ MINERALOGICAL TESTING TYPE(S)
TP - STR - 01	Tom Price	Southern Ridge	GD08STR0009	72.9 - 74.6	BIF	Dales Gorge	Extremely	Highly	YELLOW-RED-BLUE	FINE	BEDDING	XRF/XRD; Microscope
TP - STR - 09	Tom Price	Southern Ridge	GD08STR0009	171.2 - 171.5	SHALE	Mount McRae Shale	Fresh	Fresh	BLACK	VERY FINE	LAMINATIONS	XRF/XRD; Microscope
TP - STR - 11	Tom Price	Southern Ridge	GC08STR0003	189.6 - 189.7	BIF	Dales Gorge	Slightly	Slightly	GREEN-GREY	VERY FINE	BEDDING	XRF/XRD
TP - STR - 12	Tom Price	Southern Ridge	GC08STR0003	195 - 195.1	BIF	Dales Gorge	Moderately	Moderately	RED-BLUE-WHITE	FINE	BEDDING	XRF/XRD; Microscope
TP - STR - 13	Tom Price	Southern Ridge	GC08STR0003	195.45 - 195.6	SHALE	Dales Gorge	Moderately	Moderately	RED-ORANGE	VERY FINE	MASSIVE	XRF/XRD
TP - STR - 15	Tom Price	Southern Ridge	GC08STR0003	228.4 - 228.6	BIF	Dales Gorge	Slightly	Slightly	RED-BLUE-WHITE	VERY FINE	BEDDING	XRF/XRD
TP - STR - 16	Tom Price	Southern Ridge	GC08STR0003	228.6 - 228.8	BIF	Dales Gorge	Moderately	Slightly	BLUE-WHITE	VERY FINE	BEDDING	Microscope
TP - STR - 17	Tom Price	Southern Ridge	GC08STR0003	175.5 - 175.6	BIF	Dales Gorge	Highly	Highly	BLUE-RED	FINE - MED	SOME BEDDING	XRF/XRD
TP - STR - 18	Tom Price	Southern Ridge	GC08STR0003	175.6 - 175.7	BIF	Dales Gorge	Highly	Highly	BLUE-RED	FINE - MED	SOME BEDDING	Microscope
TP - STR - 19	Tom Price	Southern Ridge	GC08STR0003	178.4 - 178.6	SHALE	Dales Gorge	Moderately	Moderately	PURPLE	VERY FINE	LAMINATIONS	XRF/XRD; Microscope
TP - STR - 21	Tom Price	Southern Ridge	GC08STR0003	307.6 - 307.7	SHALE	Mount McRae Shale	Fresh	Fresh	BLACK	VERY FINE	BEDDING	XRF/XRD
TP - NTD - 02	Tom Price	North Deposit	SOUTH	695 RL	BIF	Dales Gorge	Highly	Highly	BLUE-RED	FINE	SOME BEDDING	XRF/XRD
TP - NTD - 03	Tom Price	North Deposit	SOUTH	625 RL	BIF	Dales Gorge	Moderately	Highly	BLUE	MED	MASSIVE	XRF/XRD
TP - NTD - 10	Tom Price	North Deposit	CENTRE	625 RL	SHALE	Dales Gorge	Moderately	Highly	WHITE	VERY FINE	LAMINATIONS	XRF/XRD
TP - NTD - 11	Tom Price	North Deposit	CENTRE	625 RL	SHALE	Dales Gorge	Moderately	Highly	GREY	VERY FINE	LAMINATIONS	XRF/XRD
TP - SSEV - 02	Tom Price	Section Seven	NE MAIN	670 RL	ORE	Dales Gorge	Moderately	Extremely	BLUE	FINE	MASSIVE	XRF/XRD
TP - SSEV - 03	Tom Price	Section Seven	NE MAIN	670 RL	SHALE	Mount McRae Shale	Moderately	Highly	WHITE	VERY FINE	BEDDING	XRF/XRD
TP - SSEV - 06	Tom Price	Section Seven	CENTRE	700 RL	BIF	Dales Gorge	Moderately	Moderately	WHITE-BLUE	FINE - VERY FINE	BEDDING	XRF/XRD
TP - SSEV - 07	Tom Price	Section Seven	CENTRE	680 RL	SHALE	Whaleback Shale	Moderately	Highly	WHITE-PURPLE	VERY FINE	SOME BEDDING	XRF/XRD
TP - SSEV - 10a	Tom Price	Section Seven	NE MAIN	689 RL	CANGA	Dales Gorge	Extremely	Highly	RED	FINE - GRANULAR	SOME BEDDING	XRF/XRD
TP - SSEV - 10b	Tom Price	Section Seven	NE MAIN	690 RL	BIF	Dales Gorge	Extremely	Highly	RED	FINE - GRANULAR	SOME BEDDING	XRF/XRD
TP - SSEV - 12	Tom Price	Section Seven	SE MAIN	685 RL	SHALE	Mount McRae Shale	Moderately	Highly	WHITE-RED	VERY FINE	LAMIATIONS	XRF/XRD; Microscope
PDO - 23 - 03	Paraburdoo	23 East	GD0823E0001	6.6 - 7.2	SHALE	Joffre	Highly	Highly	RED	VERY FINE	SOME BEDDING	Microscope
PDO - 23 - 04	Paraburdoo	23 East	GD0823E0001	8.2 - 8.6	BIF	Joffre	Highly	Highly	YELLOW-RED-BLUE	FINE	BEDDING	XRF/XRD
PDO - 23 - 05	Paraburdoo	23 East	GD0823E0001	30.4 - 30.55	BIF	Joffre	Moderately	Moderately	RED-BLUE	FINE	BEDDING	XRF/XRD
PDO - 23 - 06	Paraburdoo	23 East	GD0823E0001	31.7 - 34.7	BIF	Joffre	Slightly	Slightly	WHITE-BLUE	FINE - VERY FINE	BEDDING	XRF/XRD
PDO - 23 - 11	Paraburdoo	23 East	GD0823E0008	41.3 - 44.1	BIF	Dales Gorge	Moderately	Moderately	WHITE-RED-BLUE	FINE	BEDDING	XRF/XRD
PDO - 23 - 12	Paraburdoo	23 East	GD0823E0008	45.6 - 46.6	BIF	Dales Gorge	Slightly	Slightly	WHITE-RED-BLUE	FINE	BEDDING	XRF/XRD
PDO - 23 - 14	Paraburdoo	23 East	GD0823E0008	111.8 - 112.6	SHALE	Footwall zone	Moderately	Moderately	BLACK-RED	VERY FINE	SOME BEDDING	XRF/XRD
PDO - 32 - 01	Paraburdoo	32 East 6	North wall	610 RL	SHALE	Dales Gorge	Moderately	Highly	PINK-WHITE	VERY FINE	LAMIATIONS	XRF/XRD
PDO - 32 - 05	Paraburdoo	32 East 6	North wall	610 RL	SHALE	Dales Gorge	Moderately	Highly	WHITE-ORANGE	VERY FINE	LAMINATIONS	XRF/XRD
MDO - 02	Marandoo	Tail Pit	HILL 1	720 RL	BIF	Mount Newman	Highly	Highly	BLUE-RED-YELLOW	MED	BEDDING	XRF/XRD; Microscope
MDO - 04	Marandoo	Tail Pit	HILL 1	720 RL	SHALE	Mount Newman	Moderately	Moderately	YELLOW	FINE	SOME BEDDING	XRF/XRD
MDO - 10	Marandoo	Tail Pit	HILL 5	720 RL	SHALE	Mount Newman	Moderately	Highly	RED	VERY FINE	LAMINATIONS	XRF/XRD
MDO - 12	Marandoo	Ridge Pit	WEST	710 RL	BIF	Mount Newman	Slightly	Highly	BLUE	FINE - MED	BEDDING	XRF/XRD
MDO - 13	Marandoo	Ridge Pit	WEST	710 RL	SHALE	Mount Newman	Slightly	Highly	PINK-WHITE	VERY FINE	LAMINATIONS	XRF/XRD
WA - 50 - 01	West Angelas	Deposit A	WAADC5017	63.1 m	Hard Cap	West Angelas Shale	Highly	Moderately	RED	VERY FINE	MASSIVE	XRF/XRD
WA - 50 - 10	West Angelas	Deposit A	WAADC5028	72.3 m	SHALE	West Angelas Shale	Moderately	Moderately	YELLOW	VERY FINE	MASSIVE	XRF/XRD
WA - 07 - 07	West Angelas	Deposit A	WAADC0731	145.6 - 145.8	ORE	West Angelas Shale	Highly	Highly	BROWN-YELLOW	FINE	BEDDING	XRF/XRD
WA - 07 - 09	West Angelas	Deposit A	WAADC0731	164 - 169.8	SHALE	Mount Newman	Moderately	Highly	YELLOW-BROWN	VERY FINE	MASSIVE	XRF/XRD
WA - 07 - 10	West Angelas	Deposit A	WAADC0731	166.6 - 167.4	ORE	Mount Newman	Highly	Extremely	DARK RED-BROWN	FINE	SOME BEDDING	XRF/XRD; Microscope
WA - 07 - 12	West Angelas	Deposit A	WAADC0731	185.7 - 186	BIF	Mount Newman	Moderately	Moderately	WHITE-BROWN	FINE	BEDDED	XRF/XRD; Microscope
WA - 07 - 14	West Angelas	Deposit A	WAADC0731	200 m	BIF	Mount Newman	Slightly	Slightly	WHITE-BROWN	VERY FINE	BEDDING	XRF/XRD; Microscope
WA - 07 - 16	West Angelas	Deposit A	WAADC0730	13.3 - 14.8	SHALE	West Angelas Shale	Moderately	Highly	YELLOW-BROWN	VERY FINE	MASSIVE	XRF/XRD
WA - 07 - 18	West Angelas	Deposit A	WAADC0730	21.2 - 21.9	SHALE	West Angelas Shale	Moderately	Highly	PINK-BROWN	VERY FINE	LAMIATIONS	XRF/XRD
WA - 07 - 19	West Angelas	Deposit A	WAADC0730	32.2 - 32.3	SHALE	West Angelas Shale	Slightly	Highly	RED-BROWN	VERY FINE	MASSIVE	XRF/XRD
WA - 07 - 24	West Angelas	Deposit A	WAADC0730	84.2 - 84.5	BIF	Mount Newman	Moderately	Highly	YELLOW-RED-BLUE	FINE	BEDDING	XRF/XRD
WA - 07 - 25	West Angelas	Deposit A	WAADC0730	96.9 - 97.1	BIF	Mount Newman	Fresh	Fresh	GREEN-GREY	FINE	BEDDING	XRF/XRD

TABLE VIII.1 XRF AND XRD SAMPLE DESCRIPTIONS

APPENDIX IX: **XRF AND XRD SAMPLE PHOTOS**

FIGURE IX.1 XRF AND XRD BIF AND SHALE SAMPLES FROM SOUTHERN RIDGE, MOUNT TOM PRICE

FIGURE IX.2 XRF AND XRD BIF AND SHALE SAMPLES FROM NORTH DEPOSIT, MOUNT TOM PRICE

FIGURE IX.3 XRF AND XRD BIF AND SHALE SAMPLES FROM SECTION SEVEN, MOUNT TOM PRICE

FIGURE IX.4 XRF AND XRD BIF AND SHALE SAMPLES FROM 23 EAST DEPOSIT, PARABURDOO

FIGURE IX.5 XRF AND XRD BIF AND SHALE SAMPLES FROM 32 EAST 6 DEPOSIT, PARABURDOO

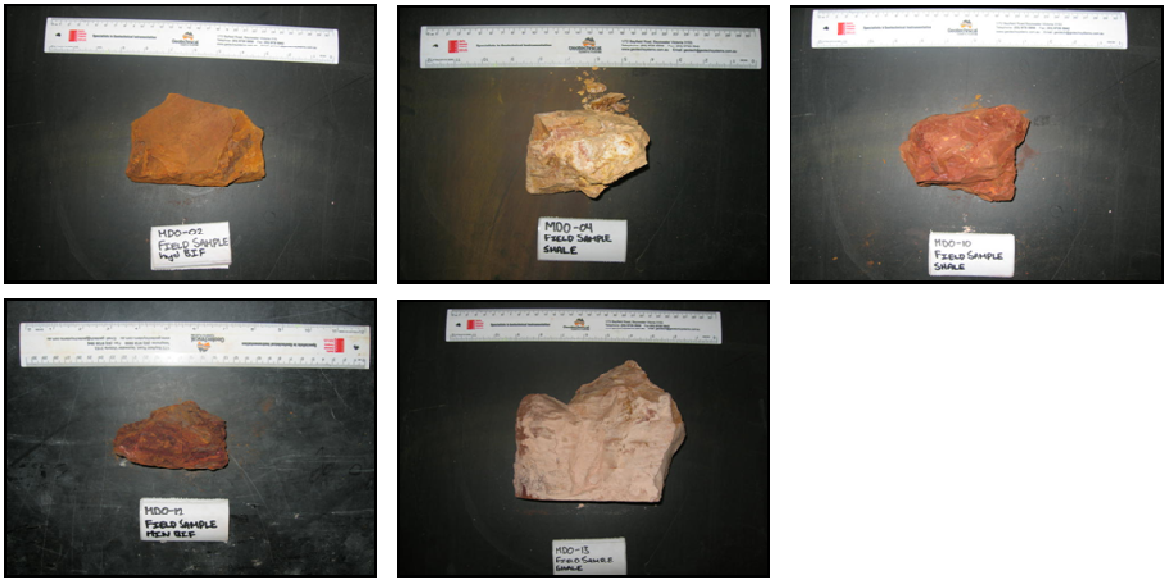

FIGURE IX.6 XRF AND XRD BIF AND SHALE SAMPLES FROM TAIL PIT AND RIDGE PIT, MARANDOO

FIGURE IX.7 XRF AND XRD BIF AND SHALE SAMPLES FROM DEPOSIT A, WEST ANGELAS

APPENDIX X: **XRF MAJOR AND MINOR ELEMENT RESULTS**

XRF Analytical Results Geochemistry Laboratory, Department of Geological Sciences, University of Canterbury, New Zealand

Your Reference	Laboratory Sample Number
TP-STR-01	34904A
TP-STR-11	34905A
TP-STR-12	34906A
TP-STR-19	34907A
TP-STR-21	34908A
TP-NTD-02	34909A
TP-NTD-03	34910A
TP-NTD-10	34911A
TP-NTD-11	34912A
PDO-23-04	34913A
PDO-23-05	34914A
PD0-23-06	34915A
PDO-23-11	34916A
PDO-23-12	34917A
TP-SSEV-02	34918A
TP-SSEV-06	34919A
TP-SSEV-07	34920A
TP-SSEV-10a	34921A
TP-SSEV-10b	34922A
PDO-32-01	34923A
MDO-04	34924A
MDO-10	34925A
MDO-12	34926A
MDO-13	34927A
WA-07-07	34928A
WA-07-12	34929A
WA-07-14	34930A
WA-07-18	34875A
WA-07-19	34876A
MDO-02	34877A
TP-SSEV-03	34878A
WA-07-09	34879A
TP-STR-17	34880A
TP-STR-15	34881A
WA-07-24	34882A
TP-SSEV-12	34883A
WA-07-25	34884A
TP-STR-09	34885A
WA-50-10	34886A
WA-07-16	34887A
TP-STR-13	34888A
WA-07-10	34889A
WA-50-01	34890A
PDO-23-14	34891A
PDO-32-05	34892A

The suffix with laboratory sample numbers (i.e. A, B or C) should be ignored when referring to trace element results.

FIGURE X.1 LABORATTORY SAMPLE NUMBERS FOR XRF MAJOR AND MINOR ELEMENT ANALYSIS

XRF Analytical Results Geochemistry Laboratory, Department of Geological Sciences, University of Canterbury, New Zealand

[Rock Majors Program]

Sample Number	SiO_2 (%)	TiO_2 (%)	Al_2O_3 (%)	Fe_2O_3T (%)	MnO (%)	MgO (%)	CaO (%)	Na_2O (%)	K_2O (%)	P_2O_5 (%)	LOI (%)	Total (%)
34904A	0.34	0.02	0.24	97.66	0.03	<0.05	0.07	<0.1	0.01	0.08	1.31	99.78
34905A	60.60	0.02	<0.2	37.67	0.02	<0.05	0.12	<0.1	<0.01	0.08	0.57	99.07
34906A	4.58	0.03	0.26	93.12	0.14	<0.05	0.06	<0.1	0.01	0.03	0.99	99.23
34907A	31.93	0.88	21.87	35.06	0.02	0.11	0.06	<0.1	0.02	0.36	9.31	99.61
34908A	52.08	0.42	12.74	9.47	0.03	13.98	0.21	<0.1	1.25	0.08	9.03	99.28
34909A	0.68	0.03	0.40	96.15	0.02	<0.05	0.06	<0.1	0.01	0.13	2.47	99.96
34910A	0.30	0.02	<0.2	98.85	0.01	<0.05	0.06	<0.1	0.01	<0.01	0.67	99.92
34911A	21.95	0.79	16.76	51.50	0.01	0.24	0.18	<0.1	0.02	0.32	7.67	99.44
34912A	29.00	0.97	23.98	33.23	0.01	0.31	0.16	<0.1	0.02	0.44	11.69	99.81
34913A	1.89	0.04	1.20	92.43	0.03	<0.05	0.08	<0.1	0.01	0.17	3.33	99.17
34914A	25.69	0.05	0.85	70.36	0.05	<0.05	0.07	<0.1	0.02	0.04	2.11	99.25
34915A	36.69	0.03	0.53	60.52	0.03	<0.05	0.07	<0.1	0.02	0.03	1.18	99.09
34916A	22.09	0.02	0.53	74.11	0.02	<0.05	0.06	<0.1	0.02	0.09	2.47	99.40
34917A	48.26	0.02	<0.2	47.88	0.01	<0.05	0.06	<0.1	0.02	0.11	2.25	98.60
34918A	0.78	0.03	0.52	95.45	0.03	<0.05	0.05	<0.1	<0.01	0.19	2.30	99.33
34919A	44.96	0.02	<0.2	52.85	0.02	<0.05	0.05	<0.1	0.03	0.05	1.22	99.19
34920A	31.65	1.06	26.02	27.26	0.03	0.13	0.07	<0.1	0.02	0.22	13.01	99.46
34921A	17.15	1.06	9.36	60.03	<0.01	<0.05	0.05	<0.1	<0.01	0.08	12.16	99.90
34922A	39.61	0.91	8.69	40.71	<0.01	<0.05	0.05	<0.1	0.01	0.06	8.99	99.03
34923A	78.56	0.48	14.18	0.32	<0.01	0.10	0.07	<0.1	0.15	0.05	5.72	99.63
34924A	42.54	0.15	34.41	7.66	<0.01	0.17	0.06	0.18	0.02	0.01	13.91	99.10
34925A	24.71	0.32	8.59	39.34	0.02	1.69	8.47	<0.1	0.14	0.13	15.58	98.99
34926A	0.89	0.02	0.56	91.40	0.03	<0.05	0.05	<0.1	<0.01	0.15	6.32	99.42
34927A	43.66	0.46	36.23	4.54	0.03	0.10	0.05	<0.1	<0.01	0.03	14.05	99.15
34928A	1.80	0.05	1.52	85.46	0.10	<0.05	0.06	<0.1	<0.01	0.06	10.32	99.36
34929A	22.31	0.02	0.38	72.34	0.03	<0.05	0.06	<0.1	0.01	0.09	4.23	99.47
34930A	44.42	0.02	<0.2	52.08	0.01	<0.05	0.06	<0.1	0.01	0.10	2.57	99.26
34875A	22.15	0.80	19.07	41.82	1.53	0.60	0.14	0.17	1.42	0.24	12.03	99.95
34876A	30.62	1.32	27.57	26.83	0.55	0.15	0.15	0.11	0.07	0.11	12.53	100.00
34877A	1.59	0.02	0.44	88.95	0.02	<0.05	0.13	0.34	0.06	0.17	7.22	98.94
34878A	68.52	0.46	18.67	2.63	<0.01	1.10	0.12	<0.1	3.22	0.05	5.20	99.96
34879A	1.99	0.05	3.78	77.99	1.05	0.06	0.16	0.28	0.06	0.37	13.27	99.05
34880A	0.68	0.02	0.32	96.14	0.02	<0.05	0.14	0.32	0.07	0.15	1.10	98.95
34881A	59.93	0.01	<0.2	38.67	0.01	<0.05	0.15	<0.1	0.04	0.05	0.47	99.33
34882A	32.26	0.03	0.28	63.85	0.01	<0.05	0.14	0.21	0.05	0.13	2.49	99.45
34883A	48.56	1.38	24.04	15.52	0.02	0.21	0.12	<0.1	0.04	0.09	9.75	99.72
34884A	59.38	0.02	<0.2	30.28	0.04	1.85	3.28	0.15	0.12	0.02	4.00	99.13
34885A	68.83	0.41	14.14	3.69	<0.01	1.21	0.12	<0.1	3.14	0.03	7.56	99.12
34886A	1.53	0.07	2.67	81.98	0.12	<0.05	0.14	0.13	0.06	0.13	12.39	99.22
34887A	48.73	0.79	18.04	19.63	0.55	0.91	0.13	<0.1	2.42	0.11	7.63	98.95
34888A	44.71	0.51	15.21	31.11	0.01	0.09	0.15	<0.1	0.05	0.57	6.53	98.94
34889A	0.77	0.02	0.39	93.50	0.05	<0.05	0.13	0.34	0.06	0.12	3.95	99.33
34890A	16.07	1.16	17.52	52.47	0.02	<0.05	0.16	0.20	0.05	0.10	11.29	99.03
34891A	30.16	0.39	10.62	29.74	17.31	<0.05	0.18	0.27	0.44	0.21	10.34	99.65
34892A	25.35	0.66	21.65	37.90	0.06	0.20	0.16	0.19	0.73	0.19	12.25	99.33

FIGURE X.2 XRF MAJOR ELEMENT ANALYSIS RESULTS

XRF Analytical Results Geochemistry Laboratory, Department of Geological Sciences, University of Canterbury, New Zealand
[Rock Trace Program]

Sample Number	V (ppm)	Cr (ppm)	Ni (ppm)	Zn (ppm)	Zr (ppm)	Nb (ppm)	Ba (ppm)	La (ppm)	Ce (ppm)	Nd (ppm)	Ga (ppm)	Pb (ppm)
34904	18	11	<3	16	10	4	134	<5	<5	<10	7	6
34905	<3	7	<3	6	8	3	28	<5	<5	<10	4	1
34906	16	13	<3	17	10	<2	204	<5	<5	<10	5	7
34907	103	172	48	53	208	22	71	31	81	36	44	12
34908	101	93	82	135	111	10	83	25	60	30	17	11
34909	7	14	<3	31	10	3	120	<5	<5	<10	4	6
34910	3	10	<3	12	7	3	162	<5	<5	<10	6	5
34911	164	163	16	55	195	16	140	<5	26	<10	29	60
34912	207	203	82	118	325	25	131	21	72	19	40	43
34913	6	26	<3	18	13	3	145	<5	<5	<10	6	6
34914	8	17	<3	15	16	4	131	<5	<5	<10	4	1
34915	7	12	<3	12	11	3	143	<5	<5	<10	3	3
34916	<3	13	<3	20	8	3	140	<5	<5	<10	3	4
34917	5	7	<3	10	7	3	92	<5	<5	<10	3	2
34918	10	8	<3	25	11	<2	195	<5	28	<10	4	7
34919	3	3	<3	10	6	3	76	<5	<5	<10	<2	3
34920	249	170	63	163	244	19	51	<5	41	<10	29	23
34921	142	51	<3	14	146	21	56	<5	34	19	16	8
34922	122	40	10	12	133	18	40	<5	17	<10	15	9
34923	25	51	8	16	218	17	72	81	137	66	21	25
34924	5	11	32	10	26	3	<20	12	9	<10	5	2
34925	55	53	10	37	128	10	421	<5	<5	<10	11	3
34926	<3	14	<3	23	7	3	80	<5	<5	<10	3	<1
34927	19	61	40	35	70	6	<20	11	11	<10	9	3
34928	15	35	<3	29	11	3	91	<5	<5	<10	4	6
34929	<3	9	<3	20	6	3	49	<5	<5	<10	5	3
34930	<3	8	<3	15	6	3	57	<5	<5	<10	3	3
34875	184	83	169	142	249	13	135	62	53	76	25	27
34876	182	199	127	81	241	20	58	30	65	39	36	22
34877	3	9	<3	20	8	3	80	<5	<5	<10	2	<1
34878	122	140	47	34	105	7	130	81	189	73	21	129
34879	13	22	<3	40	18	4	109	<5	87	20	<2	4
34880	43	34	<3	27	10	<2	97	<5	<5	<10	<2	<1
34881	4	6	<3	7	7	4	53	<5	<5	11	<2	2
34882	6	9	<3	14	8	3	61	<5	<5	<10	<2	3
34883	178	175	<3	38	292	21	23	16	64	31	37	18
34884	7	6	<3	8	10	3	28	<5	<5	<10	<2	4
34885	83	81	26	33	157	12	80	37	75	50	20	20
34886	31	39	<3	39	19	3	56	<5	<5	<10	5	3
34887	132	103	142	108	160	12	146	48	21	68	23	15
34888	108	127	7	48	152	14	442	85	163	91	27	25
34889	5	11	<3	18	8	3	101	<5	<5	36	3	<1
34890	171	272	55	28	123	13	74	<5	13	23	17	13
34891	75	114	674	1681	106	11	2714	21	95	58	18	11
34892	139	101	53	25	212	17	38	9	26	44	23	8

FIGURE X.3 XRF MINOR ELEMENT ANALYSIS RESULTS

[Rock Trace 03 Program]

Sample Number	Rb (ppm)	Sr (ppm)	Th (ppm)	Y (ppm)
34904	<1	14	<1	21
34905	<1	4	<1	15
34906	<1	8	4	21
34907	<1	14	21	52
34908	72	5	13	23
34909	1	2	<1	8
34910	1	3	<1	4
34911	<1	12	20	51
34912	<1	15	27	77
34913	<1	5	<1	11
34914	<1	7	<1	11
34915	<1	5	<1	13
34916	<1	7	2	6
34917	1	4	<1	4
34918	<1	18	<1	21
34919	3	2	<1	11
34920	<1	3	23	45
34921	<1	6	6	54
34922	<1	7	7	52
34923	13	61	21	33
34924	<1	7	3	4
34925	3	193	17	11
34926	<1	<1	2	6
34927	<1	2	6	7
34928	<1	1	2	13
34929	<1	1	5	6
34930	<1	2	<1	7
34875	56	6	21	159
34876	<1	5	22	60
34877	<1	3	4	4
34878	168	11	16	16
34879	<1	4	3	20
34880	<1	7	<1	15
34881	<1	4	<1	4
34882	<1	7	<1	10
34883	<1	26	26	39
34884	6	30	<1	5
34885	160	10	11	28
34886	<1	2	<1	14
34887	97	7	20	91
34888	<1	95	18	41
34889	<1	2	1	5
34890	<1	6	8	19
34891	6	68	16	70
34892	9	6	21	70

Sample Number	As (ppm)	Cu (ppm)	Sc (ppm)	U (ppm)
34904	25	34	<2	<4
34905	6	19	<2	<4
34906	24	48	<2	<4
34907	10	82	20	10
34908	79	59	14	8
34909	23	33	<2	<4
34910	16	29	<2	<4
34911	46	155	19	4
34912	55	211	20	10
34913	36	29	<2	<4
34914	15	25	<2	<4
34915	14	20	<2	<4
34916	18	23	<2	<4
34917	11	18	<2	<4
34918	21	31	<2	<4
34919	9	18	<2	<4
34920	104	60	34	8
34921	79	23	7	<4
34922	36	15	3	<4
34923	3	6	9	7
34924	<2	9	<2	5
34925	11	23	12	<4
34926	18	29	<2	<4
34927	18	11	5	5
34928	32	39	<2	<4
34929	13	25	<2	<4
34930	7	18	<2	<4
34875	108	74	32	<4
34876	44	61	26	8
34877	16	28	<2	<4
34878	138	26	15	<4
34879	18	43	<2	<4
34880	23	29	<2	<4
34881	9	16	<2	<4
34882	10	22	<2	<4
34883	50	24	27	7
34884	3	13	<2	4
34885	30	7	14	6
34886	21	47	10	<4
34887	39	53	16	7
34888	44	53	10	8
34889	15	37	<2	<4
34890	24	55	19	<4
34891	455	82	8	9
34892	22	22	27	<4

FIGURE X.3 XRF MINOR ELEMENT ANALYSIS RESULTS (CONTINUED)

APPENDIX XI: **XRD MINERAL ANALYSIS**

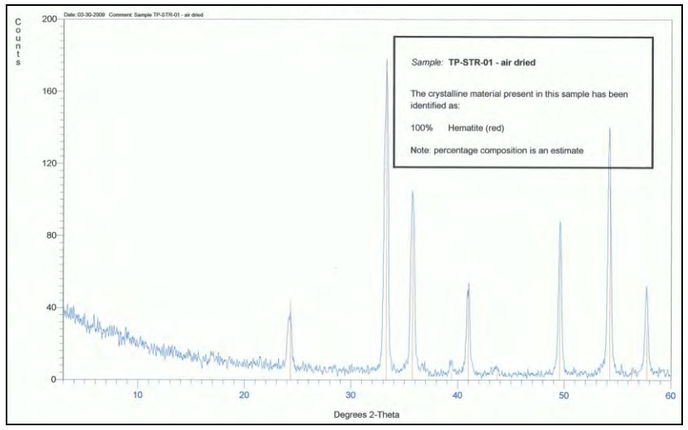

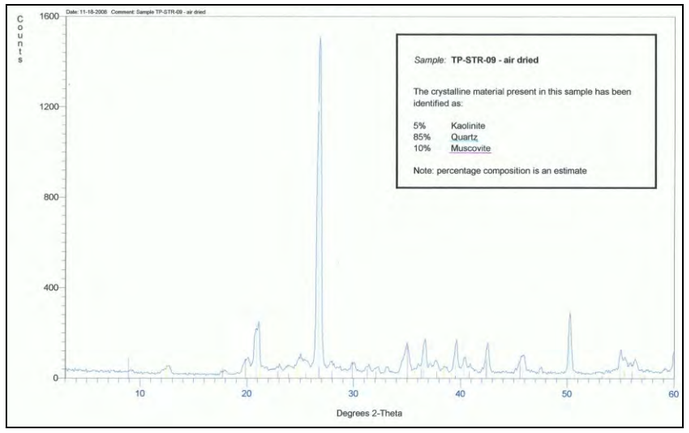

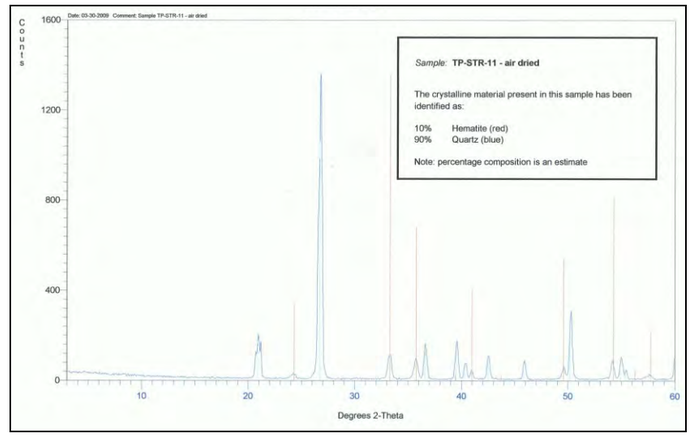

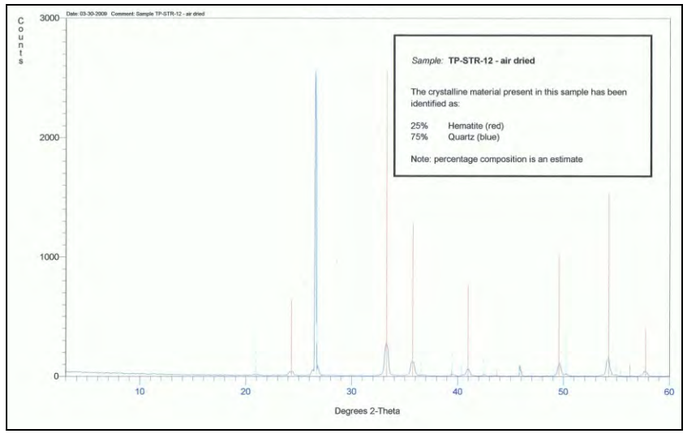

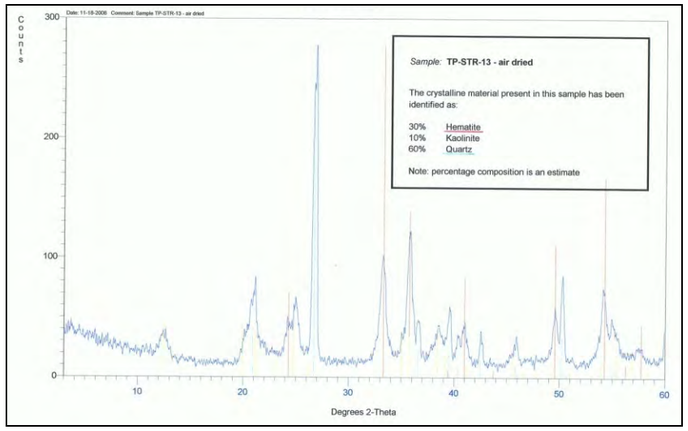

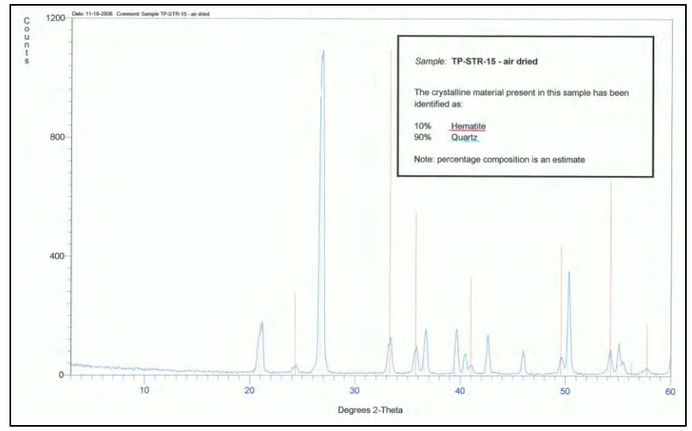

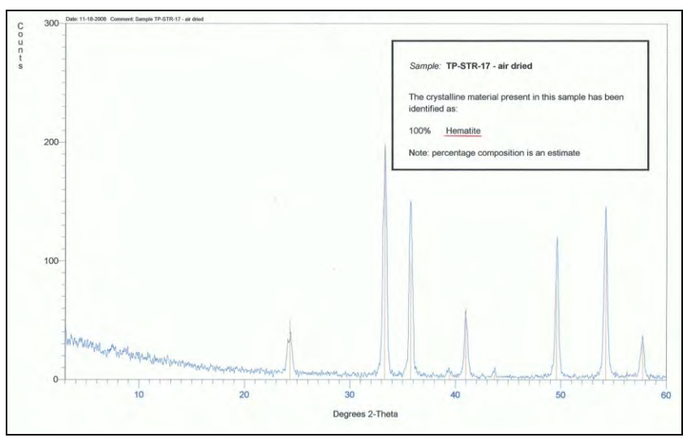

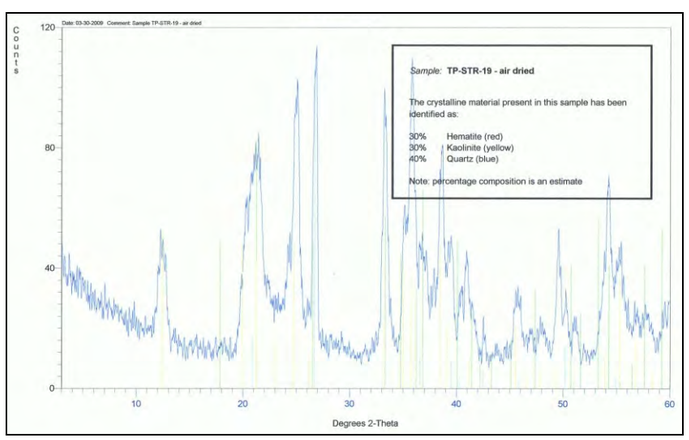

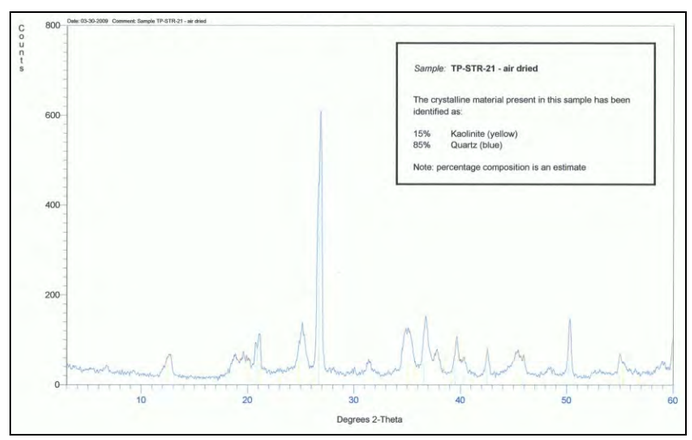

FIGURE XI.1 XRD MINERAL ANALYSIS RESULTS

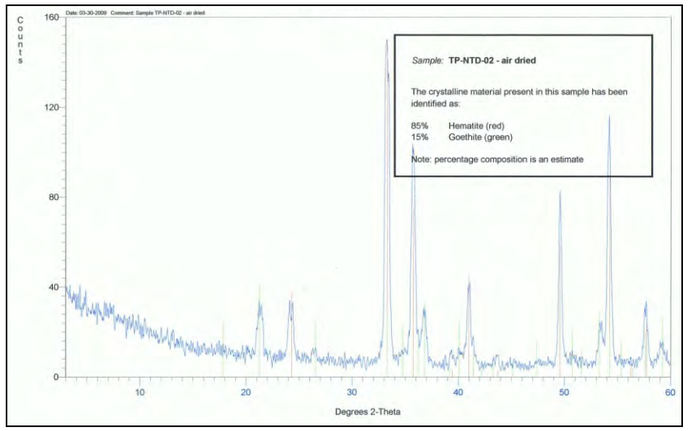

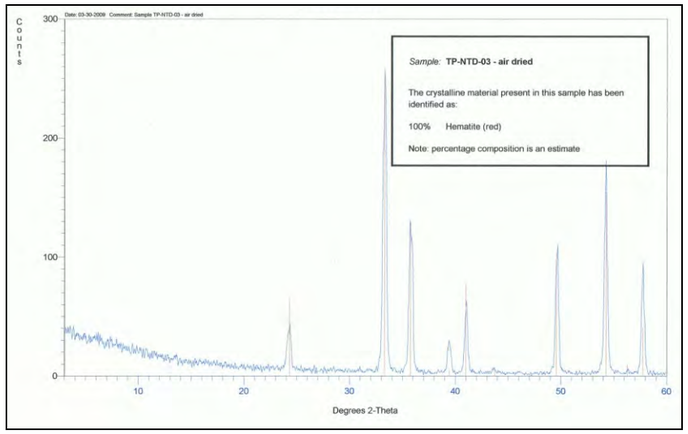

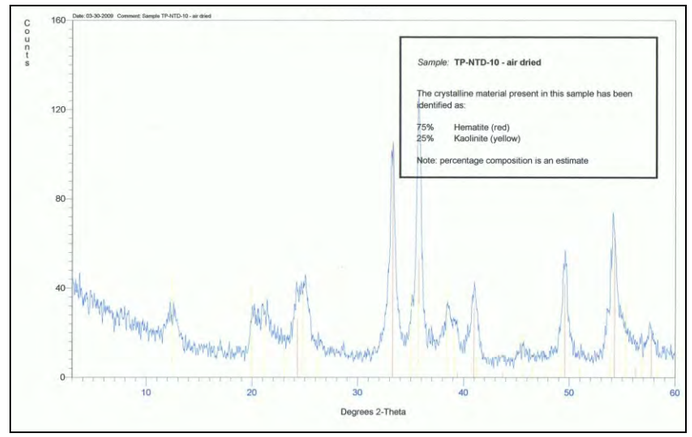

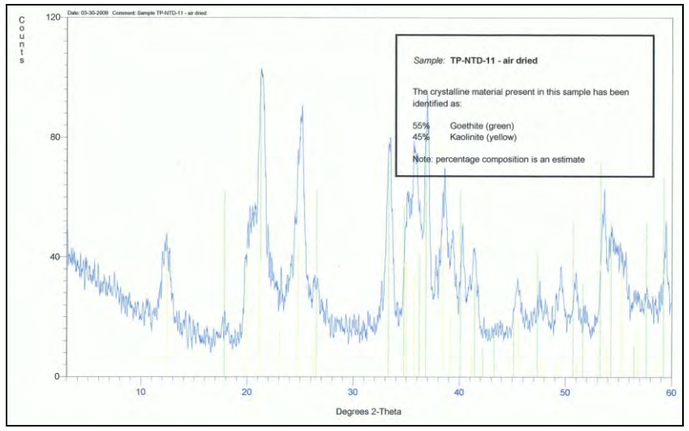

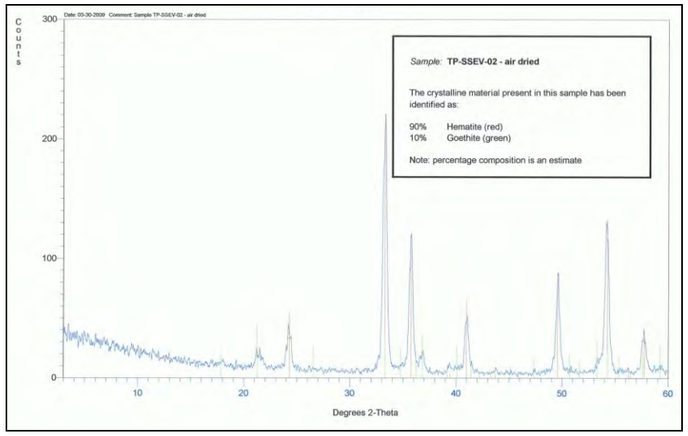

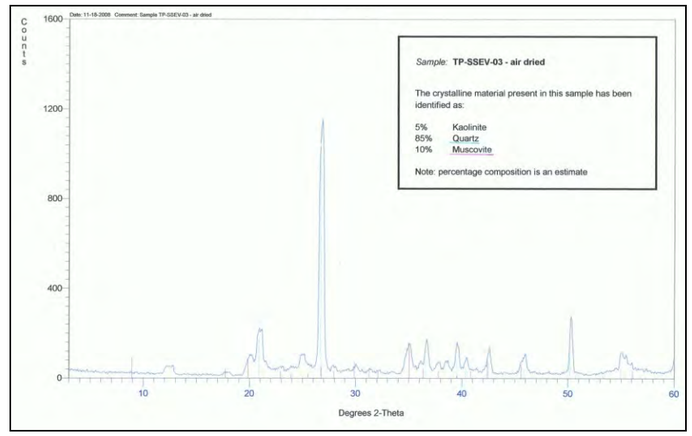

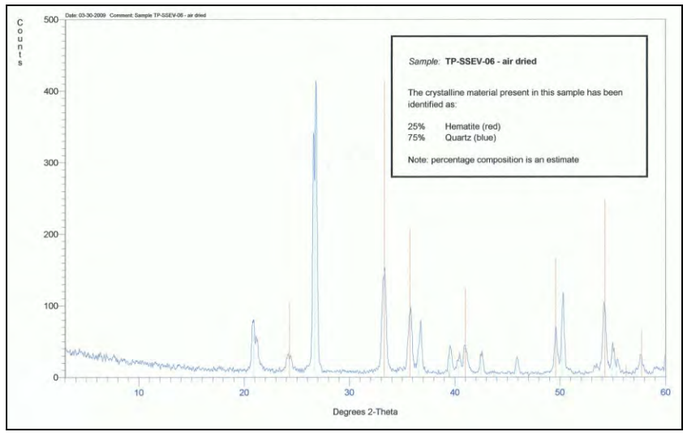

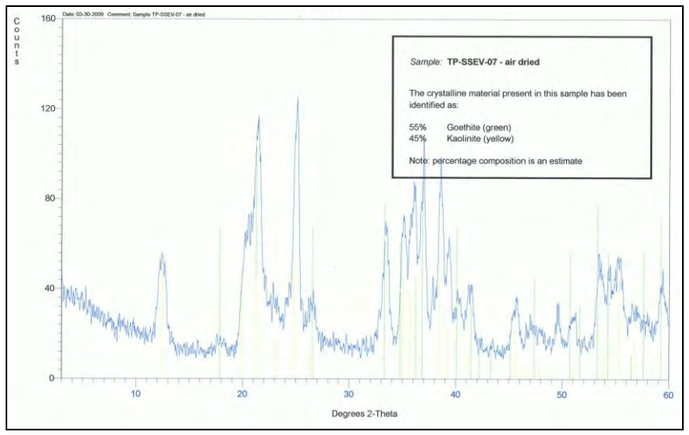

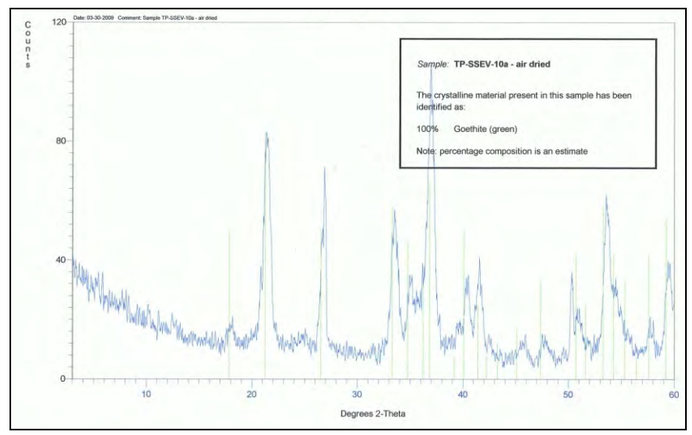

FIGURE XI.1 XRD MINERAL ANALYSIS RESULTS (CONTINUED)

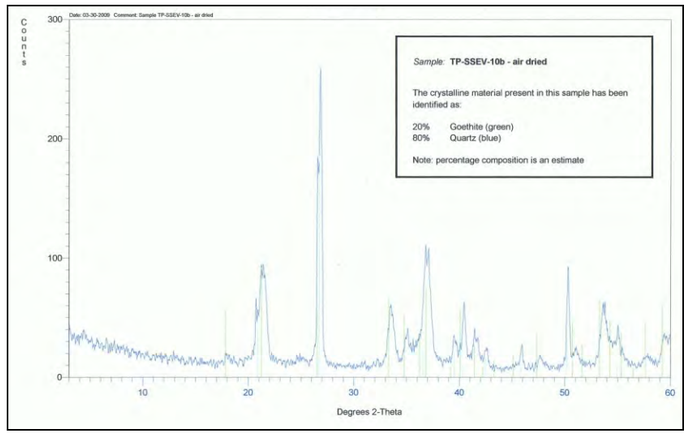

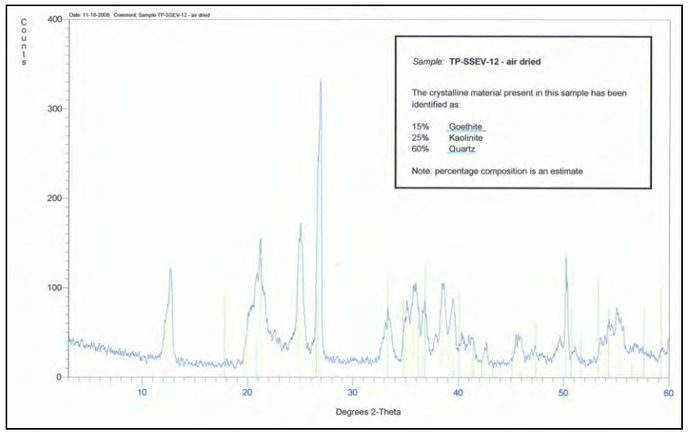

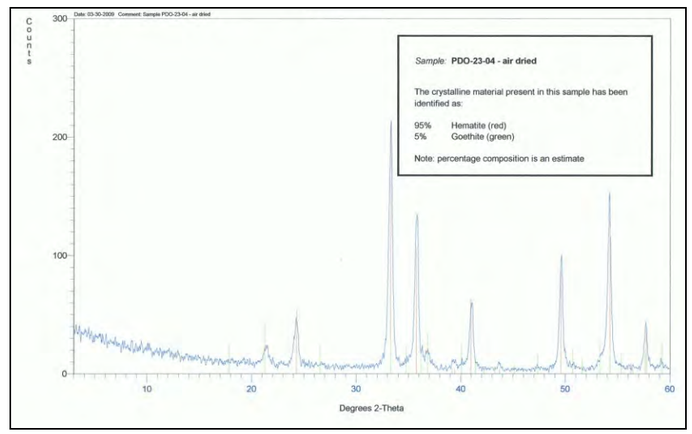

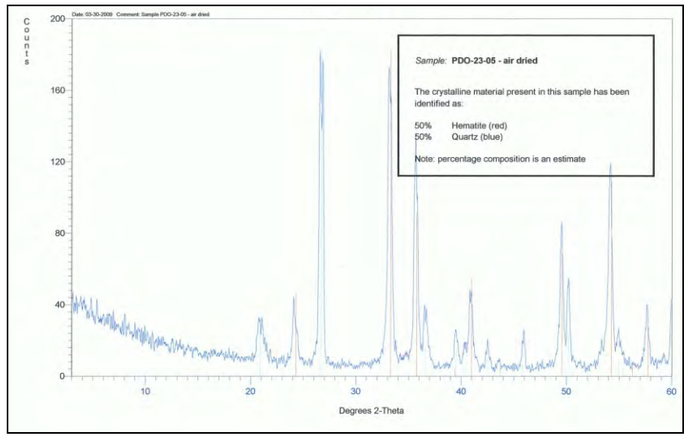

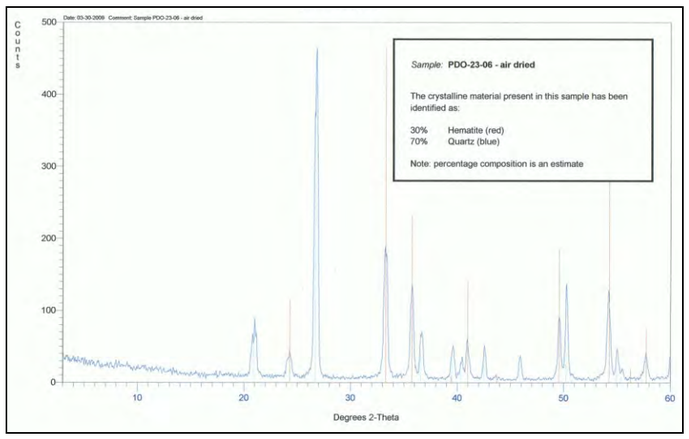

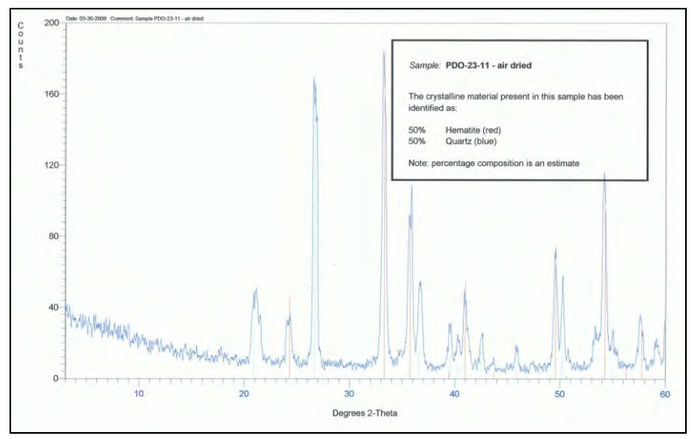

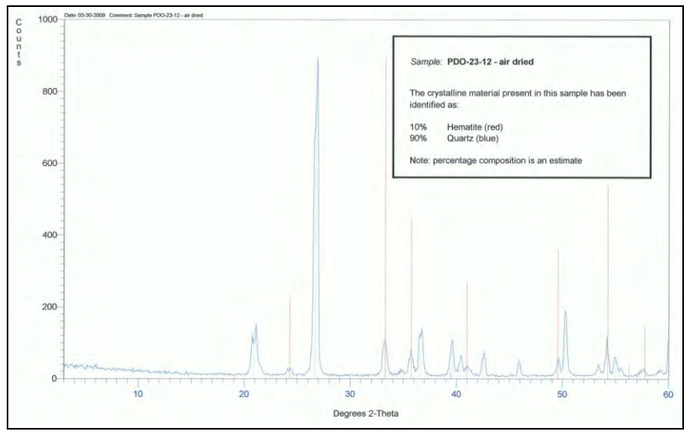

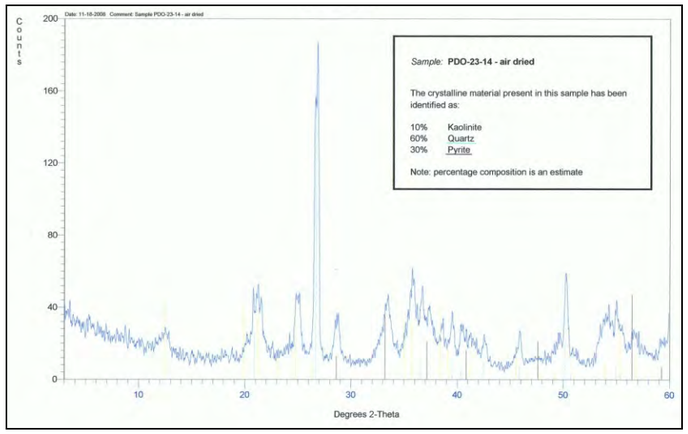

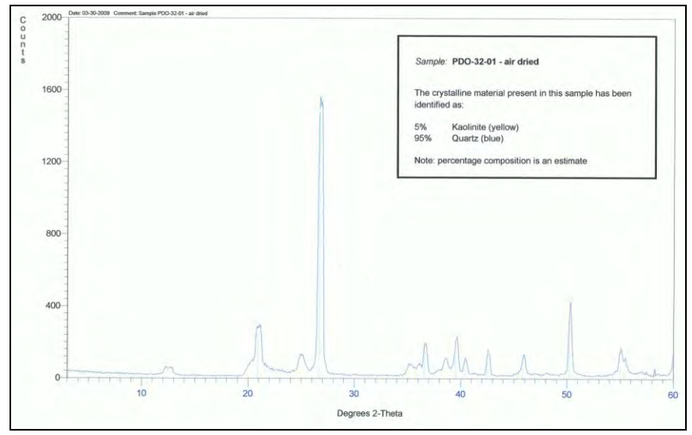

FIGURE XI.1 XRD MINERAL ANALYSIS RESULTS (CONTINUED)

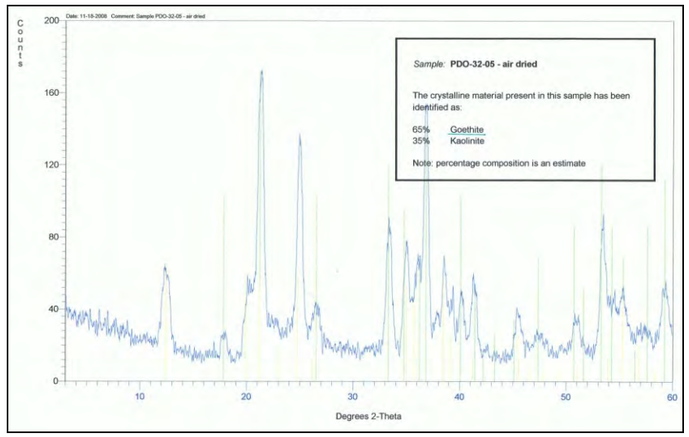

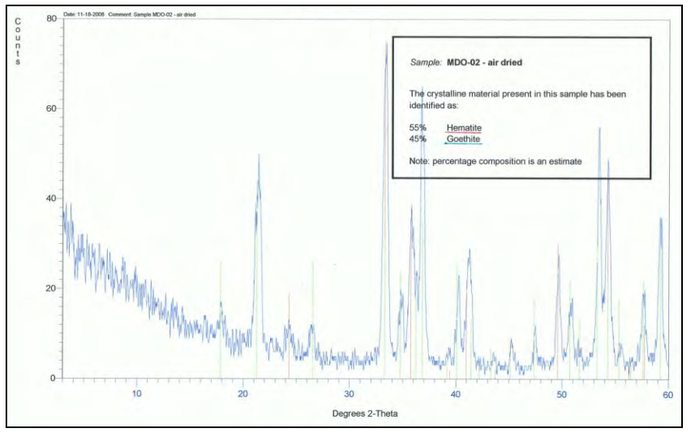

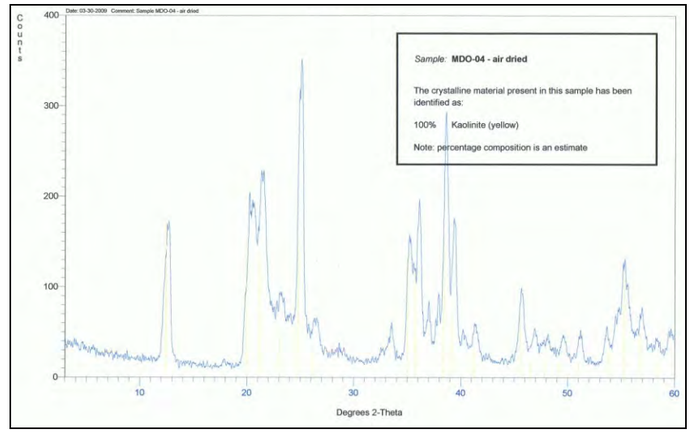

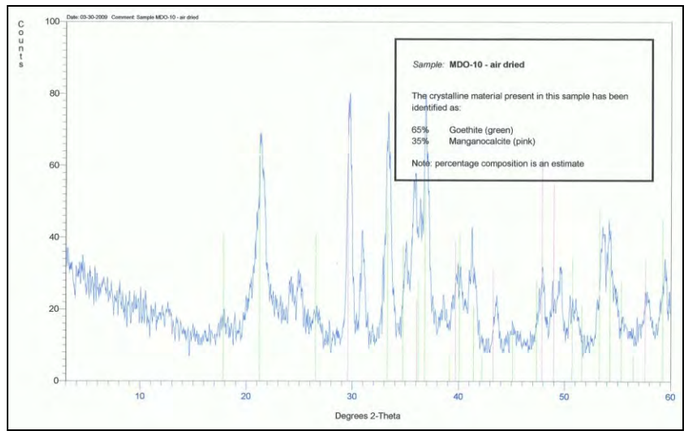

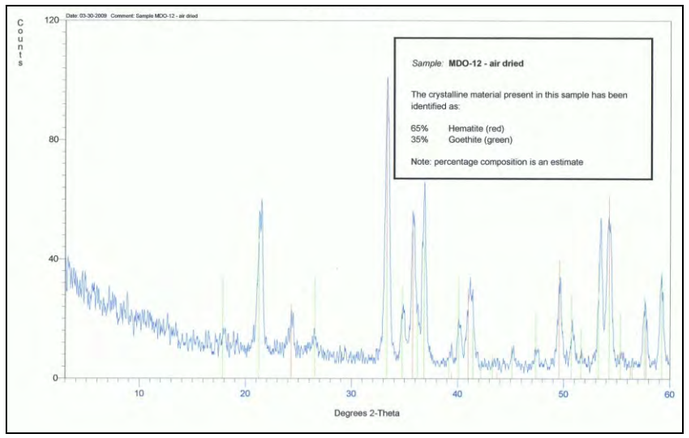

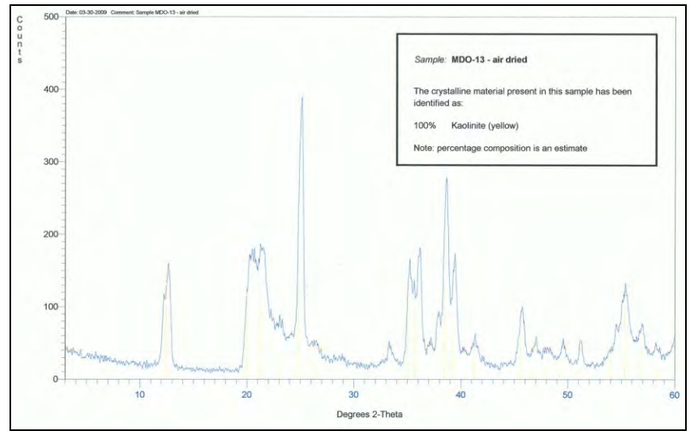

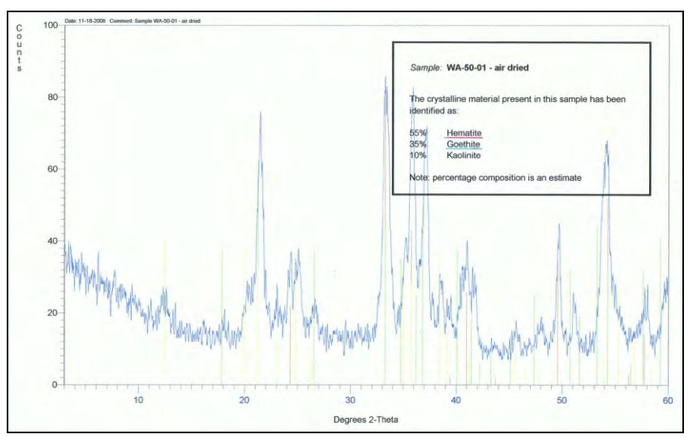

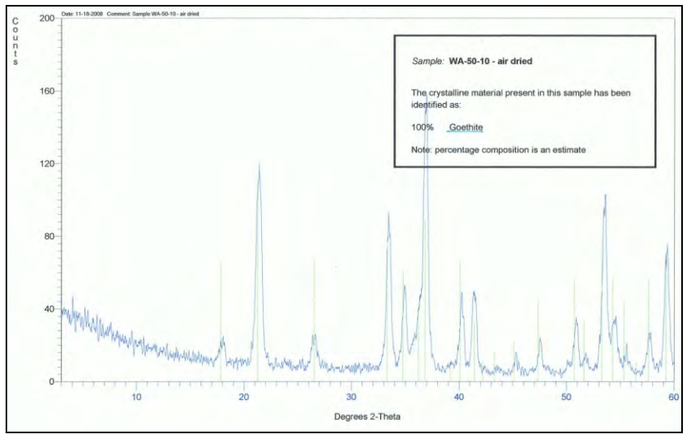

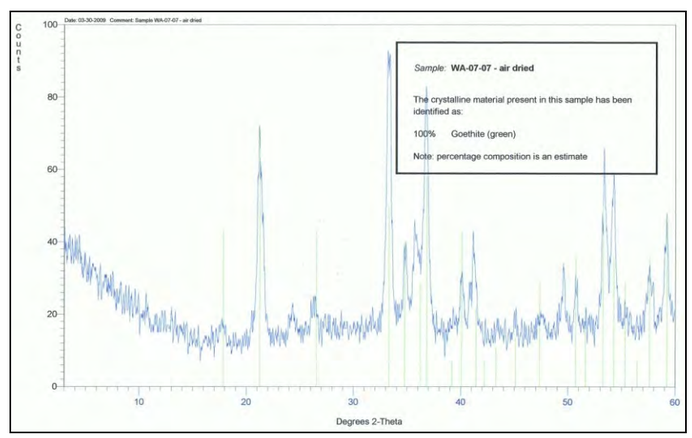

FIGURE XI.1 XRD MINERAL ANALYSIS RESULTS (CONTINUED)

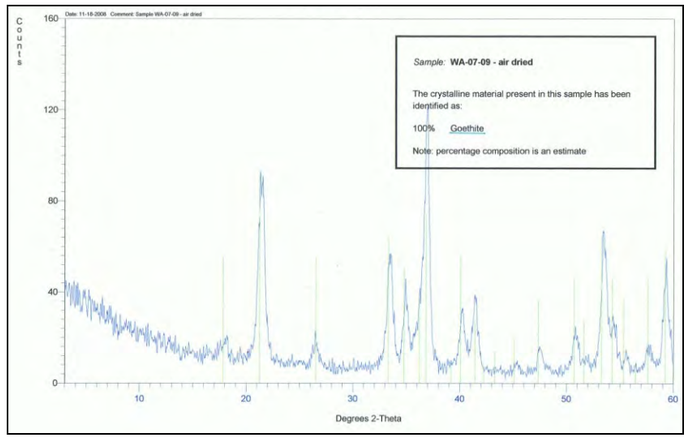

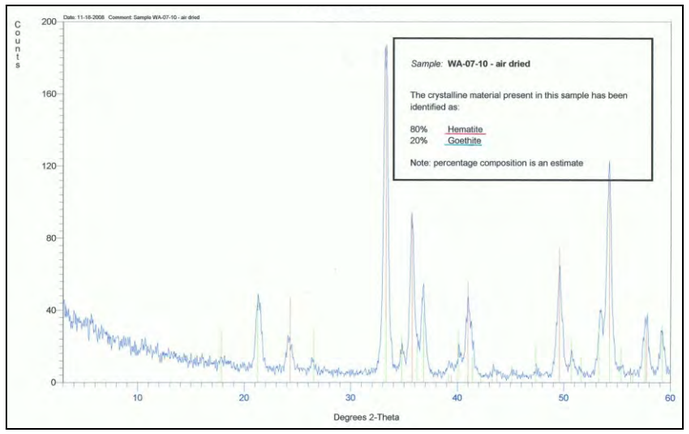

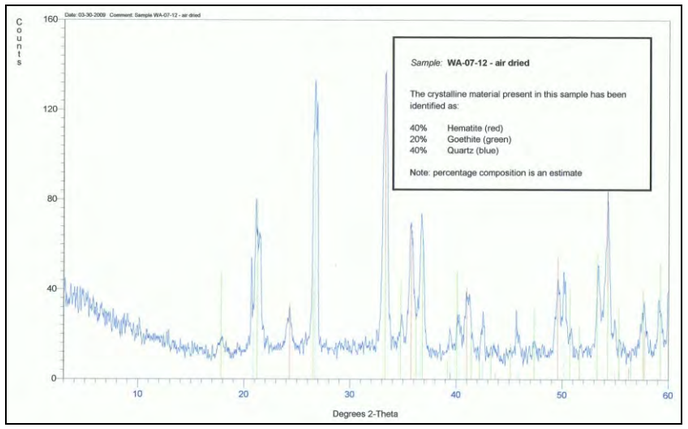

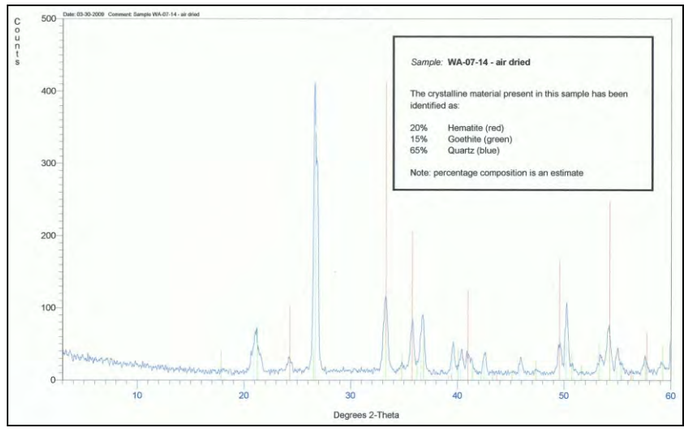

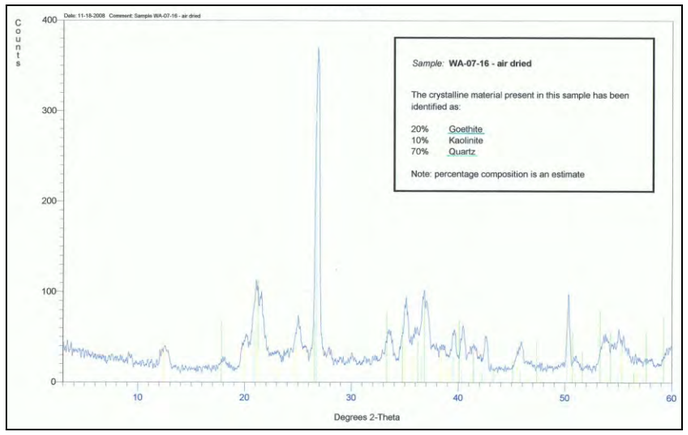

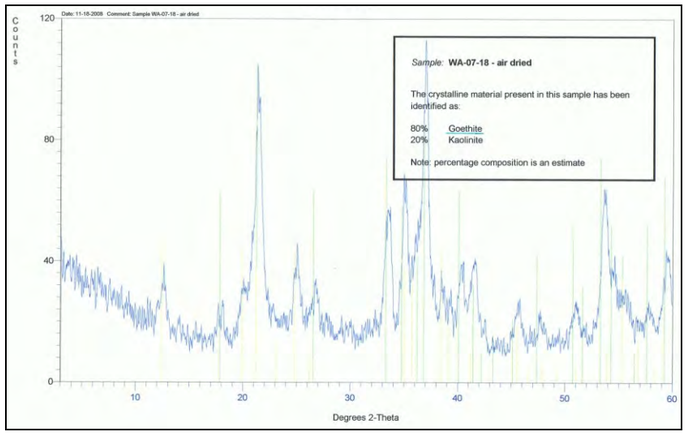

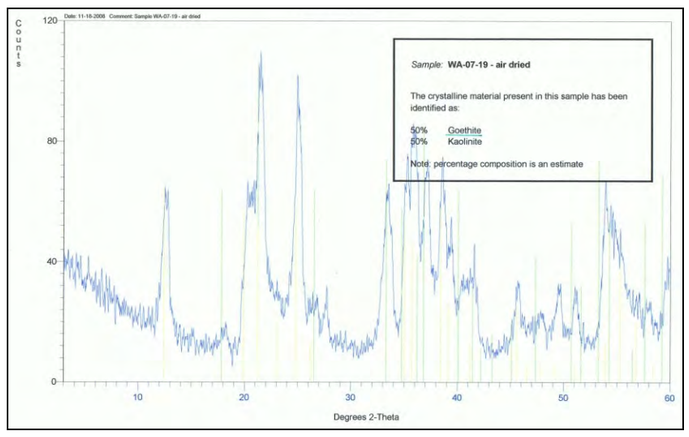

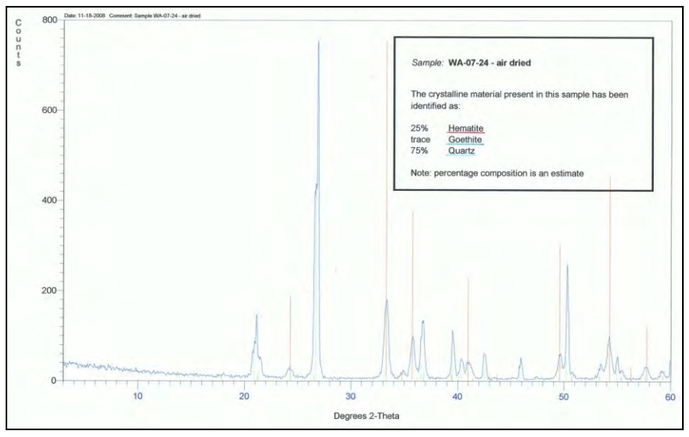

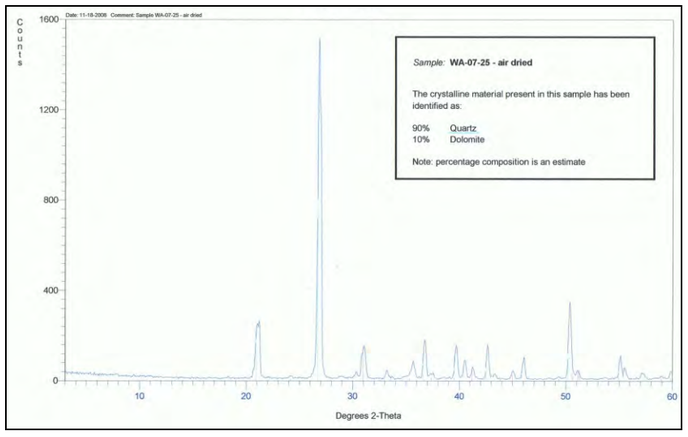

FIGURE XI.1 XRD MINERAL ANALYSIS RESULTS (CONTINUED)

Geochemical Analysis – H. Donders sample PDO-23-14

The XRD result for this sample indicates that pyrite (FeS_2) is present – the XRF major element analysis confirms this by the iron concentration and a qualitative XRF scan of the sample confirms that sulphur is also present.

This sample has a relatively high MnO concentration (determined by XRF analysis). The mineral pyrolusite (MnO) is a likely source of the high MnO value. The XRD pattern lines for pyrolusite are overlapped by the pattern lines for pyrite, which would explain why the XRD search/match process did not detect pyrolusite.

The amount on the XRD report of 30% Pyrite will effectively be 30% attributed to Pyrite/Pyrolusite.

FIGURE XI.2 FURTHER NOTE FOR XRF AND XRD TESTING